CYCLODEXTRIN COMPLEXES OF ANTIMICROBIAL AGENTS

by

NAYNA CHAUHAN

A thesis submitted for the degree of
Doctor of Philosophy
at
THE UNIVERSITY OF ASTON IN BIRMINGHAM

March 1995

The University of Aston in Birmingham.

CYCLODEXTRIN COMPLEXES OF ANTIMICROBIAL AGENTS

By
Nayna Chauhan

Submitted for the degree of Doctor of Philosophy, 1995

SUMMARY

Poorly water-soluble drugs show an increase in solubility in the presence of cyclodextrins (CyD) due to the formation of a water-soluble complex between the drug and dissolved CyD. This study investigated the interactions of β-CyD and hydroxypropyl-β-CyD (HP-β-CyD, M.S. = 0.6) with antimicrobial agents of limited solubility in an attempt to increase their microbiological efficacy. The agents studied were chlorhexidine dihydrochloride (CHX), *p*-hydroxybenzoic acid esters (methyl, ethyl, propyl and butyl) and triclosan.

The interactions between the antimicrobials and CyDs were studied in solution and solid phases. Phase solubility studies revealed an enhancement in the aqueous drug solubility in the presence of the CyD and also gave an indication of the complex stability constant (K_S). The temperature-dependence of the stability constant of the complex was modelled by the van't Hoff plot which yielded the thermodynamic parameters for complexation.

Further confirmation of the inclusion of the antimicrobials within the cavity of the CyDs in aqueous solution was obtained from proton magnetic resonance and ultraviolet absorption spectroscopies. The former method indicated that the chlorophenyl moiety of the CHX was included within the β-CyD cavity and the stoichiometry of the complex formed was 1:1.

The solid-phase complexes were prepared by freeze-drying. The inclusion complex of triclosan with HP-β-CyD was obtained from aqueous solution with the addition of ammonia. Evidence to confirm complex formation was obtained from DSC, IR and X-ray powder diffraction studies.

Dissolution studies of the solid inclusion complexes using the dispersed powder technique illustrated their superior solubilities as compared to the equimolar physical mix of the guest and CyD. It was shown that these solutions of the complex were supersaturated with respect to the free guest. This was further demonstrated by diffusion studies which showed the flux of free drug from donor solutions of the antimicrobial-CyD complex to be significantly greater than the flux from donor suspensions of drug alone.

The microbiological activities of the antimicrobial-CyD complexes were evaluated using two methods. The antibacterial effect of the butyl paraben-HP-β-CyD complex on the viability of a strain of *Pseudomonas aeruginosa* was superior to a saturated solution of butyl paraben alone. Using a diffusion model, the microbiological effect of BuP as it diffused from a donor solution of its HP-β-CyD complex was assessed. As a consequence of the relatively higher free antimicrobial concentration in this system, the effect of butyl paraben against a strain of *Escherichia coli* was greater than for an equivalent system containing a donor a suspension of drug alone.

Equations are presented which enable calculation of free and complexed guest concentrations in systems comparing different concentrations of guest and CyD in the presence and absence of a competitor.

KEY WORDS: β-cyclodextrin; hydroxypropyl-β-cyclodextrin; chlorhexidine dihydrochloride; competitor; free drug concentrations; *p*-hydroxybenzoic acid esters (parabens); inclusion complex; mathematical model; microbiological activity; triclosan; supersaturation.

To Mum and Dad
For all your love

ACKNOWLEDGEMENTS

I would like to thank my supervisor Dr Bill Irwin for his supervision, guidance and support throughout this project. I am also grateful to both Dr Tim Grattan and SmithKline Beecham, and the Department of Pharmaceutical and Biological Sciences, Aston University, for financial support.

I am also grateful to Mr Chris Bache for his excellent technical assistance and Mr Graham Smith for his graphical expertise. My thanks also go to Dr Peter Lambert and Mrs Dorothy Townley for helpful guidance and discussion for the microbiological work. Thanks also to Mr Mark Harrison, Wacker Chemicals, for the supply of the cyclodextrins.

X-ray diffractometry was carried out by Mr Roger Howell. All photographic reproductions are courtesy of the Aston University Photographic Department.

A very special thank you to Debbie Stagg for her support and friendship.

Thanks also to my parents and family for all their love, support and encouragement. Finally, I would like to thank Suresh for his continual optimism, support and understanding.

CONTENTS

LIST OF FIGURES

LIST OF TABLES

LIST OF PLATES

CHAPTER ONE
INTRODUCTION

1.1 HISTORY

Cyclodextrins (CyDs) were first isolated by Villiers in 1891 from the degradation products of starch and the description of their preparation, isolation and main characteristics was made by Schardinger in the years 1903 to 1911. Hence, CyDs are known as 'Schardinger dextrins' as well as cycloamyloses and cycloglucans. Many papers and texts have been published concerning the properties and applications of CyDs in the pharmaceutical field (Jones *et. al.*, 1984; Saenger, 1980; Szejtli, 1988; Bekers *et. al.*, 1991b).

1.2 PRODUCTION

CyDs are formed by the action of the cyclodextrin-*trans*-glycosidase enzyme (CTG) on a medium containing starch (Szejtli, 1988). As a consequence of the helical structure of the starch molecules, the primary product of the cleavage by the CTG-enzyme undergoes an intramolecular reaction and α–1,4-linked cyclic products are formed; these being known as cyclodextrins. The CyDs are separated from the reaction mixture by selective precipitation with complexing solvents, and then purified by decomposition of the complex, removal of the guest compound, and crystallisation of the CyDs from water (Clarkes, Coates and Lincoln, 1988).

It was in 1903 that Schardinger described the micro-organism *Bacillus macerans* as being the most frequent source for the CTG enzyme. Other organisms which produce this enzyme include *Klebsiella pneumonia* and *Alkaphilic bacterium* No 38-2 (Bekers *et. al.*, 1991b).

1.3 STRUCTURE AND PROPERTIES

Cyclodextrins are cyclic oligosaccharides composed of alpha-(1,4) linked D-glucose monomer units as illustrated in figure 1.1. The three most commonly used natural CyDs are alpha (α), beta (β), and gamma (γ) CyDs. The α-CyD consists of 6 glucose units, and is also known as Schardinger α-dextrin, cyclomaltohexaose, cyclohexaglucan and cyclohexamylose. The β-CyD is also known by various other names which include

Schardinger β-dextrin, cyclomaltoheptaose, cycloheptaglucan and cycloheptamylose and comprises 7 glucopyranose units. The γ-CyD consists of 8 units and is also known as Schardinger γ-CyD, cyclomaltoheptaose, cycloheptaglucan and cycloheptamylose. Of the natural CyDs, β-CyD is the most widely used, the structure of which is β-CyD is shown in figure 1.2.

The natural CyDs are all white, crystalline, homogenous, non-hygroscopic substances. CyDs with less than 6 glucose units are not formed, possibly due to steric reasons (Sundararajan and Rao, 1970). Larger CyDs have been identified, however their yields are small and their complexing abilities are not significant (Uekama and Otagiri, 1987).

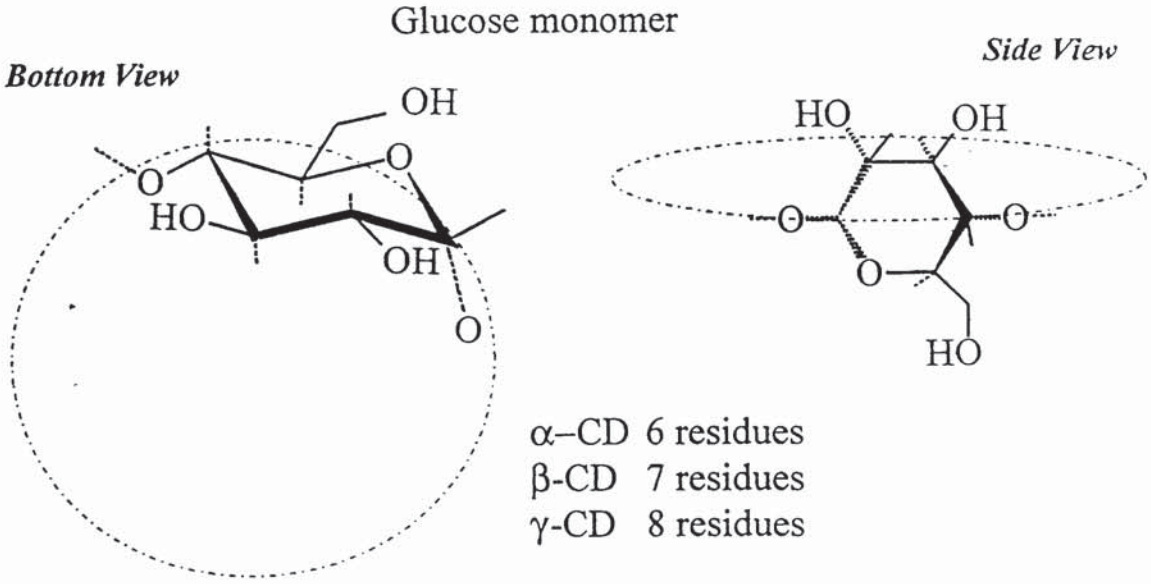

Figure 1.1 Alpha-(1,4) linked D-glucose monomer unit of cyclodextrin

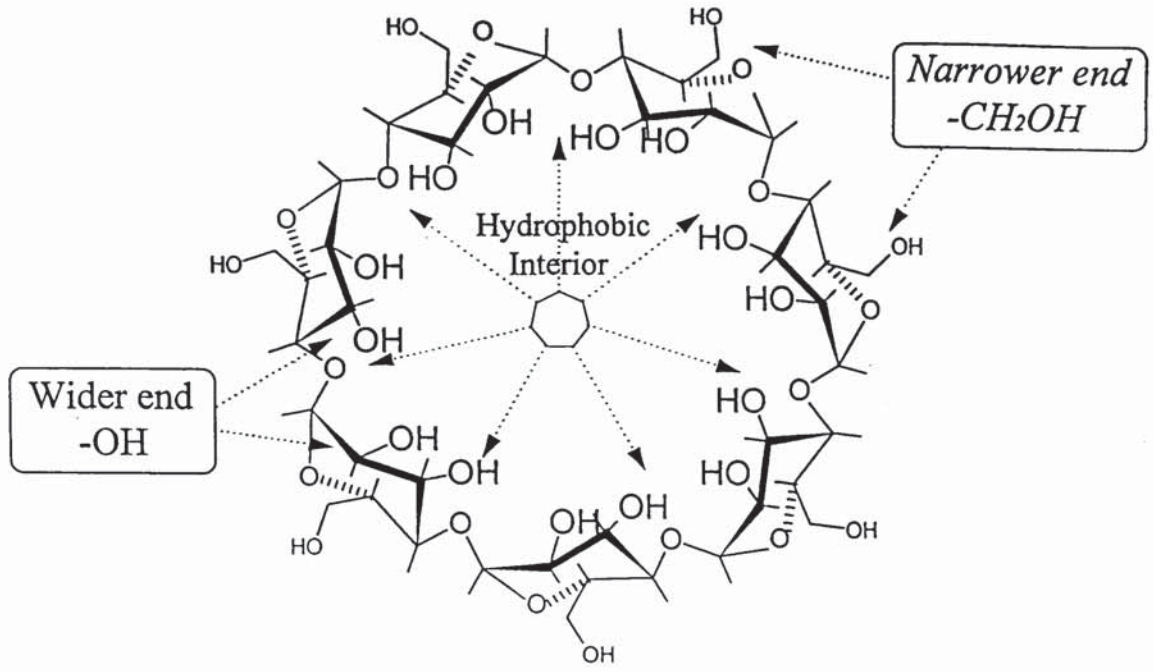

Figure 1.2 Structure of β-cyclodextrin (β-CyD)

NMR and X-ray diffraction studies (Rao and Foster, 1963; Hybl, Rundle and Williams, 1965) have revealed a C-1 chair conformation for the glucose molecules of the CyDs (as illustrated later in section 2.6.10). As a consequence of this configuration and the lack of free rotation among the glycosidic bonds, CyDs are not perfectly cylindrical molecules, but are in the shape of truncated cones. The secondary hydroxyl groups (on the C-2 and C-3 atoms of the glucose units) are located on one edge of the ring, while the primary hydroxyls are on the other side. As the primary hydroxyls can rotate freely, the effective diameter of the cavity on the side where they occur is reduced. However, rotation of the secondary hydroxyl groups is restricted as they are relatively rigid chains. Hence, the cavity at the secondary hydroxyl side is wider than that at the primary hydroxyl side (Bekers *et. al.*, 1991b). The exterior of the CyD torus is hydrophilic due to the hydroxyl functionalities. Conversely, the interior cavity is hydrophobic as it is lined with a ring of C(3)-H groups, a ring of glucosidic oxygens and another ring of C(5)-H groups. This hydrophilic/hydrophobic property is a characteristic feature of CyDs which allows the CyD to be relatively soluble in water, with the interior cavity providing a hydrophobic environment for the solubilisation of lipophilic substances. Figure 1.3 illustrates the functional structure of CyDs.

Figure 1.3 Functional structural scheme of cyclodextrins (Szejtli, 1988)

The C2-OH group of one glucose unit of the CyD molecule can form a hydrogen bond with the C3-OH group of the adjacent unit (Bekers *et. al.*, 1991b). These interactions stabilise the macrocyclic structure of the CyD molecule (Uekama and Otagiri, 1987). These intramolecular H-bonds also prevent hydration of the CyD molecule which is a possible explanation for the low solubility of β-CyD (Szejtli, 1988). In aqueous solution, β-CyD molecules tend to form head-to-tail and head-to-head dimers (figure 1.4) in order to achieve maximum contact for these interactions (Szejtli, 1991). The limited aqueous solubility of β-CyD restricts its usefulness in improving solubility, dissolution and bioavailability. However, this problem can be overcome by chemical modification of the CyD as further discussed in section 1.5, and also by the presence of certain additives. With the addition of bases (Pharr *et. al.*, 1989), the CyD is solubilised due to the deprotonation of the secondary hydroxyl group of the glucose monomer. Buvári and Barcza (1989) reported an increase in β-CyD solubility in the presence of metal salts which was due partly to their interaction with the exterior of the CyD torus ('outer sphere complexes') and partly due to changes in the activity of the water. Various water/co-solvent mixtures (Chatjigakis *et. al.*, 1992) have also been used to enhance the solubility of β-CyD. As a general rule, the solubility of the natural CyDs increases with a rise in temperature. In contrast, the aqueous solubility of the methylated derivatives is inversely proportional to temperature increase (Szejtli, 1983).

In contrast to the β-CyD, the solubility of α-CyD is greater due to the formation of an incomplete belt of hydrogen-bonds as one of the glucose units of the α-CyD molecule is distorted (Rees, 1970). γ-CyD is the most soluble of the natural CyDs due to its non-coplanar, flexible structure (Szejtli, 1988). As expected, the molecular dimensions of the

CyDs alter with the number of glucose units which will consequently effect their complex forming abilities as discussed later.

Figure 1.4 'Head-to-tail' and 'head-to-head' structures of β-CyD molecules in aqueous solution (Szejtli, 1988)

1.4 CYCLODEXTRIN DERIVATIVES

The natural CyDs can be modified by the introduction of different chemical moieties onto their hydroxyl groups leading to an alteration in the physicochemical properties of the parent CyD. There are various types of CyD derivatives which include alkylated CyDs (El-Gendy *et. al.*, 1986; Imai *et. al.*, 1988), hydroxyalkylated CyDs (Yoshida *et. al.*, 1988; Yoshida *et. al.*, 1990), ionic derivatives (Uekama *et. al.*, 1989), CyD polymers (Szeman *et. al.*, 1988) and branched CyDs (Okada *et. al.*, 1988). The physicochemical properties of the parent CyD are influenced by the nature of the substituent group and also its degree of substitution. The numerous publications dedicated to the different types of CyD derivatives and their potential uses have been summarised by Szejtli (1988 and 1992) and Bekers *et. al.* (1991b). A comprehensive review of the methods of preparation of the various derivatised CyDs has been published by Croft and Bartsch (1983).

One property in particular which is affected by chemical modification of the natural CyD is the aqueous solubility. For example, when hydroxyalkyl groups are incorporated into the β-CyD molecule, the aqueous solubilities of the derivatives are greater than 50 g/ 100 ml (Yoshida *et. al.*, 1988) compared with 1.85 g/100 ml for the parent CyD. The limited solubility of β-CyD can therefore be substantially improved by chemical modification. A similar solubility enhancement was observed with 2,6-di-O-methyl-β-CyD (DM-β-CyD, 57 g/100 ml; 25°C); the presence of the methyl groups in the CyD molecule prevent the formation of intramolecular H-bonds which would otherwise hinder its solubility (Uekama and Otagiri, 1987). In contrast, the ethylated CyD derivatives are of low aqueous solubility (diethyl-β-CyD, 0.005 g/100 ml; 25°C), enabling them to be used as sustained release carriers of water soluble drugs (Uekama *et. al.*, 1989; Hirayama *et. al.*, 1988).

One particular derivative which is important pharmaceutically, is 2-hydroxypropyl-β-CyD (HP-β-CyD) due to its enhanced aqueous solubility and lack of toxicity (Pitha and Pitha, 1985; Müller and Brauns, 1985). The structure of HP-β-CyD is illustrated in figure 1.5. HP-β-CyD has been used for the improvement of pharmaceutical properties such as solubility (Müller and Brauns, 1985; Yoshida *et. al.*, 1990), dissolution (Pitha, Harman and Michel, 1986), chemical stability (Darrington *et. al.*, 1990; Brewster *et. al.*, 1991) and bioavailability (Hosteler, Hanson and Stevens, 1992).

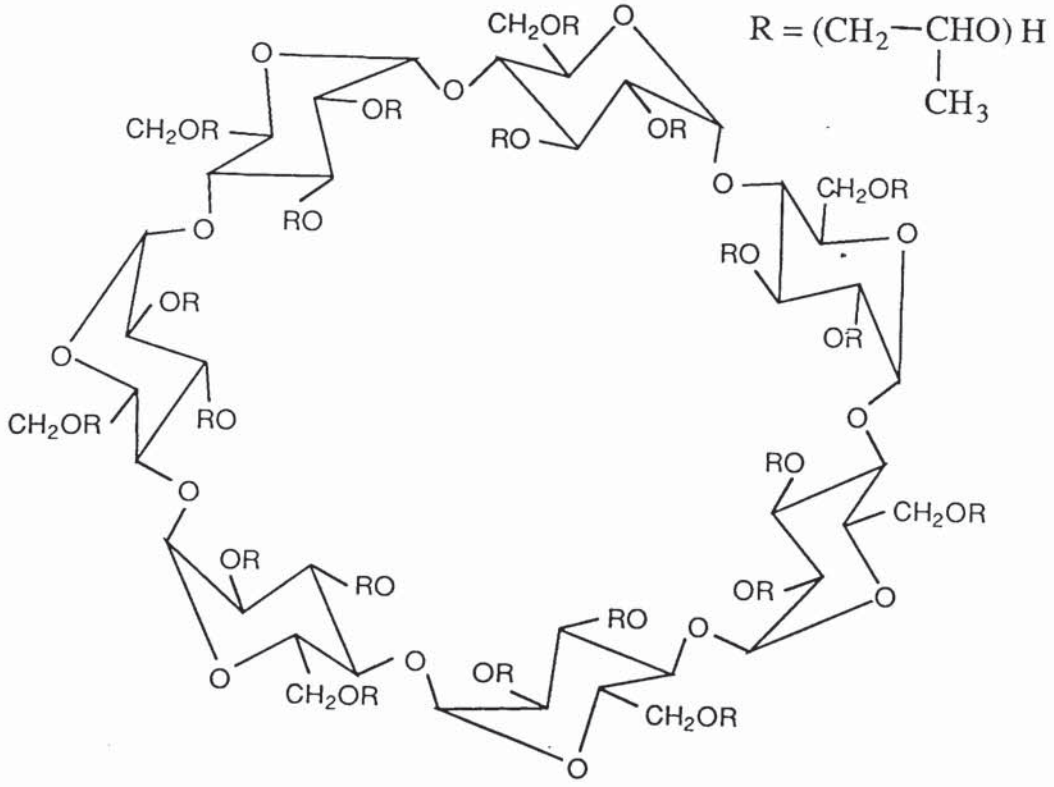

Figure 1.5 Structure of hydroxypropyl-β-cyclodextrin (HP-β-CyD)

Several methods have been reported for the preparation of the HP-β-CyD (Pitha *et. al.*, 1986; Szente and Strattan, 1991). Very simply, the procedure involves reacting propylene oxide with β-CyD with the addition of a base (usually sodium hydroxide) in an aqueous environment under specified conditions of temperature, pressure and reaction time. Since the CyDs themselves are chiral molecules, and the hydroxypropyl substituent also has an asymmetric carbon, the reaction process produces a heterogeneous mixture of thousands of isomers. The randomness of the position of the substituent causes the resulting CyD derivative to be amorphous, which contributes to its enhanced aqueous solubility as compared to the parent CyD. The extent of substitution also effects the amorphous nature of the derivative which is important for the aqueous solubility of the derivative as demonstrated by Rao and co-workers (1990). By careful control of the reaction mixture, these researchers controlled the extent of chemical substitution of the CyD derivative. Using very low concentrations of sodium hydroxide (1.5 %) and optically pure propylene oxide [(S)-propylene oxide], the number of components in the final mixture was limited. For example, the average degree of substitution of preparation 1 was found to be 8.5 by NMR, and consequently was highly water-soluble (> 50 % w/w). In contrast, preparation 2, obtained using less propylene oxide, had a average degree of substitution of 3.4 and a lower aqueous solubility of 2.1 % w/w. Furthermore, X-ray powder diffraction analysis revealed the amorphous nature of preparation 1, whereas sharp signals obtained for preparation 2 indicated its crystallinity. By using less propylene oxide, the number of possible isomeric components and also the amorphousness of preparation 2 was reduced which lead to a reduction in the aqueous solubility of the resultant HP-β-CyD.

HP-β-CyD is characterised by the extent of substitution which can be expressed in several ways. The term, degree of substitution (D.S.), is a measure of the average number of substituted hydroxyls per glucose unit of the CyD ring (Szejtli, 1992). As each CyD glucose monomer has one primary hydroxyl and two secondary hydroxyl groups, the maximum D.S. can only be 3. Molar substitution (M.S.) indicates the number of the substituent hydroxypropyl groups on each glucose unit of the CyD. The M.S. value can be used to calculate the average molecular weight of the CyD derivative, an example of the which is shown in section 2.6.3. The degree of substitution can be determined from mass spectrometry and NMR (Szente and Strattan, 1991). As previously discussed, the extent of substitution is important for the solubility characteristics of the derivative. This parameter will also effect the complex forming ability of the derivative as discussed later in section 1.5.

The aqueous solubility limit of the HP-β-CyDs has not been reported. A concentration of 70% w/w was reached by Häulser and Müller-Goymann (1993). These researchers also reported a concentration-dependent increase in viscosity which was caused by intermolecular hydrogen bonding between individual HP-β-CyD molecules.

In comparing the molecular dimensions of HP-β-CyD to the parent CyD, the interior cavity size is expected to be the same, whereas the other dimensions such as the height of the torus, diameter of the periphery, and effective volume of the cavity will differ due to the freely-rotating nature of the hydroxypropyl substituents (Szente and Strattan, 1991).

1.5 CYCLODEXTRIN INCLUSION COMPLEXES

One of the most important features of CyDs is their ability to form inclusion complexes with a wide variety of molecules. In these complexes, all or part of the guest molecule is encapsulated within the apolar cavity of the CyD host molecule.

CyDs inclusion complexes can exist both in solution and the solid phase. In an aqueous environment, water molecules reside in the CyD cavity and can therefore be considered as guest species. In the presence of hydrophobic species, however, the water molecules in the CyD cavity are preferentially displaced. Further discussion into the mechanism of these interactions are detailed later (section 1.5.5). The structure of the CyD inclusion complex in solution may differ significantly from that in the crystalline state (Szejtli, 1988). In solution, the guest molecule wholly or partly occupies the hydrophobic CyD cavity and the entire complex is surrounded and solvated by water molecules. The molar ratio of host to guest is usually 1:1 in inclusion complexes formed in dilute aqueous solutions. However, depending on the properties of the guest, such as its size and shape, 1:2, 2:1 and 2:2 guest-CyD complexes may also co-exist in solution (Szejtli, 1988). The existence of these will depend on the concentrations of both guest and CyD in the system. For example, in dilute solutions γ-CyD forms a 1:1 complex with Methyl orange, but in more concentrated solutions, a 2:1 and 2:2 guest-CyD complex can exist (Clarkes, Coates and Lincoln, 1983). The geometric considerations of the guest will be discussed later.

In solid-phase crystalline complexes, the guest is enclosed within the cavity of the CyD as well as between CyD molecules in the lattice structure. In contrast to complexes formed in solution, the crystalline complexes seldom have strict stoichiometric composition (Szejtli, 1985). The CyDs and their complexes can be crystallised from water and examined by X-ray crystallography. Depending on the size and molecular characteristics

of the guest, three possible structures may be formed: channel, cage or herring-bone (Saenger, 1980). The crystal structure of the natural CyDs and their inclusion complexes have been reviewed by Saenger (1984).

1.5.1 Complex stability constant, K_S

CyD inclusion complexes in solution are in equilibrium with their free components as shown by equation 1.1.

$$G + CyD \rightleftharpoons G\text{-}CyD \qquad (1.1)$$

where G and CyD are the free guest and CyD components and G-CyD is the complex.

The general definition of complex stability or association constant of this equilibrium process is given by the equation 1.2.

$$K_S = \frac{[G\text{-}CyD]}{[G]\,[CyD]} \quad (M^{-1}) \qquad (1.2)$$

The stability constant K_S of the complex indicates the relative affinity of a particular guest type for the CyD cavity. Phase solubility studies (Higuchi and Connors, 1965) are frequently used for the determination of K_S values and will be further discussed later. Many other methods are used for the determination of stability constants of the complexes which include UV spectroscopy (Lehner, Müller and Seydel, 1994) and NMR spectroscopy (Djedaini *et. al.*, 1990). However, it has been found that when different methods have been used to determine K_S, widely deviating values have been obtained (Szejtli, 1988). For example, the K_S value for the β-CyD complex of phenylalanine determined by ^{13}C-NMR measurements was 1000 M^{-1} (Inoue and Miyata, 1981) in contrast to the value of 20 M^{-1} as determined by freezing-point depression measurements (Suzuki *et. al.*, 1993).

The stability constant of the complex is also dependent on the temperature and pH. With increasing temperature, K_S decreases reflecting dissociation of the complex. A change in pH may cause ionisation of the guest which as a consequence has a lower affinity for the hydrophobic CyD cavity (Menard, Dedhiya and Rhodes, 1988; Catena and Bright, 1989).

The inclusion of a guest within the CyD cavity will depend on its geometric dimensions and its polarity. The extent to which both these requirements are satisfied is reflected in

the magnitude of the K_S value. The higher the K_S value the greater the affinity of the guest for the CyD cavity.

1.5.2 Geometric Capability

The guest molecule must fit entirely or at least partially into the CyD cavity (Saenger, 1980). The molecular dimensions of CyDs differ as they each contain a different number of glucose units as illustrated in figure 1.6. As a consequence of their different internal diameters, CyDs show different degrees of inclusion formation with various sized molecules, hence the respective guest-CyD complexes will have K_S values of diverse magnitudes. One example to illustrate the effect of their different cavity sizes is the inability of α-CyD to form a complex with naphthalene (2 phenyl rings) and the ability of anthracene (3 phenyl rings) to form a complex with γ-CyD but not β-CyD (Szejtli, 1988). Since the height of these guest molecules is the same, the orientation of these guest molecules within the CyD cavity must be equatorial rather than axial (figure 1.7). Table 1.1 lists some important physicochemical properties of the three natural CyDs.

Figure 1.6 Molecular dimensions of cyclodextrins (Szejtli, 1982)

Figure 1.7 Equatorial and axial inclusion of naphthalene (Szejtli, 1988)

Table 1.1 Physicochemical properties of cyclodextrins (Bekers *et. al.*, 1991b; Szejtli, 1988)

Further examples of the effect of the different cavity dimensions are illustrated in table 1.2. The diameter of a phenyl ring including van der Waals radii of proton is 0.68 nm (Inoue and Miyata, 1981). Generally therefore, guest species have a greater affinity for β-CyD as reflected by the larger K_S which is a consequence of the most favourable positioning of the guest within its cavity. However, with steroid hormones as guest species, which are relatively bulky structures, Uekama *et. al.*, (1982) observed an increase in the stability constants of the complexes formed with the natural CyDs in the order $\gamma > \beta > \alpha$, indicating that in this instance, the larger the cavity size the more favourable the fit of the guest molecule. Exceptions to this trend were seen with prednisolone which had a greater affinity for β-CyD (K_S = 3600 M^{-1}) than with γ-CyD (K_S = 3240 M^{-1}). Spironolactone, another a steroidal guest species, also showed a greater interaction with β-CyD (K_S = 24921 M^{-1}) than with γ-CyD (K_S = 11142 M^{-1}); Yusuff and York, 1991. Furthermore, the geometric compatibility of the guest will also influence the stoichiometry of the guest-CyD complexed formed. The stoichiometry of the prednisolone-β-CyD complex was 1:2 (guest-CyD respectively), whereas the respective γ-CyD complex had a stoichiometry of 2:3 (Uekama *et. al.*, 1982).

Table 1.2 Comparison of the interaction of specific guest species with the natural CyDs, α-, β- and γ-CyD on the basis of the respective guest-CyD complex K_S values (M^{-1})

Guest	α-CyD	β-CyD	γ-CyD	Reference
clofibrate	400	1350	110	Uekama *et. al.* (1983)
diazepam	24	220	120	Uekama *et. al.* (1983)
dexamethasone	169	4660	26600	Uekama *et. al.* (1982)
flurbiprofen	20	5100	460	Otagiri *et. al.* (1983)
hydrocortisone	57	1720	2240	Uekama *et. al.* (1982)
phenytoin	110	850	149	Menard *et. al.* (1988)
prednisolone	298	3600	3240	Uekama *et. al.* (1982)
salbutamol	1.1-1.2	66-69	5.1-5.2	Cabral Marques *et. al.* (1990)
spironolactone	564	24921	11142	Yusuff and York (1991)

If the guest molecule is significantly larger than the CyD cavity, complex formation may still be possible if certain groups or side chains of the guest are able to penetrate the cavity (Szejtli, 1982). Examples of such complexes include the anilinonaphthalene-1-sulphonate-β-CyD complex (ANS-β-CyD; Nishijo and Nagai, 1991) and the

indomethacin-β-CyD complex (Djedaini *et. al.*, 1990). Using NMR techniques to elucidate which part of the guest was encapsulated within the CyD cavity, it was found that, in both cases, the drug-CyD complexes were formed by the inclusion of the aromatic rings in the CyD cavity.

As previously discussed, the cavity diameter of CyD derivatives are essentially the same as their parent CyD, however, the solubilising power of the hydrophilic derivatives is usually better due to their enhanced aqueous solubilities. For example, in the presence of an aqueous CyD solution (1.5 % w/v), the solubility of progesterone was enhanced 3.1-fold with β-CyD and 88-fold with HP-β-CyD; the K_S values were 1600 M^{-1} and 1800 M^{-1} for the complexes of β-CyD and HP-β-CyD respectively (Szejtli, 1992). However, Yoshida *et. al.* (1989) found dihydroxypropyl-β-CyD (DHP-β-CyD) to be a weaker solubiliser than β-CyD itself; the K_S for the prednisolone-β-CyD complex was 1600 M^{-1} and 760 M^{-1} for the DHP-β-CyD complex. Due to the presence of the substituent groups, the CyD torus is narrower, hence the guest is sterically hindered from entering the hydrophobic cavity and consequently the complexing ability of the CyD is affected. Similar behaviour was observed by Müller and Brauns (1986) who found the CyD derivatives of lower substitution to be better solublisers than highly substituted derivatives.

As discussed earlier, the extent of substitution controls the amorphous nature of the CyD derivative which is important for its physicochemical characteristics. However, its seems that a comprise has to be reached such that the extent of substitution is sufficient to provide a highly soluble product but not too great as to sterically hinder complexation of the guest.

1.5.3 Polarity

The polarity of the guest molecule is also a consideration in complex formation. In aqueous solutions of CyDs, water molecules can be considered as guest species. However, as a consequence of the hydrophobic nature of the CyD cavity, the presence of the water molecules in the CyD cavity results in polar-apolar interactions which renders them energetically unfavourable guest molecules. The water molecules are readily displaced by appropriate hydrophobic guest species to attain apolar-apolar interactions, resulting in a more stable lower energy state. The greater the hydrophobicity of the guest molecule, the greater the stability of its CyD inclusion complex (Szejtli, 1988). Ikeda and co-workers (1975) studied the interactions between anti-inflammatory fenamate drugs and β-CyD in aqueous solution. These researchers found that compounds with larger partition coefficients showed larger complex stability constants. For example, anthranilic

acid was found to have a partition coefficient (P) of 0.11 and its respective β-CyD complex had a K_S value of 130 M^{-1}. In contrast, the K_S value for the complex of the more hydrophobic flufenamic acid (P = 39) was 1380 M^{-1}. Similar correlations between the K_S values and guest partition coefficients were also observed for the interactions between the benzodiazepenes and CyDs (Uekama *et. al.*, 1983), the phenothiazines and β-CyD (Otagiri, Uekama and Ikeda, 1975) and for the interaction of HP-β-CyD with a series of *p*-hydroxybenzoic acid esters (Lehner, Müller and Seydel, 1993).

Ikeda and co-workers (1975) also found that with bulky fenamate guest molecules, the K_S values for the respective complexes were lower than expected from their partition coefficients, indicating that steric factors as well as the hydrophobic nature of the guest influenced the extent of interactions between guest and host. The involvement of both these factors was reflected in the relative magnitudes of the K_S values for the CyD complexes of the cinnamic acid derivatives (Uekama *et. al.*, 1975); the structure of cinnamic acid is shown in figure 1.8. The partition coefficient of cinnamic acid was found to be 0.058, and, the K_S values for the its interaction with α-CyD was 3460 M^{-1}. Para-substitution of the acid with derivatives of increasing lipophilicity was followed by a greater interaction with α-CyD as reflected in the magnitude of K_S. For example, the interaction between α-CyD and the more lipophilic *p*-methylcinnamic acid (P = 0.246; K_S for complex = 13600 M^{-1}) was greater than that with cinnamic acid. In contrast, with the less lipophilic *p*-hydroxycinnamic as the guest species (P = 0.023), the relative interactions with α-CyD was reduced as indicated by the lower K_S value of 1990 M^{-1}. This trend was not observed with meta-substitution of cinnamic acid with derivatives of increasing lipophilicity. For example, although the partition coefficient of *m*-bromocinnamic acid (P = 0.116) was found to be greater than that of cinnamic acid (P = 0.058), its relative interaction with α-CyD (1390 M^{-1}) was less. These researchers proposed that complexation occurred by inclusion of the phenyl moiety of cinnamic acid within the CyD cavity. Thus, the effect of various substitutions can be explained as follows. In the para-position, the relative interactions between the guest and α-CyD are influenced by the hydrophobic nature of the guest. In the meta-position however, the presence of bulky substituents cause steric hindrance, thus, in this instance, the relative interactions between guest and host are primarily influenced by the size of the substituent. Otagiri *et. al.* (1976) observed similar behaviour for the interaction of barbiturates with β-CyD where both the lipophilic nature of the guest and steric factors influenced the interactions between guest and host. No obvious correlation has been found between the physical and chemical properties of guest molecules and the K_S values for the respective drug-CyD inclusion complexes (Szejtli, 1984)

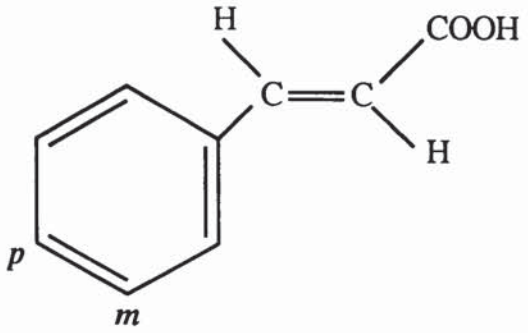

Figure 1.8 Structure of cinnamic acid (*p* indicates position of para-substitution in the phenyl ring and *m* indicates position of meta-substitution)

1.5.4 Preparation of solid complexes

No universal method exists for the preparation of CyD inclusion complexes. The reaction conditions employed are 'tailored' to the specific properties of the individual guest to be complexed. Based on the literature published on the preparation of CyD complexes, the various methods can be divided into 3 groups: liquid phase, semi-solid phase and solid phase. The practical considerations of the different methods together with their advantages and disadvantages has been reviewed (Darrouzet, 1992). A brief summary of the various methods are illustrated here using examples from the literature.

One of the most common procedures employed in the preparation of CyD inclusion complexes involves stirring or shaking an aqueous solution of CyD together with the guest or its solution (Szejtli, 1988). Depending on the thermosensitivity of the guest, heat may be applied to aid solubilisation. Furthermore, the addition of ammonium hydroxide has been successfully used to aid the solubility of weakly acidic guests (Kurozumi, Nambu and Nagai, 1975). When both the guest and CyD are completely solubilised, the water is removed by freeze-drying, spray-drying or any other suitable method. For guest-CyD systems which show the formation of soluble complexes during phase solubility studies (Type *A* solubility isotherms; Higuchi and Connors, 1965), this method is suitable for the preparation of their solid phase complexes. Phase solubility studies are discussed further in section 1.5.6. An example of a solid complex prepared by the lyophilisation method is the amphotericin-B-γ-CyD (Rajagopalan, Chen and Chow, 1986).

For guest-CyD systems which show the formation of insoluble complexes during phase solubility studies (Type B_S solubility isotherms; Higuchi and Connors, 1965), their solid complexes are precipitated from aqueous solutions containing both components. The amounts of guest and CyD to be used are estimated from solubility isotherms, added to

water and shaken until equilibrium is established. When the solution is saturated with respect to the inclusion compound, any further increases in the concentration of the complex leads to its precipitation as a microcrystalline solid which is removed from the reaction mixture by filtration and dried. This method of preparation has been used for the spironolactone-β-CyD complex (Yusuff and York, 1991) and has the advantages of being simple and also no organic solvent is needed. However, this method is often time consuming and only a low inclusion compound yield is obtained.

With insoluble guests, the co-precipitation method (Jones *et. al.*, 1984) is used. Very simply, this method involves dissolving the guest in a water-miscible solvent, such as isopropranol, prior to mixing with the CyD solution. The solvent is removed by evaporation which leads to precipitation of the complex. It is necessary to wash the recovered product with both a solvent and water to remove any residual guest and CyD respectively. The co-precipitation method enables isolation of a crystalline complex of high purity. This method was used by Amdidouche *et. al.* (1989), for the preparation of the retinoic acid-β-CyD inclusion complex.

Inclusion complexes can also be prepared in a semi-solid state such as in the kneading method and the slurry method (Darrouzet, 1992). In the former procedure, only sufficient water to form a CyD paste is used to which the solid guest is added. This combination is then mixed for long enough to allow all the CyD and guest to dissolve (Paginton, 1987). An example of a guest species complexed by this method is terfenadine (Sanghavi *et. al.*, 1995). The slurry method involves mixing the CyD with water in a ratio of 1:2 respectively and mixing at high speed to form a slurry to which the guest is added. A thick suspension is obtained which is dried and ground to obtain the inclusion complex in a powdered form.

Methods for preparing CyD inclusion complexes in the solid state involving neither water or any solvent have also been reported. Torecelli and co-workers (1991) prepared a steroidal drug (6-methylenandrosta-1,4-diene-3,17-dione)-β-CyD complex by grinding together equimolar amounts of both components. Preparation of complexes by the melting method (Szejtli, 1988) involves the use of a large excess of the guest, thus after complexation any residual guest is removed by vacuum sublimation. This method is therefore restricted to sublimable guests such as menthol. The sealed heating method has been used by Nakai *et. al.* (1987) for the preparation of complexes of benzoic acid with α-CyD and β-CyD. This method is limited to guest which have melting points below the degradation temperatures of CyDs, however, it is not really applicable on an industrial scale.

1.5.5 Cyclodextrin complexation in solution

The driving force of complexation is not fully understood, however it is thought that both enthalpy and entropy changes play a vital role in the complexation process (Szejtli, 1988). In an aqueous environment, the CyD cavity is occupied by water molecules. Since water molecules are polar, their interaction with the relatively apolar cavity is energetically unfavourable. Hence, the displacement of the water molecules by the more hydrophobic guest molecule is a favourable process.

The hydrogen-bonding capacity of the water molecules in the CyD cavity is reduced as compared to the bulk of the solvent. The molecules are therefore regarded as being of enhanced energy or enthalpy (Szejtli, 1988). The energy of the system will decrease if solvent/solvent, *i.e.* polar-polar interactions are increased. The substitution of cavity water by the guest not only reduces solvent interaction with the CyD but also reduces solvent interaction between the solvent and guest, *i.e.* apolar-polar interactions are reduced which will also lower the energy of the system.

The mechanism of the formation of inclusion complexes has been published in several papers (Cramer, Saenger and Spatz, 1967; Hersey and Robinson, 1984; Tabushi *et. al.*, 1978). Complex formation can be thought to occur in several steps:

1. The guest approaches the CyD host molecule.
2. Breakdown of the water structure within the CyD cavity with a consequent removal of water molecules from the ring.
3. Breakdown of water structure around the part of the guest molecule which is going to be included in the CyD and transport of some molecules into the solution.
4. Interactions of the substituents of the guest molecule with groups on the rim or on the inside of the CyD.
5. Possible formation of hydrogen bonds between guest and CyD.
6. Reconstruction of the water structure around the exposed parts of the guest after the inclusion process.

Steric factors are involved in steps 1, 4 and 5, the extent of which depends on the geometry of the guest. Steps 2, 3 and 6 are related to the water structure around the components involved in the reaction. No covalent bonding is involved in complexation; however, there has been much controversy surrounding the nature of the binding forces involved in inclusion process. It has been suggested that various intermolecular forces contribute to the stabilisation of these inclusion complexes (Szejtli 1988):

1. Van der Waals interactions between guest and host (Hall and Ache, 1979)
2. Hydrogen bonding between the guest and host (Cohen and Lach, 1963)
3. Hydrophobic bonding (also known as solvophobic interaction; Jencks, 1969).
4. Release of high-energy water molecules in complex formation (Griffiths and Bender, 1973)
5. Release of strain in the macromolecular ring of the CyD (change from the high-energy conformation of the water-CyD complex to the lower energy conformation of the guest-CyD complex; Szejtli, 1982). The transition of the CyD ring from strained to relaxed state on penetration of the guest is significant only in the case of α-CyD since it is only the structure of α-CyD hydrate which is distorted whereas the β- and γ-CyD structures are not (Szejtli, 1988).

The extent to which the above factors are involved depends on the nature of the guest molecule involved. The role of hydrogen bonding in CyD complexation is not universal, *i.e.* complexation is still possible with guest molecules which are unable to form hydrogen bonds such as benzene (Szejtli, 1988). The magnitude of the enthalpy change (ΔH) for the formation of hydrogen bonds is ~ 40 kJ $mole^{-1}$, which are relatively weak compared to the strength of covalent bonds, 400 kJ $mole^{-1}$. The hydrogen bond forms whenever a polar bond containing the hydrogen atom interacts with an electronegative atom such as oxygen. A schematic diagram of hydrogen bonding is illustrated in figure 1.9a.

Van der Waals forces are even weaker having an energy of ~ 4 kJ $mole^{-1}$. Four types of interactions contribute to van der Waals forces which include dipole-dipole, ion-induced dipole, dipole-induced dipole and London dispersion force. Dipole-dipole interactions, illustrated in figure 1.9bi, occur between polar molecules or molecules that possess permanent dipoles. Ion-induced dipole and dipole-induced dipole interactions occur between a molecule with a permanent dipole and a molecule without one as shown in figure 1.9bii. In the presence of the molecule which has a dipole, the other molecule is polarised which leads to a redistribution of the charge density such that an attractive interaction occurs between the two species. The London dispersion interactions arise due to the electron cloud of one molecule have a mutual attraction for the nucleus of another molecule and *vice versa* (figure 1.9iii). Parallel to the attractive forces, the electron clouds of both molecules repel one another as do the nuclei of both molecules.

Water plays a crucial role in complex formation since hydration of the CyD complex is energetically favoured when compared to hydration of the individual component. This phenomenon is known as hydrophobic interactions (figure 1.9c) and are primarily not

due to the mutual attraction between the guest and CyD, but to the intrinsic cohesion of the water (Jencks, 1969).

1.5.6 Investigation and characterisation of cyclodextrin complexes

CyD complexes are formed in both solution and solid phases. Various methods can be employed to prove that molecular entrapment of the guest has taken place. Infra-red (IR) spectroscopy, X-ray powder diffraction and thermoanalytical methods are often used to investigate the solid phase CyD complex as further discussed in sections 1.5.6.1 to 1.5.6.3. In each of these techniques, the test procedures are applied to the guest and CyD alone, their proposed inclusion complex and a physical mixture of both complex components. Not all methods are applicable with all guest types.

CyD inclusion complexation in solution can also be studied by various physicochemical methods. One method which is frequently used is phase solubility analysis (Higuchi and Connors, 1965) which is further discussed in section 1.5.6.4. Other methods include ultraviolet absorption, circular dichroism and nuclear magnetic resonance spectroscopies. Ikeda and co-workers (1975) used all three techniques to confirm the inclusion of non-steroidal anti-inflammatory fenamate drugs within the cavity of β-CyD in aqueous solution. UV absorption and NMR spectroscopies are discussed further in sections 3.6.6 and 1.5.6.5 respectively.

CD spectroscopy has also been used by Amdidouche *et. al.* (1989) to confirm the existence of the retinoic acid-β-CyD inclusion complex in aqueous solution. CyDs are chiral, non-absorbing molecules. The inclusion of achiral absorbing guests within the CyD cavity induces new CD bands in the region of the absorption bands of the optically inactive guest. These induced effects, known as Cotton effects, are only observed when the chromophore moiety of the guest is included in the cavity (Takeo and Kuge, 1972). The inclusion of chiral guest molecules within the CyD cavity may also induce changes in the CD spectra (Han and Purdie, 1984). Other investigative procedures include the use of ultrafiltration cells which have been used by Jones and Parr (1987) to assess the interactions between the acetoluides and β-CyD, and also by Yusuff and York (1991) for the study of the spironolactone-cyclodextrin system.

Another important characteristic of the drug-CyD complex which requires assessment is its dissolution. Dissolution studies aim to show both the improvement in the solubility of the guest due to its complexation, and also the enhanced rate of passage into solution (Szente, 1989).

a) hydrogen bonding

(broken line indicates H-bond)

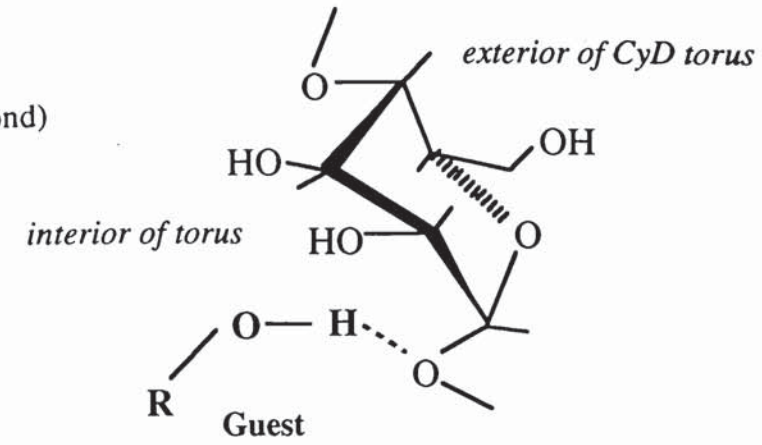

b) van der Waals forces:

i) dipole-dipole interactions

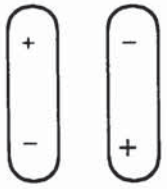

ii) dipole-induced dipole interactions

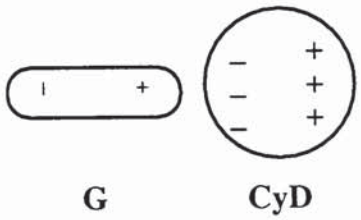

iii) London dispersion forces

(attractive force —)

(repulsive force ---)

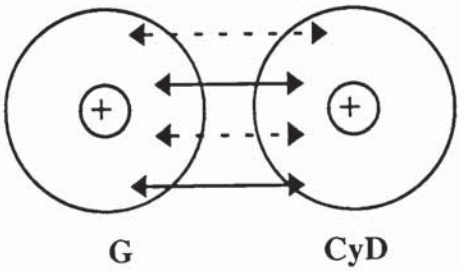

c) hydrophobic bonding

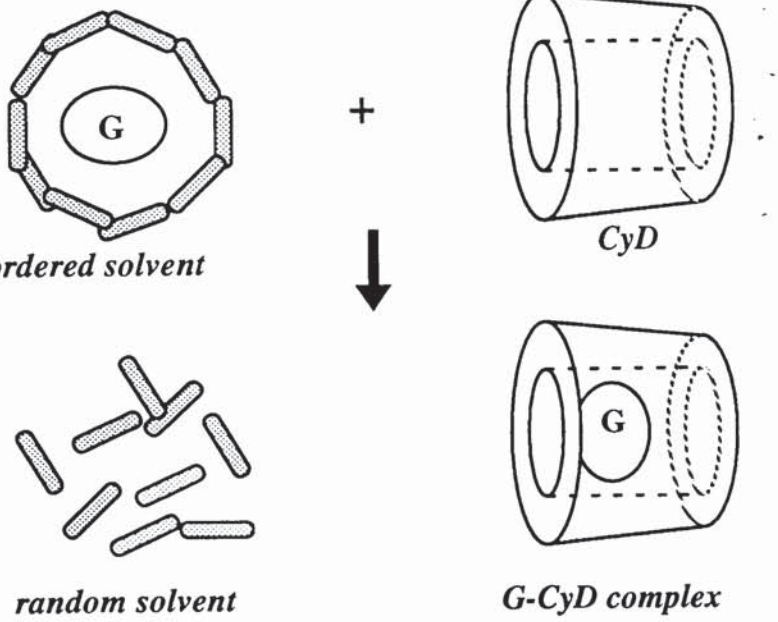

Figure 1.9 Schematic diagram illustrating the bonding mechanisms involved in CyD complexation

1.5.6.1 Differential Scanning Calorimetry (DSC)

DSC belongs to the group of thermoanalytical methods which can be used to confirm the presence of a true inclusion complex. This group of analytical procedures can differentiate between inclusion complexes and adsorbates, and can also characterise the special thermal effects due to molecular entrapment. Only guest species having melting or boiling points below the thermal degradation range of CyDs (250-300°C) can successfully be studied by thermal methods (Szente, 1989). DSC has successfully been applied in several studies to confirm complexation (Otero-Espinar *et. al.*, 1992; Cabral Marques, Hadgraft and Kellaway, 1990). In this method, the difference in energy input into a substance and a reference material is measured as a function of temperature as the specimens are subjected to a controlled temperature programme. Heat may be evolved (exothermic reaction) or absorbed (endothermic reaction) by the sample.

1.5.6.2 Infra-red spectroscopy

The ability of infra-red (IR) spectroscopy to confirm complex formation is limited. CyDs comprise the majority of the complex, thus IR spectra of the complex show characteristic absorption bands for the CyD which are hardly affected by complex formation. The bands representing the guest molecule may be shifted or their intensities altered, but since the guest species constitutes only a small percentage of the total complex mass, any alterations are obscured by the CyD (Szente, 1989). IR spectroscopy has been successfully used in the investigation of CyD complexes involving carbonyl-bearing guest species. Carbonyls show characteristic stretching in the region 1680-1700 cm^{-1} which are significantly shifted by CyD complexation (Nakai *et. al.*, 1978).

1.5.6.3 X-ray powder diffraction

X-ray powder diffraction has been employed by many researchers (Chow and Karara, 1986; Erden and Celbi, 1988; Otagiri *et. al.*, 1983) to detect inclusion complex formation in the solid state. This technique is of particular use with liquid guest molecules since liquids do not produce diffraction patterns. When the X-ray pattern of the assumed 'liquid drug-CyD complex' differs from that of the uncomplexed CyD, complex formation is confirmed. With solid guest components, a comparison has to be made between the diffractogram of the assumed complex and that of a mechanical mixture of the guest and CyD. Both the CyD and guest substance should be treated under identical conditions as the assumed complex prior to the preparation of the mechanical mixture. Comparison of the diffractograms is only possible if conditions are kept identical since CyD inclusion complex preparation processes such as freeze-drying and grinding may change the crystallinity of the pure substance and this may consequently lead to different diffraction patterns (Szejtli, 1988).

1.5.6.4 Phase solubility studies

Poorly water-soluble drugs show an increase in aqueous solubility in the presence of CyDs due to the formation of a water-soluble complex between the drug and the dissolved CyD. This interaction may be studied by phase solubility analysis (Higuchi and Connors, 1965), which determines the relationship between the total concentration of dissolved drug and the concentration of CyD added. This technique also reveals the stoichiometry of complex formation and also the complex stability constant (K_S) as defined previously in section 1.5.1.

The general procedure for phase solubility analysis involves the addition of a constant amount of drug (in excess of its normal solubility) to constant volumes of solvent, each containing increasing amounts of the CyD. Figure 1.10 illustrates the different types of phase solubility diagrams which are possible depending on the properties of the complex formed. Generally, the diagrams can be categorised into 2 main types; *Type A* and *Type B*. When the solubility of a guest increases linearly with an increase in CyD concentration, a solubility isotherm of the A_L type is observed (Higuchi and Connors, 1965). If this line deviates upwards, the solubility of the guest increases faster than the CyD concentration and an A_P diagram is seen. Negative curvature in the line is illustrated by A_N type isotherms. Solubility enhancements seen in A type systems are due to one or more molecular interactions between the host and guest components to form soluble complexes.

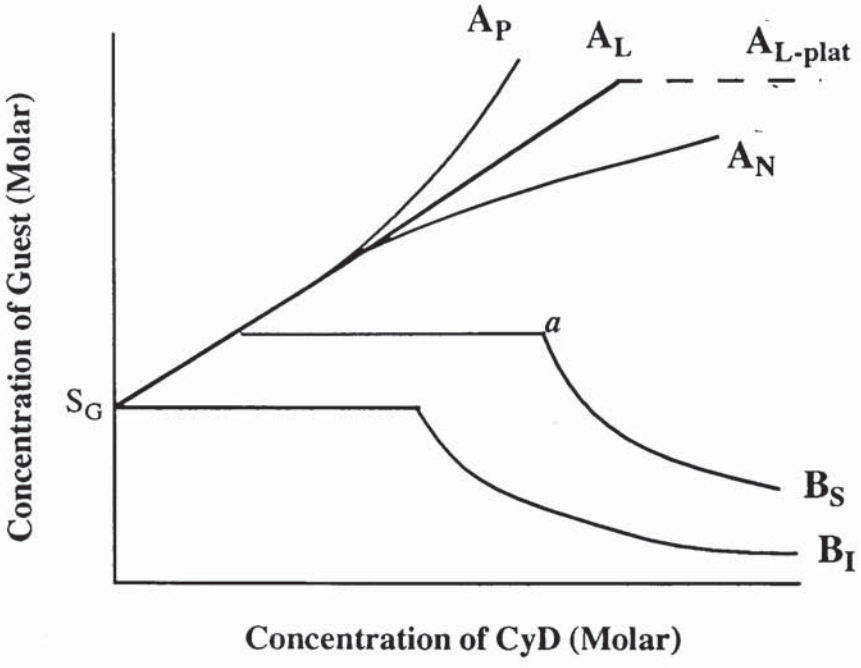

Figure 1.10 Phase solubility diagrams

If the general formula of the complex is considered to be G_xCyD_y, A_L type diagrams are observed when the CyD is of the first order in the complexes formed, for example, CyDG, $CyDG_2$, and $CyDG_3$. In the case of A_P diagrams, the order of CyD in the complexes present in these systems is greater than 1, for example, CyD_2G and CyD_3G. A_N type isotherms may occur due to several reasons (Higuchi and Connors, 1965). The presence of a large host concentration may alter the nature of the solvent which leads to a change in the K_S value. Another possible reason for negative deviation could be due to self-association of the host at higher concentrations which may affect the degree of complexation. Backensfield and co-workers (1991) found A_N type solubility diagrams for the interaction of non-steroidal anti-inflammatory drugs with hydroxypropyl CyD derivatives. The negative deviation in these systems was due to a change in pH as the solubility of drug was increased by CyD complexation.

The second type of solubility isotherms which may arise are of the B type which are observed when insoluble complexes are formed. Initially, these systems show a linear increase in guest solubility similar to A type systems. However, when all the solid guest is dissolved (point *a* on figure 1.10), the addition of further CyD results in the formation of more complex from drug in solution which is consequently precipitated. The complexation process in B type systems can be illustrated using the following scheme:

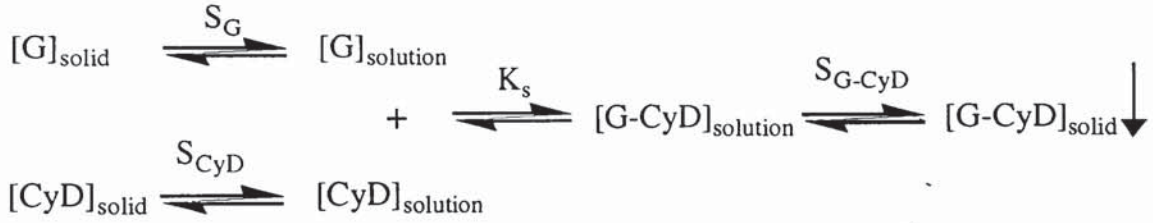

Scheme 1: Equilibration process of Type B solubility systems

where K_S = the complex stability constant
S_G = the solubility of the guest
S_{CyD} = the solubility of the CyD
$S_{G\text{-}CyD}$ = the solubility of the complex

When there is excess solid guest present in the system, the total guest concentration in solution will remain constant which corresponds to the plateau region in the solubility diagram. As more CyD is added, the equilibrium process will favour the formation of the complex. Consequently therefore, when all the guest is complexed, the guest concentration will decline due to the continuous precipitation of the complex. The

diagram observed with this situation is of the type B_S. Interaction of β-CyD with steroids resulted in B_S type solubility isotherms with consequent precipitation of the complex at higher CyD concentrations (Uekama *et. al.*, 1982).

The solubility isotherm of the B_I type is produced from a similar system as described above, the main difference being that the complex formed is so insoluble that an initial rise in guest concentration is not detected.

The plateau region of the B type diagrams is used to determine the stoichiometry of the complexes formed using the following equation (Szejtli, 1988):

$$\text{molar ratio} = \frac{\text{total guest in the system - dissolved guest at beginning of plateau}}{\text{CyD concentration difference in plateau region}} \qquad (1.3)$$

Type A diagrams may also exhibit a plateau level of guest which is unaltered by additional quantities of CyD (shown as $A_{L\text{-plat}}$ in figure 1.10) This situation may result as a consequence of complete solubilisation of the guest and therefore further increase in CyD will not further enhance the guest concentration. Another situation of this type may arise when further increases in CyD concentration is limited by its low solubility, thus saturation of the complex results with respect to the host. If, in this system, the solubility of the CyD has also been increased due to complex formation, the plateau region can be used to determine the stoichiometric ratio of the complex thus formed.

As previously discussed in section 1.5.1, CyD inclusion complexes in solution are in equilibrium with their free components, and the general definition of the complex stability or association constant of this equilibrium process is given by equation 1.2.

A plot of guest concentration against host concentration for the formation of a soluble complex should yield a straight line for Type A_L diagrams. Assuming that the G-CyD complex is formed in a 1:1 stoichiometric ratio, Higuchi and Connors (1965) have derived the following expression from which K_S can be calculated using the slope of the solubility isotherm. A detailed account of the derivation is shown in Appendix 3.

$$K_S = \frac{\text{slope}}{S_0\,(1 - \text{slope})} \qquad \text{(Equation A3.13 in Appendix 3)}$$

where S_0 represents the equilibrium solubility of the guest in the absence of CyD, *i.e.* the intercept of the solubility isotherm on the y-axis.

Equation A3.13 can also be used to calculate the K_S value from the slope of the initial rising portion of Type B_S diagrams. The stability constant obtained by this method is only an apparent constant since it has been assumed that the complex being investigated is monomeric and the stoichiometry is 1:1 (Szejtli, 1988). As discussed previously, the complex stability constant is also dependent on the temperature and pH. Other factors, such as association and the different extent of hydration of the equilibration components, may also modify the value of the stability constant, but since these effects are usually constant, reproducible stability constants can be obtained by phase solubility studies (Szejtli, 1988).

By performing phase solubility studies at various temperatures, the effect of temperature on the complex stability constant can be observed, and furthermore the thermodynamic parameters of the complexation process can be determined from the van't Hoff plot (section 2.5.5; Gelb *et. al.*, 1981). From the magnitude of these parameters, the type of bonding mechanisms involved in complex formation can be predicted. The thermodynamic changes of the inclusion process can also be found by microcalorimetric studies as used by Tong *et. al.* (1991) for the complexation of amine drugs to CyDs. This latter method however requires the use of a highly sensitive calorimeter.

1.5.6.5 Nuclear Magnetic Resonance Spectroscopy

^{1}H-NMR can be used to determine the mode of interaction between CyDs and possible guest species. Various studies of this kind have been undertaken (Demarco and Thakkar, 1970; Thakkar and Demarco,1971) which have showed that large guest molecules can form inclusion complexes if they consist of groups of a suitable size and shape which are able to fit into the β-CyD cavity. This method is based upon the fact that the CyD glucose units adopt a C-1 chair conformation as illustrated later in figure 2.34. As a result of this configuration, the C3-H and C5-H protons lining the cavity will undergo an appreciable shielding effect upon penetration of a guest molecule. The protons located on the exterior of the CyD torus, C2-H, C4-H, C6-H, are relatively unaffected. Therefore complexation with an apolar guest results in an upfield shift (lower δ value) of the C3-H and C5-H proton signals due to the magnetic anisotropy effects created by the included guest (Thakkar and Demarco, 1971), whereas downfield shifts are observed for guest protons. However, due to the relatively low guest to host ratio in terms of weight per weight, chemical shift changes in guest protons may not be detected.

Further conclusive information regarding the geometry of the guest-CyD complexed can be obtained by NMR experiments involving the nuclear overhauser effect (NOE). Using

this method Fronza *et. al.* (1992) proposed that both aromatic rings of piroxicam are alternatively included within the β-CyD cavity.

^{13}C-NMR spectroscopy can also be employed to detect shifts in the carbon atoms of the complexed guest. On the basis of such spectra, the orientation of the guest molecule within the CyD cavity may be deduced. The more intensive the interaction between the guest molecule and the wall of the cavity, the higher the shifts of the guest carbon atoms. For example, if the change in chemical shift of one guest carbon atom is zero, it can be concluded that this atom "protrudes" from the CyD cavity and is thus unaffected by the complexation process (Szejtli, 1988).

NMR spectroscopy has been used for the determination of the complex stability constant and also to obtain information concerning the stoichiometry of the complex. Djedäini *et. al.* (1990) used ^{1}H-NMR for the determination of both the K_S value and the stoichiometry of the complexed formed between indomethacin and β-CyD. Inclusion complexation of doxorubicin and daunorubicin with γ-CyD was also studied by ^{1}H-NMR (Bekers *et. al.*, 1991a) in a similar manner.

NMR has become a valuable tool in the study of CyD inclusion complexes. However, this method is limited by the low solubility of the guest and complexes in D_2O, which therefore requires the use of high frequency instrumentation for increased sensitivity. Sensitivity is important since only subtle changes in proton signals occur. ^{13}C-NMR spectroscopy requires higher concentrations than proton NMR which also presents technical difficulties.

1.5.6.6 Dissolution studies

The wettability and dissolution rates of CyD complexes are usually improved as compared to the free guest substance (Szejtli, 1985). The hydrophilic exterior of the CyD torus renders the complex more soluble than the hydrophobic drug itself, thereby improving its wetting properties. Certain processes employed in the preparation of inclusion complexes, such as freeze-drying and grinding, reduce the crystallinity of the product thus formed (Bekers *et. al.*, 1991b). Amorphous substances dissolve quicker than their respective crystalline states (Pitha and Pitha, 1985).

Dissolution rates are important for oral administration. The dissolution-absorption process of an orally administered drug can be illustrated as follows (Szejtli, 1988):

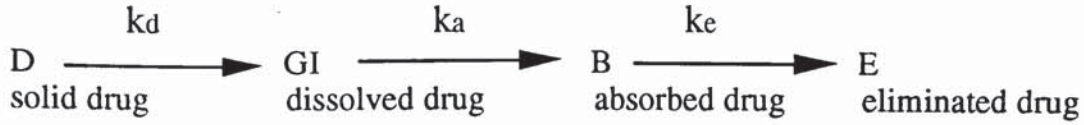

Scheme 2: Dissolution-absorption process

where D = drug in the orally administered dosage form
GI = concentration of dissolved drug in gastro-intestinal content
B = concentration of drug in blood
k_d = rate constant of dissolution
k_a = rate constant of absorption
k_e = rate constant of elimination

When the drug is very soluble, $k_d >> k_a$, it is the absorption rate which is the limiting step in the above process. However, if the drug is poorly soluble, its dissolution is the rate-limiting step in the absorption process. It is only in this latter situation that CyD inclusion complexation would be advantageous to enhance absorption. By presenting the drug as a soluble CyD inclusion complex, its dissolution rate would increase compared to the free drug alone. Following dissolution, the complex rapidly dissociates, achieving high free drug concentrations in the gastrointestinal fluid available for absorption; this consequently results in a more rapid increase in blood levels. In this present study, local delivery of the antibacterial agents is required to treat bacterial infections such as *H. pylori* in the GI tract. Therefore, the particular agent would preferentially diffuse from its high concentration in the GI fluid to the site of *H. pylori,* where a relatively low concentration of antibacterial agent would exist.

As the complex dissolves in the gastric medium, an equilibrium system governs the subsequent dissolution and dissociation of the complex as illustrated in figure 1.11 (Szejtli, 1988). The extent of dissociation will depend on the stability constant (K_S) of the complex and also the solution conditions. Theoretically, complexes of low K_S values dissociate rapidly to give high blood levels which are attained in a short time. High K_S values will shift the equilibrium in favour of complexation, therefore the concentration of free absorbable drug in the gastrointestinal fluid will be lower. Under these circumstances, the blood level peak will be seen later and the height of the peak will be reduced. In all cases, however, an enhanced biological response compared to the free drug can be expected (Szejtli, 1988).

Figure 1.11 Schematic representation of the dissolution-dissociation-absorption process of a guest-cyclodextrin (G-CyD) complex (Szejtli, 1988)

In certain cases, as illustrated by the flurbiprofen-γ-CyD inclusion complex (Otagiri *et. al.*, 1983) and the diazepam-γ-CyD complex (Uekama *et. al.*, 1983), the complexes dissolve rapidly resulting in high initial drug concentrations which exceed the equilibrium solubility of the guest alone (Figure 1.12). This supersaturation state is metastable following which subsequent precipitation of the complex components occurs, with the concentration of the drug declining to an equilibrium level. However, due to the presence of CyD in the solution, the equilibrium solubility will be higher for the complexed drug than the free drug alone.

Supersaturated systems can be considered to be metastable since eventual precipitation of the solute occurs. However, supersaturation itself will not cause crystallisation to occur. Crystallisation in addition to supersaturation requires the formation of nuclei of critical size and then growth around the nuclei. The formation of a critical nucleus occurs by random collision. Supersaturation is therefore a measure of the driving force to both nucleation and growth, and the nature and rate of these processes determine the morphological characteristics of the precipitate (Walton, 1969). At low degrees of supersaturation, small crystals may be expected to grow with a shape which corresponds to the minimum interfacial energy. At higher degrees of supersaturation, larger particular agglomerates may be obtained. Furthermore, small particles are more soluble than larger particles. Thus, two particles of different size cannot be in equilibrium with the same solution. In a situation where the solution is close to saturation, the smaller particles

dissolve, and the large particles get larger. This process of particle growth is known as Oswald ripening.

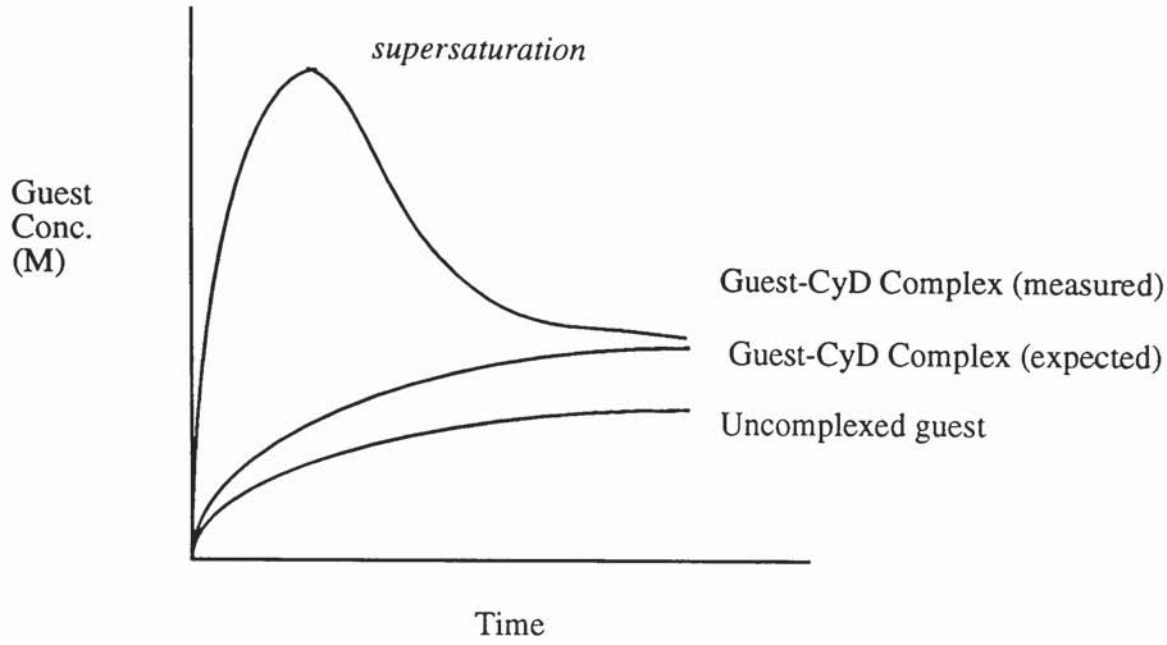

Figure 1.12 Dissolution profile of a Guest-CyD complex, illustrating the formation of a metastable supersaturated solution.

Supersaturated systems have been extensively studied in the field of transdermal delivery to maximise the rate of transdermal penetration. Emla® cream (lignocaine 2.5 %, prilocaine 2.5 %) is an example of a marketed product which exploits the supersaturation phenomena to provide rapid onset of surface anaesthesia. Kondo and Sugimoto (1987) prepared supersaturated solutions of nifedipine in volatile/non-volatile solvent systems. After application of the solution, the volatile solvent was evaporated thus concentrating the drug in the remaining vehicle; penetration from this supersaturated system was enhanced. The extent of penetration eventually decreased due to the precipitation of drug. However, when a polymer additive was added to the system, precipitation of nifedipine was retarded. Similar results have been reported by Davis and Hadgraft (1991) for the penetration of hydrocortisone acetate from co-solvent systems with the presence of hydroxypropyl methyl cellulose as an anti-nucleant polymer. Polymers are thought to inhibit crystal growth by binding to, and thus blocking, growth sites on the crystal (Sekikawa, Nakano and Arita, 1978). Polymers can also stabilise the supersaturated phenomenon observed with drug-CyD complexes. In the presence of hydroxypropylcellulose and polyvinylpyrrolidine, the supersaturated state of the

diazepam-γ-CyD was maintained for longer (Uekama *et. al.*, 1984). These researchers proposed that in the presence of these polymers, crystallisation of the drug was inhibited.

Dissolution of drug-CyD complexes can be assessed by 2 methods: the dispersed powder method and the rotating disk method. The former method involves dissolution testing of the complex in a powder form. The rotating disk method has been used by many researchers (Erden and Çelebi, 1988; Uekama *et. al.*, 1979) to assess the release of drug from a constant surface area. Dissolution of the uncomplexed drug should also be studied under identical conditions such as temperature, agitation and particle size, so that a fair comparison can be made.

1.5.7 Application of cyclodextrin inclusion complexes

The number of publications concerning the pharmaceutical application of CyDs is rising steadily. Research into new drugs can be very costly. However, research in reformulation of old drugs can prove cost-effective and may result in an improvement in the existing drug properties. Inclusion of a guest species within the hydrophobic CyD cavity results in an alteration of its physical and chemical properties. Thus due to their complexing abilities, CyDs present themselves as a valuable tool in drug delivery systems. The modifications brought about by inclusion are usually advantageous, examples of which are shown below (Szejtli, 1988 and Jones *et. al.*, 1984):

a) in the formulation of drugs:

- on complexation with CyDs, liquid compounds may be converted into solid products. For example, by the formation of powder CyD inclusion complexes of clofibrate the problems of storage and handling of this viscous oil are solved, following which development of a solid dosage form is thus possible (Uekama *et. al.*, 1983).

- incompatible compounds can be mixed when one or more reacting components are complexed. For example, this approach may be adopted during the manufacture of multivitamin products where the presence of incompatible compounds can lead to chemical instability (Frömming, 1981).

- masking of unpleasant taste or odour of a compound, *e.g.* using human subjects, Uekama *et. al.* (1983) found that the bitter taste of clofibrate was also improved by complexation. Another example is the complexation of garlic which leads to a reduction in its odour. The garlic-β-CyD product has been approved for marketing in both Germany and Hungary (Szejtli, 1991).

- reduction of side effects by complexation. For example, *in vivo* studies performed by Lin *et. al.* (1994) found that by complexation of indomethacin with both β-CyD and HP-β-CyD, gastrointestinal irritation of indomethacin was reduced.

b) improvement in the physical and chemical stability:

- compounds which would otherwise be sensitive to temperature, hydrolysis, oxidation, photodegradation *etc.* are stabilised by CyD complexation. For example, by complexation of aspartame its rate of hydrolysis in aqueous solution was reduced (Brewster *et. al.*, 1991); in the presence of HP-β-CyD, the half-life of aspartame increased from 10.7 to 13.3 minutes.

c) bioavailability of poorly soluble drugs can be improved:

- the solubility and dissolution rate of poorly soluble substances can be increased. As a consequence, the absorption of the drug is increased and hence the bioavailability. By complexation with β-CyD, the solubility of spironolactone was increased approximately 8-fold and the dissolution characteristics were also improved (Yusuff and York, 1991). Furthermore, the bioavailability of the spironolactone-β-CyD complex, compared to spironolactone powder, was 233 % (Yusuff *et. al.*, 1991)

d) as tablet excipients

- CyDs can be used as carriers and also diluents in tablet formulations of very low drug content. By tabletting of the microcrystalline complexes, the dose uniformity of a small amount of drug may be improved. The use of small amounts of highly swelling CyD polymers enables rapid disintegration of the tablet on contact with the water (Fenyvesi *et. al.*, 1984); the addition of 2.5 % cyclodextrin polymer to microcrystalline cellulose caused the disintegration time of the tablets to decrease from 22.5 to 1.7 minutes.

e) sustained-release:

- the ethylated CyD derivatives of poor water solubility serve as suitable sustained release carriers. The release rate of diltiazem from compressed tablets was significantly retarded by complexation with ethylated β-CyD (Horiuchi *et. al.*, 1990). Following oral administration of tablets containing either diltiazem alone or the diethyl-β-CyD complex to dogs, the time (t_{max}) required to reach the maximum plasma concentration (C_{max}) was prolonged with the complex; t_{max} values were 1 and 2 hours for diltiazem alone and the complex respectively.

Furthermore, C_{max} values of diltiazem and the complex respectively were ~ 69 ng/ml and ~ 24 ng/ml, indicating the sustained release effect of complexation.

f) use in separation

- As a consequence of the chiral nature of CyDs due to the glucose monomer units, they can be used for the separation of positional isomers and chiral molecules through the formation of inclusion complexes. CyDs are used extensively in HPLC for this purpose and are available as chemically-bonded silica stationary phases or may be added to mobile phases. The addition of β-CyD to the mobile phase has been shown to resolve pseudoephedrine into its enantiomers (Mularz, Cline-Love and Petersheim, 1988). Cyclodextrin-modified mobile phase have also been used to determine the complex stability constants and stoichiometries for CyD inclusion complexes (Uekama *et. al.*, 1978)

Table 1.3 contains further examples of the some of the improvement of drug properties which are possible by CyD complexation.

1.5.8 Limiting factors of cyclodextrin complexation

All drugs are not complexable by CyDs, and even those which are may not be of any pharmaceutical benefit. The three fundamental factors limiting the application of CyDs in oral preparations are as follows (Szejtli, 1984):

a) complexability (expressed as the stability constant, K_S)
b) stoichiometry of the complex
c) required dose of the complex

As previously discussed, the most important parameters which determine the complexability of a given molecule are its hydrophobicity, relative size and geometry in relation to the CyD cavity. The magnitude of the K_S value for the drug-CyD gives an indication of the relative extent of complexation and also governs the extent of dissociation of the complex. Complexes of low K_S values will dissociate rapidly, whereas drug release from complexes with high K_S values may be retarded. Hence, the release profile of a particular drug from the complex has to be considered such that the product remains efficacious.

Table 1.3 Examples of improvement of drug properties by cyclodextrin complexation (from Uekama and Otagiri, 1987).

Another limitation is based on the stoichiometry of the drug-CyD complexes. The stoichiometry of the CyD complexes will depend on the particular guest species and also the CyD involved. For example, as discussed previously, the prednisolone-β-CyD complex has a stoichiometry of 1:2 (guest:CyD) whereas the respective γ-CyD complex has a ratio of 2:3 (Uekama *et. al.*, 1982). Generally, the guests species which are suitable for complexation have molecular weights in the range of 100-400, whereas CyDs have relatively large molecular weights (972, 1135 and 1297 for α-, β- and γ-CyD respectively). Thus, 100 mg of a 1:1 stoichiometric β-CyD complex would contain about 8-26 mg active ingredient (Szejtli, 1984). However, if the guest-CyD complex had a stoichiometric ratio of 1:2 respectively, 100 mg of the complex would contain much less active ingredient. Hence, stoichiometry of the complex may limit the amount of drug which can be practically supplied by CyD complexation.

Furthermore, if the ratio of the drug in the complex is too low, one or two tablets of acceptable weight would not contain the required dose (Szejtli, 1984). Thus, for the drug complex to be therapeutically effective, a dosage of 2 tablets or more would have to be administered. This would increase the possibility of reduced compliance by the patient and hence ineffective treatment. In conclusion, therefore, for complex-forming drugs, the relationship between the required dose and the molecular weight of the drug determines the feasibility of oral administration of a drug-CyD product (Szejtli, 1991).

1.6 FATE AND BIOLOGICAL EFFECTS OF CYCLODEXTRINS

Internationally, CyDs are used in the pharmaceutical, food, cosmetic and chemical industries. In some countries, for example Japan, Germany and Italy, several orally administered drugs and some parenterals are marketed as drug-CyD complexes, as shown in table 1.4. Prior to the application of CyDs in pharmacy or in foods, their long-term safety needs to be established. The metabolism of CyDs following both oral and parenteral administration and their safety profiles are discussed here.

1.6.1 Metabolism

Following oral ingestion of the drug-CyD complex, the complex dissociates rapidly in the gastric medium. Absorption of the guest occurs rapidly whilst only an insignificant amount of unchanged CyD is absorbed intact (Szejtli, 1988).

In vivo studies performed by several researchers (Anderson *et. al.*, 1963; Szejtli, Gerlóczy and Fónagy, 1980; Gerlóczy, Fónagy and Szejtli, 1981; Gerlóczy *et. al.*, 1985) involved the oral administration of ^{14}C-β-CyD and ^{14}C-glucose to rats to compare their absorption and metabolism. The maximum radioactivity of blood derived from ^{14}C-β-CyD after its oral administration to rats was detected between the 4 th and 12 th hour and was no more than 5 % of the total administered dose. Following treatment with ^{14}C-labelled glucose, the radioactivity reached a maximum within 10 minutes of administration which was approximately 80 % of the administered radioactivity (Figure 1.13) indicating almost total absorption of glucose.

The ^{14}C in exhaled CO_2 was also measured to give an indication of the metabolism of CyDs. The amount of exhaled radioactivity (approximately 60 % of administered radioactivity) was almost identical in rats treated orally with ^{14}C-glucose, ^{14}C-starch or ^{14}C-β-CyD in a 24 hour period. With labelled glucose and starch, maximum radioactivity was detected in the first two hours as compared to the fourth and eighth hours with ^{14}C-

β-CyD (Figure 1.14). No significant difference was found in the tissue distribution of radioactivity except that higher radioactivity was found in the large intestine on the animals treated with ^{14}C-β-CyD; the large intestine contained 10-15 % radioactivity in the case of ^{14}C-β-CyD, 4-6 % in the case of ^{14}C-starch and 2 % in the case of ^{14}C-glucose.

Figure 1.13 Blood radioactivity level following oral administration of ^{14}C-β-CyD or ^{14}C-glucose in starved rats (from Gerlóczy *et. al.*, 1985)

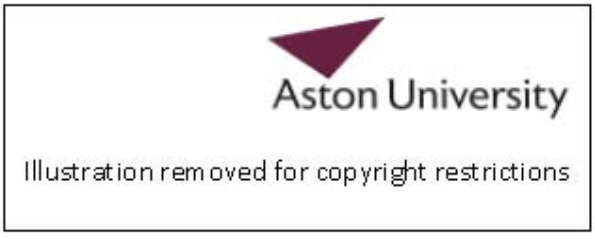

Figure 1.14 Radioactivity exhaled by rats after oral administration of ^{14}C-β-CyD or ^{14}C-glucose (Gerlóczy, Fónagy and Szejtli, 1981)

Gerlóczy and co-workers (1990) also followed the absorption, distribution and excretion of HP-β-CyD in rats following oral administration of ^{14}C-labelled HP-β-CyD. The maximum radioactivity of blood was 0.3 % of the administered dose which was detected after 30 minutes after its oral administration. The blood radioactivity declined slowly and after 24 hours only 0.1 % of the dose was detected. Approximately 3 % of administered dose was metabolised in the rat and consequently excreted as exhaled $^{14}CO_2$ in a 24 hour period. Furthermore, 2 % of the administered dose was excreted in urine and approximately 45 % in the faeces. In comparing the behaviour of HP-β-CyD to its parent CyD, the main route of excretion with the derivative seems to be *via* the faeces whereas with β-CyD, metabolism to CO_2 was the preferred route.

The results of the above studies can be summarised as follows. The appearance of radioactivity in the blood following oral administration of ^{14}C-β-CyD and ^{14}C-HP-β-CyD indicates that the CyDs are absorbed form the GI tract as glucose. The appearance of the radioactivity in the respired CO_2 is proof of *in vivo* metabolism of the CyDs. The primary products of CyD metabolism are acyclic dextrins, maltose and glucose, which undergo further metabolic and absorption processes to be finally excreted as CO_2 and H_2O (Szejtli, 1988). In comparing the metabolism of starch to CyDs, starch is metabolised in the small intestine by β-amylases which attack free end-groups, whereas CyDs are metabolised in the colon by α-amylases which attack glycosidic linkages inside the CyD ring. Once the CyD ring has been opened the metabolism of CyD follows that of starch (Szejtli, 1988). Only an insignificant amount of intact β-CyD and HP-β-CyD is absorbed from the intestinal tract. On the basis of these results, it is therefore proposed that the source of radioactivity in the blood following oral treatment is probably due glucose and glucose metabolites formed from the CyD by the action of α-amylases in the colon (Szejtli and Sebestyen, 1979; Flourié *et. al.*, 1992).

1.6.2 Toxicity

The work published on the metabolism of CyDs suggests that orally administered CyDs are harmless. Six month oral toxicity studies of β-CyD in rats (Makita *et. al.*, 1975) and dogs (Szejtli and Sebestyen, 1979) receiving up to 1.6 g/kg body weight/day showed no adverse effects with respect to weight gain, food consumption or clinical biochemical values. No signs of toxicity were revealed in pathological or histological investigations. β-CyD was also found to be devoid of any embryotoxic and teratogenic effects. Chromosomal tests performed on rats treated for 6 months did not increase the incidence of spontaneous aberration and no gene-mutating effects were revealed. Similar results were observed after administration of high oral doses (5 g/kg) of HP-β-CyD in rats

(Coussement *et. al.*, 1990). These studies further confirm the non-toxicity of orally administered CyDs.

The consequences of parenteral administration of the 3 natural CyDs (α, β, and γ) are different from their oral administration. Administration *via* the intravenous route can result in nephrotoxicity and haemolytic effects. Following their parenteral administration, the natural CyDs may accumulate in the kidneys. The CyDs form inclusion complexes with cholesterol and cholesterol-esters in the blood, which then accumulate in the kidney. The complexes dissociate in urine with most of the CyD being excreted, however the cholesterol is reabsorbed. The small amount β-CyD remaining in the kidney forms complexes with the accumulated cholesterol. Subsequent crystallisation of the complexes results due to their low solubility (Frijlink, 1991) which eventually leads to necrotic effects.

The haemolytic activity of CyDs could be a consequence of their direct interaction with membrane components such as phospholipids, proteins and cholesterol which leads to disruption of the cell membrane. The concentration of CyD causing complete haemolysis of human erythrocytes (0.25 %) in 10 mM isotonic phosphate buffer was ~ 0.01 M with β-CyD, ~ 0.02 mM with α-CyD and ~ 0.04 M with γ-CyD (Uekama and Otagiri, 1987). As a consequence of the molecular dimensions of β-CyD cavity generally being the most favourable for accommodating guest species and also due to its reduced water-solubility, the haemolytic activity of the natural CyDs decreases in the order β- > α- > γ-CyD (Bekers *et. al.*, 1991b).

The degradation rates of the natural CyDs by *Aspergillus oryzae* are different; the rates of hydrolysis for β- and γ-CyD are, respectively, almost 30 and 500 times greater than that found for α-CyD (5.8 min^{-1}; Jodál *et. al.*, 1984). The hydrolysis rate of HP-β-CyD was reported to be less than the parent CyD (Müller and Brauns, 1986). As a consequence of the high solubility and rapid enzyme degradation of γ-CyD, its haemolytic activity and nephrotoxicity are lower than that of α- and β-CyDs making it the most appropriate natural CyD for use as an injectable drug carrier. The LD_{50} for rats on intravenous administration of β-CyD was 0.788 g/kg and 1 g/kg for α-CyD (Frank, Gray and Weaver, 1976). In comparing these results with γ-CyD, the LD_{50} is 4.0 g/kg in mice and more than 2.4 g/kg in rats (Matsuda *et. al.*, 1983). The LD_{50} for HP-β-CyD has not been determined, however on the basis of published work, Brewster, Estes and Bodor (1990) suggested that the toxicity of this derivatised CyD was similar to glucose.

The toxicity profiles of the CyD derivatives following their intravenous administration are different from their respective parent CyDs which is primarily due to their differing solubilities and complexing abilities. The haemolytic activities of the hydroxyalkylated derivatives of β-CyD have been reported to be less than that of the natural CyD (Yoshida *et. al.*, 1988). With the parent β-CyD, haemolysis started at a concentration of 0.3 % w/v, whereas with the hydroxypropyl and hydroxyethyl derivatives, haemolysis was induced at 0.5 % and 2 % w/v respectively. The decrease in haemolytic toxicity of the HA-β-CyDs may be due to their reduced ability to remove cell membrane components. The introduction of hydroxyalkyl groups into the parent CyD molecule may reduce the complexing ability of the respective derivatised CyD due to steric hindrance. In contrast, DM-β-CyD, with a greater solubility and complexing ability than β-CyD itself, has been reported to have a greater haemolytic effect; with DM-β-CyD haemolysis was induced at a concentration 0.07 % w/v compared with 0.3 % w/v with the natural β-CyD (Yoshida *et. al.*, 1988) (Figure 1.15). However, with DM-β-CyD, haemolytic effects are thought to be due to its surface activity effect on the membranes rather than by inclusion of the membrane components (Stern, 1989).

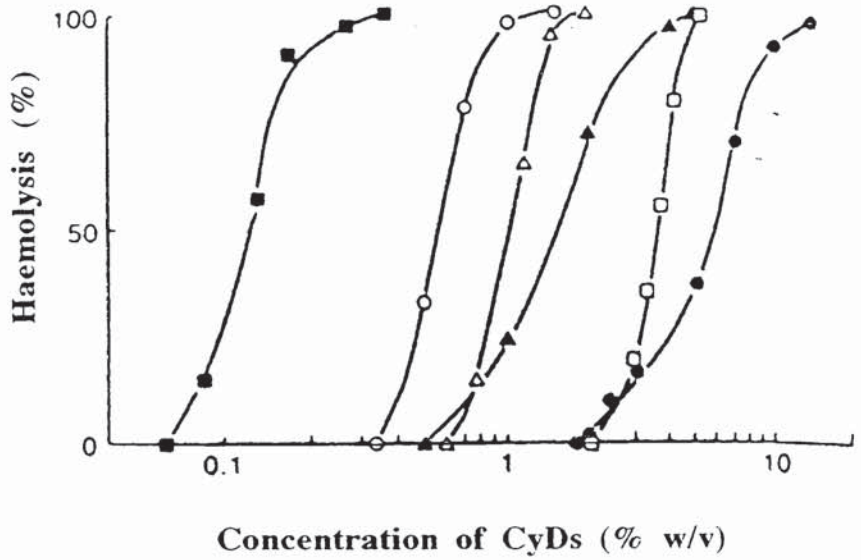

Figure 1.15 Haemolytic effects of cyclodextrins and cyclodextrin derivatives (Yoshida *et. al.*, 1988). Δ = α-CyD, o = β-CyD, □ = γ-CyD, ■ = DM-β-CyD, ▲ = HP-β-CyD, ● = HE-β-CyD.

Studies comparing the renal effect of the methylated CyDs found no significant differences in the toxic effect of β-CyD and its mono- and trimethylated derivatives, however, DM-β-CyD was found to be less toxic (Szejtli, 1983). When HP-β-CyD was administered parenterally, the inclusion complex formed between HP-β-CyD and cholesterol accumulated in the kidney, however, in contrast to the respective cholesterol-β-CyD complex, no crystallisation of the HP-β-CyD complex was observed (Frijlink *et. al.*, 1991). Hence, the nephrotoxicity of the HA-β-CyDs is less than β-CyD. Several studies (Brewster, Estes and Bodor, 1990; Coussement *et. al.*, 1990) examining the effects of acute and chronic intravenous dosing in rats and monkeys using repeated doses of up to 400 mg/kg HP-β-CyD over a 3 month period have shown no adverse effects.

Other possible parenteral routes of administration of CyDs includes the intramuscular and subcutaneous routes. The irritancy of the HP-β-CyDs at the site of injection was significantly lower than that of β-CyD and its methylated derivatives (Yoshida *et. al.*, 1988; Coussement *et. al.*, 1990).

On the basis of the data published on the toxicity of CyDs, it can be concluded that CyDs are safe when administered orally, however, HP-β-CyD has the greatest potential for use as a drug carrier in parenteral formulations.

1.7 LEGALISATION

New drug substances for human consumption are subjected to extensive toxicological studies before their legal approval. As previously discussed, complexation with the CyDs leads to a modification is several physicochemical properties of the guest which include the bioavailability and stability of drugs. Following oral administration of the drug-CyD complex, the complex dissociates in the gastrointestinal tract and only the active drug is absorbed. The question which arises here is, should the complex be treated as the 'drug' entity, although it is the free guest component which is active. Despite the fact that there is insignificant absorption of the CyD, it is most probable that extensive toxicology and metabolic studies will need to be performed on each specific drug-CyD complex before market approval.

No marketed products are currently available in the United Kingdom, however, some drug-CyD complexes are undergoing clinical trials in human subjects, *e.g.* the spironolactone-β-CyD complex (Yusuff *et. al.*, 1991). In some countries, for example Japan, Germany and Italy, several orally administered drugs and some parenterals are

marketed as drug-CyD complexes; these are shown in table 1.4 with details of the improvement in drug properties brought about by complexation.

Table 1.4 Approved and marketed drug-cyclodextrin complexes (Szejtli, 1991)

1.8 IMPROVING ACCESS TO SITES OF INFECTION

The potential application of the antimicrobial-CyD complexes studied in this work is for the local treatment of bacterial infections which have colonised sites that are difficult to access. One organism in particular which is difficult to eradicate is *Helicobacter pylori* (*H. pylori*) as further discussed in 1.8.1. Due to the numerous crevices in the oral cavity, bacterial infections at these sites are also difficult to treat. The involvement of bacteria in peridontal diseases is discussed in 1.8.2.

For the antimicrobial drug to be active against such infections, its concentration at the site of infection has to be sufficiently high. The drug must diffuse to the site of infection, the driving force of which is controlled by the concentration differential. It therefore follows that the delivery of a high concentration of antimicrobial agent would enable enhanced diffusion and hence greater activity. However, the concentration of the antimicrobial

agent may be limited by its poor aqueous solubility. Organic solvents could be used to overcome the solubility problem, however they are irritant and toxic. An attractive alternative to this is the use of cyclodextrins.

1.8.1 *Helicobacter pylori*

Helicobacter pylori (also known as *Campylobacter pylori*) was first isolated in 1982 (Warren and Marshall, 1983). It is a spiral Gram negative organism found in the upper gastrointestinal tract of humans. There has been much controversy surrounding the role of *H. pylori* in gastro-duodenal ulceration and chronic gastritis. Since the identification of *H. pylori*, the number of publications concerning this bacterium has been increasing. Some general reviews published include those by Caldwell and Marshall (1989), Wyle (1991) and Peterson (1991).

H. pylori is found beneath the mucus, mainly in the antrum of the stomach and in areas of gastric metaplasia in the duodenum (Kumar and Clark, 1990). The organism does not penetrate the epithelial cells themselves but tends to cluster around the junctions between the cells. Diagnosis of *H. pylori* can be confirmed by endoscopic biopsy or non-invasive breath urea test. The fact that *H. pylori* is a urease-producing bacterium is made use of in its detection.

The main evidence for the role of *H. pylori* in gastritis follows from the resolution of symptoms on eradication of the bacterium, however its precise mechanism of action is unknown. A brief summary on its proposed mode of action is as follows (Vines, 1994). *H. pylori* is equipped with the urease enzyme that breaks down urea in gastric juice to produce a localised alkaline medium of bicarbonate and ammonia. This enables the bacterium to survive the hostile acidic environment of the stomach. The organism burrows under the stomach's layer of protective mucus and attaches to epithelial cells where it releases a cytotoxin which causes cell damage. Consequently, the immune response is also triggered which attracts inflammatory cells to the site of damage inorder to rid the body of the bacterium. There is much debate on whether the bacterium also interferes with the acid-producing ability of the stomach. Higher acid production by *H. pylori* would explain how this bacterium causes duodenal ulcers. As more acid spills out of the stomach, cells lining the duodenum change from small intestinal to stomach-type. This allows bacteria to colonise the duodenum, setting off the inflammation that precedes a duodenal ulcer.

Different treatment regimes are being evaluated for the treatment of *H. pylori.* Due the risk of resistance, combination therapy is necessary. Current treatment includes the use

of bismuth compounds and antibiotics such as amoxycillin, erythromycin, metronidazole and tetracycline. The triple combination of bismuth, tetracycline and metronidazole is the gold standard against which all other combinations need to be evaluated, having produced cures in 85-90% of patients (Scrip, 1994). However, since this treatment has problems with patient compliance and also side effects the search continues for different combinations. One of the most promising combinations which is in development involves the use of omeprazole 20 mg twice daily, metronidazole 500 mg twice daily and clarithromycin twice daily for 14 days; cure rates of ~ 90 % were achieved with this combination. In the U.K. and Sweden, the first dual therapy combination approved for the treatment of *H. pylori* infection is omeprazole and amoxycillin. At present therefore, no single effective treatment regime exists for the consistent eradication of *H. pylori* in infected patients.

1.8.2 Oral cavity bacteria

The oral mucosa is exposed to various bacterial flora, mainly anaerobic. Bacteria are present in the saliva, on the tongue and cheeks, on the tooth surface and in the gingival crevices (between gum and tooth).

A lapse in oral hygiene leads to an accumulation of the bacteria which results in plaque formation. Plaque can be defined as a mass of bacteria in a matrix of organic material which adheres to the tooth surface (Melville and Russell, 1981). The organic material consists largely of protein and polysaccharide which is derived partly from saliva and partly produced by the organisms. Experimental studies of plaque development have shown that the early colonisers are streptococci, particularly *S. mitis*, *S. sanguis* and *S. oralis* (Marsh, 1992). Accumulation of plaque is greatest in sites sheltered from functional friction and tongue movement and thus make its removal difficult. Different varieties of organisms attach themselves to the existing plaque leading to an increase in its surface deposition. The primary cause of peridontal disease is bacterial plaque (Manson, 1983) where the implicated organisms are *Porphyromonas gingivalis*, *Actinomyces actimycetecomitans*, *Fusobacterium nucleatum*, *Wollinella recta* and *Prevatella intermedius* . Accumulation of the bacterial plaque within close proximity of the gingival crevice results in gingival inflammation.

Topical antimicrobials in dental products have four general mechanisms of action (Marsh, 1992). They can decrease the rate of new plaque accumulation, decrease or remove existing plaque, suppress growth of those species associated with disease, or inhibit the production of virulence factors (*e.g.* proteases, cytotoxics). The effects of the antimicrobial agents will be dependent on the concentration of the agent delivered to the

site of action. Agents may be present initially at relatively high concentration, however, this will only be for a short period of time since a large proportion of the agent will be lost by expectoration and swallowing. Subsequent effects are therefore dependent on the concentration of the agent retained on oral surfaces.

Current treatments for peridontal disease include an improvement in oral hygiene together with the use of topical antibacterial agents. There a number of toothpastes and mouthrinses available commercially that contain antimicrobial agents to control plaque. Examples of such products include Corsodyl® (chlorhexidine digluconate, 0.2 %) and Crest® (triclosan, 0.3 %). Studies performed to assess the efficacy of such products found a approximate 45-61 % reduction in plaque formation in subjects using chlorhexidine rinses, and a 0-30 % reduction with triclosan products (Cianco, 1992). Inorder to boost the antimicrobial activity of triclosan, it has been combined with a co-polymer (polyvinylmethyl ether maleic acid; Colgate Plax®) which increases oral retention. Triclosan has also been combined with another antibacterial agent, zinc citrate to exert an synergistic effect on bacteria (New Mendadent P®). In comparing the effect of these products relative to triclosan alone, combined with the co-polymer an approximate 60 % reduction in plaque formation was observed, whereas with zinc citrate plaque formation was reduced by 35 % (Urquatt and Addy, 1991).

Extensive colonisation by a bacterial species may lead to tooth abscess which would require systemic treatment with broad spectrum antibiotics such as amoxycillin. It would therefore seem sensible to treat the primary cause of peridontal disease which is the bacterial plaque itself. When considering the local treatment of bacterial plaque, one problem which needs to be addressed is retention of the antibacterial agent in the oral cavity for a suitable length of time such that the active drug can diffuse to the sheltered sites of plaque accumulation.

1.9 AIMS OF STUDY

The aim of this study was to observe the interactions between poorly soluble antimicrobial agents (chlorhexidine dihydrochloride, *p*-hydroxybenzoic acid esters and triclosan) and CyDs in an attempt to enhance their aqueous solubility and also their microbiological activity.

The guest species were chosen on the basis of work performed by the Microbiological Department as SmithKline Beecham where potential antimicrobial compounds for activity

against *H. pylori* were screened. The agents mentioned above were amongst the compounds which were found to be active. However, since the aqueous solubility of these agents is limited, as a consequence, their antimicrobial activity may also be restricted by solubility considerations. Another significant problem which needs to be considered for successful eradication of this bacteria is accessibility since its area of residence is difficult to reach. A similar scenario exists for the treatment of bacterial plaque in the gingival crevices. For both bacterial infections, the active agent has to reach the site of infection and the potency of the agent has to be such that eradication of the organism is achieved. Therefore, by solubilising the antimicrobial agents by CyD complexation, it was anticipated that a greater concentration of drug as the CyD complex would be delivered, thus a steeper concentration differential would be established which should facilitate the flux of active drug to the site of infection. Another objective of this study was to assess the extent of supersaturation of free drug which would lead to an enhancement in both its diffusion to the site of action and also its microbiological activity.

The following chapters discuss the preparation and investigations of the various antimicrobial-CyD complexes and aim to show the feasibility of a treatment for bacterial infections where accessibility is a problem. A further objective was to assess the microbiological activity of the antimicrobial-complexes.

CHAPTER TWO
INVESTIGATION OF THE INTERACTION OF CHLORHEXIDINE DIHYDROCHLORIDE WITH β-CYCLODEXTRIN AND HYDROXYPROPYL-β-CYCLODEXTRIN

2.1 INTRODUCTION

Chlorhexidine (1,1'-Hexamethylene-bis[5-(4-chlorophenyl)biguanide]) is a bis-biguanide antibacterial agent which has both bacteriostatic and bactericidal properties. It is effective against a wide range of Gram-positive and Gram-negative bacteria. Chlorhexidine is a strong base and is available commercially as the digluconate solution (B.P), the diacetate salt (B.P.C.) and the dihydrochloride salt; the structure of the latter is shown in figure 2.1. The solubilities of each salt differs with the digluconate being the most soluble (>70 % w/v at 20°C; Senior, 1973) and the dihydrochloride salt being the least soluble at 0.06 % w/v.

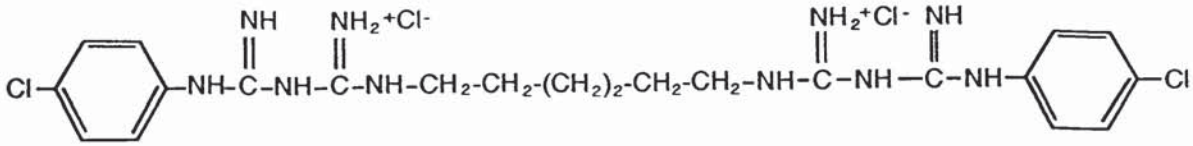

Figure 2.1 Structure of chlorhexidine dihydrochloride

At neutral and mild alkaline pH, chlorhexidine is dicationic with the positive charge distributed over its ten nitrogen atoms (Davies, 1973). In strong acid solution however, chlorhexidine is reported to carry four positive charges (Christensen and Jensen, 1974). Two pK_a values of 2.2 and 10.3 have been reported (Hugo and Longworth, 1964). The major factor influencing the antibacterial activity in bisbiguanides is the hydrophilic/lipophilic balance in the molecule (Cutler *et. al.*, 1966).

At physiological pH, the bacterial cell surface is negatively charged which facilitates the rapid adsorption of the chlorhexidine cations. Under acidic conditions, however, surface ionisation of bacteria is suppressed and as a consequence the bactericidal effect of chlorhexidine is reduced (Davies, 1973). With respect to this, a potential chlorhexidine product for the oral treatment of *Helicobacter pylori* would be delivered to a highly acidic gastric environment where the activity of the antibacterial agent would be reduced.

However, with this bacterium, the important site of action is beneath the gastric mucus where an alkaline environment exists thus enabling chlorhexidine to retain its antibacterial activity.

Various studies have been undertaken to study the mode of action of chlorhexidine against *Escherichia coli* and *Staphylococcus aureus* (Hugo and Longworth, 1964; Russell, 1969; Davies, 1969). From a review of this literature, the mode of action of chlorhexidine can be summarised as follows:

1. Adsorption of the cationic base to the bacterial surface
2. Damage to the permeability barriers which consequently facilitates entry of the bactericide to the cytoplasm
3. Precipitation of the cytoplasm and prevention of repair of cell membrane and wall

Initial *in-house* microbiological studies performed by SmithKline Beecham have found chlorhexidine dihydrochloride (CHX) to be an effective antibacterial agent against *H. pylori.* Since CHX is poorly water-soluble, it was decided to investigate the effect of CyDs in enhancing its aqueous solubility in an to attempt further increase its antibacterial activity. The CyDs employed for this study were β-CyD and its hydroxypropyl derivative (HP-β-CyD, M.S. = 0.6).

Previous work on the involvement of CHX with CyDs concerned the application of CyDs to improve the availability and taste of chlorhexidine and it salts (Gallopo and Lynch, 1989). In the presence of β-CyD, the side effects associated with chlorhexidine such as bitter taste, irritation and tooth staining were reduced. More recently, various other studies concerning the interaction of chlorhexidine with CyDs have been reported in the literature. Lehner, Müller and Seydel (1993) investigated the preservative efficiency of chlorhexidine in the presence of HP-β-CyD and Qi and co-workers (1994) examined the interaction between chlorhexidine diacetate and β-cyclodextrin using microcalorimetry, UV and NMR spectroscopic techniques.

The proceeding sections describe the experiments performed to assess the interactions involved between CHX and both β-CyD and HP-β-CyD. The CyD complexes were studied both in solid and solution phases to investigate the extent of their interaction and the degree of enhanced water-solubility of CHX.

In view of the fact that water-soluble chlorhexidine salts are commercially available (digluconate and diacetate salts), experiments were also performed to assess whether a

CyD inclusion complex of the dihydrochloride salt would have any advantage over the more soluble chlorhexidine salts.

2.2 MATERIALS

All cyclodextrins used for this study were a gift supplied by SmithKline Beecham and Wacker Chemicals (Halifax), and were used as received. Both chlorhexidine dihydrochloride and chlorhexidine digluconate were purchased from Sigma chemicals. All other chemicals and solvents were purchased from the appropriate chemical suppliers as listed in Appendix 2 and were used as received. HPLC grade solvents were used for the preparation of HPLC mobile phases whilst other chemicals were either of Analar or reagent grade as appropriate. Distilled water was used throughout for the preparation of analyte solutions.

Amicon Diaflo ultrafiltration membranes type YM1 (molecular weight cut-off 500 Daltons; 500 Da.) and YM2 (molecular weight cut-off 1000 Da.) of 25 mm diameter were purchased from Amicon Ltd, U.K. Spectra/Por cellulose ester molecularporous dialysis membrane (molecular cut-off 500 Da. and 1000 Da.; 19.7 mm diameter) was purchased from Medicell International Ltd, London. Sil-Tec Silicone membrane (0.02 inches thickness) was purchased from Technical Products Inc. of Georgia, U.S.A.

2.3 EQUIPMENT

Differential Scanning Calorimetry

Differential scanning calorimetry (DSC) was undertaken with a Perkin-Elmer DSC-4 instrument. The Thermal Analysis Data Stations (TADS) was used for data collection, handling and presentation.

High-Performance Liquid Chromatography

High-Performance Liquid Chromatography (HPLC) analysis was performed using a Waters Chromatography station. This comprised a Waters 600E system controller, a WISP 712 autoinjector and a Waters 484 ultraviolet variable wavelength detector. A sensitivity of 0.005 AUFS was used during all chromatography runs. Chromatography was performed with a stainless steel column (10 cm x 4.6 mm; column length x internal diameter), packed *in-house* with 5 µm Spherisorb ODS2 reversed-phase material.

Chromatograms were collected and integrated on a Waters Chromatography Baseline 815 workstation.

Infra-Red Spectroscopy

Infra-red (IR) spectra were recorded as KBr discs on a 2020 Galaxy FT-IR spectrophotometer.

Karl Fischer Titrimetry

Karl Fischer (KF) titrimetry was undertaken using a Metrohm 702 SM Titrino.

Thermogravimetric Analysis

Thermogravimetric analysis (TGA) was performed with a Perkin-Elmer TGS-2 Thermogravimetric Analyser. Thermal Analysis Data Stations (TADS) was used for data collection, handling and presentation.

Ultraviolet Spectroscopy

Ultraviolet (UV) absorption readings were determined using a Cecil C292 Digital Ultraviolet spectrophotometer. UV scans were recorded using a Cecil 584 Double Beam scanning spectrophotometer. In both cases, 10 mm quartz cells were employed.

X-ray powder diffraction

The powder X-ray diffraction patterns were recorded on a Phillips PW1120 X-ray diffractometer.

All pH measurements were determined with a Corning pH Meter 145 (2 decimal places) appropriately calibrated with Colourkey® buffer solutions (BDH).

A range of electronic balances were employed for weighing purposes: Sartorius 1601 MP8, an analytical A200S (4 decimal place), or a research R200D (5 decimal place).

A Kerry sonicator was utilised to aid dissolution, where required, and for solvent de-gassing.

An Edwards Modulyo freeze-dryer was employed for freeze-drying purposes throughout the study.

Centrifugation was performed using a Microcentaur centrifuge with variable speed and time functions being available.

2.4 ASSAY PROCEDURES FOR CHLORHEXIDINE DIHYDROCHLORIDE

UV absorption spectroscopy and HPLC were employed for the quantitative assay of CHX.

2.4.1 UV spectroscopy

UV spectroscopy is frequently used in pharmaceutical analysis. It involves the measurement of the amount of ultraviolet radiation absorbed by a substance in solution. As illustrated in figure 2.1 CHX possesses an aromatic moiety which confers UV absorption. The UV spectra of CHX was determined in the range 200-350 nm and the wavelength at which maximum absorbance (λ_{max}) occurred was 255 nm. All subsequent UV analyses of CHX were performed at this λ_{max}. The molar extinction coefficient (E, L mol^{-1} cm^{-1}) gives an indication of the UV absorbing affinity of a compound and for CHX was found to be 2.8×10^4 L mol^{-1} cm^{-1} at 255 nm.

To apply UV spectroscopy in quantitative analysis, the UV absorbing compound should obey Beer-Lambert's Law *i.e.* the absorbance is proportional to the concentration of absorbing substance present. To confirm this, the absorbances of CHX solutions of various concentrations were determined at the λ_{max} (255 nm). A linear plot of absorbance *versus* concentration indicated that over the CHX concentration range studied ($0.4 - 3.4 \times 10^{-5}$ M) Beer-Lambert's law was obeyed. A typical UV calibration graph for CHX is shown in figure 2.2.

2.4.2 HPLC method development

The use of HPLC provides a rapid, specific, and sensitive assay procedure suitable for quantitative analysis. The ability of this method to efficiently separate and detect a wide range of molecules of various molecular weights, polarities and chemical properties renders it a versatile analytical technique widely applied in pharmaceutical analysis. Many review articles and text are available concerning the theoretical principles and practicalities of HPLC and its application in the pharmaceutical field (Munson, 1984; Irwin and Scott, 1982; Kirschbaum, 1989).

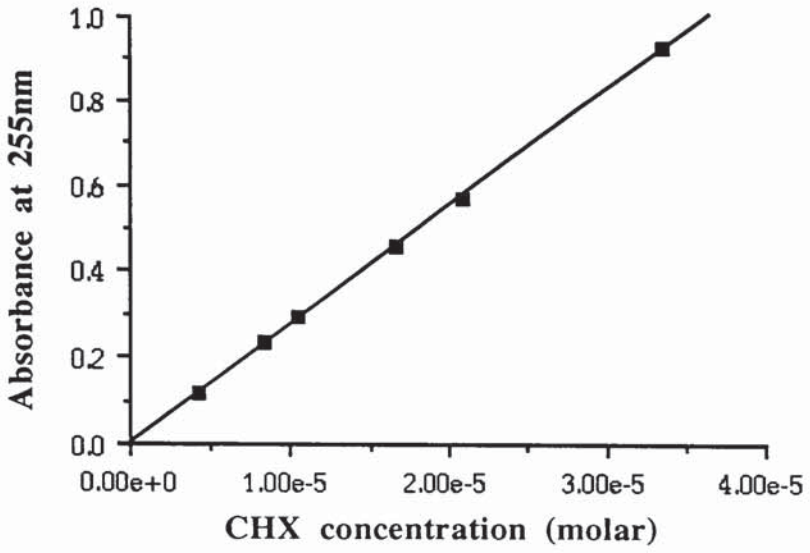

Figure 2.2 Example of a typical UV calibration graph for chlorhexidine dihydrochloride (CHX)
($y = 2.7359 \times 10^{-4}x + 1.3334 \times 10^{-3}$, $r^2 = 1.000$)

Several methods for the HPLC determination of chlorhexidine have been reported in the literature (Gaffney, Cooke and Simpson, 1984; Huston, Wainwright and Cooke, 1982; Brougham, Cheng and Pittman, 1986). By minor modification of these methods a suitable assay procedure for the efficient quantification of CHX was established. In a neutral environment (pH=7), chlorhexidine exists as a dicationic species. This property dictated the selection of a reversed-phase HPLC system with the use of an ion-pairing agent possessing an anionic moiety.

In reversed-phase HPLC, the mobile phase generally consists of water and a less polar organic solvent such as methanol or acetonitrile. Separations in these systems are due to different degrees of hydrophobicity of the solutes, the less polar solutes associating to a greater extent with the non-polar stationary phase and consequently being retained on the column longer that the more polar solutes. The rate of elution of the components is controlled by the proportion of the organic modifier in the mobile phase. By systematic and quantitative changes in solvent composition it was found that a mobile phase in the ratio of 75:25 methanol:water gave optimum peak resolution whilst maintaining a relatively short analysis time. All mobile phases were degassed by vacuum, filtration or helium sparging to eliminate dissolved gases. Dissolved gases may cause out gassing into the detector cell and also baseline drift (Li Wan Po and Irwin, 1980).

Counter-ions of opposite charge were added to the mobile phase leading to ion-pair formation with the CHX cations. The reduced charge of the ion-pairs renders them more hydrophobic and results in an increased retention of the solute. Sodium heptane sulphonate was selected as the ion-pairing agent as it has minimum absorbance at the UV maxima of CHX, 255 nm; the wavelength at which the elutes were monitored.

Due to the basicity of the solute, the extent of endcapping in the analytical column was an important consideration in-order to minimise peak-tailing. As a consequence of this, ODS2 (Octadecylsilane, C_{18}) was selected as the packing material for the solid-phase analytical column. This chemically modified silica phase has higher than normal carbon loading (~12%) to provide a greater degree of endcapping. A stainless steel column (10 cm x 4.6 mm; column length x i.d.), packed *in-house* with 5 µm Spherisorb ODS2 reversed-phase material was used for all HPLC analyses throughout the study.

To further reduce peak tailing, 0.1 % diethylamine was added to the mobile phase. The final pH of the mobile phase was adjusted to pH 3.5 with glacial acetic acid. During ion-pair reversed phase HPLC, the pH should be adjusted such that the analyte exists entirely in the desired ionic form. Thus, in the case of CHX, the final mobile phase pH of 3.5 will favour the formation of CHX cations which will readily interact with the oppositely charged counter-ions. For optimum column performance, the pH of the mobile phase should lie within the range 2.5 to 7. Below pH 2.5, the column will be susceptible to loss of bonded phase, whereas above pH 7 the silica particles are liable to dissolve. A summary of the HPLC conditions employed for the quantitative analysis of CHX are shown in table 2.1.

Following the testing of a number of candidates, propyl paraben (*n*-propyl 4-hydroxybenzoate; PrP) was selected as the internal standard. Internal standard candidates are selected by virtue of their chemical and UV absorptive characteristics such that they would be adequately separated and detected under the HPLC conditions employed for the analyte of interest. Internal standards are incorporated into samples to aid standardisation by minimising errors caused by fluctuations in injector performance. The concentration of the internal standard (I.S.) given in the table of conditions (table 2.1) is the final concentration of injected I.S. in the samples. Quantification of sample peak responses was achieved using peak area ratios (analyte:I.S.). Examples of a typical chromatogram and calibration plot are illustrated in figures 2.3 and 2.4 respectively. The concentration range of injected analytes are those given in the calibration graph. The injection volume in each case was 100 µl and a sensitivity of 0.005 AUFS was employed.

Table 2.1 HPLC conditions for the quantitative assay of chlorhexidine dihydrochloride

mobile phase	75:25 methanol-water 0.005 M sodium heptane sulphonate 0.1 % diethylamine pH 3.5 with glacial acetic acid
flow rate	1.2 ml min^{-1}
wavelength	255 nm
injection volume	100 µl
injection solvent	distilled water
sensitivity	0.005 AUFS
internal standard	Propyl paraben (5×10^{-5} M)

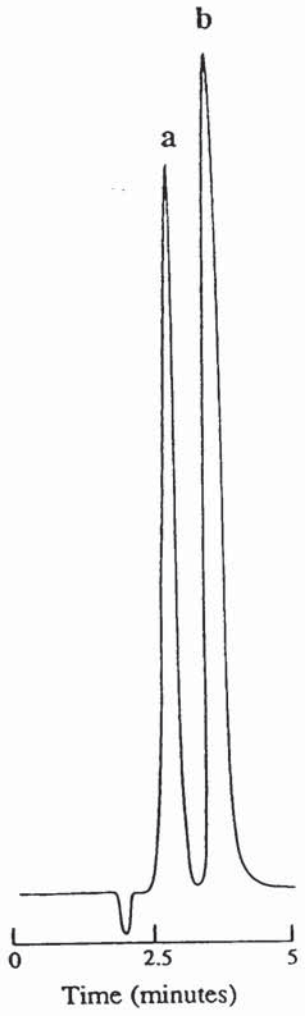

Figure 2.3 Example of a typical chromatogram of chlorhexidine dihydrochloride (peak b, 4.2×10^{-5} M; t_R = 3.5 minutes) with propyl paraben (peak a, 5×10^{-5} M; t_R = 2.7 minutes) as internal standard.

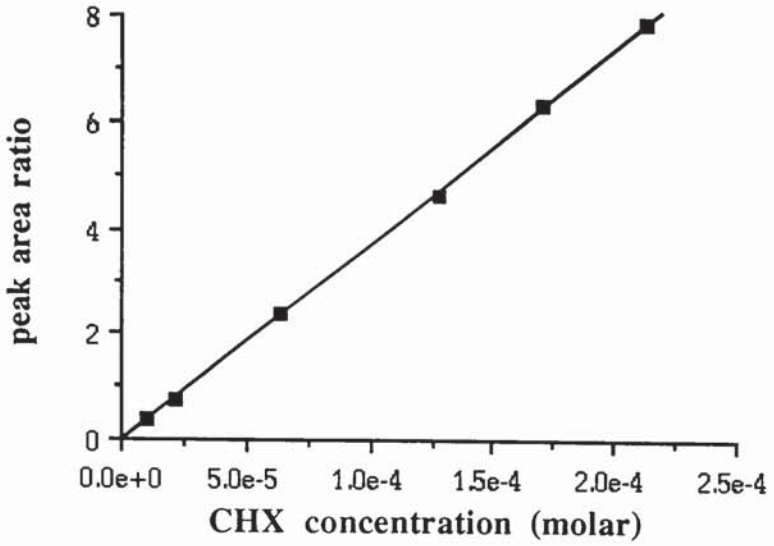

Figure 2.4 Example of a typical calibration curve for chlorhexidine dihydrochloride (CHX) with 5 x 10^{-5} M propyl paraben as I.S.
($y = 3.6787 \times 10^{-4}x - 3.7946 \times 10^{-2}$, $r^2 = 1.000$)

2.5 EXPERIMENTAL

2.5.1 Preparation of the solid phase β-CyD and HP-β-CyD complexes of chlorhexidine dihydrochloride

Equimolar quantities of the host and guest components were used. The additional weight of the water present in the CyDs as determined in section 2.5.3.2, was accounted for prior to weighing the appropriate quantities. β-CyD, 1.276 g (1 mmol) or HP-β-CyD, 1.432 g (1 mmol), were dissolved in 100 ml of distilled water and heated to 75°C in a flask. When the CyD had dissolved, 0.578 g (1 mmol) of CHX was slowly added. The mixture was left stirring until a clear solution was visible (~10 minutes), after which it was quickly cooled to room temperature by immersion in an ice water bath. The resulting solution was transferred to a freeze-drying flask (500 ml) and quickly frozen by immersion in a acetone/dry ice bath and then lyophilised to a white solid.

When larger amounts of both complex components were used, the volume of water was adjusted proportionately.

2.5.2 Preparation of equimolar physical mixes of the CyDs and chlorhexidine dihydrochloride

The physical mixture was prepared by careful mixing of 1.276 g (1 mmol) of β-CyD, or 1.432 g of HP-β-CyD with 0.578 g (1 mmol) of CHX in a ceramic mortar with gentle folding (Erden and Çelebi, 1988). The resulting mix was freeze-dried overnight in order to simulate conditions used in the preparation of the complex.

2.5.3 Investigation of the solid phase chlorhexidine dihydrochloride-CyD complexes

2.5.3.1 Differential Scanning Calorimetry

Samples for thermal analysis (β-CyD, HP-β-CyD and CHX alone, their respective freeze-dried equimolar physical mixes and the CHX-CyD complexes) were accurately weighed (4-8 mg) into an aluminium pan, covered with an aluminium lid and crimped into position. The pan was placed in the DSC oven together with a blank. The blank was prepared in the same way but did not contain the sample. The sample and blank pans were continuously purged with nitrogen gas. Thermograms were recorded over a range of 25-300°C with a programmed heating rate of 10°C min^{-1}. Initial temperature calibration was made with an indium standard which had an onset temperature of 156.6°C.

2.5.3.2 Karl Fischer Titration

Prior to sample analysis, the instrument was calibrated by the assay of a specific quantity of water, for which a certain volume of KF reagent was required to reach the reaction end-point as detected by the electrode. Six consecutive additions of 20 µl (20 mg) of water were made to the titration vessel using a glass microlitre syringe. The volume of KF reagent required on each occasion, and the mean and variance of the six volumes, were automatically printed at the end of the procedure.

For sample analysis, the solid was accurately weighed (approximately 0.5 g) and added to the solvent in the reaction vessel. The instrument was programmed to perform a delay titration (5 minute delay). At the end of each titration reaction, the volume of reagent used was printed. This procedure was repeated in triplicate for each solid sample under test. To compensate for any moisture absorption by the solvent during the delay period, a blank titration was performed in duplicate omitting the addition of any solid material. The mean volume of reagent obtained for each solid material was corrected with the mean volume for the blank titrations, after which the calibration data was used to determine the percentage water content of the CyD samples.

2.5.3.3 *Thermogravimetric Analysis*

Samples for thermal analyses included the aforementioned CyDs, CHX, equimolar physical mixes of CHX and β-CyD and CHX and HP-β-CyD (molar ratio 1:1) and the CHX-β-CyD and CHX-HP-β-CyD complexes. The physical mixes was subjected to TGA before and after freeze-drying. TGA was performed in triplicate for each test solid. Each sample was accurately weighed into an aluminium pan (5-10 mg), which was then placed onto the sample pan of the autobalance, with the reference pan empty. The sample was heated *via* a controlled temperature programme (25-150°C) whilst being continuously purged with nitrogen gas. The change in mass with increasing temperature was recorded as percentage loss, and was displayed as a thermogravimetric curve at the end of the heating process. Prior to use, a calibration procedure was performed and the autobalance was zeroed.

2.5.3.4 *Infra-Red Spectroscopy*

β-CyD, HP-β-CyD, CHX, the respective physical mixtures of the respective host and guest components and the CHX-CyD complexes were all subjected to IR analysis.

2.5.3.5 *X-ray Powder Diffraction*

Solutions of CHX, β-CyD and HP-β-CyD alone were prepared in distilled water, frozen and then freeze-dried. Using these individual lyophilised guest and host components, the respective equimolar physical mixes for CHX and each CyD were prepared in a similar manner to that described in section 2.5.2.

These freeze-dried physical mixes, together with β-CyD, HP-β-CyD, CHX, and the CyD complexes were subjected to X-ray diffraction using the following operating conditions: Ni filtered CuKα_1 radiation, voltage: 40 kV; current 20 mA; time constant: 2 sec; scanning speed 1°·2ϑ/min. For comparison, the original physical mixes as prepared in section 2.5.2 were also tested.

2.5.4 Chemical analysis of the chlorhexidine dihydrochloride-CyD complexes

Approximately 4 mg of each batch of complex was accurately weighed into screw-capped bottles, to which 1 ml of distilled water was added. For each batch of complex triplicate determinations were performed. Samples (0.5 ml) of the complex solutions were diluted 50-fold using a 25 ml volumetric flask. Prior to making up to volume with distilled water, 1 ml of PrP I.S. stock solution (1.25×10^{-3} M) was added after which 100 µl of the resultant dilution was injected under the HPLC described in section 2.4.2.

2.5.5 Phase solubility studies of chlorhexidine dihydrochloride in the presence of β- and HP-β-CyD

Solubility measurements were carried out according to the method of Higuchi and Connors (1965). Excess CHX was added to either 10 ml β-CyD solutions of various concentrations (0.00014 -0.0146 M) or 2 ml HP-β-CyD solutions (0.003-0.137 M) in screw-capped bottles. Each concentration of CyD solution was prepared in triplicate by appropriate dilution of a stock solution of either 0.0146 M β-CyD and 0.137 M HP-β-CyD respectively using distilled water as the solvent. Triplicate controls were also set up containing excess CHX in 10 ml distilled water. All suspensions were protected from light and were shaken in a water bath at the desired temperature for 4 days which was found to be sufficient time for equilibrium to be established. After this time period, a 1.5 ml aliquot from each suspension was placed in an Epindorf tube and centrifuged at 13000 *rpm* for 5 minutes. The CHX concentration of the supernatant was determined by HPLC, details of which are shown in section 2.4.2. For analysis of the β-CyD solutions, 1 ml of the supernatant was diluted 25-fold in a 25 ml volumetric flask using distilled water, but prior to making up to volume, 1 ml of the I.S. stock solution (propyl paraben, 1.25×10^{-3} M) was added. For the HP-β-CyD solutions, 0.5 ml of the supernatant was diluted 50-fold in a similar manner. In both cases, an injection volume of 100 µl was used.

The experiment was performed at 10, 25, 37 and 45°C. At each temperature, a constant amount of CHX was added to each β-CyD solution which ranged from 15 mg at 10°C to 30 mg at 45°C. Due to the high cost of the hydroxypropyl derivative, only 2 ml volumes of HP-β-CyD solution were prepared to which a constant amount of CHX was added ranging from 5 mg at 10°C to 20 mg at 45°C. A Churchill re-circulating cooling system was used to maintain the water bath at 10°C. When performing phase solubility analysis at this lower temperature, the CyD solutions and the distilled water controls were pre-cooled to 10°C for 1 hour prior to adding CHX. For all other temperatures, a thermostatically controlled shaking water-bath was used.

The concentration of CHX solubilised in each CyD solution was plotted versus CyD concentration for each CyD at each temperature. Stability constants were calculated from the linear portion of the solubility diagrams on a basis of a 1:1 stoichiometry using equation A3.13 in Appendix 3.

2.5.6 Dissolution studies in water using the dispersed powder method

Distilled water (30 ml) was placed in triplicate dissolution vessels each maintained at 37°C by a Churchill thermostatic water-pump which circulated water through a jacket surrounding the vessel body. Uniform mixing of the solvent was achieved by a small teflon coated magnetic stirring bar driven by an external motor. When the dissolution medium had reached the desired temperature, the equivalent amount of 165 mg of CHX, as the β-CyD complex (510 mg) or the equivalent amount of 380 mg of CHX as the HP-β-CyD complex (1.30 g), was accurately weighed and placed in the dissolution vessel. At appropriate time intervals, 1 ml samples were removed from each vessel with a Gilson automatic pipette and placed into Epindorf tubes. The samples were centrifuged for 5 minutes at 13000 *rpm* using a microcentrifuge. The CHX concentration of the supernatants was determined by HPLC, details of which are shown in section 2.4.2. For analysis of the β-CyD complex samples, 0.5 ml of the supernatant was diluted 50-fold in a 25 ml volumetric flask using distilled water, but prior to making up to volume, 1 ml of the I.S. stock solution (propyl paraben, 1.25×10^{-3} M) was added. For the HP-β-CyD complex samples, 0.25 ml of the supernatant was diluted 100-fold in a similar manner. In both instances, an injection volume of 100 µl was used for the HPLC assay. After sample removal, no additional solvent was added to the dissolution medium.

The above dissolution procedure was repeated with excess CHX (50 mg added to 30 ml distilled water) and the equimolar physical mixes for each CyD; 510 mg and 1.30 g of the corresponding β-CyD and HP-β-CyD mixes respectively were used. For each test powder, triplicate experiments were performed.

The dissolution experiments were performed using *Batch I* of the CHX-β-CyD complex and *Batch II* of the respective HP-β-CyD complex. The solubility of the other batches of complex for each CyD were also assessed by reducing the dissolution volume and hence using less complex. The amount of complex used varied with each batch since the CHX content was different in each case as determined in section 2.5.4. For each batch of complex, the equivalent amount of 28 mg of CHX, as the β-CyD complexes (~ 85 mg) or the equivalent amount of 64 mg of CHX as the HP-β-CyD complexes (~ 217 mg), were accurately weighed and added to 5 ml distilled water maintained at 37°C. The solubility of the each batch was determined in duplicate after 5 minutes and then after 4 days in a similar manner to that described above.

2.5.7 Dissolution studies with competing agents

The procedure employed was similar to that previously described in section 2.5.6 for the dissolution of the complex with minor modifications. On this occasion, the dissolution medium consisted of a 0.09 M phenylalanine (Phe) solution. The CHX-β-CyD complex (*Batch I*), 510 mg, was added to the 30 ml volume contained in the dissolution vessel and sampling was performed in a similar manner as before. When spironolactone (SP) was used as the competitor, 50 mg SP was placed in each dissolution vessel each containing 30 ml distilled water maintained at 37°C. This system was allowed to equilibrate for 30 minutes after which 510 mg of the complex was added and sampling carried out as previously described. Dissolutions were performed in triplicate for each competitor.

Quantification of CHX was determined by HPLC, details of which are shown in section 2.4.2. Details of sample preparation for HPLC assay were as described previously in section 2.5.6. Neither Phe or SP interfered with the assay of CHX.

2.5.8 Dissolution of chlorhexidine dihydrochloride, chlorhexidine digluconate, and the CyD complexes in HCl

2.5.8.1 Effect of increasing chloride ion concentration on the solubility of CHX in 0.1 M HCl

The solubility of CHX in the presence of increasing concentrations of chloride was determined. Using sodium chloride as the chloride source, appropriate amounts of the salt were dissolved in 100 ml volumes of 0.1 M HCl so that the final concentration of chloride ranged from 3.5 mg/ml to 6.2 mg/ml. Table 2.2 summarises the amount of NaCl used and the final concentration of chloride in the solution of HCl. The solubility of CHX at each chloride concentration was then determined as follows. The dissolution medium consisting of 20 ml 0.1 M HCl of various chloride ion concentration was placed in duplicate dissolution vessels maintained at 37°C by a Churchill thermostatic water-pump which circulated water through a jacket surrounding the vessel body. Uniform mixing of the solvent was achieved by a small teflon-coated magnetic stirring bar driven by an external motor. When the dissolution medium had reached the desired temperature, 20 mg (excess) CHX was added. At appropriate time intervals over a 3 hour period, 1 ml samples were removed from the test suspension with a Gilson automatic pipette and placed into Epindorf tubes. The samples were centrifuged for 5 minutes at 13000 *rpm* using a microcentrifuge. A sample of the supernatant (0.5 ml) was diluted 50-fold in a 25 ml volumetric flask using distilled water prior to quantification of CHX concentration by UV spectroscopy at 255 nm as discussed in section 2.4.1.

Table 2.2 Concentration and amount of chloride added to 100 ml of 0.1 M HCl as NaCl

Weight of NaCl added to 100 ml 0.1 M HCl (mg)	concentration of chloride mg/ml	Molar
0	3.55	0.100
89	4.44	0.125
178	5.33	0.150
266	6.21	0.175

2.5.8.2 Solubility of chlorhexidine dihydrochloride in 0.15 M HCl

The solubility of CHX in 0.15 M HCl was performed in a similar manner to that described in section 2.5.8.1 using 0.15 M HCl as the dissolution medium.

2.5.8.3 Solubility of chlorhexidine digluconate in 0.15 M HCl

The solubility of chlorhexidine digluconate (CHG) in acid was determined in a manner similar to CHX with modifications. The volume of 0.15 M HCl used was 19 ml to which 1 ml of the 20% v/v CHG solution was added. Due to the larger concentration of chlorhexidine being used, the supernatants recovered after centrifugation of the samples were diluted 50 to 1000-fold prior to quantification of CHX concentration by UV spectroscopy.

The above procedure was repeated adding larger volumes of CHG at time zero. The volume of acid used was adjusted accordingly such that the initial total volume of acid plus CHG was 20 ml. Table 2.3 contains the volume of CHG and HCl used and the theoretical concentrations of CHG at time zero. An example of how the CHG concentration was calculated is shown below:

Example calculation:

A 20 % v/v solution of CHG was used, which is equivalent to a molar concentration of 0.236 M. When 1 ml of this solution is added to 19 ml acid, a 20-fold dilution of CHG is performed, therefore the concentration of CHG is 0.236/20 = 0.0118 M

The other CHG concentrations were calculated in a similar manner.

Table 2.3 Concentration of chlorhexidine digluconate (CHG) at time zero

CHG volume (ml)	HCl volume (ml)	CHG concentration (M)
1.0	19.0	0.0118
1.5	18.5	0.0177
2.0	18.0	0.0236
2.5	17.5	0.0295

2.5.8.4 Solubility of the CHX-β-CyD and CHX-HP-β-CyD complexes in 0.15 M HCl

The solubility of the CyD complex in acid was assessed in a manner similar to its dissolution in water as described in section 2.5. The volume of acid used as the dissolution medium on this occasion was 20 ml to which the equivalent amount of 110 mg of CHX, as the β-CyD complex (340 mg), or the equivalent amount of 253 mg as the HP-β-CyD complex (866 mg) was added. At appropriate time intervals over a 2-day period, 1 ml samples were removed from the test suspensions and were centrifuged. The supernatants (0.5 ml) recovered from the β-CyD complex system were diluted 50-fold in a 25 ml volumetric flask with the addition of 1 ml PrP I.S. stock solution (1.25×10^{-3} M) prior to making up to volume. With the HP-β-CyD complex, 0.25 ml samples of the supernatants were diluted 100-fold in a similar manner. In both instances, quantification of CHX in the final samples was achieved by the injection of 100 µl under the HPLC conditions described in section 2.4.2. For each CyD complex, duplicate experiments were performed.

2.5.9 Dissolution studies in water using the rotating disk method

2.5.9.1 Design of dissolution apparatus

A Caleva dissolution apparatus was modified for use which consisted of 6 one litre dissolution vessels contained in a thermostatically controlled water bath. The aqueous dissolution medium contained in 100 ml beakers were held in each one litre vessel by means of a plastic support. The litre vessels contained in the water bath were also filled with water so that the dissolution medium was maintained at 37°C. For dissolution testing, 300 mg of the test powder was compressed into discs using an infra-red press which had a diameter of 13 mm. A compression pressure of 2000 kg/cm^2 for 2 minutes was used. These disks were placed into a teflon die in which only one surface of the disk was exposed. This disk holder was attached to a metal rod which was connected to the stirring motor of the Caleva dissolution apparatus in place of the normal stirring paddles. It was possible to perform six tests simultaneously. A diagrammatic representation of the apparatus is shown in figure 2.5.

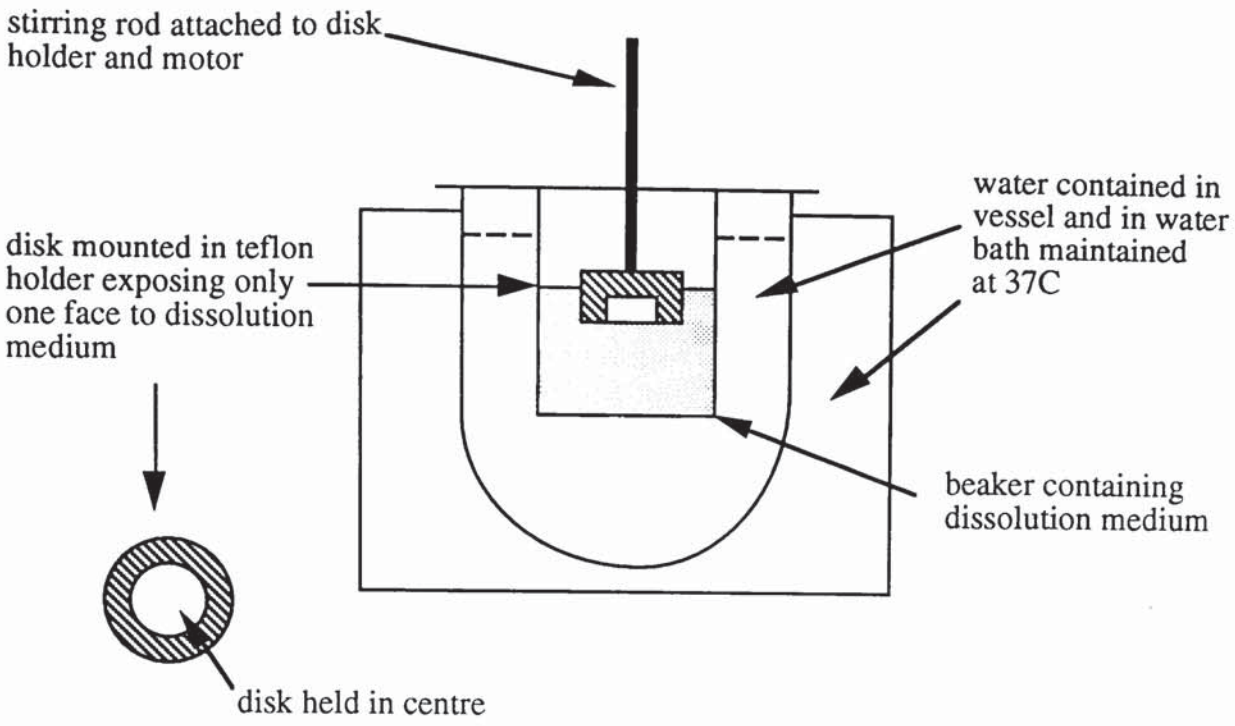

Figure 2.5 Diagrammatic representation of apparatus used for dissolution testing of compressed disks of CyD complexes

2.5.9.2 Dissolution testing

The dissolution medium (50 ml distilled water) contained in beakers was maintained at 37°C by a thermostatically controlled water bath. Once equilibrium had been established, rotation of the metal rods was started at a speed of 100 *rpm*, and the disks attached to the teflon holders were immersed into the dissolution medium. Samples (1 ml) were removed from each beaker at appropriate time intervals (usually every 2.5 minutes) up to a period of 30 minutes. These samples were diluted 2-fold by the addition of 1 ml of PrP I.S. stock solution (1×10^{-4} M) and their CHX concentrations were determined by HPLC using an injection volume of 100 µl as described in section 2.4.2. The volume of the dissolution medium was kept constant by replacement with distilled water. This procedure produced a dilution of the dissolution medium. It was necessary, therefore, to adjust each successive sample concentration for the dilution produced by all previous samples. This was performed by applying the following correction factor:

$$C_t = C_{mt} + V_s \frac{\sum_{t=1}^{t=n-1} C_m}{V_d} \qquad (2.1)$$

where C_t is the true concentration of drug in the dissolution vessel at time t, which would be found without dilution, C_{mt} is the current measured concentration of drug in the dissolution vessel, V_s is the volume of sample removed for analysis, V_d is the volume of the dissolution medium, and ΣC_m is the summed total of the previous measured concentrations (t =1 to n-1).

Samples for tablet dissolution testing included disks prepared from CHX alone, the respective equimolar physical mixes, the CHX-CyD complexes and from a 50 % w/w CHX/cellulose mixture. The dissolution of each type of disk was performed six times or more.

2..5.9.3 Tablet hardness testing

The hardness of the compressed disks of the CHX-CyD complex was tested with a Scheulinger 4M Instrument. For each CyD complex, 6 replicates were performed.

2.5.10 Diffusion studies on the CHX-β-CyD complex

2.5.10.1 General procedure

Franz diffusion cells consisting of donor and receiver chambers were used for the diffusion experiments. Experiments were performed using various types of membrane which included Amicon Diaflo ultrafiltration membranes of type YM1 (molecular weight cut-off 500 Da.) and YM2 (molecular weight cut-off 1000 Da.), Spectra/Por cellulose ester molecularporous dialysis membrane (molecular cut-off 500 Da. and 1000 Da.) and silicone membrane (0.02 inches thickness). The Amicon membranes were presented as 25 mm discs. The Spectra/Por dialysis membrane was presented in a continuous tubular form (19.7 mm diameter) of which a piece 3 cm in length was cut for use. With silicone membrane, a piece of approximately 3 cm^2 was cut for use. All membranes were washed in distilled water before use. The experimental procedure was essentially the same for all membrane types. Distilled water was used as the receiver solvent which was maintained at 37°C by a Churchill thermostatic water pump which circulated water through a jacket surrounding the cell body. However, prior to filling the receiver chamber, the water was initially boiled, sonicated and then cooled to 37°C. This procedure was essential for the elimination of air bubbles. A small magnetic flea was also added to the receiver chamber which was then clamped above a Camlab Variomag multipoint stirrer enabling uniform mixing of the receiver phase at a rate of 100 *rpm.* The use of this stirrer unit permitted the receiver solvents to be stirred at the same rate in each experiment. The washed membrane was then carefully mounted onto the donor cell with Parafilm. With the Spectra/Por membrane, the membrane was cut open and was mounted onto the donor cell so that the inner surface would be in direct contact with the donor sample. The donor cell was then

secured to the receptor chamber with Parafilm and held together by a spring clamp. The test sample was added to the donor compartment which was stirred by a glass rod driven by an external motor. Both the donor chamber and the receiver compartment sampling port were covered with parafilm to prevent evaporation of the solutions. All experiments were performed in triplicate. A diagrammatic representation of the Franz diffusion cell is illustrated in figure 2.6.

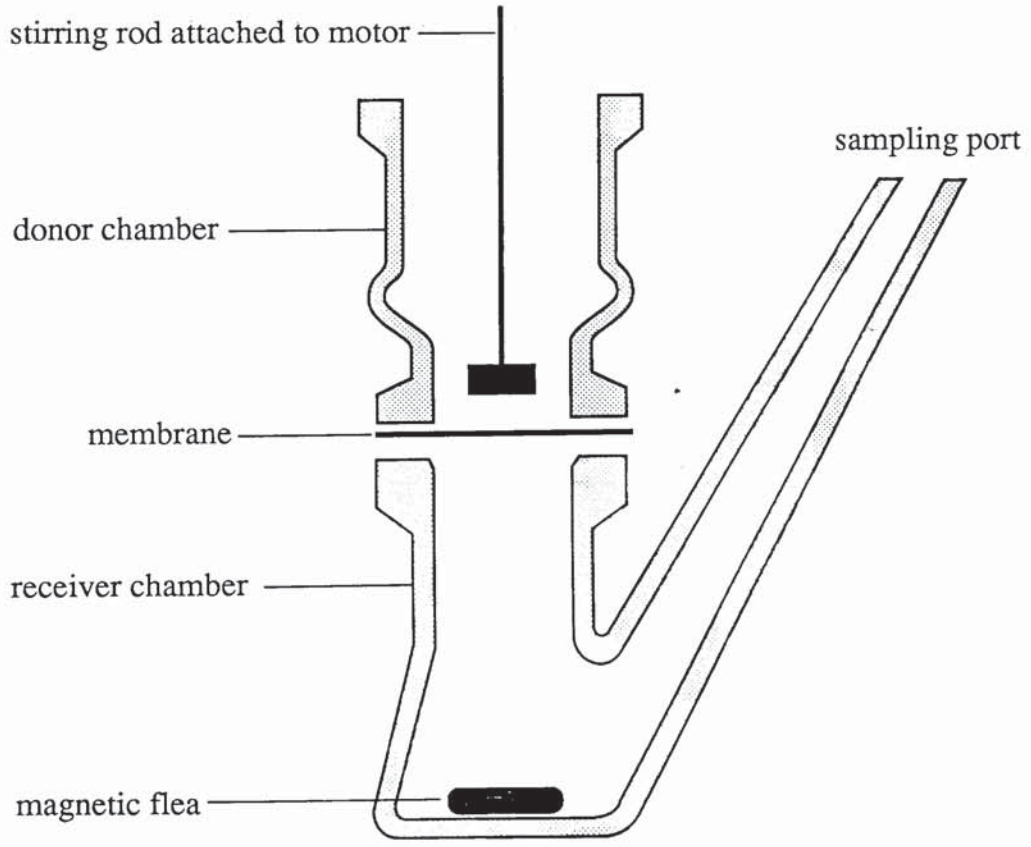

Figure 2.6 Diagram of Franz diffusion cell

At set time points (usually every 5 minutes up to 1.5 hours) 1 ml samples were removed from the receiver compartment, placed in a 1 ml quartz cuvette (1 cm path length) and their UV absorbance at 255 nm determined against distilled water as the reference solution. After UV assay the samples were returned to the receiver compartment. However, when the UV absorbance was greater than one, 200 µl of the receiver sample was transferred to an Epindorf tube to which 1 ml of distilled water was added. The UV absorbance of this 6-fold dilution was then determined. The volume of the receiver cell was maintained constant by replacement with 200 µl distilled water. This procedure produced a dilution of the receiver phase. It was necessary, therefore, to adjust each successive sample concentration for the dilution produced by all previous samples. This was performed by applying a similar correction factor to that described in section 2.5.9 (equation 2.1). However, in this case, C_t is the true concentration of drug in the receiver phase at time t, which would be found without dilution, C_{mt} is the current measured concentration of drug in the receiver compartment, V_s is the volume of sample removed for analysis, V_d is the volume of the receiver medium, and ΣC_m is the summed total of the previous measured concentrations (t =1 to n-1). This correction factor was applied to experimental data using a BASIC computer program written by W. J. Irwin, which also converted the molar concentrations to µmoles cm^{-2} membrane.

2.5.10.2 Diffusion of CHX from donor suspensions of free and complexed CHX using Amicon membranes of 1000 Da. molecular weight cut-off limit

The experimental procedure described in section 2.5.10.1 was followed, however, since this was only a preliminary assessment of the diffusion behaviour of free and complexed CHX, only one Franz cell was used for each test sample. A pre-saturated CHX suspension of CHX was prepared by adding excess drug (10 mg) to 10 ml of water and shaking overnight at 37°C. To the donor chamber, 5 ml of the pre-saturated suspension was added. Receiver samples were assayed by UV spectroscopy at 255 nm as described in 2.5.10.1. The concentration of CHX in the donor chamber was determined after 5 minutes of initiation of the experiment and at the end of the 1.5 hours study period by centrifuging 1 ml of the donor suspension at 13000 *rpm* for 5 minutes. The recovered supernatant was diluted 100-fold, and its UV absorbance determined at 255 nm.

To assess the diffusion of CHX from its β-CyD complex, 5 ml distilled water pre-heated to 37°C, was placed in the donor chamber to which 85 mg of the CHX-β-CyD complex (equivalent to 28 mg CHX) was added. Sampling of the receiver phase was done as previously described in 2.5.10.1. The CHX concentration of the donor was determined in a similar manner to that described for the donor suspension of CHX alone, however, on this occasion, the supernatants were diluted 500-fold prior to UV assay.

2.5.10.3 *Diffusion of β-CyD through various membranes from a saturated donor solution*

The diffusion behaviour of β-CyD was assessed through all 3 membrane types (Amicon, Spectra/Por and silicone) of both 500 Da. and 1000 Da. molecular cut-off limits where appropriate. The general experimental procedure described in section 2.5.10.1 was followed with each membrane using a saturated solution of β-CyD (0.0145 M) as the donor phase. For each membrane, the procedure was performed in triplicate. However, on this occasion no sampling of the receiver phase was done until after 5 hours when the receiver solution from each diffusion cell was carefully poured into a round bottom flask. The receiver solutions were then frozen by immersion into a dry ice-acetone bath and then lyophilised.

2.5.10.4 *Diffusion of CHX through various membranes from a donor suspension of drug alone*

The diffusion behaviour of CHX from a donor suspension of drug alone was assessed using all 3 membrane types. The procedure described in section 2.5.10.2 for the transport of CHX through Amicon membrane of 1000 Da. was followed replacing this latter membrane with Amicon and Spectra/Por membranes, both of 500 Da. molecular cut-off limits and silicone membrane.

2.5.10 Nuclear magnetic resonance spectroscopy for the study of inclusion complexation

β-CyD (12.77 mg) and CHX (5.78 mg) were each dissolved in 10 ml D_2O to give 1 mM stock solutions. Various quantities of the two solutions were mixed such that the final volume of all samples was constant and the total concentration was 1 mM. Each sample was left in a water-bath and shaken continuously at 37°C for approximately 8 hours. The experimental conditions were as follows: relaxation time 2 s, acquisition time 8 s, temperature 310 K (37°C), and approximately 5000 scans were collected for each spectrum. The chemical shifts were referred to the residual HOD signal in the solvent. Changes in chemical shifts were calculated by subtracting the chemical shift value of a proton in the complexed state from that of the same proton in the free state. Spectra were recorded with a Bruker AC 250 spectrophotometer at 250 MHz.

2.6 RESULTS AND DISCUSSION

2.6.1 Preparation of the solid phase β-CyD and HP-β-CyD complexes of chlorhexidine dihydrochloride

As previously discussed in section 1.5.4, various methods have been used for the preparation of solid complexes. The method of preparation will essentially depend on the properties of the guest. In this instance, CHX has low water solubility (60 mg/100 ml), 20°C), thus a purely aqueous system was used for preparation of the inclusion complex. The basis for the method of preparation of the CHX complexes was taken from Gallopo and Lynch (1989) who prepared the solid CyD complexes of CHX using the freeze-drying method. However, these researchers used excess (1.5 times) CyD as compared to the amount of CHX. From consideration of the CHX structure (figure 2.1), a 1:1 or 1:2 (CHX:CyD) complex could theoretically exist due to encapsulation of either one or both chlorophenyl rings respectively. The initial aim of this study was to prepare the 1:1 CyD solid phase complex, thus equimolar quantities of both CHX and CyD were used to prepare the complex. A white amorphous powder was obtained after lyophilization for the β-CyD and HP-β-CyD complexes of CHX.

The interactions in the solid complexes of CHX with β-CyD and HP-β-CyD were investigated using various techniques as described in section 2.5.3, and were compared to the corresponding physical mixes of the same molar ratio.

2.6.2 Investigation of the solid phase chlorhexidine dihydrochloride-CyD complexes

2.6.2.1 DSC

The thermogram of CHX (figure 2.7A) revealed an endotherm with an onset of approximately 260°C, which corresponds to the melting point of CHX (Merck Index). Following this, an exothermic peak was observed due to its consequent degradation as the heating process continued.

The β-CyD thermogram (figure 2.7B) showed a broad endotherm in the temperature range 90-120°C corresponding to the loss of water. In comparing this to the HP-β-CyD thermogram (figure 2.7C), the endotherm over this temperature range is less significant which is a direct consequence of the fact that the latter CyD contains less water as discussed later.

From the DSC thermograms, it can be seen that the melting point of CHX and the degradation temperature of CyDs are close together. Thermal analyses of the physical mixes (figures 2.5D and 2.5F for β-CyD and HP-β-CyD respectively) revealed an

endothermic peak at 260°C, followed by an exothermic peak. However, the thermograms of both CyD complexes (figure 2.7E and 2.7G for β-CyD and HP-β-CyD respectively) showed the endotherm for CHX to be almost completely absent as compared to their respective physical mixes. This reduction in the endothermic peak of CHX may be attributed to the formation of an inclusion compound. These thermograms also showed broad endotherms in the temperature range corresponding to the evaporation of water, suggesting that if a complex were present, a certain amount of water was also associated with its structure which has been quantified by thermogravimetric analysis as discussed in the following section.

Even though the melting point of CHX and the degradation temperature of the CyD were within close proximity of each other, it was evident from DSC analysis that CHX formed an inclusion complex with both β-CyD and HP-β-CyD.

2.6.2.2 Determination of water content by KF titration and TGA

KF titration and TGA are commonly used techniques for determination of water-content of pharmaceutical solids. Both these methods were employed to determine the water-content of the natural CyDs, α-, β- and γ-CyD and their respective hydroxypropyl derivatives (MS = 0.6). The moisture content of the CyD complexes were determined solely by TGA as this technique could be performed with a smaller sample weight. The moisture content will have a significant affect on the mechanical properties of the CyD complexes, as it directly affects their usefulness in tabletting (Szente, 1989). Properties affected by hydration include granularity, clumping tendency and also flow properties.

Karl Fischer Titration

The KF titration method involves the use of two indicator electrodes. Very simply, the technique can be described as follows (Johnson, 1988). The titrant used, Karl Fischer (KF) reagent, consists of a mixture of iodine, sulphur dioxide and pyridine dissolved in methanol. Iodide ions are liberated within the titration vessel which are involved in the reaction with water as shown in equation 2.2 (where R = pyridine, C_5H_5N). Once all the water has reacted, excess iodine is detected by an indicator electrode which results in an automatic halt in its generation. The indicator electrode consists of two platinum wires across which an a.c. (alternating current) is applied. In the presence of excess iodine a marked drop in voltage across these electrodes occurs which consequently halts its liberation. In this way, a quantitative relationship exists between the charge passed and the iodide generated from the reagent.

$$H_2O + R.I_2 + R.SO_2 + R + CH_3OH \longrightarrow 2R.HI + R.CH_3OSO_3H \qquad (2.2)$$

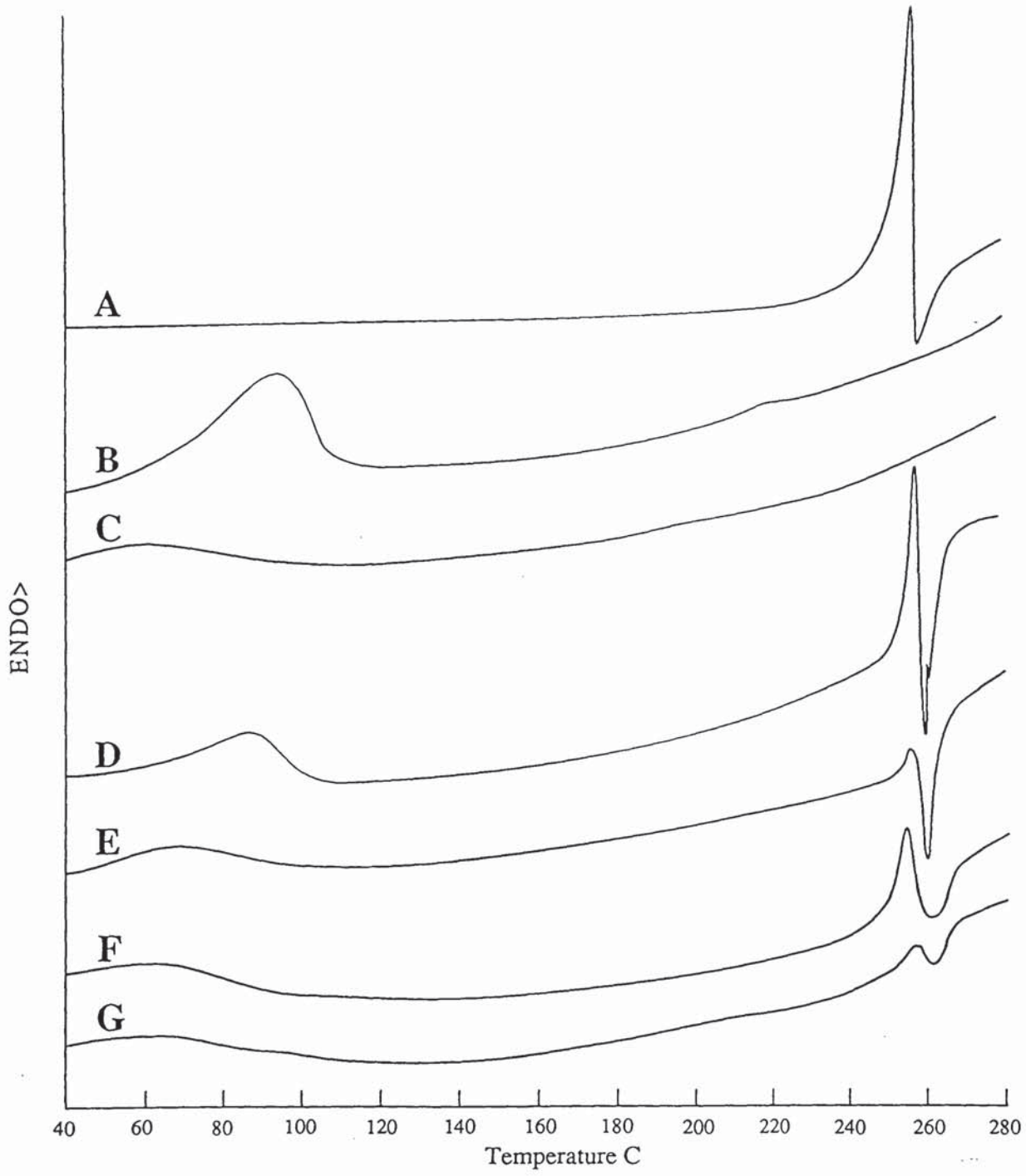

Figure 2.7 DSC thermograms of: A) CHX, B) β-CyD, C) HP-β-CyD, D) the physical mixture of CHX and β-CyD (molar ratio 1:1), E) the CHX-β-CyD complex, F) the physical mixture of CHX-HP-β-CyD (molar ratio 1:1), and G) the CHX-HP-β-CyD complex

The water content of both solids and liquids can be quantified using Karl Fischer titration. For solid test materials, a delay titration is performed which allows the sample sufficient time to dissolve in the solvent before the KF reagent is added. The delay time can be increased appropriately depending on the solubility of the solid.

From the calibration procedure, the mean volume of KF reagent required for titration of 20 µl (20 mg) of water was 3.907 ml (n=6, s.d.=1.00). The standard deviation value obtained was considered to be acceptable in accordance with the standard operating procedure for the instrument. Using these data, the weight of water corresponding to a specific volume of KF reagent was found as follows:

20 mg / 3.9070 = 5.119 mg/ml

Therefore, 1 ml of KF reagent was equivalent to 5.119 mg of water. Using this relationship the water content of the CyDs were calculated as shown in table 2.4.

Thermogravimetric Analysis

TGA can be used to provide quantitative data for the change in mass with increasing temperature. In the present study, the samples were heated *via* a controlled temperature programme (25 - 150°C) and the percentage weight loss was measured. During the heating programme, a gradual decline in sample mass occurred until reaching a plateau level at a temperature of approximately 110°C. As the heating process continued to 150°C, no further decrease in mass was observed. Since the boiling point of water is 100°C, the weight loss observed in this temperature range indicated the evaporation of water. The extent of water loss is dependant on the structure of the hydrated species. If the water molecules are tightly bound, for example by forming an integral part of the complex, a higher temperature may be needed for evaporation to occur. If water is loosely bound to the exterior of the complex, a lower temperature will be sufficient for evaporation to occur. An example of a typical thermogravimetric curve obtained is illustrated in figure 2.8. When heating was continued to above 250°C, weight loss occurred rapidly due to degradation of the CyD as expected.

The percentage moisture content of the CyDs as found from KF titration and TGA are contained in table 2.4. In comparing the values obtained *via* both methods, it can be seen that they were in close agreement. The natural CyDs have a higher water-content than their respective hydroxypropyl derivatives. This can be explained by the fact that the parent CyDs are crystalline hydrates containing a certain amount of water of crystallisation. The percentages of crystal water are 10.2, 13.2-14.5 and 8.13-17.7 %

for α, β and γ-CyD respectively (Szejtli, 1988). In addition, water molecules are taken up by the cavity of the CyDs, with the number of water molecules increasing as the CyD cavity size increase; 6, 11 and 17 water molecules are encapsulated by α-, β-, γ-CyD respectively (Parrish). The water content of a freeze-dried sample of β-CyD was found to contain 8.04 % water, compared with 12.58 % water for an untreated sample, indicating that a certain proportion of water was retained to maintain its crystal structure. In contrast to the parent CyDs, their hydroxypropyl derivatives are amorphous powders. As discussed earlier in section 1.4, production of the derivatives results in the final product being a heterogeneous mixture of thousands of isomers which causes the derivatives to be amorphous. The molecular mass of β-CyD and HP-β-CyD was corrected for the water content prior to use in this study. The % w/w water content used in each case were the means of the values found from KF and TGA studies and were 12.52 % for β-CyD and 3.58 % for HP-β-CyD.

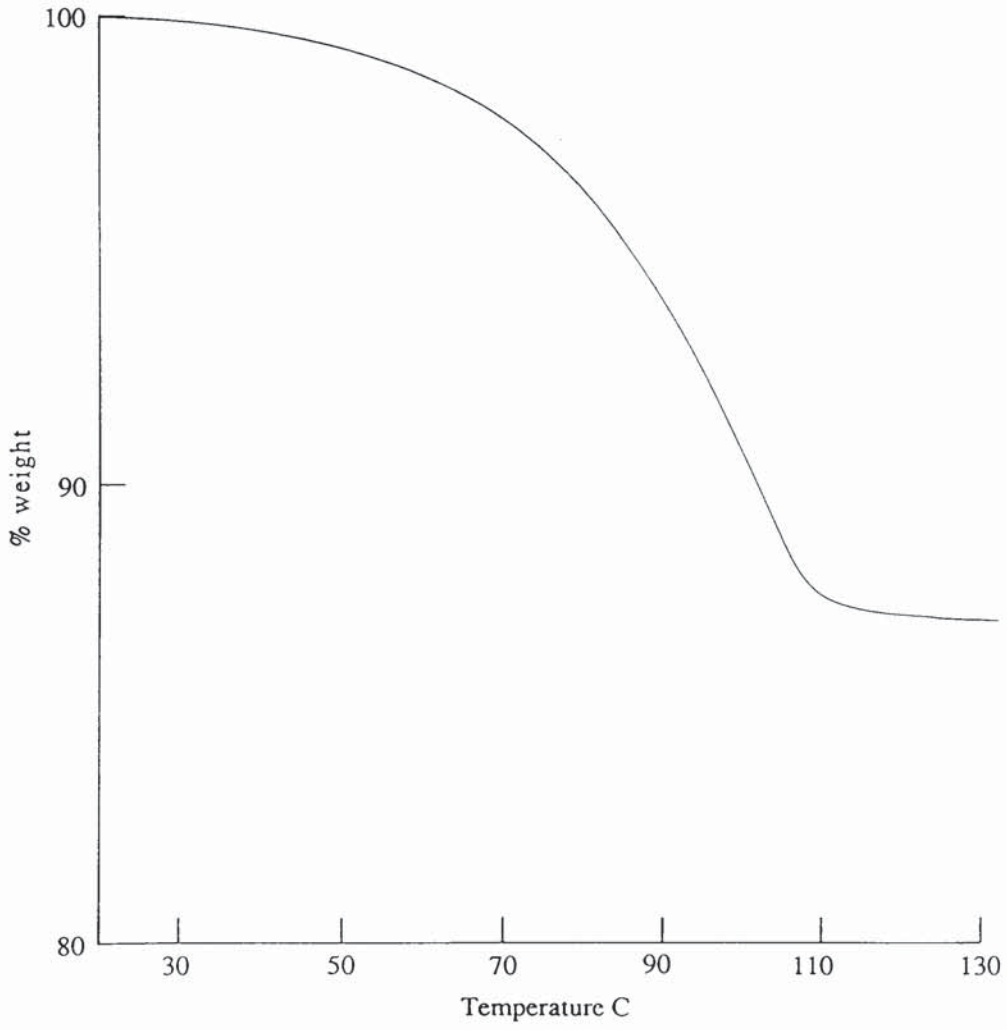

Figure 2.8 Example of typical thermogram of β-CyD obtained by TGA

Table 2.4 Percentage water-content of cyclodextrins (n = 3)

Cyclodextrin	KF titration mean % w/w ± s.d.	TGA mean % w/w ± s.d.
α-CyD	4.43 ± 0.15	4.92 ± 0.18
β-CyD	12.45 ± 0.71	12.58 ± 0.53
β-CyD (freeze-dried)	-----	8.04 ± 0.05
γ-CyD	5.13 ± 0.25	5.76 ± 0.25
hydroxypropyl-α-CyD	3.50 ± 0.10	3.98 ± 0.36
hydroxypropyl-β-CyD	3.28 ± 0.26	3.88 ± 0.14
hydroxypropyl-γ-CyD	2.70 ± 0.17	2.85 ± 0.56

The water-content of CHX, its CyD complexes (β-CyD and HP-β-CyD), and their physical mixes, as found by TGA, are shown in table 2.5 The CHX used in the study was found to contain minimal moisture (0.51 %).

The different batches of β-CyD complex, which were prepared on separate occasions, show varying degrees of hydration which are possibly due to variations in freeze-dryer efficiency. Similarly, differences were seen between the various batches of HP-β-CyD complex.

The water content of all batches of β-CyD complex are low compared to the hydration of intact β-CyD (12.52%) and the freeze-dried β-CyD (8.04 %). The CHX-β-CyD complex was prepared by the freeze drying method which resulted in an amorphous product as will be further confirmed by results of X-ray powder diffraction in section 2.6.2.4. The amorphous nature of the product indicates a loss of crystal structure and therefore a loss in crystal water. Hence, the hydration of the complex can be expected to be less than that of β-CyD alone. The effect of freeze-drying on the degree of hydration is illustrated well by comparing the water-content of the equimolar physical mix of CHX and β-CyD before and after the drying process. The freeze-dried mixture had a water-content of 2.85 % (± 0.22) whereas the untreated mix was found to contain 9.08 % (± 0.32) water. Since CHX itself is virtually dry, the majority of the water in the mix was probably due to the presence of β-CyD. The greater moisture content of the β-CyD complex (~ 5-7 % w/w) compared to the freeze-dried (2.85 % w/w) mix is due to the fact that the complex was prepared in an aqueous medium.

Table 2.5 Percentage water-content of free and complexed CHX as determined by TGA ($n = 3$)

Sample	mean % w/w water content ± s.d.
CHX	0.51 ± 0.02
CHX-β-CyD complex:	
Batch I	6.77 ± 0.28
Batch II	7.17 ± 0.48
Batch III	5.02 ± 0.04
Batch IV	6.30 ± 0.11
Batch V	5.96 ± 0.55
CHX-β-CyD physical mix (untreated)	9.08 ± 0.32
CHX-β-CyD physical mix (f/d)	2.85 ± 0.22
CHX-HP-β-CyD complex:	
Batch I	5.20 ± 0.57
Batch II	5.52 ± 0.49
Batch III	2.97 ± 0.41
CHX-HP-β-CyD physical mix	4.29 ± 0.33
CHX-HP-β-CyD physical mix (f/d)	3.37 ± 0.17

2.6.2.3 IR Spectroscopy

The β-CyD and HP-β-CyD spectra revealed absorption bands at the following frequencies due to certain functional moieties present in their structure:

3250-3500 cm^{-1}	OH stretching vibration
2900 cm^{-1}	C-H stretching vibration
1000-1200 cm^{-1}	C-OH stretching vibration

The spectrum of CHX also showed specific absorption bands due to the presence of the biguanide group:

3250 cm^{-1}	N-H stretching vibration
1500-1600 cm^{-1}	RC-NH-CR stretching vibration

The spectra of the equimolar physical mixes of both CyDs showed a combination of absorption bands due to the presence of both the CyD and CHX. The majority of the bands seen in the spectrum for both the β-CyD and HP-β-CyD complexes were similar to

those of the respective CyD alone. Figure 2.9 illustrates examples of spectra obtained for the CHX-β-CyD system. As discussed previously, since the CyD constitutes a high proportion of the total complex, inclusion of the guest may not induce any major changes. From these results it was concluded that IR spectroscopy could not be used to confirm the existence of a true inclusion complex.

2.6.2.4 X-ray Powder Diffraction

X-ray powder diffraction was performed on CHX, β-CyD, HP-β-CyD, the respective physical mixes of the CHX and CyDs and their complexes. The diffractograms of both CHX (figure 2.10A) and β-CyD (figure 2.10B) revealed continuous sharp peaks indicating their crystalline properties. This is in contrast to the behaviour of HP-β-CyD (figure 2.11B) which produced a diffractogram showing only one diffuse peak illustrating its amorphous nature.

The diffraction patterns of the physical mixes of CHX with both CyDs were simply the superposition of each component; the diffractograms for the CHX-β-CyD and CHX-HP-β-CyD mixes are shown in figures 2.10C and 2.11C respectively. The freeze-dried physical mixes (figure 2.10D and 2.11D for β-CyD and HP-β-CyD respectively), showed fewer peaks with reduced intensities than the respective intact physical mixes. The reduced crystallinity of the freeze-dried mixtures is probably a direct consequence of the lyophilisation process. X-ray diffraction studies performed on a freeze-dried equimolar mixture of α-CyD and methyl *p*-hydroxybenzoate showed the mix to be of an amorphous nature compared to untreated mix (Oguchi *et. al.*, 1989). The rate of freezing will also effect the degree of crystallinity in the final product. Rapid freezing results in a relatively amorphous product as compared to slow freezing. During the present study, all solutions were frozen rapidly with the aid of an acetone/dry ice bath. Both CyD complexes (figures 2.10E and 2.11E illustrate the diffractograms of the CHX-β-CyD and CHX-HP-β-CyD complexes respectively) gave diffuse patterns with hardly any distinctive peaks. The lack of crystallinity of the complexes suggests that all of CHX was encapsulated within the CyD cavities. X-ray diffraction studies have revealed significant differences between the freeze-dried control physical mixtures and the respective CHX-CyD complexes which further confirms that true inclusion complexes were formed.

Physical assessment of the CHX-CyD complexes, have revealed conclusive evidence that the complexes was formed in the solid state. Further investigations of the solid complexes include analysis of their chemical content (section 2.6.3), and dissolution and diffusion studies which are discussed later in sections 2.6.5 to 2.6.9. The interactions

between CHX and the CyDs in solution were also studied using phase solubility analysis (section 2.6.4) and NMR techniques (2.6.10).

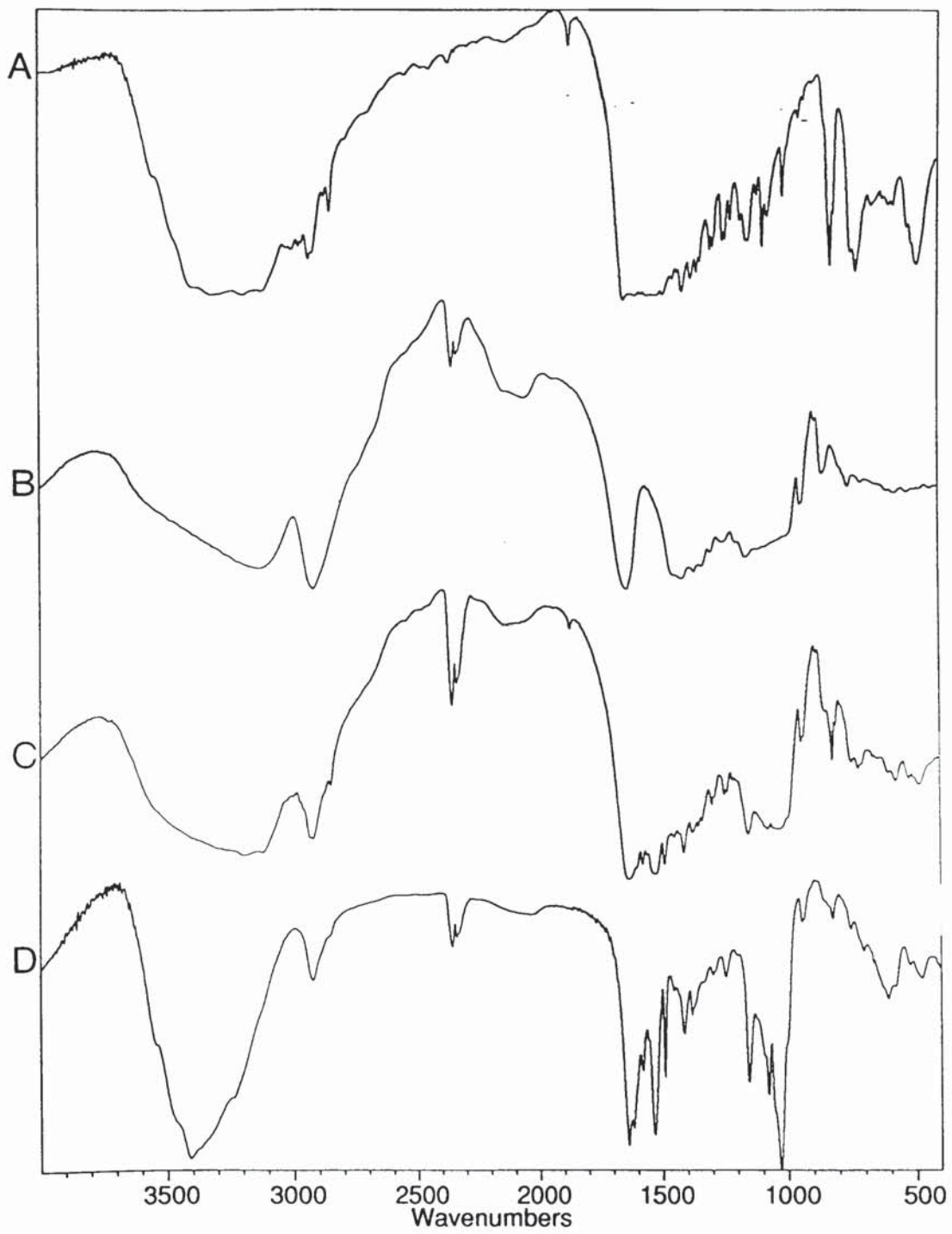

Figure 2.9 Examples of IR spectra: A) CHX, B) β-CyD, C) physical mix of CHX and β-CyD (molar ratio 1:1), D) CHX-β-CyD complex

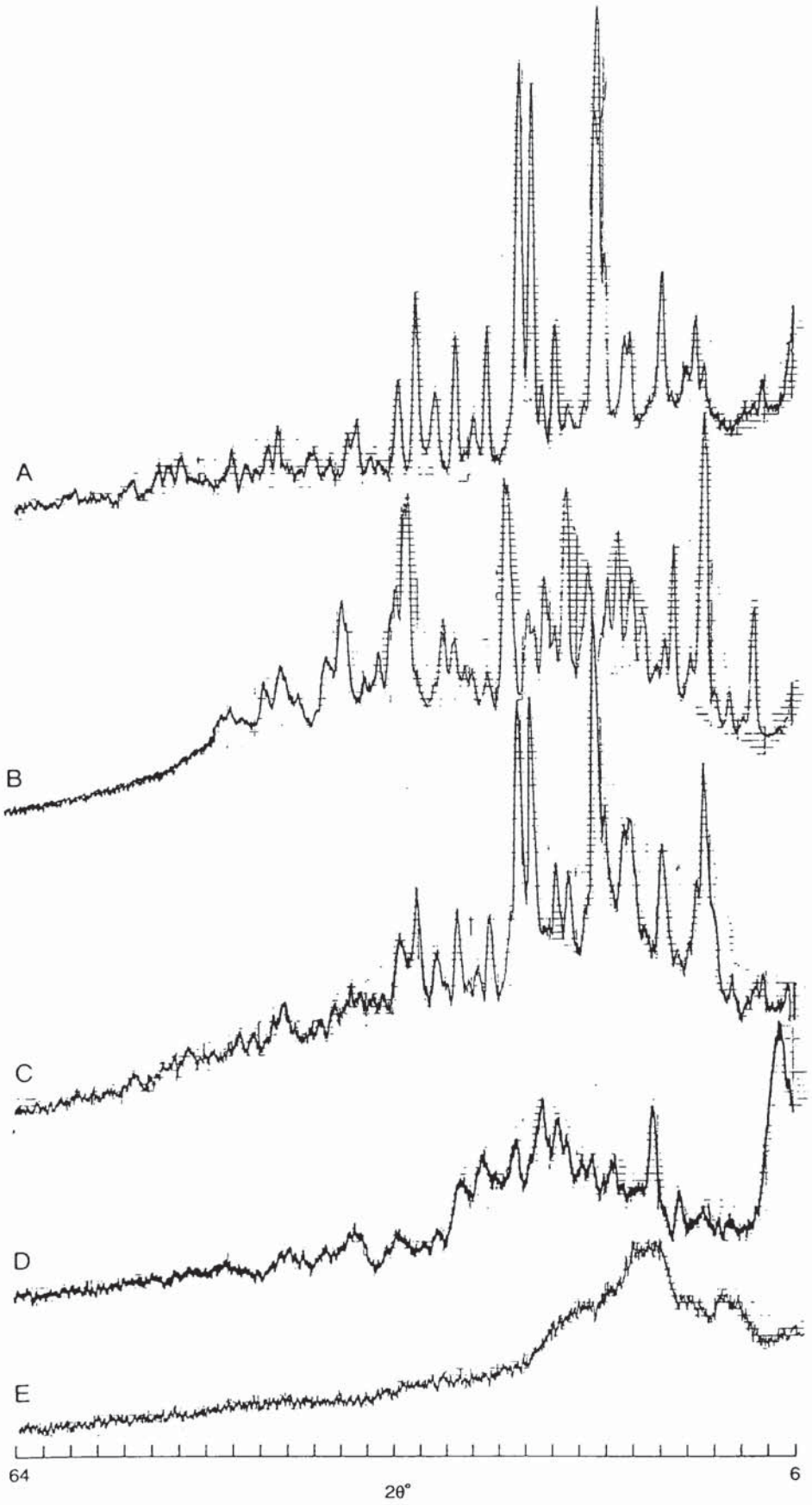

Figure 2.10 Examples of X-ray powder diffractograms: A) CHX, B) β-CyD, C) intact equimolar physical mix of CHX and β-CyD, D) freeze-dried equimolar physical mix of CHX and β-CyD, E) CHX-β-CyD complex

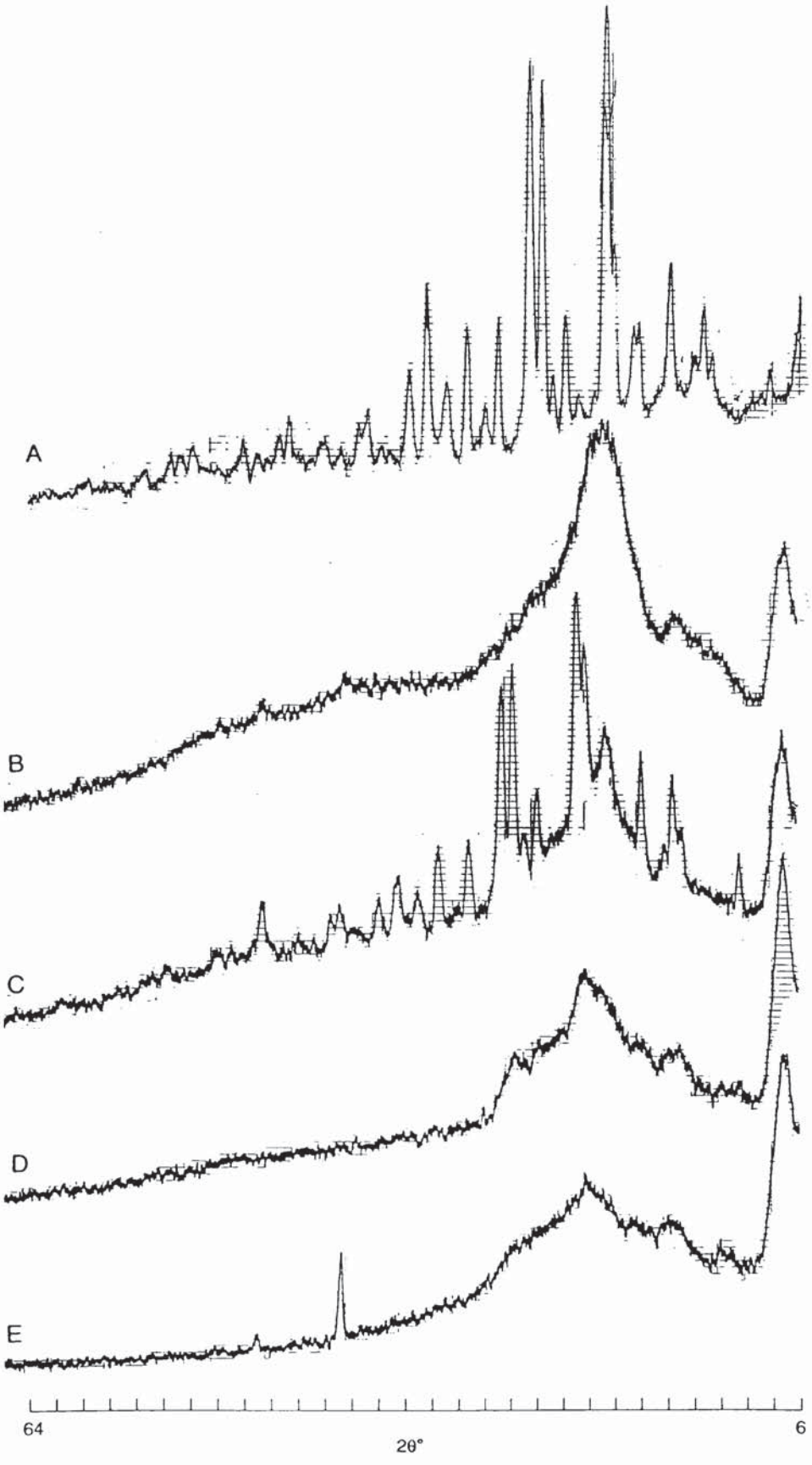

Figure 2.11 Examples of X-ray powder diffractograms: A) CHX, B) HP-β-CyD, C) intact equimolar physical mix of CHX and HP-β-CyD, D) freeze-dried equimolar physical mix of CHX and HP-β-CyD, E) CHX-HP-β-CyD complex

2.6.3 Chemical analysis of the chlorhexidine dihydrochloride-CyD complexes

The chemical content of CHX per weight of complex was determined by dissolving a known weight of complex in a specific volume of distilled water and determining the CHX concentration of the resulting solution. The amount of complex used (4 mg/ml) was below saturation such that no solid material was present. The drug content of all batches of β-CyD and HP-β-CyD complexes was determined. Each batch of complex was prepared on a separate occasion.

The theoretical weight of the 1:1 CHX-β-CyD and the 1:1 CHX-HP-β-CyD complex can be considered to be the sum of the molecular weights (M.W.) of both CHX and β-CyD and CHX plus HP-β-CyD, *i.e.*:

For the CHX-β-CyD complex:

1134.37 (β-CyD M.W.) + 578.4 (CHX M.W.) = 1712.77

However, the water content of the complex as determined by TGA (section 2.6.2.2) should also be accounted for as follows:

CHX-β-CyD complex: *Batch I*

water content = 6.77 % w/w,

therefore, 1712.77 x 1.0677 = 1828.7 = theoretical molecular weight of complex

The theoretical percentage weight of CHX per weight of *Batch I* complex is therefore:

578.4/1828.72 x 100 = **31.63 % w/w CHX**

Similarly for the CHX-HP-β-CyD complex:

M.W. of HP-β-CyD = (1134.37 + [0.6 x 58 x 7]) = 1377.97

where 0.6 = molecular substitution of parent β-CyD with hydroxypropyl groups

58 = molecular weight of hydroxypropyl group

7 = number of glucose molecules in CyD ring

1134.37 = M.W. of β-CyD alone

therefore M.W. of complex is as follows:

1377.97 (HP-β-CyD M.W.) + 578.4 (CHX M.W.) = 1956.37

CHX-HP-β-CyD complex: *Batch I*

water content = 5.20 % w/w,

therefore, 1956.37 x 1.052 = 2058.1 = theoretical molecular weight of complex

The theoretical percentage weight of CHX per weight of *Batch I* complex is therefore:

578.4/2058.1 x 100 = **28.10 % w/w CHX**

The theoretical drug content of CHX for each batch of complex for both CyDs was determined in a similar manner using the TGA results and are tabulated in table 2.6 for the β-CyD complexes and table 2.7 for the HP-β-CyD complexes. Also, shown are the respective stoichiometric ratios of CHX and CyD in the respective complexes.

An example calculation of the experimental drug content is shown below:
4.26 mg (in 1 ml distilled water) of *Batch I* CHX-β-CyD complex gave a CHX concentration of 2.2325 mM which is equivalent to 1.291 mg CHX per ml
thus, 1.291/4.26 x 100 = 30.31 %, *i.e.* % CHX per complex weight

The chemical content of all complex batches for both CyDs were calculated in a similar manner.

Table 2.6 Theoretical and experimental determinations of the chlorhexidine dihydrochloride (CHX) content of its β-CyD complexes. (Values represent the mean ± s.d., $n = 3$)

	% w/w CHX		stoichiometry (CyD:CHX)
	Theoretical value	Experimental value	
Batch I	31.62 ± 0.08	30.57 ± 0.92	1:0.97 ± 0.03
Batch II	31.50 ± 0.14	29.61 ± 0.72	1:0.94 ± 0.03
Batch III	32.14 ± 0.01	31.47 ± 0.41	1:0.98 ± 0.01
Batch IV	31.76 ± 0.03	31.24 ± 0.11	1:0.98 ± 0.01
Batch V	31.86 ± 0.16	30.12 ± 0.66	1:0.95 ± 0.02

Table 2.7 Theoretical and experimental determinations of the chlorhexidine dihydrochloride (CHX) content of its HP-β-CyD complexes. (Values represent the mean ± s.d., $n = 3$)

	% w/w CHX		stoichiometry (CyD:CHX)
	Theoretical value	Experimental value	
Batch I	28.09 ± 0.15	26.04 ± 0.29	1:0.93 ± 0.02
Batch II	28.01 ± 0.13	29.18 ± 0.80	1:1.04 ± 0.03
Batch III	28.70 ± 0.11	28.24 ± 0.25	1:0.98 ± 0.01

The theoretical chemical content values for each batch of complex differs slightly for each CyD which is direct consequence of their differing degrees of hydration which were taken into account when the calculating the theoretical molecular weight of the complexes. The theoretical and experimental values of drug content for each complex batch are similar to the expected theoretical values. If the stoichiometry of all batches of complex are considered, the ratio of CHX is within the range of 0.91 to 1.0 for the β-CyD complex and 0.91 to 1.07 for the HP-β-CyD complex. Ideally, a 1:1 stoichiometric ratio was expected for both CyD complexes since during their preparation equimolar quantities were used. However, although the minimum value deviated 9 % from the ideal 1:1 stoichiometric ratio, these experimentally determined values were accepted as being satisfactory since all complexes were prepared on a relatively small scale with no more than 10 g being prepared on each occasion, thus variations between batches were expected.

Ideally, the complex should have been washed with a suitable solvent to remove any free CHX and also uncomplexed CyD. If an organic solvent had been used, the free components themselves would not have been readily soluble. Furthermore, there was a risk of the solvent-CyD complex being formed. If water had been used for the washing process, both components are soluble, however, there was then a danger of the complex itself dissolving and therefore dissociating into its free components. Thus, for subsequent dissolution experiments, the CHX-CyD complexes were used as prepared without any pre-washing.

2.6.4 Phase solubility studies of chlorhexidine dihydrochloride in the presence of β-CyD and HP-β-CyD

Phase solubility studies were performed on CHX in the presence of β-CyD and also HP-β-CyD at various temperatures.

2.6.4.1 Interaction of CHX with β-CyD

All solubility isotherms obtained at the different temperatures showed a linear increase in CHX solubility up to the maximum concentration of β-CyD (0.0146 M). The solubility diagrams can be classified as the A_L type which indicate the formation of a soluble complex between β-CyD and CHX due to the formation of one or more molecular interactions between host and guest respectively (Higuchi and Connors, 1965). Figure 2.12 illustrates the solubility diagram obtained for the CHX-β-CyD system.

The slope of each diagram was found by linear regression, which was subsequently used to calculate the K_S values using equation A3.13 in Appendix 3.

$$K_S = \frac{\text{slope}}{S_0(1 - \text{slope})} \qquad \text{(A3.13)}$$

where S_0 represents the equilibrium solubility of CHX in the absence of CyD (the intercept on the y-axis).

Table 2.8 contains the slope of each line, S_0 and the K_S values found at each temperature using the above equation. Also, shown are the experimental values obtained for the equilibrium solubility of CHX alone, $S_{0\text{-Exp}}$.

The solubility of CHX alone and in the various β-CyD solutions increased with a rise in temperature. The saturation solubility of CHX increased from 0.732 mM (± 0.016) at 10°C to 2.736 mM (± 0.055) at 45°C. The S_0 solubility values found by linear regression were in close agreement with the experimental values of CHX solubility. In contrast to the effect of temperature on the solubility of CHX alone, in the presence of CyD the extent of CHX solubilisation decreased with a rise in temperature; at 10°C, an approximate 2.9-fold increase in CHX solubility was observed with the maximum concentration of β-CyD (0.0146 M) and at 45°C, the solubility of CHX was increased approximately 1.5-fold. The slope followed a similar trend showing a decrease from 0.09770 at 10°C to 0.09034 at 45°C. Furthermore, the stability constant of the CHX-β-CyD complex also decreased from 146 M^{-1} (10°C) to 36 M^{-1} (45°C) over the temperature range studied. These results therefore indicate that at higher temperature, the proportion of complexed drug was less than at lower temperatures which is a direct consequence of dissociation of the complex. The slope at 37°C, however, did not follow this general trend, but showed a higher than expected value (0.09845). The solubility isotherm of 37°C system indicates the possibility that the first 3 data points may have caused deviation of the slope. By omitting these data from linear regression, the slope was reduced to 0.097886 (from 0.09845) which is closer to the values obtained at the other temperatures (range 0.09034 to 0.09770). This illustrates the sensitive nature of the slope, and therefore also the magnitude of K_S, to slight changes in the data values.

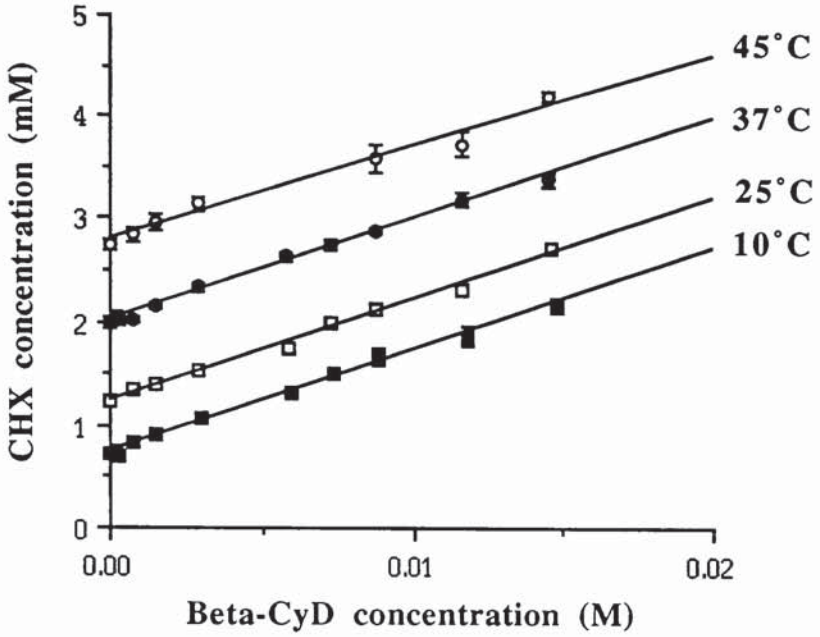

Figure 2.12 Phase solubility diagram of CHX-β-CyD system in distilled water at various temperatures. Points represent mean ± s.d., $n = 3$.

Table 2.8 Summary of solubility data for the CHX-β-CyD phase solubility system ($S_{0\text{-}Exp}$ are the experimental values for the equilibrium solubility of CHX in the absence of CyD and are the mean ± s.d., $n = 3$).

Temperature (°C)	Slope	S_0 ($M \times 10^3$)	$S_{0\text{-}Exp}$ ($M \times 10^3$)	K_S (M^{-1})	r^2
10	0.09770	0.7424	0.7322 ± 0.016	146	0.995
25	0.09738	1.2495	1.2356 ± 0.023	86	0.993
37	0.09845	2.0083	1.9936 ± 0.049	54	0.994
45	0.09034	2.7923	2.7361 ± 0.055	36	0.981

At all temperatures, the slope of the solubility diagram was less than one, from which a 1:1 stoichiometry for the complex was assumed (Higuchi and Connors, 1965). If, however, the slope was greater than one, the general formula of the complex formed is considered to be G_xCyD_y, where x is greater than one, *e.g.*, G_2CyD, G_3CyD and G_4CyD. In these systems, equation A3.13 in Appendix 3 cannot be used for the calculation of the stability constant of the complex (Higuchi and Connors, 1965) since a 1:1 stoichiometry for the complex can not be assumed.

K_S values ranged from 146 M^{-1} at 10°C to 36 M^{-1} at 45°C. The magnitude of these K_S values indicate a relatively weak interaction between CHX and β-CyD. K_S values can range form 10 to 20,000 M^{-1} or more. As previously discussed, certain factors affect the magnitude of K_S which include the hydrophobic nature of the guest and also steric factors involved in inclusion of the guest within the CyD cavity. The CHX molecule comprises 2 chlorophenyl moieties linked together by biguanide groups and a methylene chain as shown in figure 2.1. On the basis of the geometry of this guest type, it is therefore unlikely that the complete CHX molecule is encapsulated within the CyD cavity. Furthermore, as previously discussed bisbiguanides contain both hydrophilic and hydrophobic functionalities, and it therefore follows that it is these latter moieties which will interact with the CyD cavity. However, since CHX has 2 aromatic moieties it is possible that both chlorophenyl moieties are encapsulated. During the course of this work, Qi and co-workers reported the interaction between chlorhexidine diacetate and β-CyD in solution by UV spectroscopy and reported the existence of both 1:1 and 1:2 CHX-β-CyD complexes in solution. Furthermore, the K_S values for these complexes were 287 M^{-1} and 268 M^{-1} respectively. The differences between these values and the present study may be due the different conditions under which complexation was studied. As previously discussed, determination of K_S values by different methods can lead to widely deviating values. The K_S values for the CHX-β-CyD complex for the present study were calculated on the assumption that a 1:1 stoichiometric complex was formed in solution. NMR spectroscopy has been used to determine the stoichiometry of the CHX-β-CyD complex and to elucidate the possible mode of inclusion of CHX as discussed later.

When complexes of low stability are administered orally, rapid dissociation occurs in the gastrointestinal fluid resulting in high free drug concentrations, which should theoretically lead to rapid increases in blood levels. With consideration of the aims of this study as discussed in section 1.8, absorption of CHX is not required; however, rapid dissociation of the complex would provide a high free drug concentration for an enhanced local antimicrobial effect (further discussed in section 2.6.8; dissolution of complex). Thus, complexes of low K_S values may prove beneficial when a rapid biological response is required. Low stability constants for other guest species have also been reported. Cabral Marques *et. al.* (1990), found K_S values of 66-69 M^{-1} for the β-CyD complex inclusion complex of salbutamol. K_S values between 13 and 81 M^{-1} for β-CyD complexes with thiazides were found by Corrigan and Stanley (1982). Uekama *et. al.* (1983), reported similar low K_S values in benzodiazepine systems and suggested that the results were due the low lipophilicity of the guests and also to their poor compatibility to the CyD cavity.

As the temperature was decreased, the interaction between CHX and β-CyD became stronger as seen with an increase in K_S values. This reflects dissociation of the complex at the higher temperatures and shows the expected exothermic nature of the complexation process. The effect of temperature on the equilibrium constant was illustrated by the van't Hoff plot which was obtained by plotting ln K_S against absolute temperature as shown in figure 2.13.

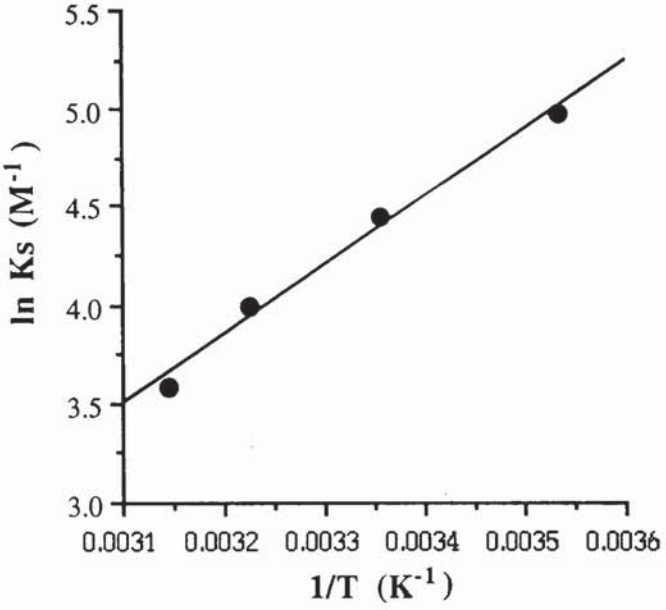

Figure 2.13 Temperature dependence of the equilibrium constant of the CHX-β-CyD complex illustrated by the van't Hoff plot
($y = -7.4578 + 3532.7x$, $r^2 = 0.989$)

The van't Hoff equation is as follows:

$$\ln K = \frac{\Delta S}{R} - \frac{\Delta H}{R} \cdot \frac{1}{T} \qquad (2.3)$$

where, K = complex stability constant K_S (M^{-1})
S = entropy, J K mol^{-1}
H = enthalpy, kJ mol^{-1}
T = absolute temperature (Kelvin, K)
R = gas constant, 8.314 J mol^{-1} K^{-1}

The van't Hoff plot was close to linear over the temperature range employed ($r^2 = 0.989$). Linear regression was employed to find the equation of the plot from which the thermodynamic parameters of the inclusion process were found. The intercept on the y-axis, when 1/T was equal to zero, is equal to $\Delta S/R$ and the gradient of the plot is equal to $-\Delta H/R$. Table 2.9 contains the thermodynamic parameters of complexation as found from the graph.

Table 2.9 Thermodynamic parameters of the CHX-β-CyD complexation process

ΔH	-29. 4 kJ mol^{-1}
ΔS	- 62 J K mol^{-1}

The change in free energy, ΔG was found using the following equation:

$$\Delta G = - RT\ln K \qquad (2.4)$$

The K_S values for the CHX-β-CyD complex as found during phase solubility analysis were substituted in the above equation together with the respective temperatures (absolute temperature, K) at which the phase solubility experiment was performed. This was repeated using all temperatures; the corresponding ΔG values are illustrated in table 2.10.

Table 2.10 Free energy change (ΔG) for the CHX-β-CyD complexation reaction performed at various temperatures

Temperature (°C)	ΔG kJ mol^{-1}
10	-11.73
25	-11.04
37	-10.28
45	-9.47

The free energy change is a measure of the useful work that a system is capable of doing. If ΔG is negative, work will be done by the system and the reaction will proceed. Thus, from the ΔG values obtained for the CHX-β-CyD system, the negative values indicated that complex formation was a feasible process at all temperatures. With increasing temperature, the magnitude of ΔG also increased which further confirms the fact that, at higher temperatures, complex formation is less favoured. Thus the proportion of

complexed drug will be less with a shift in the equilibrium process such that the complex dissociates into its free components as illustrated in scheme 3.

Scheme 3: The effect of temperature on the dissociation equilibrium of the complex

As previously discussed, Qi and co-workers reported the existence of both 1:1 and 1:2 chlorhexidine diacetate:β-CyD complexes. Using microcalorimetry, the thermodynamic parameters for this complexation process were found to be: for the 1:1 complex, ΔH = -24.6 ± 1.9 kJ mol^{-1}, ΔS = -36 J K mol^{-1}, ΔG = -14 kJ mol^{-1} (25°C) and for the 1:2 complex, ΔH = -35.6 ± 6.6 kJ mol^{-1}, ΔS = -73 J K mol^{-1}, ΔG = -13.9 kJ mol^{-1} (25°C). This data correlated well with the data obtained during the present study (ΔH = 29.4 kJ mol^{-1}, ΔS = -62 J K mol^{-1}, ΔG = -11.04 kJ mol^{-1} at 25°C).

Several CyD review articles (Clarke, Coates and Lincoln, 1988; Saenger, 1980) contain many examples of the thermodynamic parameters for the complex formation between CyDs and a variety of guest molecules. When ΔH is plotted *versus* ΔS, a linear relationship is observed, known as a 'compensation' effect. This correlation means that in the various guest-CyD systems, parallel changes were seen in both the entropy and enthalpy which compensated from each other and thus, as a consequence, only minor changes were seen in the free energy of the complexation process. This relationship implies that a similar mechanism must operate in the different guest-CyD systems which contributes to this compensation effect. Since the guest substrates employed varied widely in their chemical structure, the common link between the different guest-CyD systems were the solvent and the host (Clarkes, Coates and Lincoln, 1988). Compensation effects of this nature have been observed in aqueous solution (Lumry and Rajendra, 1970), which were a result of changes in the solvation of the solutes participating in the reaction. With consideration of this entropy-enthalpy compensation phenomena, is most likely that changes in solvation of both the guest and CyD play an important role in determining the stability of the resultant inclusion complex.

A reaction in which the solvent becomes more disordered will usually proceed with a favourable entropy change but the solvent disordering will be accompanied by the breaking of some solvent-solvent bonds which will result in an unfavourable enthalpy change. This is a very simplistic description of the compensation effect which is limited to highly ordered and hydrogen bonded solvents such as water (Lewis and Hansen, 1973).

As can be seen above, the enthalpy of formation of the CHX-β-CyD inclusion complex is negative (ΔH = -29.4 kJ mol^{-1}), indicating that complex formation is exothermic. Hence, there is a release of energy which favours formation of the complex (Otero-Espinar *et. al.*, 1992). The enthalpy change for the formation of the naproxen-β-CyD complex in aqueous solution (pH=1) was found to be -22.5 kJ mol^{-1}, from which it was suggested that hydrogen bonds between the guest and host participated in the formation of the complex (Otero-Espinar *et. al.*, 1992). It is also possible that hydrogen bonds were involved in the formation of the CHX-β-CyD complex; hydrogen bonds may have been formed between the nitrogen atoms of the CHX molecule and the CyD, between CHX and the solvent, and between the solvent molecules themselves. As previously discussed, other bonding mechanisms which may also play a role in the guest-host interactions include van der Waals-London dispersion forces, hydrophobic bonding interactions and energy release by substitution of the water molecules contained within the CyD.

The large ΔH value (-29.4 kJ mol^{-1}) for the formation of the CHX-β-CyD complex, could more than compensate for the unfavourable ΔS value (-62 J K mol^{-1}). If ΔH is small, the entropy value will be large indicating a greater degree of disorder after complex formation. However, if ΔH is large, the entropy is negative and complex formation will result in a higher order of the system (Szejtli, 1988). For example, the enthalpy of formation for the naproxen-β-CyD complex at pH 5 was relatively small at -9.04 kJ mol^{-1} whereas the entropy value was 20.75 J K^{-1} mol^{-1} (Otero-Espinar *et. al.*, 1992). In contrast, Tong *et. al.* (1991) reported an unfavourable entropy change (-45.4 J K^{-1} mol^{-1}) for the formation of the orphenadrine hydrochloride-β-CyD complex but this was compensated for by the favourable enthalpy change (-31.27 kJ mol^{-1}).

In the CHX-β-CyD system, the unfavourable entropy change indicates an increased order in the system. The entropy change during the complexation process depends on whether there is an increase or decrease in the order of the water structure in the system (Frank and Evans, 1945). Water plays a crucial role in complex formation since hydration of the CyD complex is energetically favoured when compared to hydration of the components. This phenomenon is known as hydrophobic interaction, and is primarily due to the intrinsic cohesion of water in the bulk solvent rather than to the mutual attraction of the two relatively apolar components (Jencks, 1969).

The thermodynamics involved in the formation of the CHX-β-CyD complex can be summarised as follows. The large enthalpy change found for the formation of the CHX-β-CyD complex results from the formation of hydrogen bonds between the guest and

host and between the water molecules that become part of the bulk water during the reaction (*i.e.* water displaced from the CyD cavity becomes bulk water and as such is hydrogen bonded). The net result must be a gain in the number of hydrogen bonds. The unfavourable entropy change is assumed to result from the greater ordering of the displaced water molecules in the bulk water structure (Lewis and Hansen, 1973). It is probable that the unfavourable entropy change was compensated for by the favourable enthalpy change. Therefore, in conclusion, the results indicated that the formation of the CHX-β-CyD complex in solution was an energetically feasible process.

2.6.4.2 Interaction of CHX with HP-β-CyD

HP-β-CyD has a greater aqueous solubility than the parent β-CyD, thus HP-β-CyD solutions of up to 0.137 M (~ 20%) were used during phase solubility studies. As discussed previously in section 1.4, aqueous solutions of up to 70 % w/v HP-β-CyD have been prepared. However, with increasing concentration, the viscosity also increases. Therefore, the HP-β-CyD solutions prepared for this study were no greater than 20 % w/v.

At all temperatures, the solubility of CHX increased with increasing HP-β-CyD concentration. With the maximum concentration of HP-β-CyD (0.137 M) used, an approximate 4-fold enhancement in CHX solubility was observed. This was greater than the solubility enhancement observed with β-CyD (approximately 2-fold), however, the maximum concentration of β-CyD used was limited to 0.0146 M due to its relatively poor water-solubility.

In contrast to the HP-β-CyD system, the CHX-β-CyD system showed linearity (Type A_L diagram) over the entire concentration range of β-CyD (0.00014 - 0.0146 M), whereas, the solubility diagrams of the CHX-HP-β-CyD system were of the A_N type. Figure 2.14 illustrates the solubility diagram for the CHX-HP-β-CyD system at the different temperatures. The initial portion of the solubility isotherms up to HP-β-CyD concentrations of 0.03 M were relatively linear, thus linear regression was applied to these data points to obtain the slope and S_0 values which were then used for the subsequent calculation of K_S using equation A3.13 in Appendix 3. The initial portion of the phase diagrams are illustrated in figure 2.15 with the respective solubility data contained in table 2.11.

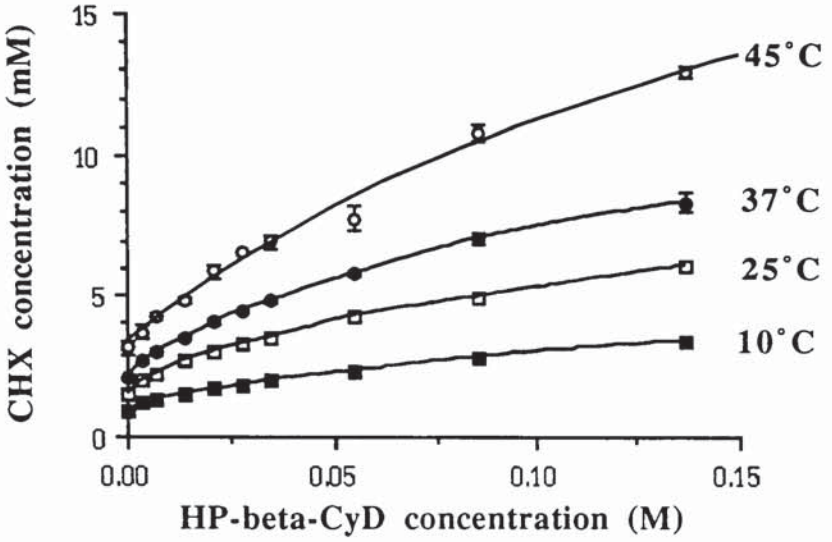

Figure 2.14 Phase solubility diagram of CHX-HP-β-CyD system in distilled water at various temperatures. Points represent mean ± s.d., $n = 3$.

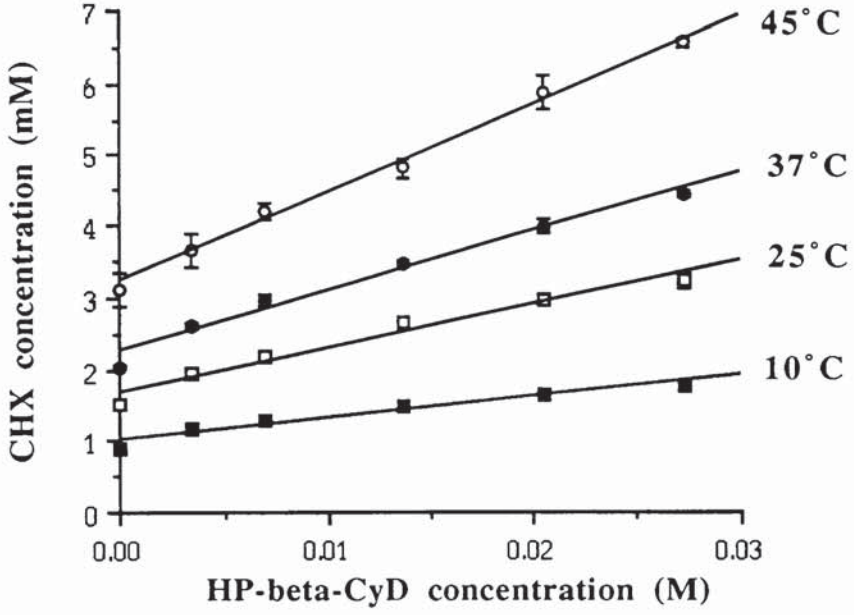

Figure 2.15 Initial portion of phase solubility diagram of CHX-HP-β-CyD system in distilled water at various temperatures. Points represent mean ± s.d., $n = 3$

Table 2.11 Summary of solubility data for the CHX-HP-β-CyD system illustrated in figure 2.15. ($S_{0\text{-}Exp}$ are the experimental values for the equilibrium solubility of CHX in the absence of CyD and are the mean ± s.d., $n = 3$)

Temperature (°C)	Slope	S_0 ($M \times 10^3$)	$S_{0\text{-}Exp}$ ($M \times 10^3$)	K_S (M^{-1})	r^2
10	0.02926	1.0197	0.8819 ± 0.067	30	0.954
25	0.06094	1.6816	1.4021 ± 0.081	39	0.966
37	0.08367	2.2429	2.0215 ± 0.054	41	0.979
45	0.12464	3.2091	3.0126 ± 0.140	44	0.994

The slopes of the solubility isotherms for the HP-β-CyD system increased with a rise in temperature. In contrast, the β-CyD system followed the opposite trend. On this basis, it therefore seems that the complexing ability of HP-β-CyD increased with increasing temperature.

As shown in table 2.11, the S_0 values found from linear regression deviated from the experimentally determined solubilities of CHX as indicated by $S_{0\text{-}Exp}$. The deviations are due to the fact that linear regression was applied which draws a line of best fit through the data points. Since even the initial portions of these phase solubility diagrams have a slight tendency to deviate from linearity, the intercept is placed higher than the experimentally determined solubility values. The relative linearity of the CHX-HP-β-CyD diagram is reflected in the respective correlation coefficient (r^2) values at each temperature.

There is little difference between the K_S values at the temperatures measured, but in contrast to the β-CyD system, the HP-β-CyD complexes show an increase in K_S with a rise in temperature. These K_S values may not be a true representation of the interaction of CHX with HP-β-CyD as the overall relative linearity of the phase diagram was low. Thus, by using linear regression, the resulting K_S values may be distorted.

The data obtained at 45°C showed greater linearity than at the other temperatures ($r^2 = 0.994$). Comparing the K_S values for the interaction of CHX with both β-CyD and HP-β-CyD at 45°C, *i.e.* 36 M^{-1} and 44 M^{-1} respectively, it can be seen that similar values were obtained, suggesting that the affinity of CHX for both β-CyD and HP-β-CyD was alike at this temperature. Furthermore, at 45°C, the solubility enhancement with 0.0136 M HP-β-CyD was 1.5-fold and with 0.0146 M β-CyD an equivalent solubility

enhancement was observed. At the other temperatures, the K_S values for the HP-β-CyD complexes were lower than the respective values for the β-CyD system suggesting that the complexing ability of parent CyD was greater. As discussed previously in section 1.5.1, the cavity diameter of HP-β-CyD is essentially similar to the parent β-CyD. Thus, the complexing ability of both CyDs could be expected to be similar. However, the dimensions of the β-CyD cavity volume are affected by derivatisation due to rotation of the hydroxypropyl substituents. This modification may consequently affect the extent of penetration of the guest into hydrophobic cavity. HP-β-CyD is generally considered to more effective than β-CyD due to its greater aqueous solubility. However, there have been instances where HP-β-CyD is a weaker solubiliser that the parent β-CyD itself. Using equimolar CyD concentrations (15 mg/ml), Szejtli (1992) found a 90-fold enhancement in the solubility of digoxin in the presence of β-CyD, whereas with HP-β-CyD only a 57-fold increase was observed.

As discussed previously, the A_N type behaviour of the CHX-HP-β-CyD phase solubility system may result from a large host concentration affecting the nature of the solvent. Thus, it is possible that with increasing HP-β-CyD concentration the viscosity of the solvent increases due to intermolecular hydrogen bonding between the CyD molecules. An experiment which could be performed to confirm whether the increased host viscosity is responsible for the A_N type behaviour, is to add sufficient glucose to solutions of β-CyD such that the viscosity is equal to the HP-β-CyD solutions.

Another explanation for the negative deviation seen in the CHX-HP-β-CyD system could be due to the effect of pH. Similar A_N type diagrams were seen for the interaction of hydroxypropyl CyD derivatives with piroxicam, diclofenac and indomethacin (Backensfeld, Bernd and Kolter, 1991). These researchers found that with an increase in guest concentration by solubilisation with the CyD, the pH decreased which affected the saturation concentration of free drug. When measuring the pH of the CHX-HP-β-CyD solutions, it was found that a saturated solution of CHX alone (2.028 ± 0.024 mM; 37°C) had a pH of 6.43, whereas a solution of CHX with 0.068 M HP-β-CyD (6.137 ± 0.056 mM CHX) had a pH of 6.03. Hence, the theory put forward by Backensfeld and co-workers may also help explain the solubility behaviour of the CHX-HP-β-CyD system. However, since chlorhexidine has pK_a values of 2.2 and 10.3, this relatively small change in pH will have a marginal effect. The increase in CHX concentration by CyD solubilisation will also increase the effective amount of hydrochloride in solution which will lower the pH. Prior to complexation of CHX by the CyD, the CHX itself has to be solubilised. However, as shown later in section 2.6.7, the solubility of CHX in 0.1 M HCl (0.267 mM ± 0.015 mM) was lower than that in distilled water (~ 2 mM) but

this was due to the common ion effect of the chloride ions rather than due to the acidity of the solution. The solubility of CHX in 0.1 M HCl was further reduced with increasing concentrations of chloride. Thus, it is possible that at higher CyD concentrations, the subsequent solubility enhancement of CHX solubility leads to an increase in the relative concentration of chloride in solution, and as a consequence the solubility of CHX alone in solution is limited. In respect of this, the amount of CHX alone in solution cannot increase linearly which results in an A_N type diagram.

The negative deviations in the HP-β-CyD system were most pronounced at higher CyD concentrations which were not possible with β-CyD due to its limited solubility. Thus it is possible that at lower concentrations of HP-β-CyD in a similar range to that used for the β-CyD phase solubility study, the negative deviation effect may be eliminated.

During the course of this work, Lehner and co-workers (1994) reported the interaction of chlorhexidine diacetate with HP-β-CyD in solution by phase solubility studies and also UV spectroscopy. In contrast to the present study, phase solubility studies revealed type A_L solubility diagrams even at high HP-β-CyD concentrations (17 % w/v). With increasing CyD, the solubility of the chlorhexidine salt was increased and thus the concentration of acetate ions in solution also increases. Since chlorhexidine diacetate it is relatively water-soluble it is probable that its solubility will be not effected by the increased concentration of acetate ions. With CHX however, its solubility was reduced with increasing chloride concentrations. Thus, due to the solubility difference between the chlorhexidine salts, their respective phase solubility behaviour differed. Furthermore, the K_S of the chlorhexidine diacetate-β-CyD complex was found by UV spectroscopy to be 399 M^{-1} (25°C) which is approximately 10 times greater than the respective value found for the CHX-HP-β-CyD complex (39 M^{-1}). However, as previously discussed, K_S values determined by different methods can show great variation.

To summarise, phase solubility studies have shown the interaction of CHX with both β-CyD and HP-β-CyD in solution with the formation of soluble complexes. K_S values ranged from 30 to 146 M^{-1} indicating the relatively weak interaction between the guest and host components. Inclusion of CHX with the β-CyD cavity in solution is further investigated by NMR spectroscopy from which the stoichiometry and the structure of the complex is predicted.

2.6.5 Dissolution studies in water using the dispersed powder method

Dissolution studies were performed using excess CHX-CyD complexes to determine their saturation solubilities.

2.6.5.1 Dissolution of the CHX-β-CyD system

The equilibrium solubility of CHX in water at 37°C was found to 2.116 ± 0.099 mM which correlated well with the solubility found during phase solubility studies performed at this temperature (section 2.6.4). The equimolar physical mix of CHX and β-CyD had an equilibrium solubility of 4.004 ± 0.370 mM, which was approximately 2-fold greater than the solubility of CHX itself. The β-CyD complex exhibited an initial peak CHX concentration (9.293 ± 0.383 mM) which was approximately 4.7 times greater than the saturation solubility of CHX alone. Following this maxima, the solubility of the complex gradually declined but eventually reached an equilibrium concentration of 4.246 ± 0.164 mM after 4 days. This concentration was similar to the value approached by the physical mix after this time period. Figures 2.16 and 2.17 compare the initial and extended dissolution behaviour of CHX, the equimolar physical mix and the CHX-β-CyD complex.

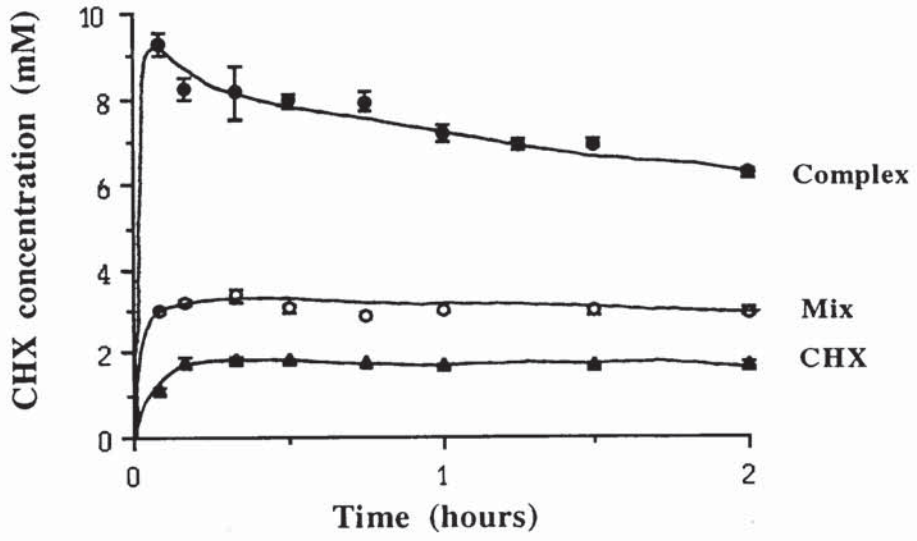

Figure 2.16 Dissolution profiles of CHX, its equimolar physical mix with β-CyD and its β-CyD complex in water at 37°C, measured by the dispersed powder method. Point represents the mean ± s.d., $n = 3$.

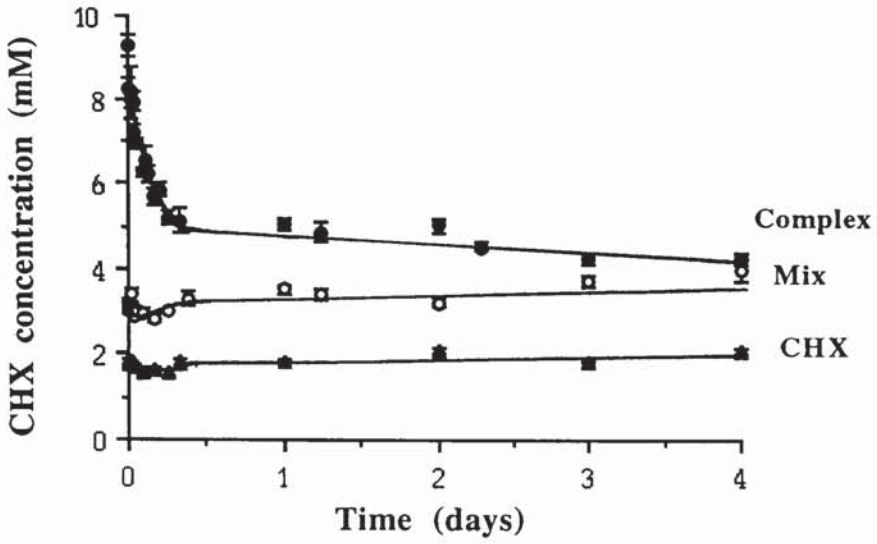

Figure 2.17 Extended dissolution profiles of CHX its equimolar physical mix with β-CyD, and its β-CyD complex in water at 37°C, measured by the dispersed powder method. Points represent the mean ± s.d., $n = 3$

The initial high CHX concentration following dissolution of the CHX-β-CyD complex was due to the formation of a metastable supersaturated solution, following which a decline in drug concentration was observed. The rapid fall in complex solubility may be explained by consideration of the dissociation of the complex in the dissolution medium. The stability constant for the CHX-β-CyD complex (54 M^{-1} at 37°C; phase solubility studies, section 2.6.4), is relatively small indicating a weak interaction between CHX and β-CyD. Dissolution of the complex results in its rapid dissociation which consequently results in the precipitation of free drug during the dissolution process. HPLC assay of the residual solid in the dissolution medium confirmed that CHX itself had precipitated. As mentioned previously, similar dissolution behaviour was observed with the diazepam-γ-CyD complex which had a K_S of 120 M^{-1} (Uekama *et. al.*, 1984) and the flurbiprofen-γ-CyD complex which had a K_S of 460 M^{-1} (Otagiri *et. al.*, 1983). In contrast, the β-CyD complexes of diazepam and flurbiprofen had K_S values of 220 M^{-1} and 5100 M^{-1} respectively, indicating a much more favourable fit of the guest within the CyD cavity as compared to γ-CyD. Furthermore, neither of these β-CyD complexes exhibited supersaturation behaviour. These data therefore suggest that the supersaturation phenomenon observed on dissolution of the complex occurs only when the interaction between the guest and CyD is relatively weak.

The equilibrium solubility of the complex, and the physical mix were approximately 2-fold greater than the solubility of CHX itself. This solubility enhancement correlated well with the phase solubility studies which also revealed a 2-fold increase in CHX solubility with saturated β-CyD solutions.

2.6.5.2 Dissolution of the CHX-HP-β-CyD system

The solubility of the equimolar physical mix of CHX and HP-β-CyD after 4 days was 4.217 ± 0.282 mM which is approximately twice the solubility of CHX alone. In a similar manner to that observed for the CHX-β-CyD complex, a supersaturation effect was observed upon dissolution of the CHX-HP-β-CyD complex. The peak solubility of the HP-β-CyD complex occurred at 5 minutes at a concentration of 21.029 ± 0.885 mM, which was approximately 11-fold greater than the saturation solubility of CHX alone. As observed with the CHX-β-CyD system, the solubility of the CHX-HP-β-CyD gradually declined to an equilibrium level (4.853 ± 0.482 mM) over a 4 day period. Furthermore, the solubility of the physical mix was similar to the concentration of the equilibrium solubility of the complex over this time period (4.217 ± 0.282 mM). Figures 2.18 and 2.19 compare the initial and extended dissolution behaviour of CHX, the equimolar physical mix and the CHX-HP-β-CyD complex.

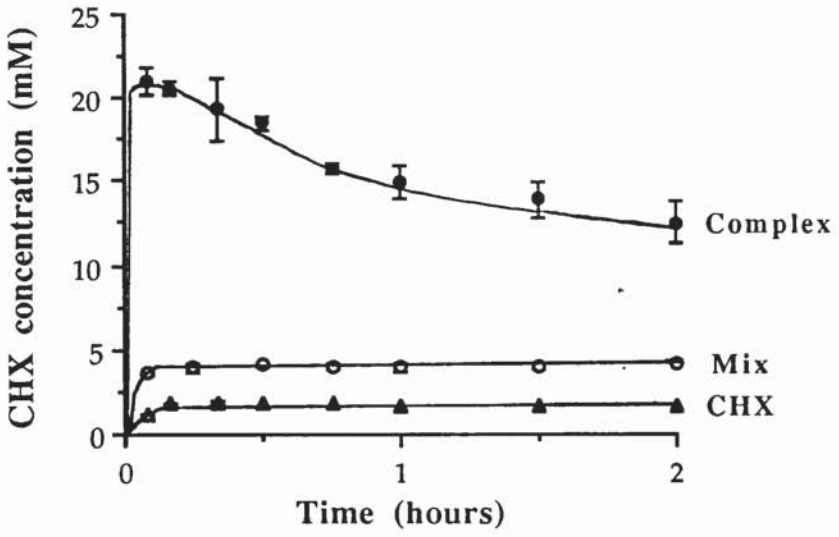

Figure 2.18 Dissolution profiles of CHX, its equimolar physical mix with HP-β-CyD, and its HP-β-CyD complex in water at 37°C, measured by the dispersed powder method. Points represent the mean ± s.d., $n = 3$.

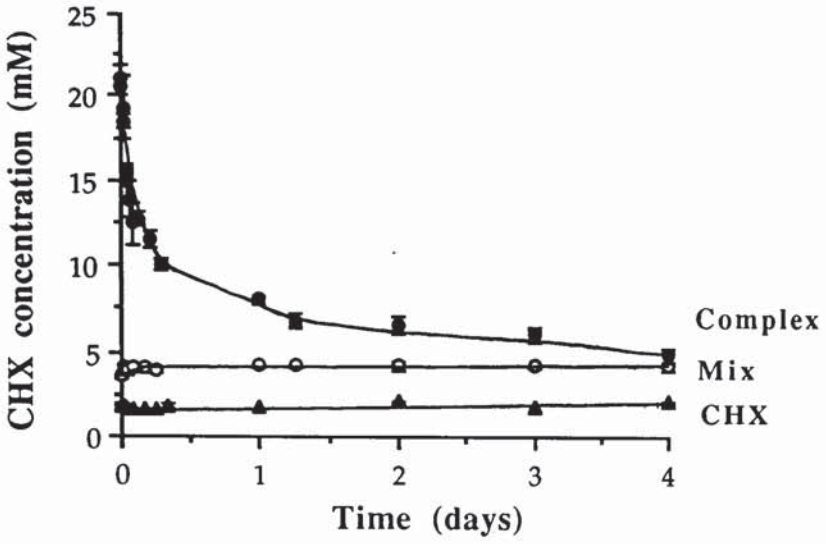

Figure 2.19 Extended dissolution profiles of CHX, its equimolar physical mix with HP-β-CyD, and its HP-β-CyD complex in water at 37°C, measured by the dispersed powder method. Points represent the mean ± s.d., $n = 3$.

The initial solubility of the CHX-HP-β-CyD complex (21.029 ± 0.885 mM) was approximately twice the solubility of the corresponding β-CyD complex (9.293 ± 0.383 mM) which may be a direct consequence of the hydroxypropyl CyD derivative being more water-soluble than its parent CyD. Again, the dissolution behaviour of the HP-β-CyD complex can be explained by the relatively low K_S value of 40 M^{-1} (phase solubility studies, section 2.6.4) which consequently results in rapid dissociation of the complex and hence eventual precipitation of CHX.

The equilibrium solubility of the CHX-HP-β-CyD complex (4.853 ± 0.482 mM) was approximately twice the solubility of CHX alone (2.116 ± 0.099 mM). The dissolution experiment was performed by adding 1.30 g of CHX-HP-β-CyD complex (*Batch II*) to 30 ml dissolution medium. Although, precipitation of free CHX occurs during the dissolution process, any free HP-β-CyD is in solution. The theoretical concentration of HP-β-CyD following dissolution of the complex was approximately 0.021 M and was calculated as follows.

From chemical analysis of the CHX-HP-β-CyD complex (section 2.6.3), the percentage weight of CHX per complex weight was found to be 29.18 %. It therefore follows that the percentage of HP-β-CyD per complex weight is equal to 70.82 %.

The weight of HP-β-CyD in 1.30 g of complex is therefore, 0.9207 g, which is dissolved in 30 ml distilled water as the dissolution medium. The concentration of HP-β-CyD is therefore 30.7 mg/ml which is equivalent to 0.021 M.

During phase-solubility analysis at 37°C (section 2.6.4), an approximate HP-β-CyD concentration of 0.021 M increased the solubility of CHX 2-fold which is similar to the solubility enhancement observed with dissolution studies.

The solubility of all batches of complexes was assessed to observe the solubility enhancement, the dissolution profile and the reproducibility of complex preparation. Table 2.12 contains the solubility of all CHX-CyD complex batches at 5 minutes during the dissolution process and the equilibrium solubility of the complex assessed after 4 days. For comparison, the solubility of corresponding CHX-CyD physical mixes are also included as well as the saturation solubility of CHX at 37°C.

Table 2.12 Solubility of the various batches of the CHX-CyD complexes. Concentrations are means of duplicate determinations ± s.d.

	Solubility at 5 minutes (CHX concentation, mM)	Solubility after 4 days (CHX concentration, mM)
CHX alone	1.086 ± 0.121	2.116 ± 0.099
CHX-β-CyD complex		
Batch I	9.293 ± 0.383	4.246 ± 0.164
Batch II	10.238 ± 0.125	4.325 ± 0.505
Batch III	9.581 ± 0.187	4.027 ± 0.412
Batch IV	11.150 ± 0.194	4.295 ± 0.338
Batch V	10.515 ± 0.174	4.113 ± 0.252
1:1 physical mix	2.981 ± 0.070	4.004 ± 0.370
CHX-HP-β-CyD complex		
Batch I	21.593 ± 0.387	4.571 ± 0.221
Batch II	21.029 ± 0.885	4.853 ± 0.482
Batch III	23.228 ± 0.249	4.682 ± 0.384
1:1 physical mix	3.562 ± 0.134	4.217 ± 0.282

The solubilities of the different batches of complex for each CyD were similar, indicating that the method of preparation was reproducible. As illustrated by the data, the solubility of the different batches of complex eventually declined to an equilibrium level which was similar to the solubility of the corresponding physical mix. The CHX-CyD complexes were prepared by the freeze-drying method. Since all complexes were prepared on different occasions, minor changes in freeze-dryer efficiency may have affected the amorphous nature of the freeze-dried complexes which consequently showed slight differences in solubility.

Dissolution studies have shown the superior solubilities of both CHX-CyD complexes as compared to drug alone. The supersaturation phenomena observed on dissolution of the solid drug-CyD inclusion complexes can be exploited in drug delivery systems where drug access is a problem. In the treatment against *H. pylori*, supersaturated solutions of antimicrobial agents, such as CHX, may be able to penetrate the mucin layer of the stomach wall with greater efficiency than subsaturated solutions.

Researchers (Van Doorne, Bosch, and Lerk, 1988; Van Doorne and Bosch, 1991) have shown that antibacterial-CyD complexes themselves possess low, if any, microbiological activity. If this also holds for the CHX-CyD inclusion complexes, then even though a 4.7-fold and 10.5-fold enhancement in CHX solubility was observed with the β-CyD and HP-β-CyD complexes respectively, the complexed CHX is likely to have no activity. The total CHX concentration obtained during complex dissolution consists of the solubility of CHX alone, the equilibrium solubility of the complex and the solubility of the supersaturated CHX which may be exist as free drug or complexed. Using the dissolution data obtained for the CHX-β-CyD complex, figure 2.20 illustrates these different contributions to the total CHX concentration.

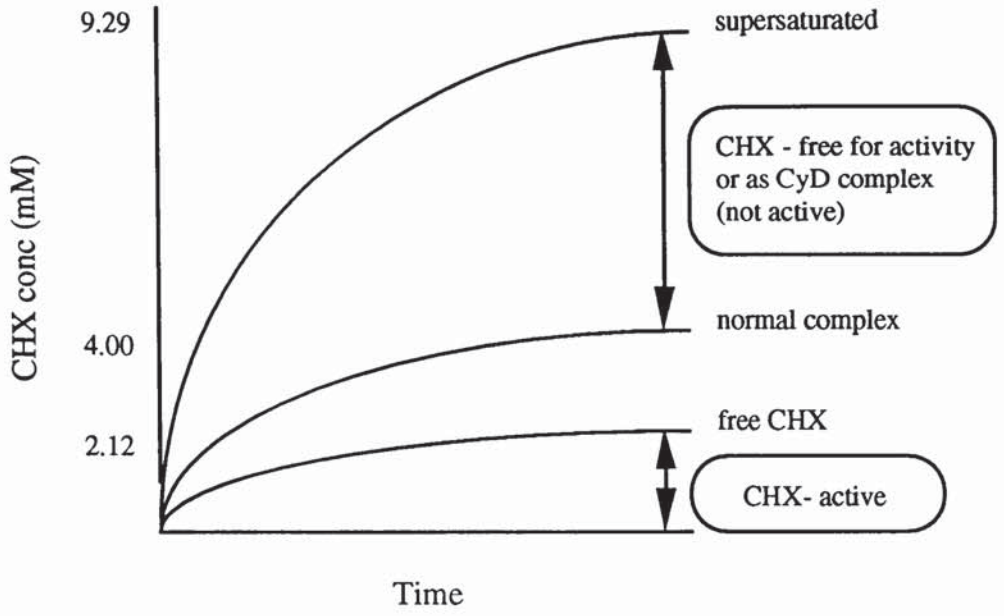

Figure 2.20 Diagrammatic representation of the availability of free CHX from the dissolution of the β-CyD complex.
(Concentrations correspond to the dissolution data obtained)

To estimate the concentration of free drug in the guest-CyD system, Irwin *et. al.* (1994) have derived the following model (equation A4.20; derivation given in Appendix 4):

$$[A] = \frac{\sqrt{1 + 4K_A.[A_0]} - 1}{2K_A} \qquad \text{(A4.20)}$$

where $[A_0]$ is the initial concentration of guest, [A] is the concentration of free guest and K_A is the complex stability constant for the A-CyD complex. Using this model, the concentration of free CHX for both β-CyD and HP-β-CyD systems was calculated using the solubility of the complexes at 5 minutes and at equilibrium after 4 days. As shown in table 2.13, the concentration of free drug in both CHX-CyD systems is greater than the saturation solubility of CHX itself indicating that these systems were supersaturated with respect to CHX. Upon dissolution of the CHX-β-CyD complex, the initial concentration of free CHX (6.8 mM) is approximately 3 times greater than the solubility of CHX, and with the HP-β-CyD complex the concentration of free CHX is enhanced approximately 6-fold. Although, the solubility of the complexes declined after reaching an optimum, even at equilibrium the CyD systems were supersaturated with respect to free CHX. Figure 2.21 illustrates the concentrations of free and complexed CHX with each CyD system at peak solubility and at equilibrium.

Table 2.13 Concentration of free CHX following dissolution of excess CHX-CyD complexes calculated using equation A4.20 in Appendix 4.

	CHX-β-CyD *(Batch I)*	CHX-HP-β-CyD *(Batch II)*
K_S, M^{-1}	54	40
5 minutes:		
total CHX concentration	9.293	21.029
concentration of free CHX	6.8	13.6
Conc. at 4 days (equilibrium):		
total CHX concentration	4.246	4.853
concentration of free CHX	3.6	4.2

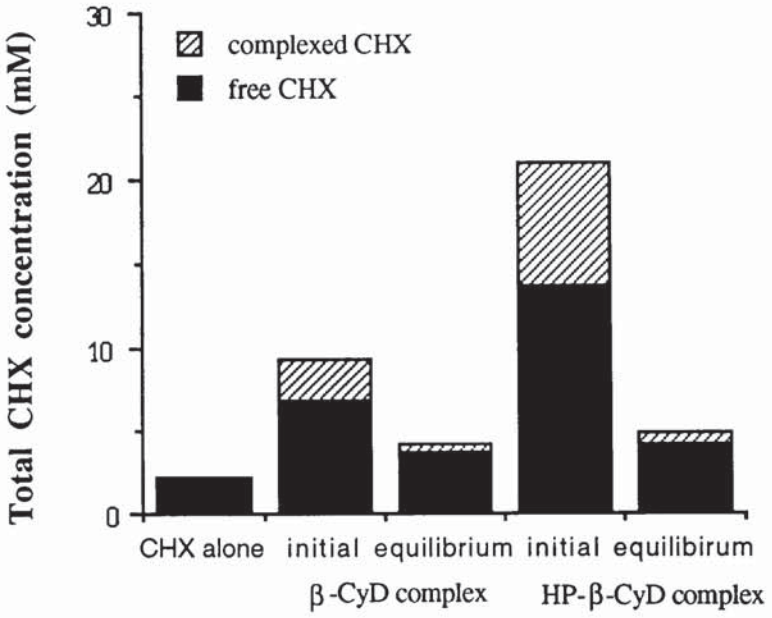

Figure 2.21 Diagrammatic representation of the concentrations of free and complexed CHX following dissolution of excess CHX-β-CyD and CHX-HP-β-CyD complexes. (CHX alone represents the solubility of CHX itself; Initial represents the concentrations at 5 minutes, and, equilibrium represents the equilibrium solubility of the complexes determined after 4 days)

On the basis of these data, it is therefore possible that solutions of the CHX-CyD complexes will have an enhanced antimicrobial activity compared to CHX alone, due to the greater concentration of free, and therefore, active drug. The microbiological testing of the complexes will be discussed later in chapter 5.

One other way to enhance the availability of free CHX, is to displace the complexed CHX from the CyD cavity by use of a more hydrophobic agent as a competitor. Tokumura *et. al.* (1986), has shown an enhancement in the bioavailability of cinnarizine from its β-CyD complex with phenylalanine as a competitor. The use of competitors is discussed later in section 2.6.6.

If the dissolution process is considered with respect to oral treatment against *H. pylori*, the free CHX as released from the CyD complex has to diffuse across the gastric mucus to the site of infection. The diffusion rate of the complex itself, is likely to be slow in comparison with the free drug due to its relatively large molecular weight. The diffusion behaviour of the CHX-β-CyD system is discussed later in section 2.6.9. Theoretically, dissolution of the complex in the gastric medium would result in a reservoir of CHX, both free and complexed, and furthermore, the concentration of free CHX would be supersaturated. Therefore, on the basis of concentration, the maximal flux of free CHX across the gastric mucus is possible. As a result of the concentration differential, a steep concentration gradient would exist across the mucus barrier which should further facilitate diffusion of free drug. Diffusion of CHX from the gastric medium to the site of bacterial infection should also promote further dissociation of the complex. In this way, the drug-CyD complex would provide a reservoir of antimicrobial agent which enhances diffusion of free drug to the site of infection. The proposed mechanism of attack is illustrated in figure 2.22. In this mode of action, oral administration of CHX as a CyD inclusion complex should enhance the availability of free active CHX for diffusion to the site of *H. pylori* infection and consequent uptake into the bacterium. In contrast, diffusion of CHX to the site of action from a saturated CHX solution would be less efficient due to the reduced concentration gradient which would exist.

This possible application of the CHX-CyD complex against *H.pylori* infection aims to illustrate the potential use of an antimicrobial-CyD product for the treatment of any bacterial infection where drug access is a problem. One major disadvantage with CHX is due to its cationic nature which would interact with the negatively charged gastric mucus *via* electrostatic interactions.

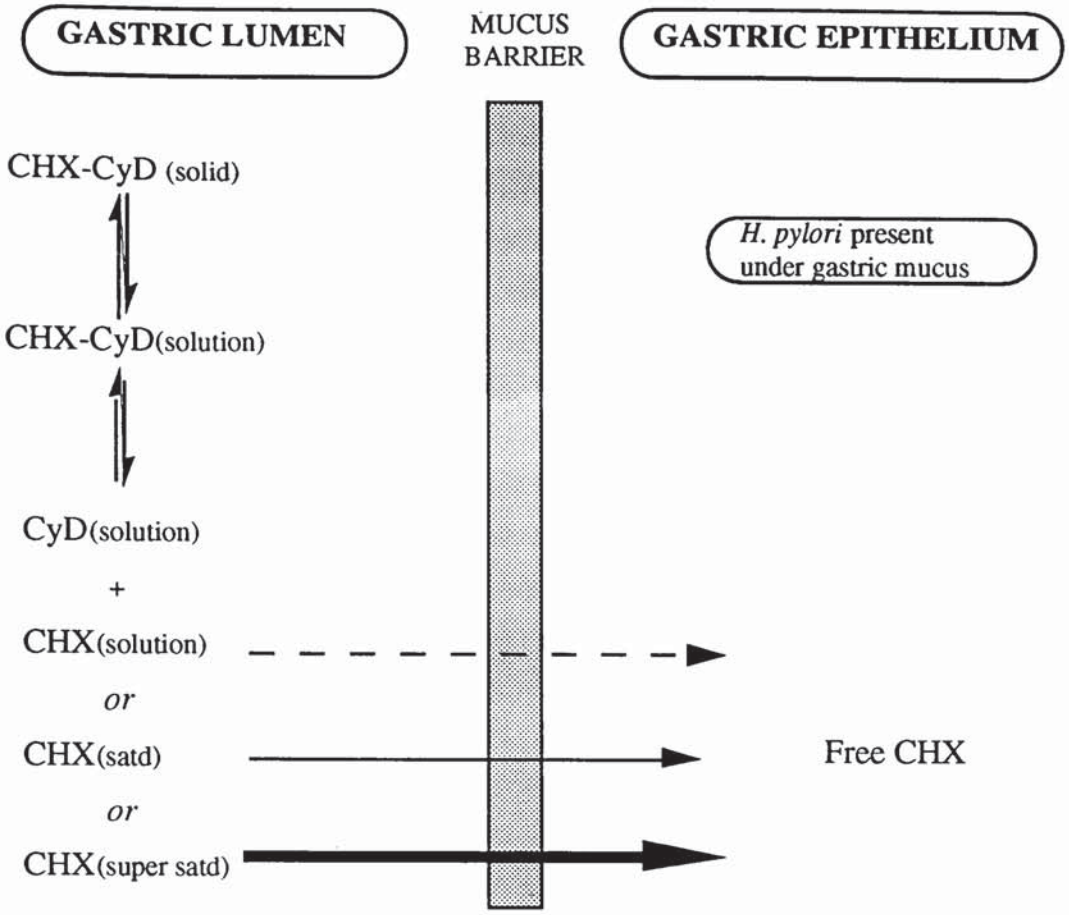

Figure 2.22 Proposed mechanism of action of CHX against *H.pylori* infection, following its oral administration as the β-CyD or HP-β-CyD complex

If the CHX-β-CyD complex is considered as a potential product against *H. pylori* infections, the complex would have to be administered orally in a suitable dosage form. Assuming a 20 ml volume for a fasting stomach, on the basis of the solubilities of the various components determined at 37°C as shown in table 2.12, the amount of CHX in solution in the stomach would be 24 mg. The equilibrium solubility of the β-CyD complex was 4.004 mM CHX *i.e.* 46 mg of CHX in 20 ml. Using equation A4.20 to estimate the relative contributions of free and complexed drug to this total, at equilibrium, approximately 39 mg of the total CHX is free and only 7 mg will be complexed. Since the solubility of CHX alone is 24 mg, at equilibrium, 15 mg of CHX will exist as a supersaturated solution. The solubility of the CHX-β-CyD complex was increased approximately 4.7-fold (9.293 mM), which is equivalent to 108 mg of CHX in 20 ml. Again using equation A4.20, this comprises 24 mg of CHX in solution as free, 29 mg as the complex and 55 mg as the supersaturated solution. Since the percentage weight of CHX per complex weight content of CHX is approximately 30 %, to deliver this weight of CHX (108 mg of which 79 mg will be free drug), approximately twice this weight of

CyD is required which give a mass of ~ 325 mg. A similar calculation performed on the CHX-HP-β-CyD complex gives a mass of ~ 730 mg. With the addition of tablet excipients, it is possible that a potential CHX-β-CyD product could be administered as one 500 mg tablet or two 200-250 mg tablets and the CHX-HP-β-CyD as two 500 mg tablets. As discussed previously, with a dosage of more than 2 tablets there is a possibility that patient compliance will be reduced and hence treatment will be ineffective. Other factors which need to be considered include the frequency of dosing which will depend on the retention and efficacy of the product at the site of action.

The above hypothetical dosage regime has been based on the solubility of the CHX-CyD system in distilled water. However, administration to the acidic environment of the stomach may effect their relative solubilities and therefore the final dosing calculations. The solubility of CHX and its CyD complexes in acid are discussed later in section 2.6.7. Since more soluble chlorhexidine products are available (diacetate and digluconate salts), the dissolution behaviour of the CHX-CyD complexes were also compared to chlorhexidine digluconate to assess their advantage, if any, over the soluble salt.

2.6.6 Dissolution studies with competing agents

Initial dissolution studies of the CHX-β-CyD complex have shown an approximate 4.7-fold enhancement in CHX solubility on dissolution of the complex (section 2.6.5). As discussed and quantified, this total CHX concentration (9.293 mM) corresponds to free CHX (~ 6.8 mM) and also complexed CHX (~ 2.5 mM). To enhance the microbiological potential of CHX, the amount of free CHX in solution needs to be maximised.

One possible way to enhance the availability of free CHX further is to displace that complexed by an appropriate competitive guest type. Figure 2.23 illustrates the role of a competing agent in the dissolution process of the complex. Theoretically, CyD complexes of drugs of a greater hydrophobicity than CHX would have a greater K_S assuming that their geometric properties were also favourable. It is therefore these guest types which would be suitable competitors. As previously discussed Tokumura *et. al.* (1986) found an enhancement in the bioavailability of cinnarizine from its β-CyD complex with DL-phenylalanine (Phe) as a competitor. However, the K_S of the cinnarizine-β-CyD complex was found to be 6.2×10^3 M^{-1} (Tokumura *et. al.*, 1984) whereas there seems to be little agreement for the phenylalanine-β-CyD complex K_S. Literature values for the stability constant of the β-CyD inclusion complex of Phe vary widely from 20 M^{-1} (Suzuki *et. al.*, 1993) to 1000 M^{-1} (Inoue and Miyata, 1981). In considering both these K_S values, the affinity of Phe for the CyD cavity is less than the affinity of cinnarizine as reflected by the magnitude of its K_S. In this system, the

competitive effect of Phe cannot be explained by simply considering the respective K_S values. Since Phe is relatively water-soluble (1.4 g/100 ml) a high concentration of competitor was used which may have counteracted the effect of the relatively small K_S value.

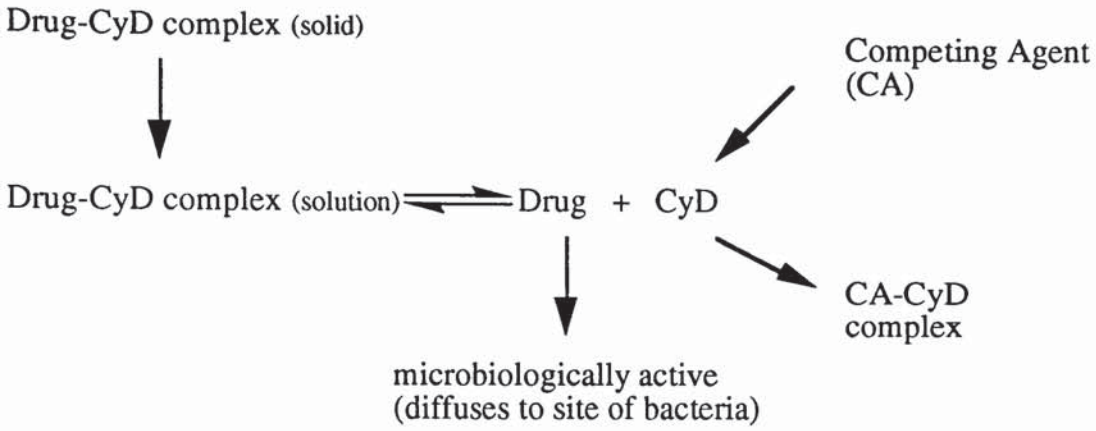

Figure 2.23 Proposed role of a competing agent in the dissolution-dissociation process of the complex

Studies in these laboratories (A K Dwivedi) have shown spironolactone (SP) to be an effective competitor in displacing n-butyl-*p*-hydroxybenzoate from its respective β-CyD inclusion complex (K_S = 2561 M^{-1} at 25°C; Uekama *et. al.*, 1980). In contrast to Phe, spironolactone has limited water-solubility and also has a greater affinity for the β-CyD cavity as indicated by the K_S of 9198 M^{-1} (37°C; Yusuff and York, 1990).

The CHX-β-CyD complex has a K_S of 54 M^{-1} (section 2.6.4) which is lower than that for the corresponding SP complex, and can be considered to be either similar to or less than the value for the Phe complex. SP and Phe were therefore used as competitors for the CHX-β-CyD complex due to their greater affinity for complexation by the CyD. Dissolution studies of the CHX-β-CyD complex were performed in the presence of both these competitors to observe their effect, if any, on the displacement of CHX from the CyD cavity. A competitive effect may result in an increase in the total concentration of CHX measured due to an increase in free CHX. It is also probable that maximum solubility of the complex will remain unchanged, even though the proportion of free CHX in solution may have increased.

The concentration of Phe used as the competitor was ten times greater than the maximum CHX concentration seen on complex dissolution *i.e.* 0.09 M. For SP, a 2 x S_0 concentration was used , where S_0 is the equilibrium solubility of CHX alone (~ 2.0 mM

at 37°C). Since the solubility of SP is limited, excess SP was used such that a theoretical concentration of 4 mM was possible if all were solubilised. The above quantities of competitor were used such that sufficient competitor was present to displace CHX.

Figure 2.24 compares the dissolution profiles of the CHX-β-CyD complex in the presence of the competitors to that in distilled water alone. As illustrated, the presence of neither competitor had any significant effect on further increasing the total concentration of CHX on dissolution of the complex. However, it is probable that the amount of free CHX in solution may have increased which may be revealed by diffusion experiments as discussed later in section 2.6.9. Many researchers (Otagiri *et. al.*, 1983) have shown a decrease in the diffusion rate of guest from a solution of the complex as compared to a solution of guest alone, both solutions being equivalent in concentration. This behaviour is expected since in the solution of the complex both free and complexed guest will exist, however, as the molecular weight of the complex will be greater than the free guest component its diffusion will be slower. If an appropriate competitor is added to the solution of the complex, complexed guest may be displaced from the CyD cavity thus the diffusion rate may be enhanced due to the increase in free drug.

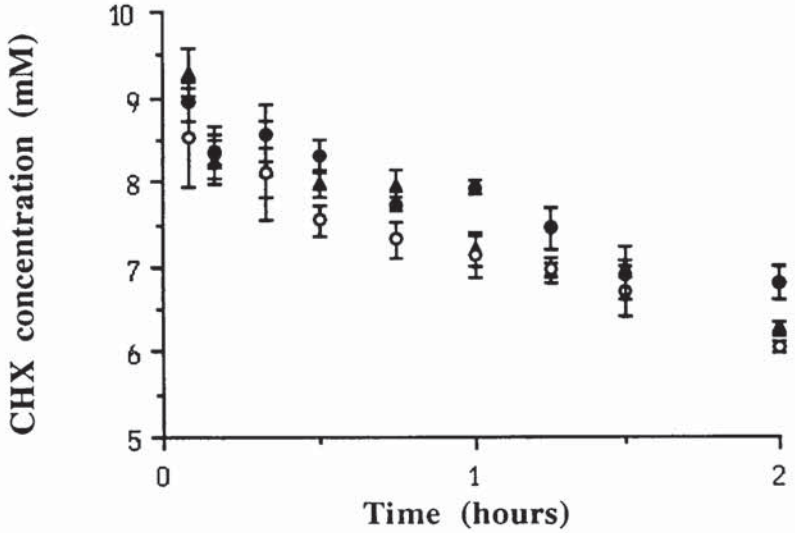

Figure 2.24 Dissolution profiles of CHX-β-CyD complex in water alone (▲) and in the presence of phenylalanine (o) and spironolactone (●) at 37°C. Points represents the mean ± s.d., $n = 3$.

2.6.7 Dissolution of chlorhexidine digluconate, chlorhexidine dihydrochloride and CHX-CyD complexes in HCl

Chlorhexidine digluconate (CHG) is a soluble salt of chlorhexidine and is commercially available as a 20 % v/v solution. CHG is miscible with water whereas the dihydrochloride salt of chlorhexidine (CHX) is only sparingly water-soluble (60 mg per 100 ml, 25°C). It could be asked why CyDs need to be used to improve the solubility of CHX when a soluble salt of chlorhexidine already exists. It may also be that the activity (not just the concentration) is important to optimise diffusion across the mucus barrier. Theoretically, when the more soluble chlorhexidine salt, CHG, is placed in the acidic environment of the stomach, the dihydrochloride salt would be formed and as a consequence would precipitate due to its low solubility. In considering the application of CyDs to enhance the solubility of CHX, it is important to observe this precipitation effect *in vitro*.

The dissolution experiments were performed in acid to assess whether in practice the CHX-CyD complex offers any advantage over the administration of the soluble digluconate salt. The solubilities of the dihydrochloride and digluconate salts of chlorhexidine salts were compared to the solubility of the CHX-β-CyD and CHX-HP-β-CyD complexes in an acidic environment. The pH of gastric juice is documented to be within the range 1.2 to 1.7 (Documenta Geigy, 1965), thus 0.15 M HCl was used as the dissolution medium as it was found to have a pH of ~ 1.5.

Furthermore, the effect of chloride ion concentration on the solubility of CHX was also assessed. For these experiments, 0.1 M HCl was used as the dissolution medium to which increasing amounts of NaCl were added (concentration range of chloride used: 0.1 to 0.175 M). The normal chloride content of the gastric juice is 500-600 mg/100 ml, *i.e.* approximately 0.155 M.

2.6.7.1 Effect of increasing chloride ion concentration on the solubility of CHX in 0.1 M HCl

The solubility of CHX in the presence of increasing chloride concentrations was assessed over 6 hours. As illustrated in figure 2.25, after approximately 3 hours, equilibrium had been established. Thus, the data points collated after this time period were used to find the mean solubility of CHX at the various chloride concentrations. As the chloride concentration was increased from 0.1 M to 0.175 M, the solubility of CHX decreased approximately 1.8-fold from 0.267 ± 0.015 mM to 0.149 ± 0.010 mM respectively. The solubility of CHX in 0.1 M HCl was approximately 8 times less than its solubility in distilled water (2.116 ± 0.099 mM, section 2.6.7).

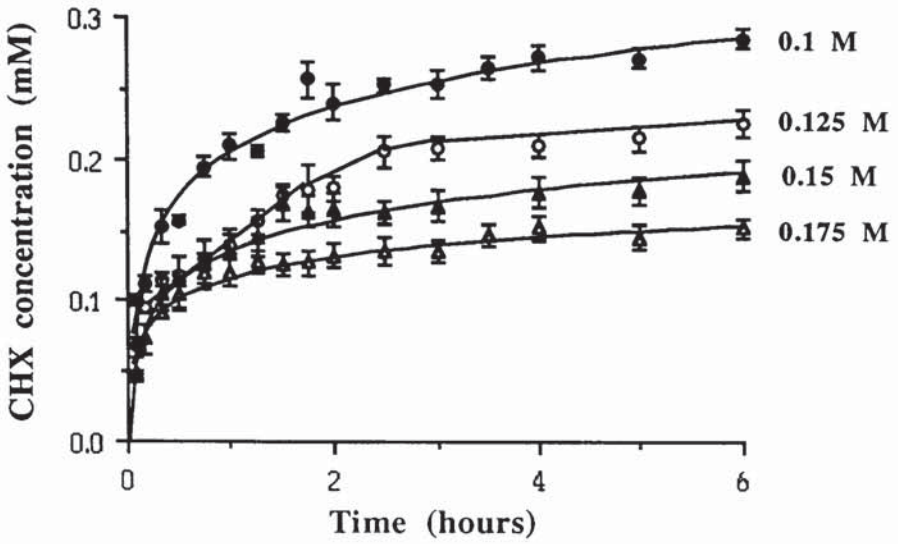

Figure 2.25 The effect of increasing chloride concentrations on the solubility of CHX in 0.1 M HCl at 37°C. Points represent the mean ± s.d., $n = 2$.

The reduced solubility of CHX with increasing chloride concentration is due to the common ion effect. The addition of a common ion reduces the solubility of a slightly soluble salt. This 'salting out' results from the removal of water molecules as solvent due to the competing hydration of other ions. Hydrochloride salts often exhibit suboptimal solubility in gastric juice due to the abundance of chloride ions (Wells and Aulton, 1988). Examples of weakly basic drugs which exhibit this behaviour include chlortetracycline and triamterene.

For CHX, the equilibrium of a saturated solution of the salt in contact with undissolved solid may be represented by:

$$CHX.2HCl_{solid} \rightleftharpoons CHX.2HCl_{solution} \rightleftharpoons CHX.2H^{+}_{ions} + 2Cl^{-}_{ions} \quad (2.5)$$

where, on this occasion CHX.2HCl indicates chlorhexidine dihydrochloride.

The equilibrium constant, K, for this reversible reaction is given by:

$$K = \frac{[CHX.2H^{+}]\,[Cl^{-}]^2}{[CHX.2HCl]} \quad (2.6)$$

If CHX is assumed to be a sparingly soluble salt *i.e.* [CHX.2H$^+$] >> [CHX.2HCl], the concentration of the solid is regarded as being constant, following which the solubility product of CHX can be represented by:

$$K_{sol} = [[CHX.2H^+] [Cl^-]^2 \quad (2.7)$$

If K_{sol} is exceeded by the product of the concentration of the ions, then the equilibrium shown in equation 2.5 moves towards the left to restore equilibrium, and CHX will be precipitated. Thus, if the [Cl$^-$] is increased, the concentration of [CHX.2H$^+$] is expected to decrease in order to maintain a constant solubility product. Using the solubility data of CHX at each chloride concentration, equation 2.7 was used for the calculation of the K_{sol} to determine whether this was a constant value. However, in this case, the total chloride concentration will be the concentration of chloride in the dissolution medium ([Cl_{med}]; ranging from 0.1 M to 0.175 M) plus the concentration of chloride present as solubilised CHX. Since, CHX is a dihydrochloride salt, this latter chloride concentration is twice the solubility concentration of CHX *i.e.* 2[CHX.2H$^+$]. The solubility product is therefore:

$$K_{sol} = [CHX.2H^+] \times ([Cl_{med}] + 2[CHX.2H^+])^2 \quad (2.8)$$

The values obtained for K_{sol} are summarised in table 2.14

Table 2.14 Summary of solubility product calculated using solubility of CHX in the presence of increasing chloride ion concentration. Values represent the mean ± s.d.

Concentration of chloride in dissolution medium (M)	Solubility of CHX (mM)	K_{sol} (x 10^6 mol^3 l^{-3})
0.1	0.267 ± 0.015	2.68 ± 0.16
0.125	0.210 ± 0.009	3.29 ± 0.14
0.15	0.174 ± 0.013	3.92 ± 0.30
0.175	0.149 ± 0.010	4.57 ± 0.30

Although the solubility of CHX is reduced with increasing chloride concentration, the solubility product of CHX does not remain constant but increases linearly as shown in figure 2.26. This indicates that the common-ion effect is less pronounced than predicted from equations 2.5 to 2.7, and thus CHX is not a sparingly soluble salt.

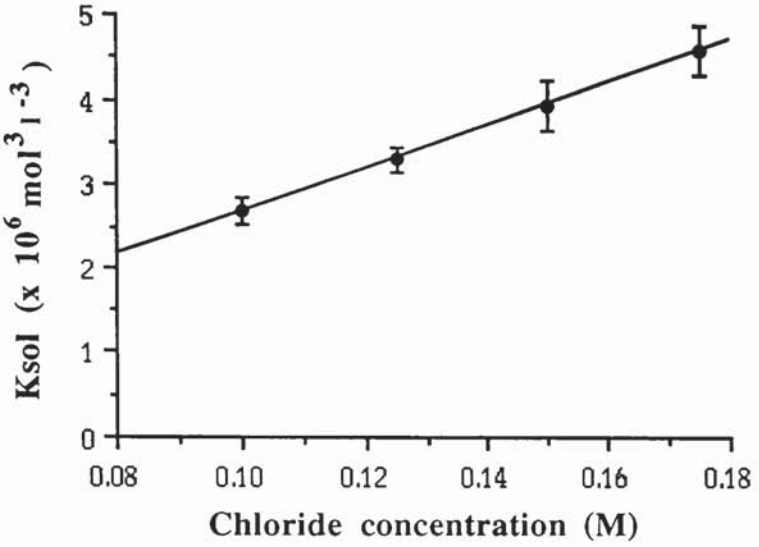

Figure 2.26 Solubility product of CHX (K_{sol}) as a function of chloride concentration ($r^2 = 1.000$)

2.6.7.2 Solubility of CHX and CHG in 0.15 M HCl

The solubility of CHX in 0.15 M acid was approximately 11 times less than its solubility in distilled water; 0.185 ± 0.011 mM compared with 2.116 ± 0.099 mM respectively. The solubility of CHX in 0.15 M HCl was similar to its solubility in 0.1 M HCl containing a total chloride concentration of 0.15 M (0.174 ± 0.013 mM) as determined in section 2.6.7.1. The reduced solubility of CHX in 0.15 M HCl is due to the common-ion effect as discussed previously.

At all CHG concentrations, with the exception of the lowest concentration of 11.8 mM used, a rapid decline in chlorhexidine concentration was observed. A milky white precipitate appeared in the dissolution vessels which was assumed to be the sparingly soluble dihydrochloride salt of chlorhexidine. The initial fall in chlorhexidine concentration was the greatest with the highest CHG concentration of 29.5 mM. At all CHG concentrations, again with the exception of 11.8 mM CHG, the decrease in chlorhexidine concentration was initially steep after which the decline continued but at a much slower rate until reaching a steady plateau. In these suspensions, the presence of solid material probably promoted crystal growth which further enhanced the precipitation of CHX. The final chlorhexidine concentrations of these suspensions measured after 3 hours were greater than the solubility of the dihydrochloride salt itself under the same conditions, as shown in table 2.15. Figure 2.27 illustrates the dissolution of CHX and CHG in 0.15 M HCl.

Table 2.15 Final measured concentration of chlorhexidine following the addition of CHX and various concentrations of CHG to 0.15 M HCl at 37°C.

	Final concentration of chlorhexidine (mM)
CHX (excess added)	0.185 ± 0.011
Initial concentration of CHG:	
11.8 mM	11.6
17.7 mM	1.5
23.6 mM	1.8
29.5 mM	1.7

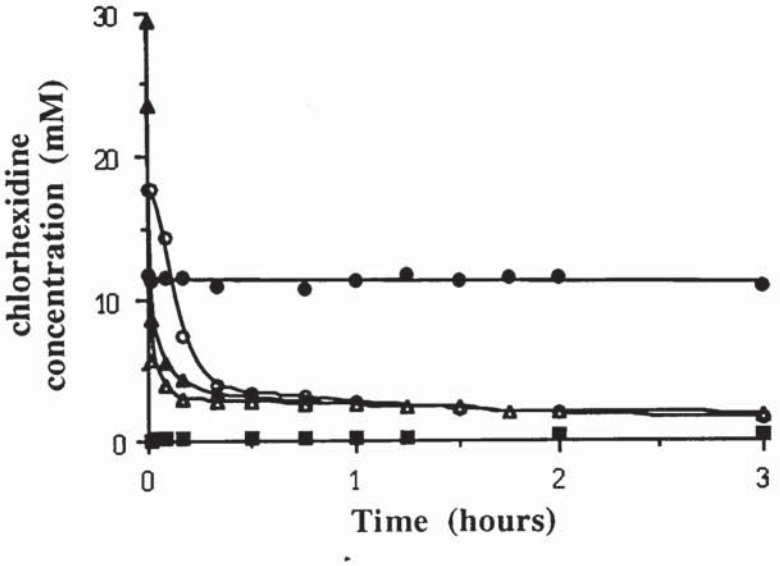

Figure 2.27 Solubility of chlorhexidine dihydrochloride (■) and various concentrations of chlorhexidine digluconate and in 0.15 M HCl at 37°C (● 11.8 mM; o 17.7 mM; ▲ 23.6 mM; Δ 29.5 mM).

The minimum chlorhexidine concentration obtained during CHG dissolution was 1.5 mM, which is 8 times greater than the acid solubility of CHX (0.185 mM). Even though the concentration of HCl is relatively large which would favour the formation of the dihydrochloride salt from CHG, some of the digluconate will remain associated with chlorhexidine. Hence, the total solubilised chlorhexidine is a combination of it existing as both the digluconate salt and also the dihydrochloride salt, with the former salt dominating. Since, the solubility of CHX in acid is already known to be 0.185 mM, the remaining chlorhexidine in solution can be assumed to be the digluconate salt. For

example, with a initial concentration of 17.7 mM CHG, the final concentration of chlorhexidine was 1.5 mM, thus 0.185 mM of this total was due to CHX and, 1.315 mM was present as CHG.

With 11.8 mM CHG no decrease in chlorhexidine concentration was observed over the 3-hour assay period, and the test solution was also devoid of any solid material. This concentration of CHG seems to be a threshold point above which CHG is rapidly precipitated as CHX. In comparing this chlorhexidine concentration to the solubility of the CyD complexes in distilled water (section 2.6.5), the CHX-β-CyD complex, which had a maximum solubility of 9.293 ± 0.383 mM offered no advantage in the solubility enhancement of CHX. However, the HP-β-CyD complex had a maximum solubility of 21.029 ± 0.885 mM, which is greater than the solubility of CHG in acid. For fair comparison the solubility of both CyD complexes in acid was also assessed.

2.6.7.3 Solubility of the CHX-CyD complexes in 0.15 M HCl

The initial dissolution behaviour of both CHX-CyD complexes in 0.15 M HCl was similar to their solubility in distilled water. At 5 minutes the solubility of the CHX-β-CyD complex in distilled water was 9.293 ± 0.252 mM which was comparable to the solubility in acid at the same time point, 10.334 ± 0.276 mM. Similarly, the solubility of the CHX-HP-β-CyD complex in water was 21.029 ± 0.885 mM whereas the solubility in 0.15 M HCl was 20.325 ± 0.140 mM. With both complexes, once maximum solubility had been reached, their solubility gradually declined. However, in an acidic dissolution medium both CyD complexes maintained a higher solubility as compared to their behaviour in distilled water. The initial 3 hour dissolution profiles of the CHX-β-CyD and CHX-HP-β-CyD complexes in both distilled water and 0.15 M HCl are shown in figure 2.28 and 2.29 respectively (dissolution data in water taken from section 2.6.4). The dissolution process in acid was followed for 2 days after which the final measurements were taken. These data together with the solubilities at 5 minutes and 3 hours are summarised in table 2.16. Although the solubility of the complexes in acid were initially higher, after 48 hours their solubilities was similar to the solubility of the complexes in distilled water measured after the same duration. It therefore seems that equilibrium is established at the same time in both solvents, however, the rate of precipitation of the solid an acidic medium was initially slower.

Table 2.16 Solubility of excess CHX-CyD complexes in distilled water and 0.15 M HCl at 37°C at various time points. Concentrations are in mM and represent the mean ± s.d., $n = 3$ for water data and $n = 2$ for acid data

Time	β-CyD complex		HP-β-CyD complex	
	distilled water	acid	distilled water	acid
5 minutes	9.293 ± 0.271	10.334 ± 0.276	21.029 ± 0.885	20.325 ± 0.140
3 hours	6.198 ± 0.199	9.843 ± 0.252	12.724 ± 0.402	18.276 ± 0.036
48 hours	5.042 ± 0.110	4.945 ± 0.201	6.856 ± 0.512	6.085 ± 0.510

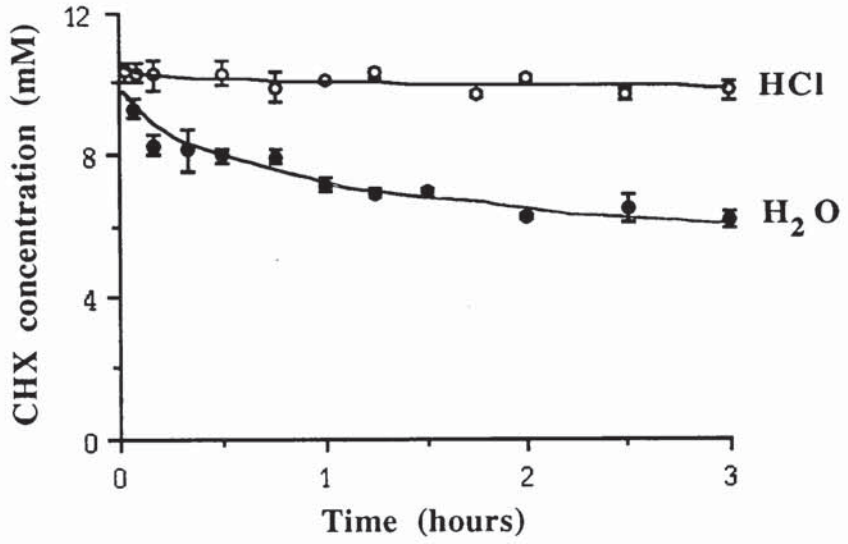

Figure 2.28 Dissolution profiles of the CHX-β-CyD complex in distilled water and 0.15 M HCl at 37°C. Points represent the mean ± s.d., $n = 3$ for water data and $n = 2$ for acid data

The supersaturation effect of the complex was attenuated in an acidic environment suggesting that dissociation equilibrium of the complex was affected. It has already been shown that the solubility of CHX in HCl is reduced due to the common-ion effect. One possibility therefore, is that the presence of chloride ions in the dissolution medium temporarily moves the position of equilibrium so that the dissociation of the complex into its free components is reduced.

When considering oral delivery of potential products to the GI tract, only the initial 2 hours of the dissolution process are important since the residence time in the stomach is limited. Thus, even though the solubilities of the complexes eventually declined, the initial high CHX concentrations may still be beneficial.

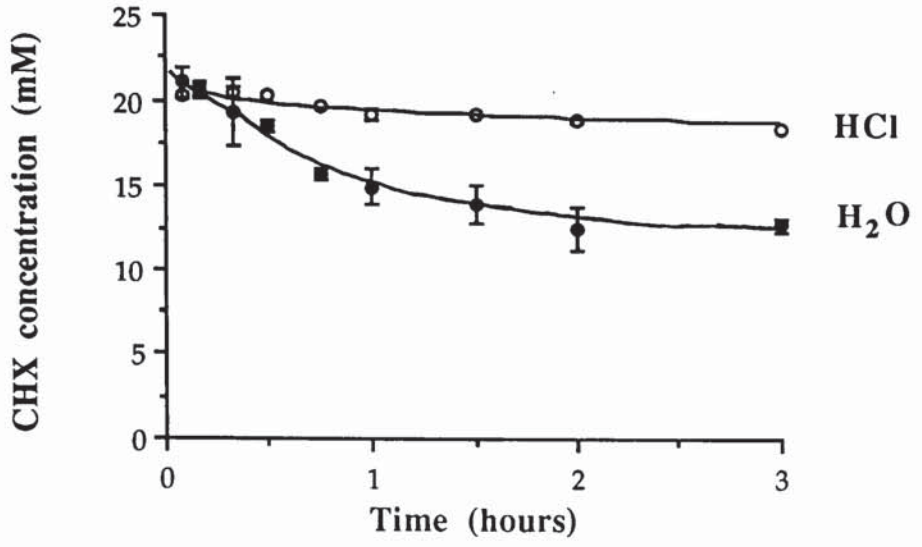

Figure 2.29 Dissolution profiles of the CHX-HP-β-CyD complex in distilled water and 0.15 M HCl at 37°C. Points represent the mean ± s.d., $n = 3$ for water data and $n = 2$ for acid data

In comparing the solubility profiles of CHG with the CyD complexes, it can be seen that only the CHX-HP-β-CyD complex has a greater initial solubility (20.325 ± 0.140 mM) than that achievable with CHG (11.8 mM). If the diffusion of antimicrobial agent to the site of bacterial infection is considered, by administration of CHG, the total amount of chlorhexidine is free and therefore would readily diffuse to the site of action. Theoretically however, by administration of a CHX-CyD complex, a reservoir of CHX would exist from which diffusion could occur. Dissolution of the CyD complexes results in both free and complexed CHX. As previously shown (section 2.6.4), the concentration of free CHX in the supersaturated system of the CHX-β-CyD complex was 6.8 mM and that for the CHX-HP-β-CyD complex was 13.6 mM. The concentration of available CHX is therefore greater than the solubility of CHX itself and consequently maximum diffusional flux is possible. Furthermore, the concentration of free drug in the HP-β-CyD complex is greater than that obtainable with administration of the soluble digluconate salt. In addition, a competitor can also be used to enhance the concentration of free drug further.

2.6.8 Dissolution studies in water using the rotating disk method

The dissolution of a solid in a liquid can be considered to consist of 2 phases. The first of these involves liberation of the solute molecules from the solid, which is followed by transport of these molecules away from solid-liquid interface to the bulk of the liquid

phase under the influence of diffusion or convection. The rate of dissolution of a solid in a liquid may be described quantitatively by the Noyes-Whitney equation (equation 2.9)

$$\frac{dm}{dt} = \frac{D.\,A\,(C_S - C)}{h} \qquad (2.9)$$

where m is the mass of the solute that has passed into solution in time t, *i.e.*, dm/dt represents the rate of dissolution, D is the diffusion coefficient of the solvent, A is the surface area of the dissolving solid, C_S is the concentration of drug in the saturated diffusion layer, C is the solute concentration at time t, and h is the thickness of the boundary layer. Units of the rate of dissolution are mass time^{-1}.

If sink conditions apply *i.e.* Cs >> C, then equation 2.9 can be simplified to:

$$\frac{dm}{dt} = \frac{D.A.C_S}{h} \qquad (2.10)$$

Furthermore, the dissolution rate constant, k, is equal to:

$$k = \frac{D}{h} \qquad \text{(units of length time}^{-1}\text{)} \qquad (2.11)$$

It therefore follows that:

$$\frac{dm}{dt} = k.\,A.C_S$$

which on rearrangement gives:

$$k = \frac{dm/dt}{A.C_S} \qquad (2.12)$$

In this study, dissolution occurred from disks which maintained a constant surface area throughout the procedure. The amount of drug released from the disk was plotted as a function of time. Using linear regression, the slope of the dissolution profile was found which was divided by the exposed surface area of the disk to give the amount of substance dissolved per unit time and unit surface area, *i.e.*, the intrinsic dissolution rate (IDR) which can be represented as the following term (Wells, 1988):

$$IDR = k.C_S \quad (2.13)$$

The disks of CHX alone showed a linear release of drug over the study period, with a intrinsic dissolution rate of (1.3302×10^{-2}) mM cm^{-2} min^{-1}. Instant disruption of the surface was observed when disks prepared from the physical mixes of CHX and CyDs were immersed in the dissolution medium. Thus, for comparison against dissolution of the complex, disks prepared from a 50 % weight per weight mix of cellulose and CHX were used. Pitha *et. al.* (1987) used a similar cellulose/guest mix as a control for the testosterone-γ-CyD complex. The intrinsic dissolution rate of these CHX/cellulose disks was found to be (0.3520×10^{-2}) mM cm^{-2} min^{-1}.

For both CHX-CyD complexes, sampling was performed for a shorter time due to disruption of the disk surface. However, up to the final sampling point shown in figure 2.30, dissolution occurred from an intact surface. The intrinsic dissolution rates were (6.4973×10^{-2}) mM cm^{-2} min^{-1} and (4.4809×10^{-2}) mM cm^{-2} min^{-1} for the β-CyD and HP-β-CyD complexes respectively. The dissolution profiles of the various test samples are illustrated in figure 2.30 with their intrinsic dissolution rates summarised in table 2.17.

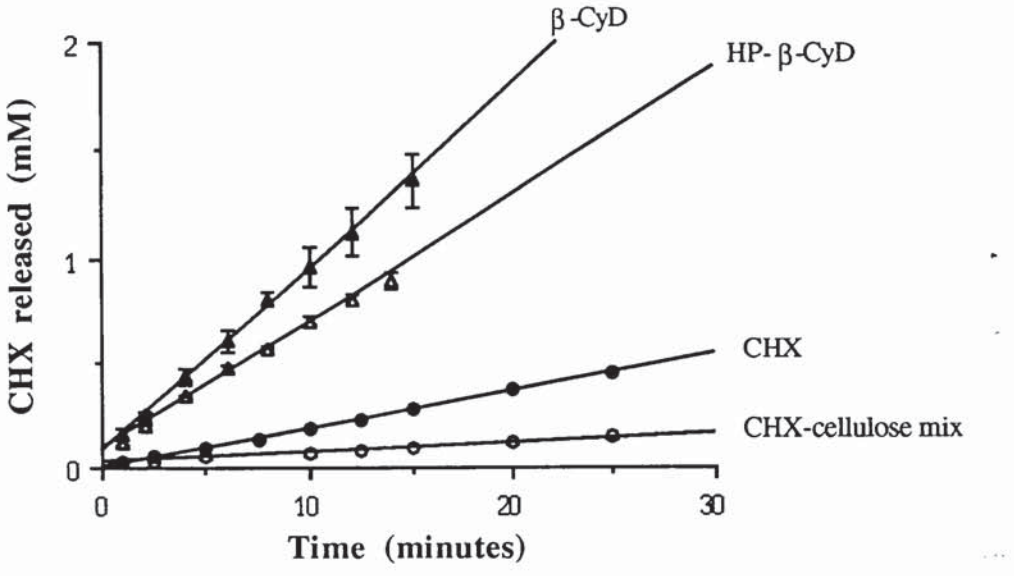

Figure 2.30 Dissolution profiles of CHX from disks prepared from CHX alone, 50 % w/w CHX/cellulose mix, CHX-β-CyD complex, CHX-HP-β-CyD complex. Points represent the mean ± s.d. of six or more replicates.

Table 2.17 Intrinsic dissolution rates of the CHX-CyD systems

Sample	slope ($\times 10^2$)	r^2	Intrinsic dissolution rate (mM cm^{-2} min^{-1}) $\times 10^2$
CHX	1.7652	0.999	1.3302
CHX/cellulose (50:50 w/w)	0.4671	0.994	0.3520
β-CyD-CHX complex	8.6219	0.999	6.4973
HP-β-CyD-CHX complex	5.9462	0.996	4.4809

The intrinsic dissolution rate of CHX was approximately 4-times greater than that for the CHX-cellulose disk. The reduced dissolution of the CHX/cellulose disks was expected since theoretically, only half of the surface of these disks comprised CHX molecules. With the disks of CHX however, the surface of the disk exposed to the dissolution medium consisted solely of CHX molecules. As shown by equation 2.11, k is affected by the diffusion coefficient of the solute and the thickness of the boundary layer. The diffusion coefficient of the solute is affected by the viscosity of the dissolution medium and the size of the diffusing molecule. Thus, in the case of cellulose, the molecule is relatively large and consequently its diffusion will be slower. The thickness of the boundary layer is affected by the degree of agitation, which in turn depends on factors such as the speed of stirring, size and position of stirrers. Since all experiments were performed with the same dissolution apparatus and a constant rotating speed, the effect of these variables of the boundary layer can be considered to be constant.

In comparing the dissolution profiles and the corresponding rates, it is evident that the solubility and intrinsic dissolution rate of CHX was significantly increased by forming complexes with both β-CyD and HP-β-CyD; dissolution rates increased approximately 5-fold and 3.4-fold for the β-CyD and HP-β-CyD complexes respectively. The enhanced dissolution behaviour of the complexes can also be attributed to their amorphous nature.

Surprisingly, the intrinsic dissolution rate of the β-CyD complex was approximately 1.5-fold greater than the rate for the HP-β-CyD complex. A greater rate may have expected for the latter CyD complex due its greater aqueous solubility. Parallel to the release of CHX from the disks, CyD is also solubilised in the dissolution medium. It is therefore possible that concentration of HP-β-CyD solubilised was sufficient to affect the viscosity of the dissolution medium which consequently lead to a lower that expected intrinsic dissolution rate for CHX.

The difference in hardness between the β-CyD and HP-β-CyD disks may also affect their intrinsic dissolution rates. Table 2.18 contains the results of the tablet hardness test performed on the compressed CHX-CyD complex disks. As can be seen, a greater force was required to break the HP-β-CyD complex disks indicating their greater hardness. This property may have contributed to the lower dissolution rate of the HP-β-CyD complex since tablet hardness will consequently effect solvent penetration of the disk surface and therefore release of drug into the dissolution medium.

Table 2.18 Hardness of compressed disks of solid-phase CHX-CyD complexes
Values represent the mean ± s.d., $n \geq 6$.

Sample	Hardness (N)
β-CyD-CHX complex	64.50 ± 6.67
HP-β-CyD-CHX complex	80.17 ± 7.31

To conclude therefore, dissolution testing by the rotating disk method has further confirmed the enhanced solubility and dissolution of CHX due to complexation with β-CyD and HP-β-CyD.

2.6.9 Diffusion studies performed on the CHX-β-CyD system

Many examples of the use of CyDs to enhance the aqueous solubility of poorly water-soluble drugs have been reported in the literature. Even though the total concentration of drug solution may have been increased, the availability of free drug from the water-soluble inclusion complex is important for its clinical efficacy. For systemic treatment, the amount of free drug is important for its absorption across the GI tract into the general circulation. The potential application of an antimicrobial-CyD drug in this study is for treatment against localised bacterial infections such in the oral cavity and in the GI tract (*H. pylori*). Since it has been reported that only free drug is microbiologically effective (Van Doorne, Bosch and Lerk, 1988), diffusion studies were undertaken to assess the amount of free antimicrobial agent available following dissolution and dissociation of its CyD complex.

Diffusion studies have been performed using systems comprising donor and receptor compartments with either semi-permeable cellulose dialysis membrane (Otagiri *et. al.*, 1983; Seo *et. al.*, 1983; Uekama *et. al.*, 1983) or silicone (silastic) membrane (Orienti *et. al.*, 1991) between them. With the former membrane, free drug, free CyD and

complexed drug are able to diffuse through to the receiver compartment. The diffusion of complexed drug through a semi-permeable membrane is expected to be lower than drug alone due to its larger molecular size. With silicone membrane, compounds are transported by initially dissolving in the membrane and then diffusing out into the receiver solvent. This mechanism of transport necessitates the diffusing solute to be of a lipophilic nature. Hence, silicone membrane is impermeable to CyDs and, therefore, also to the CyD complexes due to their hydrophilic nature. Thus, the concentration of drug in the receiver compartment is dependant upon the concentration of free drug only. Since the complex stability constant governs the dissociation of the complex, the diffusional behaviour of the drug will be dependant on this parameter. The diffusion of flurbiprofen (Otagiri *et. al.*, 1983) was greater from an aqueous solution of its γ-CyD complex (K_S = 460 M^{-1}) than its β-CyD complex (K_S = 5100 M^{-1}) indicating that the higher the stability constant the smaller the permeation of the drug. The diffusion behaviour will also depend on whether the CyD complexes are presented as solutions or suspensions in the receiver phase, this will be discussed later in section 3.6.7.1.

To assess the diffusion behaviour of CHX from its β-CyD complex, experiments were performed using suspensions of CHX alone and the CHX-β-CyD complex as the donor phases. Various membranes were used which included silicone membrane as discussed above, and also membranes of specific molecular weight cut-off limits. The ideal membrane will enable diffusion of free CHX into the receiver compartment whilst retaining free β-CyD and the complex in the donor phase. The mechanism of transport through molecular cut-off membranes is by diffusion of material through pores of a specific size. Thus, only compounds of molecular weights below the specified molecular weight cut-off level will be transported. However, the molecular weight cut-off point is not absolute and will depend on the nature of the molecule. For example, a relatively small molecular weight compound may adopt a rigid linear conformation restricting is transport through the membrane pores. In contrast, a molecule of a larger molecular weight and a spherical nature may have easier access through the pores. Amicon Diaflo ultrafiltration membranes type YM1 (molecular weight cut-off 500 Da.) and YM2 (molecular weight cut-off 1000 Da.), and Spectra/Por cellulose ester dialysis membranes of molecular weight cut-offs of 500 and 1000 Da. were assessed.

A typical diffusion profile of a drug diffusing through a membrane is illustrated in figure 2.31. It is characterised by a period of non-steady state diffusion (non-linear portion of graph) followed by steady-state penetration (linear portion of graph) where there is a net balance in the rate of entry and exit of drug into and out of the membrane.

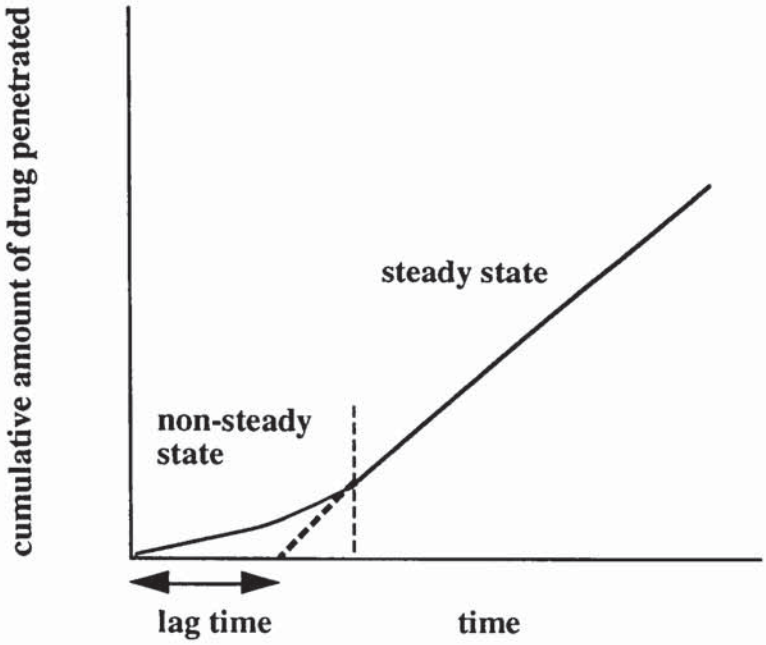

Figure 2.31 Schematic representation of a typical diffusion profile of a drug through membrane

The simplest way of modelling the diffusion process is by the application of Fick's first law of diffusion to the steady-state phase. The law states that the rate of transfer of a diffusing substance through a unit area of a section (the flux) is proportional to the concentration gradient across the entire barrier phase.

$$J = -D \frac{dc}{dx} \tag{2.14}$$

where J is the rate of transfer per unit area of surface (the flux), with the units of μmoles cm^{-2} $hour^{-1}$, dc/dx is the concentration gradient across the membrane and D is the diffusion coefficient with units cm^2 $hour^{-1}$. The flux of the penetrant corresponds to the slope of the steady-state diffusion curve in figure 2.31.

For a drug diffusing across a membrane of thickness, h, the concentration gradient may be written as:

$$\frac{C_1 - C_2}{-h} = -\frac{\Delta C}{h} \tag{2.15}$$

where C_1 and C_2 are the concentrations within the membrane, at the donor and receiver compartment side of the membrane respectively. Diagrammatic representation of the concentration gradient is illustrated in figure 2.32.

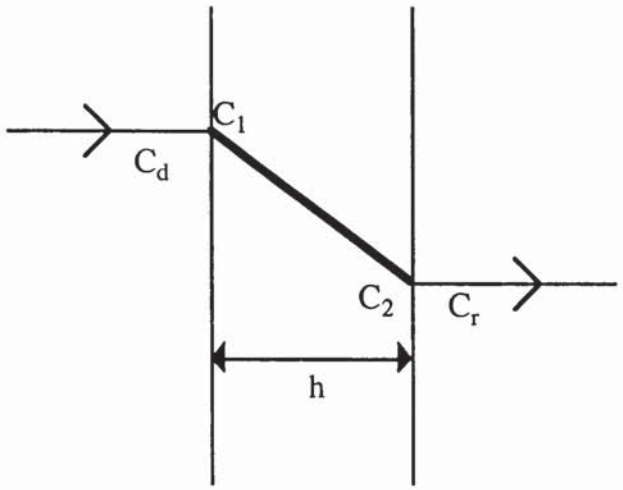

Figure 2.32 Diagrammatic representation of the concentration gradient across the membrane (C_d is the concentration at the donor side of the membrane and C_r is the concentration entering the receiver compartment; C_1 and C_2 are the concentrations within the membrane, at the donor and receiver compartment side of the membrane respectively; h is membrane thickness)

If, however, the barrier is not simply an inert structural barrier to diffusion but one with an affinity for the applied solute, partitioning into the membrane is also important. For this reason the parameter, P, the membrane-vehicle partition coefficient is introduced where:

$$P = \frac{C_1}{C_d} = \frac{C_2}{C_r} \qquad (2.16)$$

From equation 2.16 it follows that as:

$$dc = C_1 - C_2 = PC_d - PC_r = P(C_d - C_r) = P.\Delta C \qquad (2.17)$$

the flux may therefore be written as:

$$J = \frac{D.\ P.\Delta C}{h} \qquad (2.18)$$

It is possible to combine P, D and h into a single constant K_p, the permeability coefficient.

$$K_p = \frac{P.\ D}{h} \qquad (2.19)$$

The units of K_p are cm hour^{-1} (h^{-1}). Therefore by substituting K_p into equation 2.18 it can be shown that:

$$J = K_p.\Delta C \qquad (2.20)$$

If sink conditions apply, *i.e.* the depletion of the donor compartment is negligible, ΔC approximates to C_V, the applied drug concentration and the concentration in the receiver phase remains effectively zero. Hence equation 2.20 becomes:

$$J = K_p.C_V \qquad (2.21)$$

Using this equation, it is possible to determine the permeability coefficient, K_p, by dividing the steady-state slope of figure 2.31 by the initial concentration of drug applied to the donor compartment.

Prior to establishment of steady-state diffusion, there is a period where the flux of the drug is gradually increasing (non-steady state) as shown in figure 2.31. The linear portion of the line can be extrapolated to the x-axis in order to define a lag time, t_L, which is dependent upon the membrane diffusion coefficient D, and the thickness of the membrane h as shown in equation 2.22.

$$t_L = \frac{h^2}{6D} \qquad (2.22)$$

The determination of the lag time permits estimation of the diffusion coefficient, providing there is no binding. It should also be noted that the equations 2.15-2.17 are

only applicable to the steady-state phase provided there are no significant interactions, such as binding between the drug and the membrane constituents.

2.6.9.1 Diffusion of CHX from donor suspensions of free and complexed CHX using Amicon membranes of 1000 Da. molecular cut-off level

Preliminary diffusion studies were performed with Amicon membranes of 1000 Da. molecular cut-off level. Suspensions of CHX alone and the CHX-β-CyD complex were used as the donor phase. The concentration of CHX-β-CyD complex (17 mg/ml) used was equivalent to that used during previous dissolution studies (section 2.6.5) inorder to obtain a supersaturated solution from which maximal flux of CHX was possible. The diffusion of CHX from suspensions of free and complexed drug was assessed over 1.5 hours and are illustrated in figure 2.33. The permeation profile for CHX diffusion from a suspension of free drug was linear over this period of study, indicating steady-state diffusion. Using the linear portion of the rate curve, the steady-state flux of CHX from a donor suspension of free drug found to by linear regression was (4.1007×10^{-3}) μmoles cm^{-2} min^{-1}. Diffusion of CHX from the complex however, showed a constant diffusion rate over the first 40 minutes after which it declined. Using the first 9 data points up to this sampling time, the flux of CHX from a suspension of its β-CyD complex found by linear regression was (1.3330×10^{-2}) μmoles cm^{-2} min^{-1}.

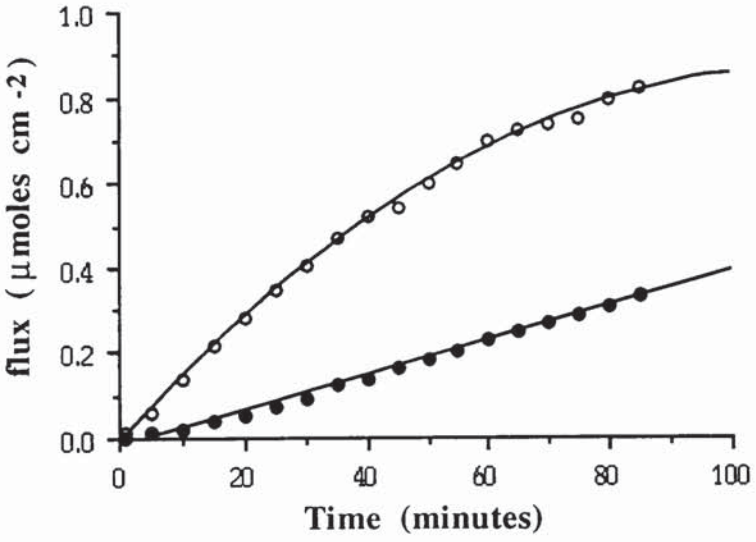

Figure 2.33 Transport of CHX through Amicon membrane (1000 Da. molecular cut-off level) from aqueous suspension of drug alone (•) and the CHX-β-CyD complex (o)

The concentration of CHX in the donor suspension of drug alone was maintained at a constant level (2.081± 0.050 mM) over the study period. As expected, the solubility of the complex was initially high at a concentration of 9.567 ± 0.125 mM, after which it declined to 5.866 ± 0.217 mM over the 1.5 hour study period. These concentrations correspond to both free and complexed CHX. Thus, using equation A4.20 in Appendix 4, the concentrations of free CHX in the CHX-β-CyD system were calculated and are summarised in table 2.19.

Table 2.19 Concentration of free CHX in the donor suspension of CHX-β-CyD complex calculated using equation A4.20 in Appendix 4 and K_S for CHX-β-CyD complex, 54 M^{-1}

Time (minutes)	Total CHX concentration of donor suspension (mM)	Concentration of total CHX concentration as free (mM)
5	9.567 ± 0.125	6.95
90	5.866 ± 0.217	4.68

Theoretically, since only the molecular weight of CHX is less than 1000 Da., only free CHX should diffuse through to the receptor compartment. The free CHX concentration in the CHX-β-CyD system can therefore be related to the flux measurements. The initial concentration of free drug in the suspension of the complex was 6.95 mM, which is approximately 2.3 times greater than the saturation solubility of CHX itself (2.081± 0.050 mM). Thus, the CHX-β-CyD system was supersaturated with respect to free CHX and so maximum flux can be expected. The flux of CHX from the donor suspension of the CHX-β-CyD complex was approximately 3 times greater than the flux from the free drug suspension which correlated well with the increase in free drug concentrations. The concentration of free CHX in suspension of the complex after 90 minutes was 4.68 mM and thus was still supersaturated. However, the rate of transport of CHX from this system was reduced after approximately 40 minutes which could be due to the reduced concentration differential between the donor and receiver phases.

This preliminary experiment has therefore shown the enhanced transport of CHX from its CHX-β-CyD complex due to supersaturation of free drug. Up to now it has been assumed that only free CHX is transported through the Amicon membrane used, however, it needs to be confirmed experimentally that β-CyD is too large a molecule to be transported.

2.6.9.2 *Diffusion of β-CyD and CHX through various membranes from donor phases of each component alone*

Control experiments were performed to determine whether β-CyD itself diffused through membranes of various types and pore sizes (Amicon, Spectra/Por and silicone membrane). The freeze-dried receiver samples obtained from using the 1000 Da. molecular cut-off membranes of Amicon and Spectra/Por showed the presence of solid white material. However, no residue was recovered from the freeze-dried receiver samples obtained from using the 500 Da. molecular cut-off membranes of Amicon and Spectra/Por and silicone membrane. These results indicate that, despite the molecular weight of β-CyD being greater than 1000 Da, the molecule was able to pass through the pores of these membranes, possibly due to its spherical nature. On the basis of these observations, it is therefore probable that during the preliminary experiments performed to assess the flux of CHX from its β-CyD complex, β-CyD may have been transported into the receiver compartment either as free or as the complex. The 1000 Da. molecular cut-off membrane is thus unsuitable for the determination of free drug diffusion. However, the pore size of the 500 Da. membrane restricted the transport of β-CyD, and, as previously discussed, β-CyD is unable to penetrate silicone membrane due to its hydrophilic nature. These results indicate that these membranes may be appropriate for the assessment of free drug diffusion, however, prior to their use, their permeability to CHX needs to be assessed.

Since the molecular weight cut-off levels are not absolute, there was a possibility that transport of CHX through the lower molecular weight cut membrane (500 Da.) may occur. However, when these membranes were used, no CHX was detected in the receiver compartment by UV spectroscopy at 255 nm. Similar experiments performed with silicone membrane also showed the impermeable nature of CHX to this membrane.

Due to the incompatibility of CHX with the range of membranes available, no further diffusion experiments were performed on the CHX-β-CyD system. To confirm the proposed theory on enhanced drug diffusion from the CyD complex and the effect of competitors, other guest candidates for CyD complexation where chosen. These had properties to allow them to be used by the available diffusion membranes. The results of these are in chapters 3 and 4.

A future consideration is the use of radiolabelled CHX and β-CyD (^{3}H-CHX and ^{14}C-β-CyD) to monitor the diffusion of the individual components. The effect of competitors on free drug concentrations can thus also be assessed.

2.6.10 Nuclear magnetic resonance spectroscopy for the study of the CHX-β-CyD inclusion complex

^{1}H-NMR was employed in the present study to determine the stoichiometry of the CHX-β-CyD inclusion complex by using the Continuous Variation Method (Job, 1928) and also to determine the mode of interaction between CHX and β-CyD.

The Continuous Variation Method is based on the fact that if a physical parameter directly related to the concentration of complex can be measured and plotted as a function of r (the ratio of the two complex components), its maximal will occur at $r = (n+1)^{-1}$, where the complex has a stoichiometry of 1:n (Djedäini *et. al.*, 1990). When this technique is employed in NMR spectroscopy, the physical parameter considered is the chemical shift. Two possible spectral changes may be observed due to the complexation of the guest. Firstly, the presence of a complex may give rise to separate signals, different from the free components. Secondly, only shifts of the spectral lines of the free components alone may be observed, which is due to fast exchange between the free and bound states. In this latter situation, if the signal belonging to the CyD is considered, the quantity $\Delta\delta \cdot [CyD]_t$ will be proportional to complex concentration, [C], and should be plotted against the ratio r. The total concentration of CyD and guest are denoted as $[CyD]_t$ and $[G]_t$ respectively. The quantity $\Delta\delta$ represents the chemical shift difference between free CyD (obtained in the absence of guest) and the observed value for a given ratio of CyD to guest (Djedäini *et. al.*, 1990). A similar plot can be constructed with consideration of the chemical shift changes seen in the guest.

The influence of β-CyD on the ^{1}H-NMR spectra of CHX and *vice versa* were studied in D_2O on the basis that inclusion complexation took place in solution. Signals for the protons of β-CyD were assigned on the basis of previous work by Demarco and Thakkar (1970) as illustrated in figure 2.34a.

No assignment for the chemical shifts of protons of CHX were found in the literature. The corresponding protons for the signals of the CHX spectrum were therefore deduced from a consideration of its chemical structure. Figure 2.35a illustrates the proton spectrum of CHX alone. The electronegativity of the neighbouring atoms of a proton will affect its chemical shift (δ); protons in the vicinity of high electronegative groups resonate at lower field and have higher δ values. Electronegative groups thus have a deshielding effect meaning that a lower value of the applied magnetic field is needed to bring the protons to resonance. As seen in the CHX structure, electronegative chlorine groups are present on the aromatic moieties, which could be responsible for the lower field proton signals. However, the main influence on the aromatic ring is due to the biguanide group

which also exerts a deshielding effect. Hence, the lower field signals (represented as *1* in figure 2.35a) correspond to the protons in the vicinity of the -NH- group. With consideration of other groups present in the CHX structure, the other signals have been assigned to the protons as shown in figure 2.35a.

From the spectra of the different samples of CyD and CHX, the changes in chemical shift observed for both components are contained in Tables 2.20 and 2.21 respectively. No new peaks appeared in the spectra of the mixed solutions which implied that the complexation was a dynamic process and the included drug was continuously exchanging between the free and bound states (Djedäini *et. al.*, 1990). The total concentration of the β-CyD and CHX was kept constant (1 mM) and the ratio of CyD to CHX and was varied between 0.2 and 0.8. Job plots (Job, 1928) were constructed by plotting $\Delta\delta\cdot[CyD]_t$ and $\Delta\delta\cdot[CHX]_t$ as a function of r, the ratio of CyD to CHX or *vice versa*; example plots are shown in figure 2.36. Although the shape of the Job plots are not highly symmetrical, the maximum does not deviate significantly from a guest/host ratio of 0.5, indicating the predominant existence of a 1:1 stoichiometry. The concentration of the components present and also the frequency of the instrument used will affect spectrum resolution and consequently affect the quality of the data used to construct the Job Plots. The stoichiometry of the indomethacin-β-CyD inclusion complex was determined in a similar manner by Djedäini and co-workers (1990) who obtained highly symmetrical Job Plots for both the CyD and respective guest. However, in contrast to the present study where 1 mM solution of guest and host were used together with a 250 MHz instrument, 10 mM concentrations were used in the indomethacin study and a 600 MHz instrument was employed.

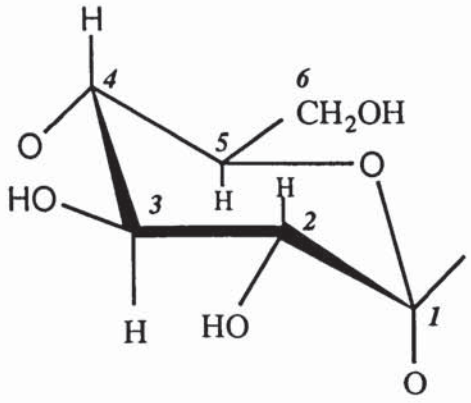

Figure 2.34a C-1 chair confirmation of glucose monomer of β-Cyclodextrin Numbers relate to carbon number. Carbons 3, 5 and 6 are located inside CyD cavity and carbons 1, 2 and 4 are on the exterior of the torus.

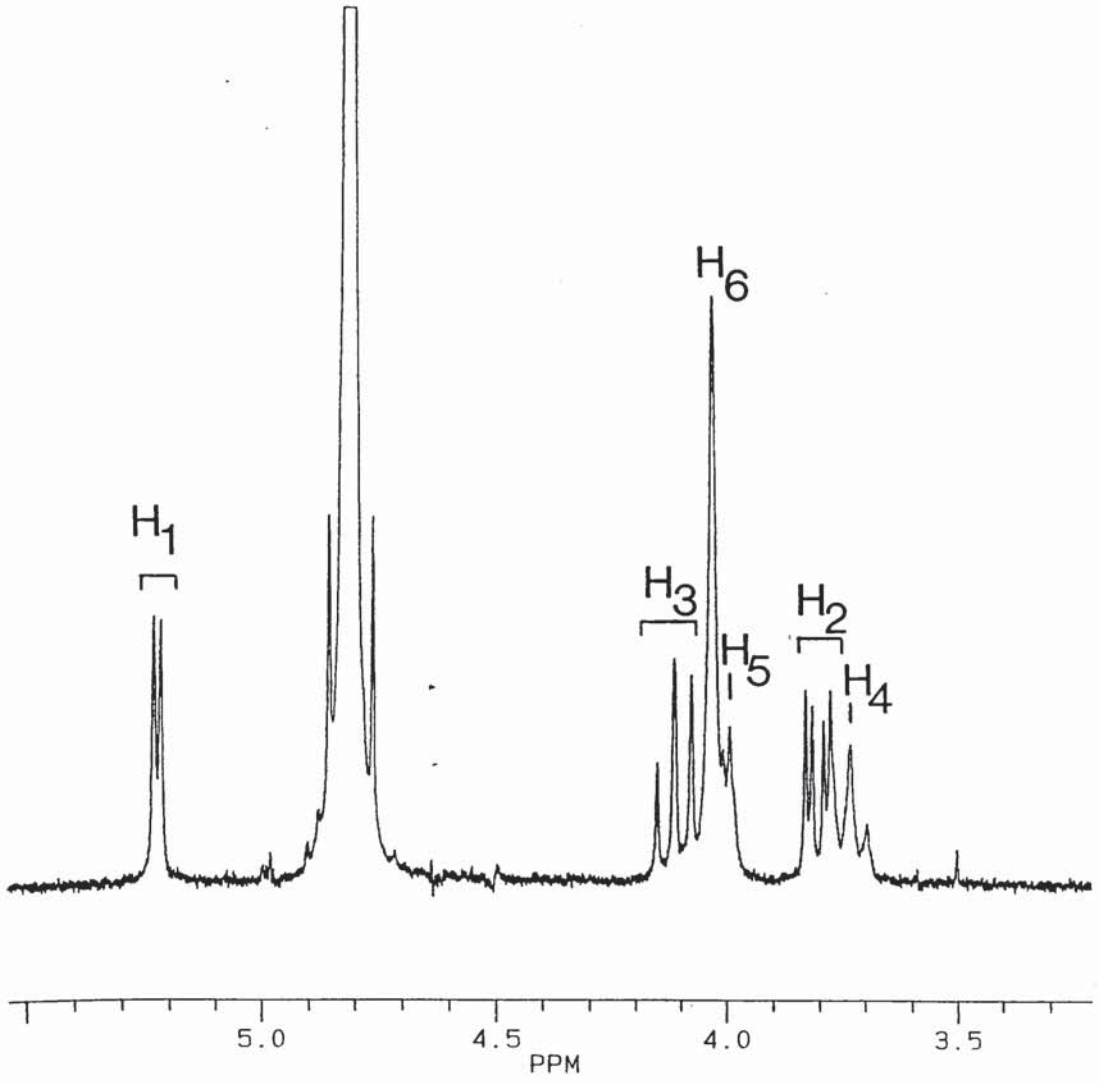

Figure 2.34b The 250 MHz ^{1}H-NMR spectrum of β-Cyclodextrin. H-1 to H-6 indicate the signals for protons on carbons 1 to 6 as shown in figure 2.34a

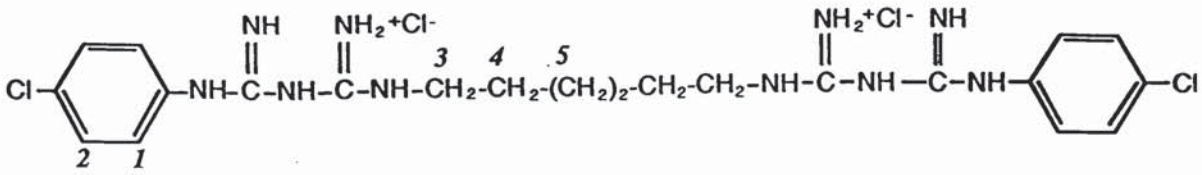

Figure 2.35a Assignment of protons of chlorhexidine dihydrochloride to the corresponding signals in the ^{1}H-NMR spectrum in figure 2.35b

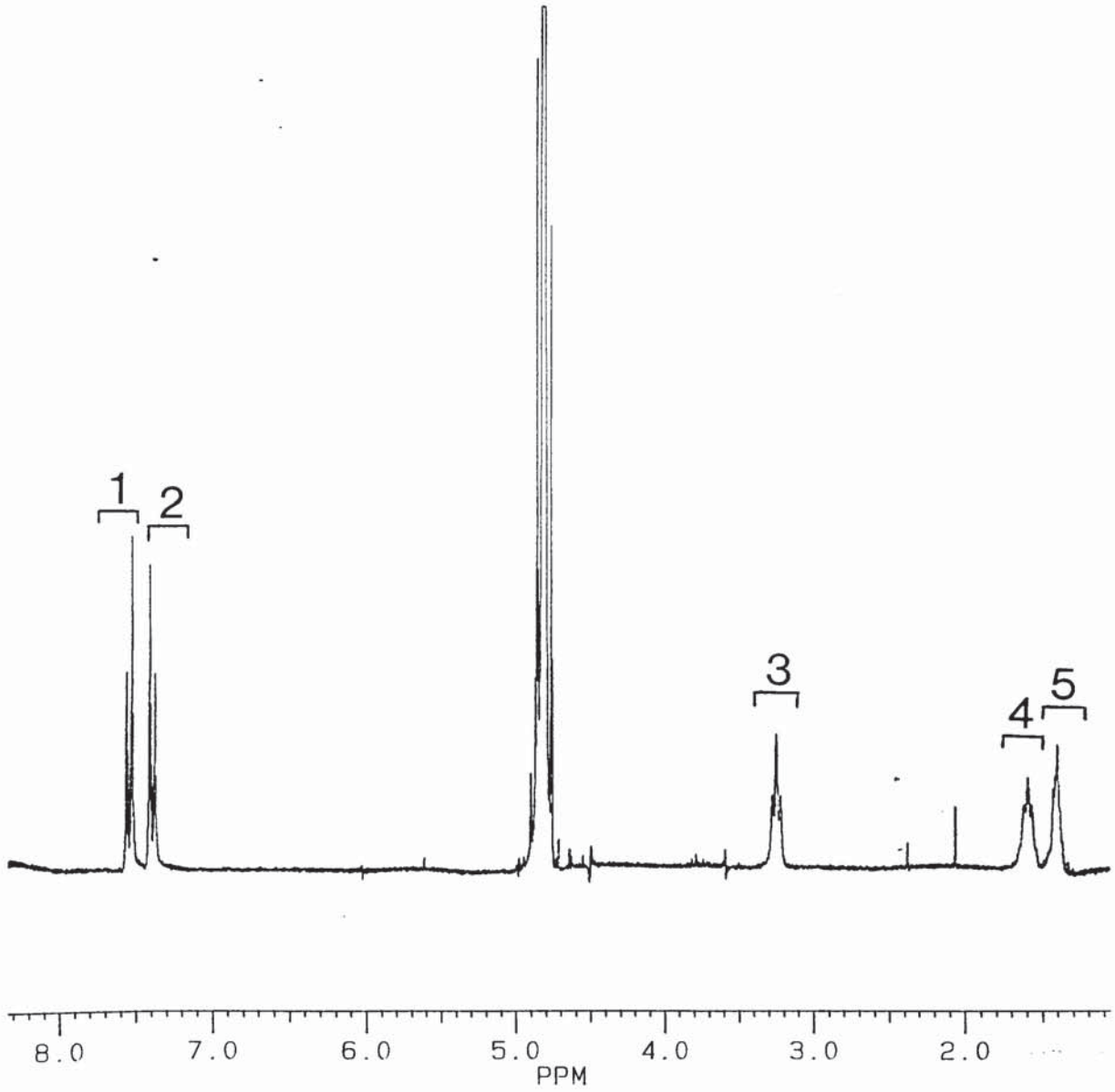

Figure 2.35b The 250MHz ^{1}H-NMR spectrum of chlorhexidine dihydrochloride. (The signals have been assigned to the protons as numbered in the structure in figure 2.35b)

Table 2.20 Changes in chemical shifts (δ) of β-CyD protons in the presence of CHX

β-CyD/CHX ratio (mM)	Proton (δ ppm)					
	H-1 (5.224)	H-2 (3.803)	H-3 (4.114)	H-4 (3.733)	H-5 (3.993)	H-6 (4.032)
0.2	0.006	-0.009	0.032	0.003	0.023	0.013
0.3	0.006	-0.008	0.033	0.005	0.026	0.012
0.4	0.005	-0.007	0.026	0.003	0.020	0.012
0.5	0.004	-0.006	0.023	0.003	0.020	0.011
0.6	0.002	-0.005	0.017	0.001	0.014	0.007
0.7	0.001	-0.004	0.012	0.001	0.011	0.004
0.8	0.001	-0.004	0.010	0.000	0.009	0.004

Change in chemical shift = $\delta_{CyD} - \delta_{CyD/CHX}$

Table 2.21 Changes in chemical shifts (δ) of CHX protons in the presence of β-CyD

CHX/β-CyD ratio (mM)	Proton (δ ppm)				
	P-1 (7.538)	P-2 (7.387)	P-3 (3.247)	P-4 (1.588)	P-5 (1.394)
0.2	0.023	-0.025	0.006	0.014	0.019
0.3	0.020	-0.024	0.006	0.013	0.018
0.4	0.019	-0.019	0.006	0.014	0.018
0.5	0.016	-0.015	0.005	0.011	0.014
0.6	0.013	-0.012	0.005	0.009	0.012
0.7	0.010	-0.008	0.002	0.006	0.007
0.8	0.008	-0.007	0.001	0.004	0.006

Change in chemical shift = $\delta_{CHX} - \delta_{CyD/CHX}$

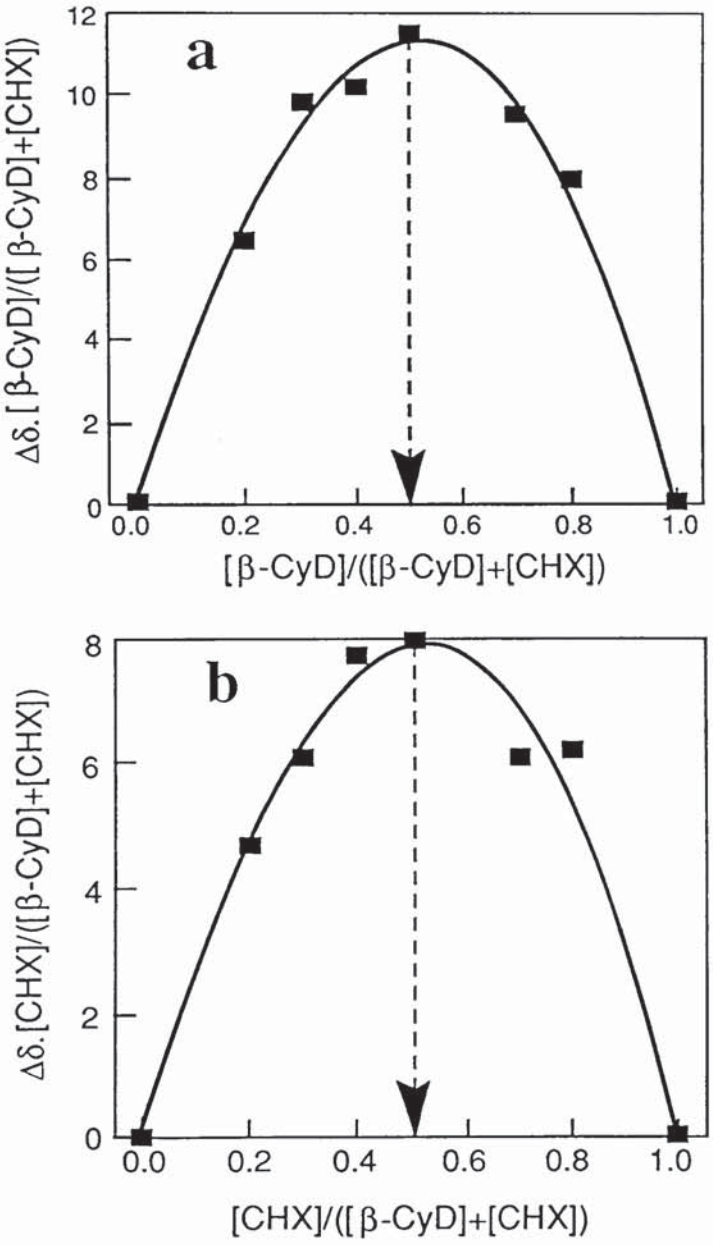

Figure 2.36 Continuous variation plot (Job Plot) for protons of (a) β-CyD (H-3) and (b) CHX (P-1)

All protons, of both the guest and host, exhibited the greatest chemical shift change at the lowest concentration of guest and host respectively, *i.e.* 0.2 mM, which can be explained as follows. In the presence of high concentrations of host (0.8 mM), most of the CHX in solution (0.2 mM) existed as the complex, and consequently the largest chemical shift change was observed. The reverse of this system is a high guest concentration (0.8 mM CHX) and a low host concentration (0.2 mM β-CyD). In the latter case, a large proportion of the total host will be complexed and thus the greatest chemical shift changes for the β-CyD protons were observed at a concentration of 0.2 mM.

All β-CyD protons, except for H-2, exhibited upfield chemical shift changes in the presence of CHX. The shift of the signal due to proton H-3 was most prominent followed by protons H-5 and H-6. The magnitude of the changes observed for protons H-1, H-2, H-4 were relatively small suggesting no significant interaction occurred between these exterior CyD protons and the guest. The upfield shifts of the signals of β-CyD result mainly from the magnetic anisotropy of the chlorophenyl moiety of CHX. Furthermore, the greater shift in protons H-3 and H-5, which are located in the CyD cavity, indicate that the guest was included in the cavity. However, the predominant chemical shift change of the H-3 protons compared with that of the H-5 protons suggests that on the ^{1}H-NMR time scale, more CHX entered the cavity from the wider H-3 side of the torus as expected.

All protons of CHX were shifted upfield except for P-2 which showed a downfield shift. Many researchers have found guest protons to be shift downfield (Cabral Marques *et. al.*, 1990; Ueda and Nagai, 1980; Suzuki and Sasaki, 1979). Low field shifts may be induced by steric perturbation, van der Waals shifts or diamagnetic anisotropy of particular bonds or regions of the host (Ueda and Nagai, 1980; Suzuki and Sasaki, 1979). The downfield change of proton P-2 suggests that inclusion of the CHX within the CyD cavity was achieved *via* the chlorophenyl moiety but only to a shallow extent. This relatively weak interaction is consistent with the results obtained by the solubility method (section 2.6.4) which revealed the K_S of the CHX-β-CyD complex to be 54 M^{-1}.

NMR studies of interaction between 8-anilinonaphthalene-1-sulphonate and β-CyD (Nishiijo and Nagai, 1991) revealed upfield shifts for some guest protons when included in the CyD which were thought to be due to C-C bond anisotropy of β-CyD. Therefore, if the upfield changes observed for the CHX protons also indicate inclusion within the CyD cavity, virtually all the CHX molecule would be encapsulated. For this proposed mode of inclusion, the biguanide region of the CHX molecule would occupy the centre of the CyD cavity. However, the biguanide group is relatively polar and would

consequently have a low affinity for the CyD cavity. It is therefore unlikely that this mode of interaction occurred.

The chemical shifts of the CHX protons (with the exception of P-2) moved upfield. This effect may suggest self-association of the CHX molecules and has also been reported by Bergeron and Rowan (1976) for *p*-nitrophenolate. With consideration of the geometry of the guest molecule together with the NMR data, the mode of inclusion of CHX is thought to be *via* the aromatic moiety. Figure 2.37 illustrates the proposed structure of the CHX-β-CyD complex as concluded from the NMR study. A consideration for further work is to perform NMR experiments involving the nuclear Overhauser effect (NOE) to obtain conclusive information regarding the geometry of the guest-CyD inclusion complex. As discussed previously, this method is concerned with the spatial relationship of the protons and has been used by Fronza *et. al.* (1992) for the prediction of the structure of the piroxicam-β-CyD complex.

As previously discussed, Qi, Nishihata and Ryting (1994) recently reported data on the interaction between chlorhexidine diacetate and β-CyD. By using ^{1}H-NMR spectroscopy, these researchers also found that inclusion of the chlorhexidine molecule in the CyD cavity occurred *via* the chlorophenyl moiety. In contrast however, they concluded that the interaction occurred *via* the primary hydroxyl side of the torus as proton H-5 of the CyD exhibited the greatest chemical shift change. Furthermore, the aromatic protons of chlorhexidine was shifted downfield due to the deshielding effect of the CyD cavity, and the protons H-3, H-5 and H-6 of the CyD experienced an upfield shift which was thought to be due to the shielding effect of the aromatic π electrons of chlorhexidine. These findings therefore correlated well with the NMR results of the present study.

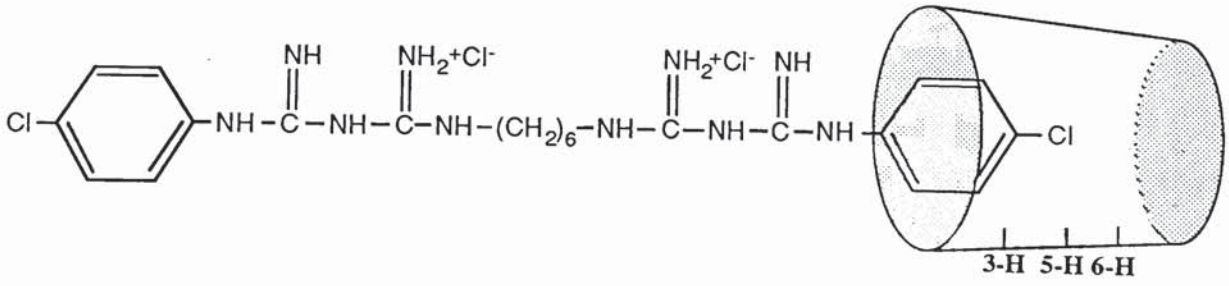

Figure 2.37 Model of the proposed structure of the β-CyD inclusion complex of chlorhexidine dihydrochloride

CHX has 2 chlorophenyl moieties, thus it is possible that a CHX-β-CyD complex could exist as a 1:2 or 1:2 complex. As discussed previously, Qi, Nishihata and Ryting (1994) reported the existence of both 1:1 and 1:2 CHX-β-CyD complexes in solution from UV analysis. However, the Job plots indicated that under the conditions of this study, the CHX-β-CyD complex formed in solution had a 1:1 stoichiometric ratio. On the basis of the data collated during the present study, the proposed orientation of CHX within the CyD cavity, together with the low complex stability constant reveal a relatively weak interaction between CHX and CyD indicating there is rapid exchange between free and complexed states.

To summarise, the ^{1}H-NMR study further confirmed the existence of a CHX-β-CyD inclusion complex in solution which has a probable stoichiometric ratio of 1:1. Complex formation occurred by partial inclusion of the aromatic moiety in the CyD cavity which can be further illustrated by the use of Stuart models as shown in plates 2.1 to 2.3.

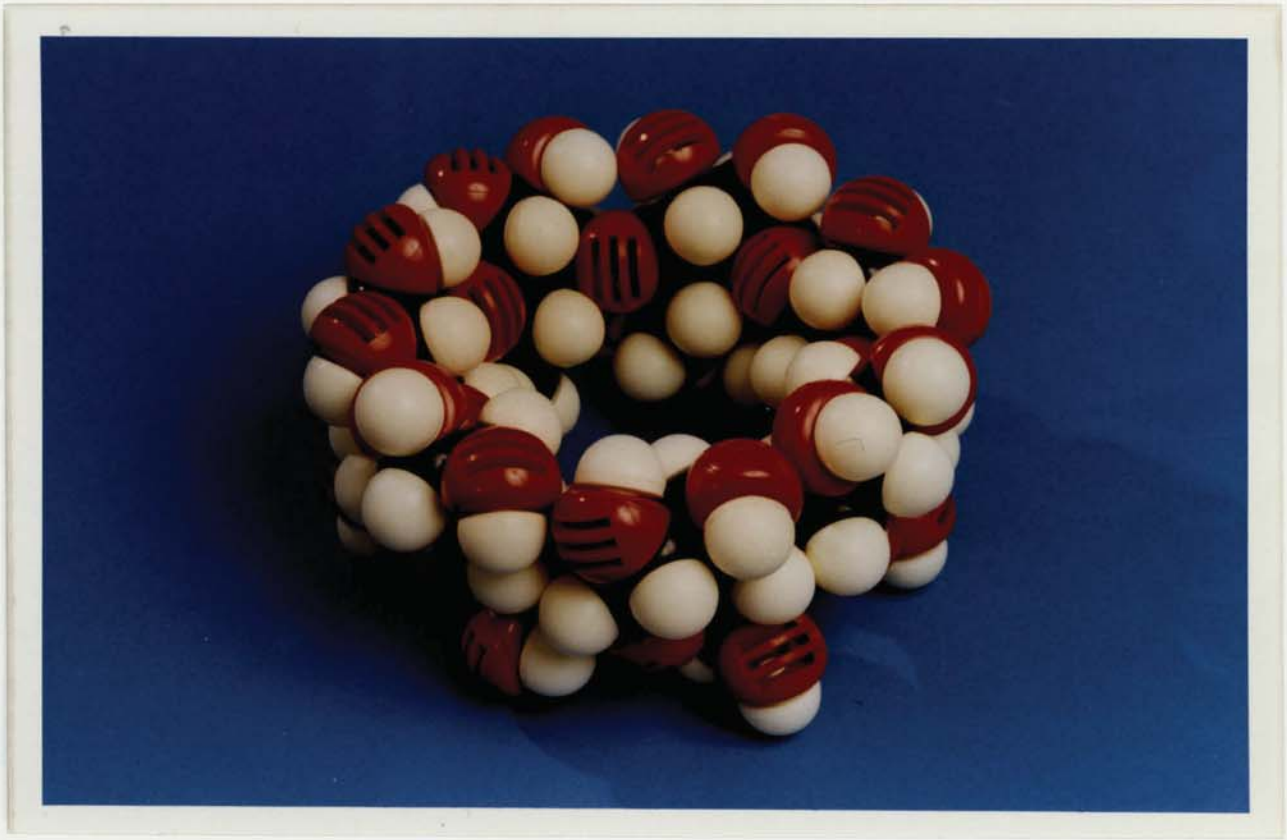

Plate 2.1 Stuart Model of β-Cyclodextrin

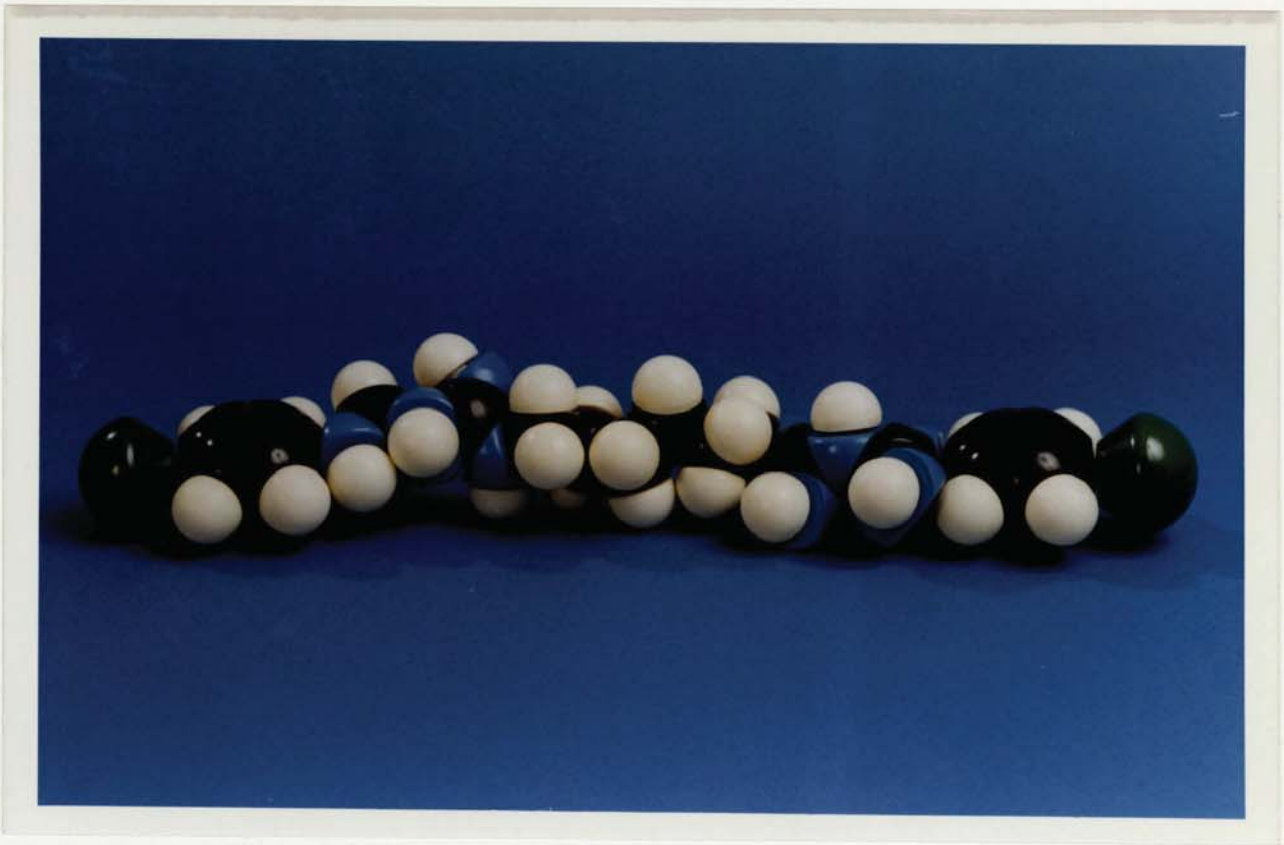

Plate 2.2 Stuart Model of chlorhexidine

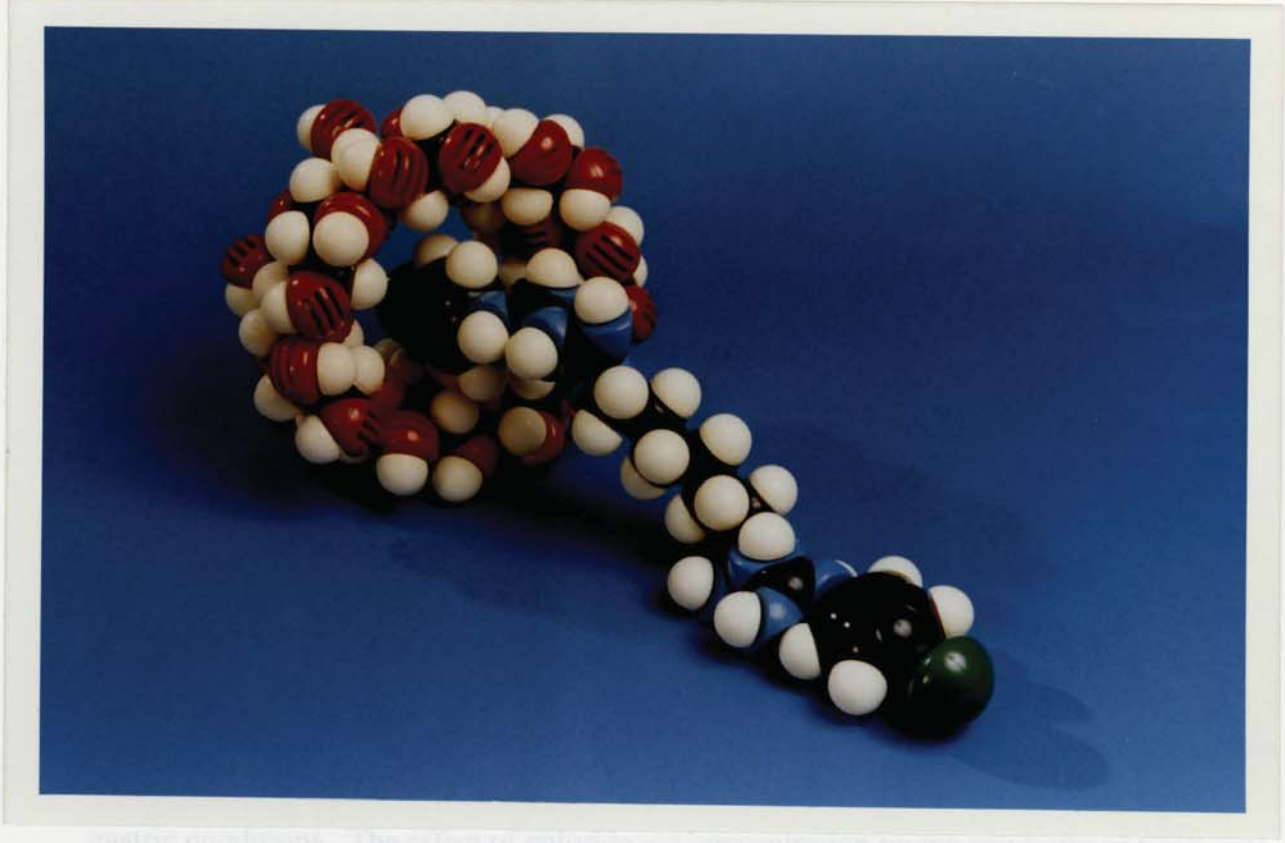

Plate 2.3 Stuart Model of proposed structure of CHX-β-CyD complex

2.7 CONCLUSIONS

The interactions between CHX and the CyDs, β-CyD and HP-β-CyD were studied in both solution and solid phases. The solid complexes were prepared by the freeze-drying method. The solid complexes of CHX-CyD have been examined by DSC, IR spectroscopy and X-ray diffractometry in comparison with the corresponding equimolar physical mixtures. DSC and X-ray diffractometry revealed significant differences between the behaviour of physical mixtures and the complexes from which true inclusion complex formation was confirmed. IR analysis revealed no significant differences since this technique is limited to carbonyl bearing guest species.

Dissolution studies performed on the solid CHX-CyD complexes showed the enhanced solubility of the complexes as compared to CHX alone. The solubility of the CHX-HP-β-CyD complex was greater than the respective β-CyD complex due to the greater aqueous solubility of the CyD derivative. Following dissolution of the CHX-CyD complexes, metastable supersaturated suspensions were formed. In these systems, the concentration of the drug in the non-complexed from was greater than the saturation solubility of CHX itself. Dissolution studies were also performed in the presence of phenylalanine and spironolactone as competing agents. Although there was no further increase in solubility of the CHX-CyD complexes, the concentration of free CHX may have been increased due to displacement by the competitor, and thus more would be available for activity. Therefore, diffusion of free CHX from these supersaturated systems was expected to be greater than from a suspension of CHX alone. Diffusion studies were performed with various membranes. However, due to the properties of CHX, no suitable membranes were available to allow selective diffusion of free drug only. Another possible way to monitor the diffusion of the free CHX is to use radiolabelled guest and host components. The effect of competitors on free CHX concentration could then also be assessed.

Dissolution studies performed using the rotating disk method revealed the enhanced intrinsic dissolution rate of the CHX-CyD complexes as compared to drug alone. This enhancement can be attributed to the increased solubility of CHX due to inclusion within the CyD cavity, and also due to the amorphous nature of the complexes.

Further dissolution studies comparing the solubility of the more soluble chlorhexidine salt, CHG to the CHX-CyD complexes were performed in HCl in an attempt to simulate gastric conditions. The effect of chloride ion concentration on the solubility of CHX was also observed following which it was found that in the presence of increased chloride, the

solubility of CHX was reduced due to the common-ion effect. At a concentration of 11.8 mM, the solubility of CHG in 0.15 M HCl was maintained. However, at higher initial concentrations of CHG, the CHX salt was formed which precipitated due to its limited water-solubility and the effect of the chloride ions present in solution. The solubility behaviour of the CHX-CyD complexes in 0.15 M HCl were initially similar to their behaviour in distilled water showing the formation of metastable supersaturated systems. With the CHX-HP-β-CyD system, the concentration of free CHX was greater than 11.8 mM. Thus, this latter CyD complex offers a greater advantage than the commercially available CHG for the delivery of a higher concentration of active chlorhexidine to the site of bacterial infection.

The interactions between CHX and the CyDs in solution were studied by phase solubility studies. With increasing concentrations of CyDs, the solubility of CHX was enhanced due to formation of a soluble complex with a probable stoichiometry of 1:1. The CHX-β-CyD system showed A_L type solubility; in contrast, the CHX-HP-β-CyD system was of the A_N type. The A_N type behaviour was thought to be due to the effect of the increased chloride concentration on the solubility of CHX as well to solvent effects. Using the CHX-β-CyD system, the temperature-dependence of the complex stability constant was illustrated. With a rise in temperature, K_S values decreased due to dissociation of the complex. Although, the thermodynamic parameters for complexation showed a favourable enthalpic change but an unfavourable entropic change, inclusion of CHX within the β-CyD cavity was energetically feasible as indicated by the favourable free energy change.

NMR spectroscopy was used to investigate the stoichiometry of the CHX-β-CyD in solution, and the mode of interaction between the guest and host. Job plots indicated a maxima when equimolar concentrations of guest and host were present indicating a stoichiometry of 1:1 for the complex. On the basis of the chemical shift changes, the CHX-β-CyD complex was formed by inclusion of the chlorophenyl moiety of CHX into the cavity *via* the wider secondary hydroxyl side of the CyD torus. Future work would include NOE experiments to confirm the predicted structure of the CHX-β-CyD further.

In conclusion, it has been shown that dissolution of the CHX-CyD complexes leads to supersaturated systems with respect to CHX alone. The diffusion of CHX this system will thus be greater than from a saturated solution of CHX, and, thus an enhanced microbiological effect is also expected. Furthermore, based on the solubility data, the potential CHX-CyD products could be delivered as two 200-500 mg tablets. However,

the retention of such products also needs to be considered so that sufficient drug can diffuse to the site of action.

CHAPTER THREE
INVESTIGATION OF THE INTERACTION OF THE *p*-HYDROXYBENZOIC ACID ESTERS WITH HYDROXYPROPYL-β-CYCLODEXTRIN

3.1 INTRODUCTION

The alkyl esters of *p*-hydroxybenzoic acid (parabens) possess both antifungal and antibacterial properties similar to their parent acid. Parabens are bacteriostatic in nature with their primary mechanism of action being inhibition of amino acid uptake processes in bacteria (Eklund, 1980). The antimicrobial activity of benzoic acid is due to its undissociated form, therefore since the acid has a pK_a of 4.2, it is effective at a pH of 4 or below, but relatively inactive at higher pH. The hydroxybenzoic acid esters (methyl, ethyl, propyl, and butyl) however, have pK_a values in the range 8 - 8.5 (Albert and Serjeant, 1984) and are therefore less readily ionised. Hence, the parabens have the advantage that they are active over a broader pH range (4 - 8), though their optimum activity is displayed in acidic solutions. The activity of the parabens increases with increasing alkyl chain length; however, a parallel decrease in aqueous solubility occurs. The general chemical structure of the esters is illustrated in figure 3.1 and a summary of their general properties is listed in table 3.1.

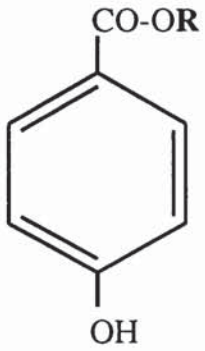

	R
methyl	$-CH_3$
ethyl	$-CH_2CH_3$
propyl	$-(CH_2)_2CH_3$
butyl	$-(CH_2)_3CH_3$

Figure 3.1 General chemical structure of the parabens

The parabens are used as pharmaceutical preservatives in oral preparations and products for external use. Methyl paraben, the most soluble ester, is usually used in aqueous preparations at concentrations of 0.1 to 0.2 %, whereas the higher esters are used in near saturated solutions. Two or more hydroxybenzoate esters are frequently used together so that a higher total concentration of preservative in solution can be achieved, and also, the

mixture of the esters may have an additive effect leading to their more extensive antimicrobial activity (Aalto *et. al.*, 1952).

Table 3.1 Some general properties of the parabens (Merck Index; Lehner, Müller and Seydel, 1993)

	Methyl (MeP)	Ethyl (EtP)	Propyl (PrP)	Butyl (BuP)
Molecular weight (Da.)	152.1	166.2	180.2	194.2
Melting point (°C)	125-128	115-118	95-98	68-69
Solubility (mg/100 ml)	250	75	40	15.4
Log P	1.85	2.33	2.87	3.44

One possible way to overcome the problem of low paraben concentration is by using the more water-soluble sodium derivatives of the esters, however, their ionisation will be dependant on the pH of the final solution. Another solution to the solubility problem could be the use of cyclodextrins as solubilisers of the parabens. Increasing the usable concentration of these preservative agents may enable their wider application.

Several researchers have studied the interactions between the alkyl hydroxybenzoates and the CyDs. The first study published in 1963 by Cohen and Lach assessed the interactions between the parabens and α- and β-CyD using phase solubility studies. With an increase in alkyl chain length from methyl to butyl paraben, the guest-host interaction also increased as indicated by the magnitude of the complex stability constants. Similar work was carried out by Uekama and co-workers (1980), using 12 parabens of increasing alkyl chain length which ranged from methyl to dodecyl paraben. In the presence of the CyDs, an initial increase in paraben solubility was observed, however, at higher CyD concentrations the paraben-CyD complexes were precipitated. As would be expected, the K_S values increased with increasing alkyl chain length, however, with long chain alkyl parabens, saturation level of K_S (~4500 M^{-1}) was attained indicating that there is an optimum guest molecule size for inclusion in the CyD cavity. The solid complexes isolated from phase solubility studies were subjected to DSC, IR spectroscopy and X-ray diffraction studies, all of which confirmed inclusion of the guest in the CyD cavity. Dissolution studies illustrated the superior solubility of the paraben-CyD complexes as compared to drug alone. Uekama and co-workers (1980) also carried out antimicrobial tests and found the MICs of parabens were increased in the presence of the CyDs. More recently, several researchers have studied the interactions between the parabens and HP-β-CyD (Lehner, Müller and Seydel, 1993; Matsuda *et. al.*, 1993). The latter work was concerned with the search of appropriate agents for the preservation of pharmaceutical

liquid formulations. It was found that the greater the interaction between the alkyl ester and HP-β-CyD, the greater the effect on the preservative action of the parabens. In contrast to the earlier work, soluble paraben-HP-β-CyD complexes were formed.

As discussed above, several studies concerning the interactions between the parabens and CyDs have already been reported in the literature. However, as yet, their has been no publications regarding the activity of a 1:1 paraben-CyD complex and also the effect of CyD complexation on paraben diffusion. One of the objectives of the present study was to investigate the effect of HP-β-CyD in enhancing the aqueous solubility of the parabens in an attempt to further increase their antimicrobial activity. The extent of the parabens-HP-β-CyD interactions were studied in both solution and solid phases, and, in addition, the antimicrobial activity of the 1:1 BuP-HP-β-CyD complex was also assessed. The potential application of a paraben-CyD product was against the treatment of localised bacterial infections such as *H. pylori* in the G.I. tract and oral cavity bacteria. This study, therefore, aims to compare and contrast the experimental data obtained with the recently published findings.

3.2 MATERIALS

Methyl, ethyl, propyl and butyl esters of *p*-hydroxybenzoic acid were purchased form Sigma Chemicals and were used as supplied. Details of all other chemicals and solvents used are listed in Appendix 2.

3.3 EQUIPMENT

Details of all equipment used are contained in section 2.3.

3.4 ASSAY PROCEDURES

UV spectroscopy and HPLC were used for quantification of parabens. Details of these assay procedures will be discussed in this section.

3.4.1 UV spectroscopy

The UV spectrum of each paraben was determined in the range 200-340 nm from which λ_{max} was found. All subsequent UV analyses of the parabens were performed at their

respective λ_{max} values which was found to be 256 nm for all esters. Quantification of the unknown paraben solutions was achieved from calibration graphs constructed by measuring the absorbance of aqueous solutions of the appropriate paraben of various concentration at λ_{max}. An example of the UV calibration graph for MeP is illustrated in figure 3.2 with the corresponding statistical parameters in table 3.2. Also shown in table 3.2, are typical statistical parameters for UV calibrations graphs of the remaining alkyl hydroxybenzoates together with the concentration range employed for each paraben.

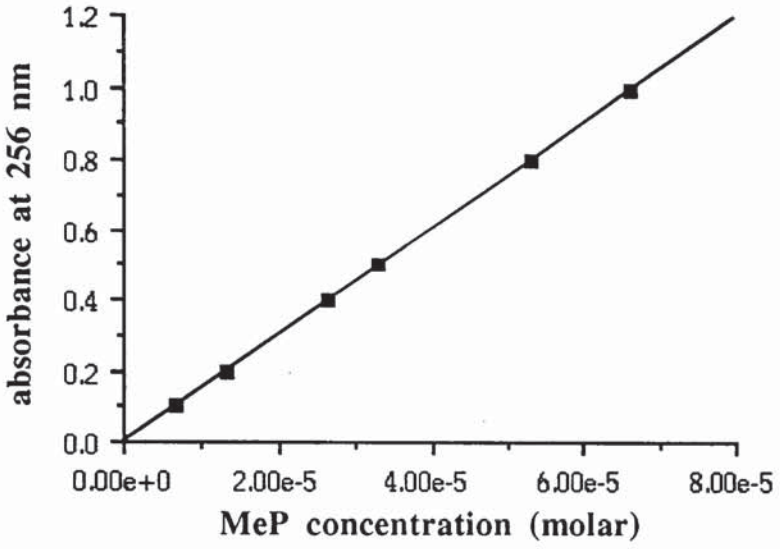

Figure 3.2 Example of the UV calibration graph for the methyl paraben (MeP)

Table 3.2 Calibration statistics and the concentration range for the UV calibration plots of paraben derivatives

Paraben	Concentration range (M)	Slope ($\times 10^{-4}$)	Intercept ($\times 10^{3}$)	Correlation coefficient
methyl	0.66 - 6.5 x 10^{-5}	1.5121	1.1667	1.000
ethyl	0.80 - 6.5 x 10^{-5}	1.4973	-0.0737	1.000
propyl	0.84 - 6.7 x 10^{-5}	1.5078	6.2604	1.000
butyl	0.95 - 7.1 x 10^{-5}	1.5319	0.0195	1.000

3.4.2 HPLC method development

Reversed-phase HPLC was employed for the quantification of all parabens. UV detection of the eluates was performed at 256 nm, the λ_{max} for each paraben as determined during UV analysis (section 3.4.1). Mobile phases consisted of methanol and water mixed in various ratios depending on the hydrophobicity of the ester, and was delivered at a flow rate of 1 ml min^{-1} to a stainless steel column (10 cm x 4.6 mm; column length x i.d.), *in-house* packed with 5 µm Spherisorb ODS2 reversed-phase material. Depending on which paraben was to be quantified, one of the remaining alkyl hydroxybenzoates was used as the internal standard (I.S.) such that, under the HPLC conditions employed, both solutes were adequately separated whilst maintaining a relatively short analysis time. A summary of the HPLC conditions used for the quantification of each paraben are contained in table 3.3 which also contains details of the I.S. used and its final concentration in the injected samples. A sensitivity of 0.005 AUFS was employed for all analyses together with an injection volume of 100 µl. Distilled water was used as the injection solvent for all samples. Quantification of sample peak responses was achieved using peak area ratios (analyte:I.S.). An example of a chromatogram from the MeP system together with a typical calibration plot are illustrated in figure 3.3. The respective statistical parameters for this plot, together with typical parameters obtained for the remaining alkyl hydroxybenzoates are contained in table 3.4. The concentration range of parabens injected are those shown in the table of conditions (table 3.3).

Table 3.3 Summary of HPLC conditions employed for the quantification of the paraben derivatives

Paraben	Methyl	Ethyl	Propyl	Butyl
concentration range ($M \times 10^4$)	0.06 - 1.50	0.06 - 1.50	0.06 - 1.80	0.06 - 2.00
mobile phase (methanol:water ratio)	55:45	65:35	65:35	65:35
retention time (minutes)	3.48	3.60	4.55	6.02
internal standard (I.S.)	ethyl paraben	propyl paraben	ethyl paraben	propyl paraben
I.S. concentration ($M \times 10^5$)	7.220	6.659	7.220	6.659
I.S. retention time	4.52	4.55	3.60	4.27

A)

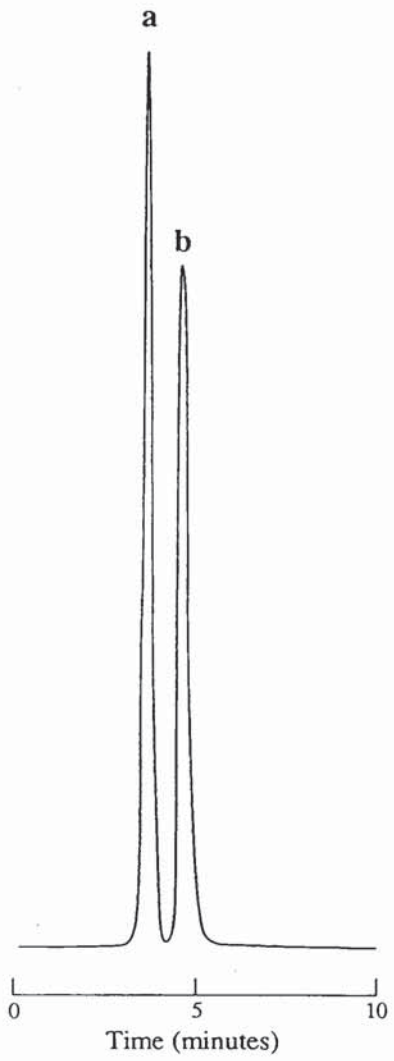

B)

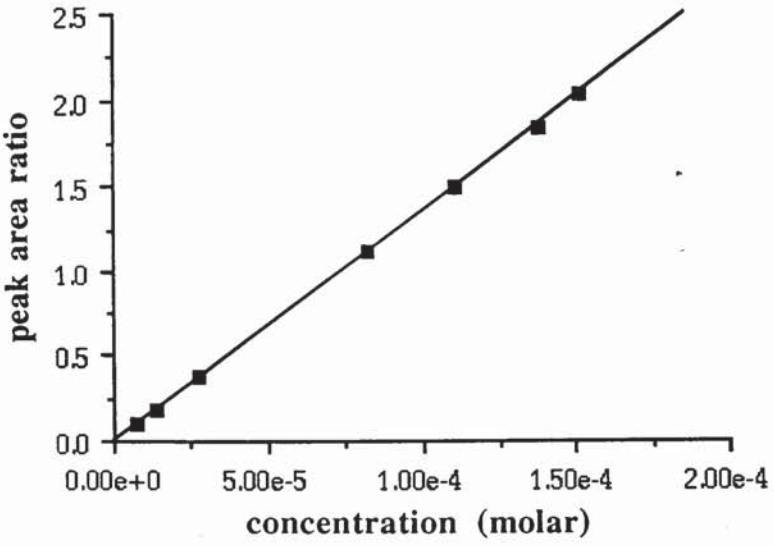

Figure 3.3 Examples of A) a typical chromatogram of methyl paraben (peak a, 8.25×10^{-5} M) with ethyl paraben (peak b, 7.22×10^{-5} M) as internal standard and B) typical calibration graph for methyl paraben

Table 3.4 Summary of the parabens HPLC calibration statistics

paraben	slope ($\times 10^{-4}$)	intercept ($\times 10^{3}$)	r^2
Methyl	1.3348	6.3194	1.000
Ethyl	1.6494	9.0744	1.000
Propyl	1.3470	9.7072	0.999
Butyl	1.5965	18.7021	1.000

3.5 EXPERIMENTAL

3.5.1 Preparation of the solid HP-β-CyD complexes of the *p*-hydroxybenzoic acid esters (parabens)

3.5.1.1 Preparation of the methyl paraben-HP-β-CyD complex

To 100 ml of distilled water, sufficient HP-β-CyD (11.4236g) and MeP (1.2176 g) were added such that the final concentration of each component in solution was approximately 0.08 M. The resulting mixture was heated to 60°C whilst stirring. Once all solid material had dissolved (after approximately 15 minutes) the solution was quickly cooled to room temperature by immersion into a ice bath. The solution was then transferred to a freeze-drying flask (500 ml) and quickly frozen by immersion in an acetone/dry ice bath and then lyophilised using an Edward Modulyo freeze-dryer.

3.5.1.2 Preparation of the ethyl paraben-HP-β-CyD complex

To 100 ml distilled water, sufficient HP-β-CyD (12.852 g) and ethyl paraben (1.4958 g) were added such that the final concentration of each component was approximately 0.09 M. The procedure described for the preparation of the MeP-HP-β-CyD complex (section 3.5.1.1) was then followed. With ethyl paraben, however, a longer time period was required for all solid material to dissolve (3 hours). The resulting solution was frozen and then freeze dried.

3.5.1.3 Preparation of the propyl paraben-HP-β-CyD complex

To 100 ml distilled water, sufficient HP-β-CyD (7.3197 g) and propyl paraben (0.901 g) were added such that the final concentration of each component was approximately 0.05 M. The procedure described for the preparation of the MeP-HP-β-CyD complex (section 3.5.1.1) was then followed, however on this occasion the mixture was left stirring at 60°C for 24 hours after which a clear solution was visible. The resulting

solution was frozen and then lyophilised in a similar manner to that described in section 3.5.1.1 for the methyl paraben-HP-β-CyD complex.

3.5.1.4 Preparation of the butyl paraben-HP-β-CyD complex

To 100 ml distilled water, sufficient HP-β-CyD (2.2846 g) and butyl paraben (0.3107 g) were added such that the final concentration of each component was 0.016 M. On this occasion the reaction mixture was stirred at 50°C for 7 days after which all material had dissolved. The solution was cooled to room temperature as previously described (section 3.5.1.1), transferred to a freeze-drying flask (500 ml) and quickly frozen by immersion in a acetone/dry ice bath and then lyophilised. The solid product recovered from freeze drying was washed twice with 10 ml diethyl ether and then freeze dried for a further 24 hours.

For larger scale preparation of the complexes, a greater volume of paraben/HP-β-CyD solution was prepared at the same concentration of paraben as described above.

3.5.2 Preparation of the equimolar physical mixes of HP-β-CyD and the *p*-hydroxybenzoic acid esters

The physical mixes were prepared by careful mixing of equimolar quantities (0.5 mmoles) of each paraben with 0.5 mmoles of HP-β-CyD (0.7139 g) in a similar manner to that described in section 2.5.2.

3.5.3 Investigation of the solid phase paraben-HP-β-CyD complexes

The solid phase paraben-HP-β-CyD complexes and the corresponding equimolar physical mixtures were subjected to DSC, TGA, IR spectroscopy and X-ray powder diffraction analysis. The experimental procedures followed were similar to those described for the investigation of the CHX-CyD complexes in section 2.5.3.

3.5.4 Chemical analysis of the paraben-HP-β-CyD complexes

For chemical analysis of the MeP and EtP-HP-β-CyD complexes, 5 mg of the respective complexes were accurately weighed and dissolved in 1 ml distilled water. For the analysis of the PrP and BuP-HP-β-CyD complexes, 10 mg of the respective complex was dissolved in 1 ml of distilled water. The paraben content of the dissolved complexes was determined by diluting 0.5 ml of the solution 50-fold using a 25 ml volumetric flask, however prior to making up to volume, 1 ml of internal standard stock solution was added. For the quantification of MeP and PrP, EtP (1.81×10^{-3} M) was used as the I.S. solution, and for the EtP and BuP assays, PrP solution (1.66×10^{-3} M)

was used as the I.S. All parabens were assayed by HPLC using an injection volume of 100 µl as described in section 3.4.2.

3.5.5 Determination of the solubility limit of the butyl paraben-HP-β-CyD

To 1 ml of distilled water maintained at 37°C in a water bath, increasing amounts of the BuP-HP-β-CyD complex were added in multiples of 25 mg in an attempt to reach a solubility limit. However, even after a total weight of 325 mg of complex had been added, a solution remained. The BuP concentration of the solution of the complex was determined by diluting 100 µl to 10 ml in a volumetric flask, followed by dilution of 0.5 ml of this initial dilution to 25 ml. However, prior to making up to volume, 1 ml PrP I.S. solution (1.66×10^{-3} M) was added. This final solution was assayed by HPLC using an injection volume of 100 µl as described in section 3.4.2.

3.5.6 Phase solubility studies of the paraben esters in the presence of HP-β-CyD

The experimental procedure followed was similar to that described in section 2.5.5 for the CHX-HP-β-CyD system. A constant but excess amount of paraben (MeP, EtP, PrP and BuP) was added to 2 ml aqueous solutions of HP-β-CyD of various concentrations (0.002 - 0.069 M) and the suspensions were shaken in a water bath at 37°C. With BuP, the procedure was repeated at 10, 25 and 45°C. The following amounts of the various parabens were added to the CyD solutions: 30 mg MeP; 30 mg EtP; 25 mg PrP; 20 mg of BuP was used at 10°C, 25 mg at 25°C, and 30 mg at 37°C and 35 mg at 45°C. Controls were also set up containing the same amount of paraben added to distilled water. The experiments were performed in triplicate with each paraben at each temperature. After equilibrium for 4 days, a 1.5 ml aliquot from each suspension was centrifuged at 13000 *rpm* for 5 minutes. The supernatants were diluted 25 to 500-fold. A 25-fold dilution was performed by diluting 1 ml of supernatant to 25 ml in a volumetric flask, however prior to making up to volume, 1 ml of I.S. stock solution was added. A 500-fold dilution was performed by initially adding 1 ml of the supernatant to 1 ml distilled water. A further 250-fold dilution was performed by placing 100 µl of the initial 2-fold dilution together with 1 ml I.S. solution in a 25 ml volumetric flask and making up to volume. Ethyl paraben I.S. solution (1.81×10^{-5} M) was incorporated into the MeP and PrP HPLC samples, and propyl paraben solution (6.7×10^{-5} M) was used as the I.S. for EtP and BuP HPLC samples. Quantification of paraben concentrations was achieved by injecting a volume of 100 µl under the appropriate HPLC conditions described for each paraben in section 3.4.2. Solubility diagrams were constructed for each paraben by plotting the concentration of ester solubilised *versus* HP-β-CyD concentration. Stability

constants were calculated from the linear portion of the solubility diagrams on the basis of a 1:1 stoichiometry using equation A3.13 in Appendix 3.

3.5.7 Analysis of the interactions between butyl paraben and HP-β-CyD in solution using UV spectroscopy

UV spectra of 4.13 x 10^{-5} M butyl paraben (BuP) in distilled water with increasing concentrations of HP-β-CyD (0.00001-0.100 M) were recorded on a Cecil 594 Double beam Spectrophotometer. The prepared solutions were shaken at 25°C and equilibrated overnight. The UV spectra of each solution was recorded using, as a reference, a HP-β-CyD solution of the same concentration.

3.5.8 Diffusion studies of parabens through silicone membrane from donor phases of free drug and the respective paraben-HP-β-CyD complex solutions

3.5.8.1 General procedure

Franz diffusion cells were employed for diffusion studies. The cells were assembled as previously described and illustrated in section 2.5.10. However, on this occasion, experiments were performed using only silicone membrane as the barrier between donor and receiver compartments. All experiments were performed in triplicate.

Quantification of drug diffusion into the receiver phase was achieved by UV spectroscopy. At set time points (usually every 30 minutes up to 7 hours) 1 ml samples were removed from the receiver compartment, placed in a 1 ml quartz cuvette (1 cm path length) and their UV absorbance at 256 nm determined against distilled water as the reference solution. After UV assay, the samples were returned to the receiver compartment. However, when the UV absorbance was greater than one, 200 µl of the receiver sample was transferred to an Epindorf tube to which 1 ml of distilled water was added. The UV absorbance of this 6-fold dilution was then determined. The volume of the receiver cell was maintained constant by replacement with 200 µl distilled water. This procedure produced a dilution of the receiver phase. Each successive sample concentration was adjusted for the dilution produced by all previous samples by applying a similar correction factor to that described in section 2.5.10 (equation 2.1). This correction factor was applied to experimental data using a BASIC computer program written by W. J. Irwin, which also converted the molar concentrations to µmoles cm^{-2} membrane.

$$C_t = C_{mt} + V_s \frac{\sum_{t=1}^{t=n-1} C_m}{V_d} \qquad (2.1)$$

where, C_t is the true concentration of drug in the receiver phase at time t, which would be found without dilution, C_{mt} is the current measured concentration of drug in the receiver compartment, V_s is the volume of sample removed for analysis, V_d is the volume of the receiver medium, and ΣC_m is the summed total of the previous measured concentrations (t =1 to n-1).

3.5.8.2 Diffusion of parabens through silicone membrane from a donor suspension of paraben alone

The general experimental procedure followed was as described in section 3.5.8.1. Pre-saturated suspensions of MeP, EtP, PrP, and BuP were prepared by adding excess drug to 20 ml distilled water and shaking overnight at 37°C. To each donor chamber, 5 ml of the pre-saturated suspension was added. Receiver samples were assayed by UV spectroscopy at 256 nm as described in 3.5.8.1. At time zero, the concentration of paraben in the donor chamber was also determined by centrifuging 1.5 ml of the donor suspension at 13000 *rpm* for 5 minutes. The recovered supernatant was diluted 25-fold, and its UV absorbance determined at 256 nm. Triplicate determinations were performed.

A further experiment was performed using a saturated solution of BuP (no excess solid present) as the donor phase. The experimental procedure followed was as described above, however, on this occasion, the concentration of the donor solution at the end of the experiment was also determined by diluting 0.5 ml of the donor solution to 10 ml in a volumetric flask. The UV absorbance of the 20-fold dilution was determined at 256 nm.

3.5.8.3 Diffusion of HP-β-CyD through silicone membrane

To assess the diffusion behaviour of HP-β-CyD through silicone membrane, the general experimental procedure described in section 3.5.8.1 was followed using 0.069 M HP-β-CyD solution as the donor phase. However, on this occasion no sampling of the receiver phase was done until after 7 hours when the receiver solution from each diffusion cell was carefully poured into a round bottom flask. The receiver solutions were then frozen by immersion into an acetone/dry ice bath and then lyophilised.

3.5.8.4 Diffusion of parabens through silicone membrane from donor solutions of the paraben-HP-β-CyD complexes

The experimental procedure described in section 3.5.8.1 was followed. For each paraben, MeP being the exception, the amount of HP-β-CyD complex used was sufficient to give a total paraben concentration 40 times the saturation solubility of paraben itself. The following weights of paraben-HP-β-CyD complex (actual paraben weight given in parentheses) were therefore dissolved in 2 ml distilled water contained in

the donor compartments: 1.101 g (0.116 g) EtP complex; 0.402 g (0.043 g) PrP complex; 0.240 g (0.023 g) BuP complex. With MeP, 0.560 g (0.0562 g) of its HP-β-CyD complex was added to 2 ml distilled water which would give a total MeP concentration ten times the saturation solubility of MeP alone.

Sampling of the receiver solutions during all experiments was performed using UV spectroscopy as described in section 3.5.8.1. The concentration of the donor solutions was determined at the beginning and end of the experiment, *i.e.* at time zero and 7 hours. A 2500-fold dilution was performed by initially transferring 100 µl of the donor solution to a 10 ml volumetric flask and making up to volume. This was followed by diluting 1 ml of the initial 100-fold dilution 25-fold in a 25 ml volumetric flask and measuring the UV absorbance of the final solution at 256 nm. Duplicate determinations were performed for each donor solution.

A further experiment was performed using sufficient BuP complex (6 mg dissolved in 2 ml distilled water) to give a total BuP concentration equivalent to the saturation solubility of BuP itself. Sampling of the receiver solution was performed as described above. The concentration of the donor solution was determined by diluting 0.5 ml of the solution of the BuP-HP-β-CyD complex in a 10 ml volumetric flask and measuring the UV absorbance of the final solution at 256 nm.

3.5.9 Diffusion of butyl paraben in the presence of competitors

Franz diffusion cells were employed and assembled as described and illustrated in section 2.5.10. The experimental protocol was as described in section 3.5.8.1

3.5.9.1 Diffusion of ascorbyl palmitate through silicone membrane

To assess the diffusion behaviour of ascorbyl palmitate (AsP) through silicone membrane, the general experimental procedure described in section 3.5.9 was followed. A pre-saturated suspension of AsP was prepared by adding excess AsP (10 mg) to 20 ml distilled water and shaking overnight at 37°C. To each donor chamber, 2 ml of the AsP suspension was added. On this occasion, sampling of the receiver solution was performed every 2 hours, with the UV absorbance being determined at 256 nm.

3.5.9.2 Diffusion of BuP through silicone membrane from donor phases of drug alone and the BuP-HP-β-CyD complex in the presence of AsP

The experimental procedures described in section 3.5.8.2 and 3.5.8.4 for assessing the diffusion of BuP from free and complexed donor phases respectively were followed with a few modifications. To assess the effect of AsP on the diffusion of BuP from its HP-β-

complex, 0.240 g BuP complex was added to 2 ml of a pre-saturated AsP suspension contained in the donor compartment. Sampling of the receiver solution was carried out every 15 minutes between the first and third hours of the procedure after which sampling was continued every 30 minutes until the end of the experiment. The concentration of BuP in the receiver samples was determined by HPLC analysis. To 1 ml of the receiver solution, 1 ml PrP I.S. solution (1.3×10^{-4} M) was added and 100 µl of this 2-fold dilution was injected under the HPLC conditions described in section 3.4.2. The volume of the receiver phase was kept constant by replacement with an equal volume of distilled water. The data obtained from HPLC analysis was adjusted using the correction factor described in 3.5.8.1.

The concentration of the donor suspension of AsP/BuP-HP-β-CyD complex was determined at the start and end of the experimental procedure by removal of 0.5 ml samples from the donor chamber and centrifugation at 13000 *rpm* for 5 minutes. The recovered supernatants were diluted 2000-fold by initially placing 100 µl of the supernatant in a 10 ml volumetric flask and making up to volume. This 100-fold dilution was further diluted by adding 100 µl to 0.9 ml distilled water and 1 ml PrP I.S. solution (1.3×10^{-4} M) contained in a HPLC vial. This procedure was repeated in duplicate for each donor solution. Using an injection volume of 100 µl, the final samples contained in the HPLC vials were assayed under the HPLC conditions described for BuP in section 3.4.2. The presence of AsP did not interfere with the BuP assay.

For an appropriate control to this procedure, the diffusion of BuP from a pre-saturated suspension of BuP with AsP was assessed. The latter suspension was prepared by shaking excess BuP and AsP in distilled water overnight at 37°C. To each donor compartment, 2 ml of the BuP/AsP suspension was added. Receiver samples (1 ml) were removed every 30 minutes up to the end of the experiment and diluted 2-fold with PrP I.S. (1.3×10^{-4} M) solution prior to their assay by HPLC as described above in section 3.4.2. The BuP concentration of the donor suspensions was determined by centrifuging 0.5 ml samples at 13000 rpm for 5 minutes and adding 100 µl of the recovered supernatant to 0.9 ml distilled water and 1 ml PrP I.S. solution (1.3×10^{-4} M) contained in a HPLC vial. Using an injection volume of 100 µl, the final samples contained in the HPLC vials were assayed under the HPLC conditions described for BuP in section 3.4.2.

3.5.9.3 *Diffusion of BuP through silicone membrane from donor phases of drug alone and the BuP-HP-β-CyD complex in the presence of the sodium dodecyl sulphate (SDS) and dodecyl trimethylammonium bromide (DTAB)*

The experimental procedures described in section 3.5.8.2 and 3.5.8.4 for assessing the diffusion of BuP from donor phases respectively were followed with some modifications. To assess the diffusion behaviour of BuP from its HP-β-CyD complex in the presence of SDS, 2 ml of 7.5 mM SDS solution previously heated to 37°C was placed in each donor compartment to which 0.240 g BuP complex was added. The concentration of the receiver solution was monitored using UV spectroscopy by sampling every 15 minutes between the first and third hours of the procedure after which sampling was continued every 30 minutes until the end of the experiment. The concentration of the donor solutions was determined at the start and end of the experiment by the centrifuging 0.5 ml of the donor solution at 13000 rpm for 5 minutes. A 2500-fold dilution was performed by initially transferring 100 µl of the recovered supernatant to a 10 ml volumetric flask and making up to volume. This was followed by diluting 1 ml of the initial 100-fold dilution 25-fold in a 25 ml volumetric flask and measuring the UV absorbance of the final solution at 256 nm. Duplicate determinations were performed for each donor solution.

For an appropriate control experiment, the general procedure described in section 3.5.8.1 was followed using 7.5 mM SDS solution as the donor phase. After 7 hours of exposure of the membrane to SDS, the diffusion apparatus was carefully dismantled leaving the membrane mounted on the donor compartments. The donor chambers and the surface of the membrane exposed to SDS were rinsed with distilled water to remove any remaining SDS. The receiver cell was also rinsed with distilled water and refilled with fresh solvent. The diffusion apparatus was reassembled and 2 ml of a pre-saturated aqueous BuP suspension was placed in each donor chamber. The experimental procedure described in section 3.5.8.2 for the diffusion of BuP from a free drug suspension was then followed.

The effect of DTAB on BuP diffusion was assessed in exactly the same way as above replacing the SDS solution with 13.5 mM DTAB solution. The presence of DTAB or SDS did not interfere with the UV spectroscopic assay of BuP.

3.5.10 Phase solubility study of ascorbyl palmitate in the presence of HP-β-CyD at 37°C

The experimental procedure followed was similar to that described in section 3.5.6 for the paraben-HP-β-CyD systems. A constant but excess amount of AsP (5 mg) was added to

2 ml aqueous solutions of HP-β-CyD of various concentrations (0.002 - 0.069 M) and the suspensions were shaken in a water bath at 37°C. Controls were also set up containing the same amount of AsP added to distilled water. After equilibrium for 2 days, 1 ml samples from each suspension was centrifuged at 13000 rpm for 5 minutes. To 100 µl of the supernatant, 100 µl of triclosan I.S. solution (1.95×10^{-3} M) was added together with 100 µl of a solvent mixture which consisted of acetonitrile, propan-2-ol and butan-1-ol in the ratio 2:1:1 respectively. The triclosan I.S. stock solution was also prepared in this solvent mixture. The samples were assayed by HPLC using the following conditions (personal communication, T. Grattan, SmithKline Beecham): mobile phase consisting of 62 % acetonitrile, 15 % 2.5 mM sodium dihydrogen orthophosphate solution, 15 % propan-2-ol, 5 % butan-1-ol and 3 % of a 50 % glacial acetic acid-water mixture was delivered to a 10 cm ODS2 Spherisorb column at a flow rate of 1.2 ml min^{-1}; UV detection of the elutes was monitored at 250 nm; a sensitivity of 0.005 AUFS was employed for all analyses together with an injection volume of 200 µl; the injection solvent consisted of distilled water and the solvent mixture in the ratio of 1:2. Quantification of sample peak responses was achieved using peak area ratios (AsP:I.S.). The concentration range of the AsP calibration solutions was $0.05 - 3.31 \times 10^{-4}$ M. The phase solubility diagram for AsP was constructed by plotting the concentration of AsP solubilised *versus* HP-β-CyD concentration. Stability constants were calculated from the linear portion of the solubility diagrams on the basis of a 1:1 stoichiometry.

3.6 RESULTS AND DISCUSSION

3.6.1 Preparation of the paraben-HP-β-CyD complexes

The complexes were prepared by a method recently used by Lehner and co-workers (1993) to prepare the propyl paraben-HP-β-CyD complex. Equimolar ratios of the parabens and HP-β-CyD were used for the preparation of each complex, however, the concentration of components varied depending on the paraben. Initially, various concentrations of the components were used for the preparation of the BuP-HP-β-CyD complex which ranged from 2 x S_{BuP} to 25 x S_{BuP}, where S_{BuP} is equal to the solubility of BuP in water according to the Merck Index (7.93×10^{-4} M; 15 mg/100 ml). At all concentrations, up to a concentration of 20 x S_{BuP}, excess BuP was initially present which was gradually solubilised due to the presence of HP-β-CyD, however the time required for solution formation was dependant on how much BuP was added. With a concentration of 20 x S_{BuP}, all solid was solubilised after 7 days shaking at 50°C, however, with 25 x S_{BuP}, solid material still remained after 10 days. On this basis, the

complex was therefore prepared using equimolar quantities of HP-β-CyD and BuP such that the final molar concentration of each component was 20 x S_{BuP}, *i.e.* 0.016 M.

For the preparation of the HP-β-CyD complexes of EtP and PrP, similar equimolar concentrations were used such that the final concentration of paraben would be 20 times its solubility according to the Merck Index. Using a similar 20-fold concentration for the MeP complex resulted in a very viscous solution due to the high concentration of HP-β-CyD (0.32 M; ~ 46 % w/v) which led to difficulties in freeze drying. The MeP-HP-β-CyD complex was, therefore, prepared using equimolar concentrations such that the final MeP concentration was 5 times the solubility of the paraben itself.

With a decrease in aqueous solubility of the parabens from the methyl to butyl ester, more time was required for the solutions of the complex to form. The reaction mixtures for all parabens, BuP being the exception, were heated at 60°C to aid dissolution of the solid material. A lower temperature was used during the preparation of the BuP-HP-β-CyD complex due to the melting point of this paraben being ~ 68°C. When the resulting BuP-HP-β-CyD solution was being frozen, precipitation of solid occurred which was most likely to be BuP due to its limited solubility; thus, the product recovered on freeze-drying was washed with diethyl ether to remove any free BuP. During the freezing of the other paraben complex solutions no precipitation was seen, thus, no washing process was performed on their freeze-dried products.

3.6.2 Investigation of the solid-phase paraben-HP-β-CyD complexes

Various methods were used for the characterisation of the solid phase CyD complexes, which included DSC, TGA, IR spectroscopy and X-ray powder diffraction.

DSC analysis of BuP alone showed a melting endotherm at approximately 69°C (figure 3.7A), which was also present in the thermograms of the equimolar BuP-HP-β-CyD physical mix (figure 3.7C) and the complex prior to washing with diethyl ether (figure 3.7D). However, the BuP peak appeared to have completely disappeared in the thermogram for the washed complex (figure 3.7E) indicating that any free BuP had been removed during the washing procedure and also that a real inclusion complex was formed between BuP and HP-β-CyD. Example thermograms of the BuP-HP-β-CyD system are illustrated in figure 3.7.

DSC thermograms obtained for the MeP, EtP and PrP-HP-β-CyD complex also showed similar results. In all cases, the endotherm corresponding to the melting point of paraben was present in the thermogram of the respective equimolar physical mixes but was absent

from the thermograms of the CyD complexes. Figures 3.4 to 3.7 illustrate the thermograms obtained for the various paraben-CyD systems. Since on a weight per weight basis the ratio of paraben to HP-β-CyD is low (~ 9.6 -12 % w/w), the relative size of the free drug peak in the physical mix thermograms was small, however, this increased with increasing alkyl chain length of the esters as expected.

From DSC analysis it was evident that real inclusion complexes were formed between the parabens and HP-β-CyD. The thermal behaviour of the parabens in the respective complex systems may be a consequence of the reduced intermolecular association between the individual guest molecules due to their monomolecular dispersion within the CyD cavity (Nakai *et. al.*, 1980).

Further evidence of complexation was obtained from IR absorption spectroscopy. The parabens-HP-β-CyD complexes were ideal candidates for this method of investigation as the guest species have carbonyl moieties (C=O). The IR spectra for the BuP-HP-β-CyD system in the carbonyl stretching region are shown in figure 3.8. The strong absorption band at 1675 cm^{-1} in the BuP spectrum (figure 3.8A) is due to the presence of the carbonyl group. No shift in this peak was observed in the physical mixture spectrum (figure 3.8C), however its intensity was reduced which is due to the low guest to host ratio of mix. The carbonyl peak of the BuP-HP-β-CyD complex shifted to 1710 cm^{-1} (figure 3.8D) with a decrease in intensity. The displacement and reduction in intensity in the stretching band corresponding to the BuP carbonyl moiety is indicative of an interaction between BuP and the HP-β-CyD. The shift to a higher frequency may be due to the breakdown of intermolecular hydrogen bonding associated with the BuP molecules (Bellamy, 1958). The shift of the carbonyl stretching band of the included guest to a higher frequency has also been observed in the aspirin-β-CyD system (Nakai *et. al.*, 1978), the ibuprofen-β-CyD complex system (Chow and Karara, 1985) and with CyD complexes of steroid hormones (Uekama *et. al.*, 1985).

IR analysis of the MeP, EtP, and PrP-HP-β-CyD systems also showed similar shifts in the carbonyl absorption band in the spectra of their respective complexes which further confirms the existence of the paraben-HP-β-CyD inclusion complexes.

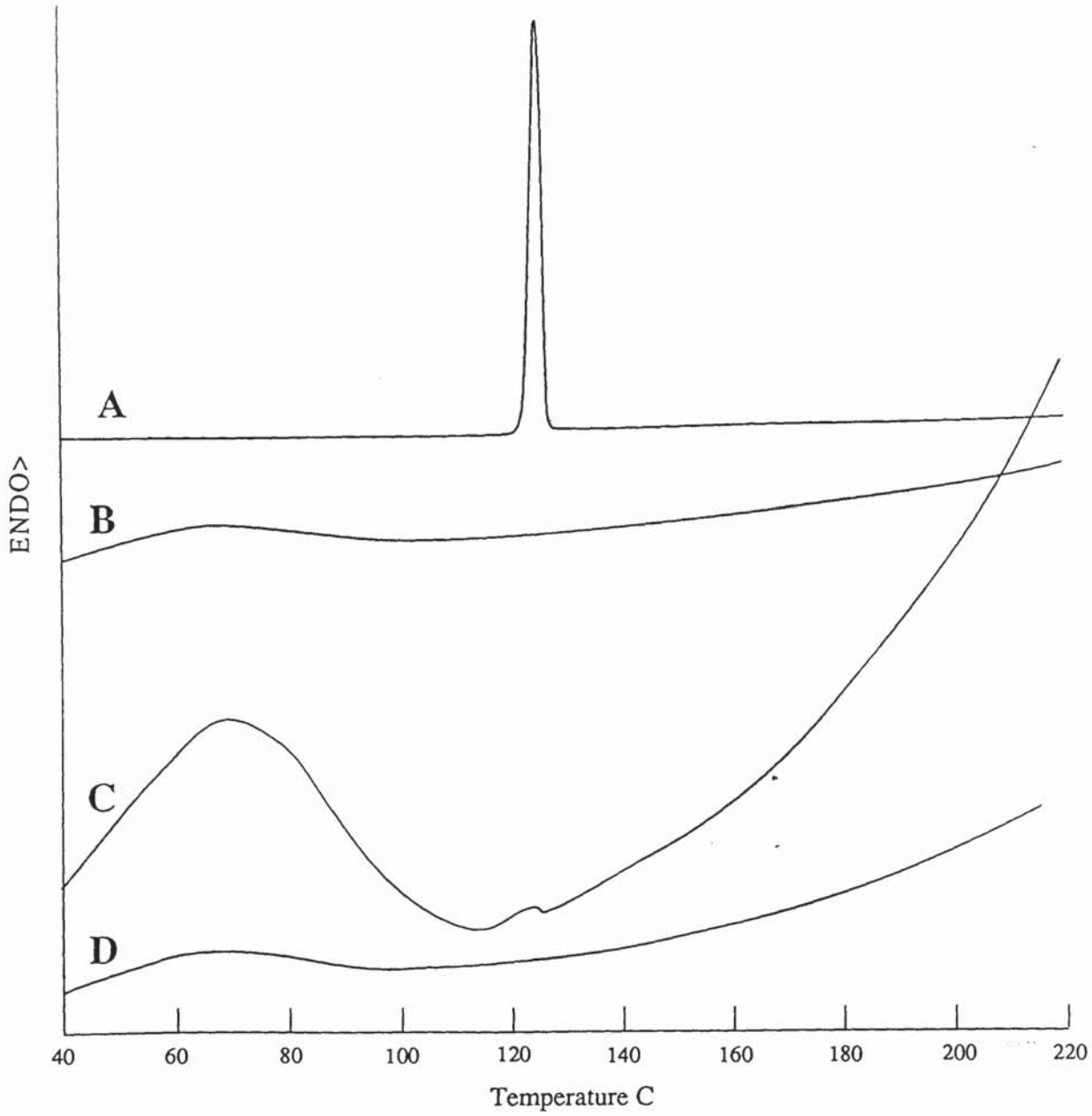

Figure 3.4 DSC thermograms of: A) methyl paraben (MeP), B) HP-β-CyD, C) the physical mixture of MeP and HP-β-CyD (molar ratio 1:1), and D) the MeP-HP-β-CyD complex

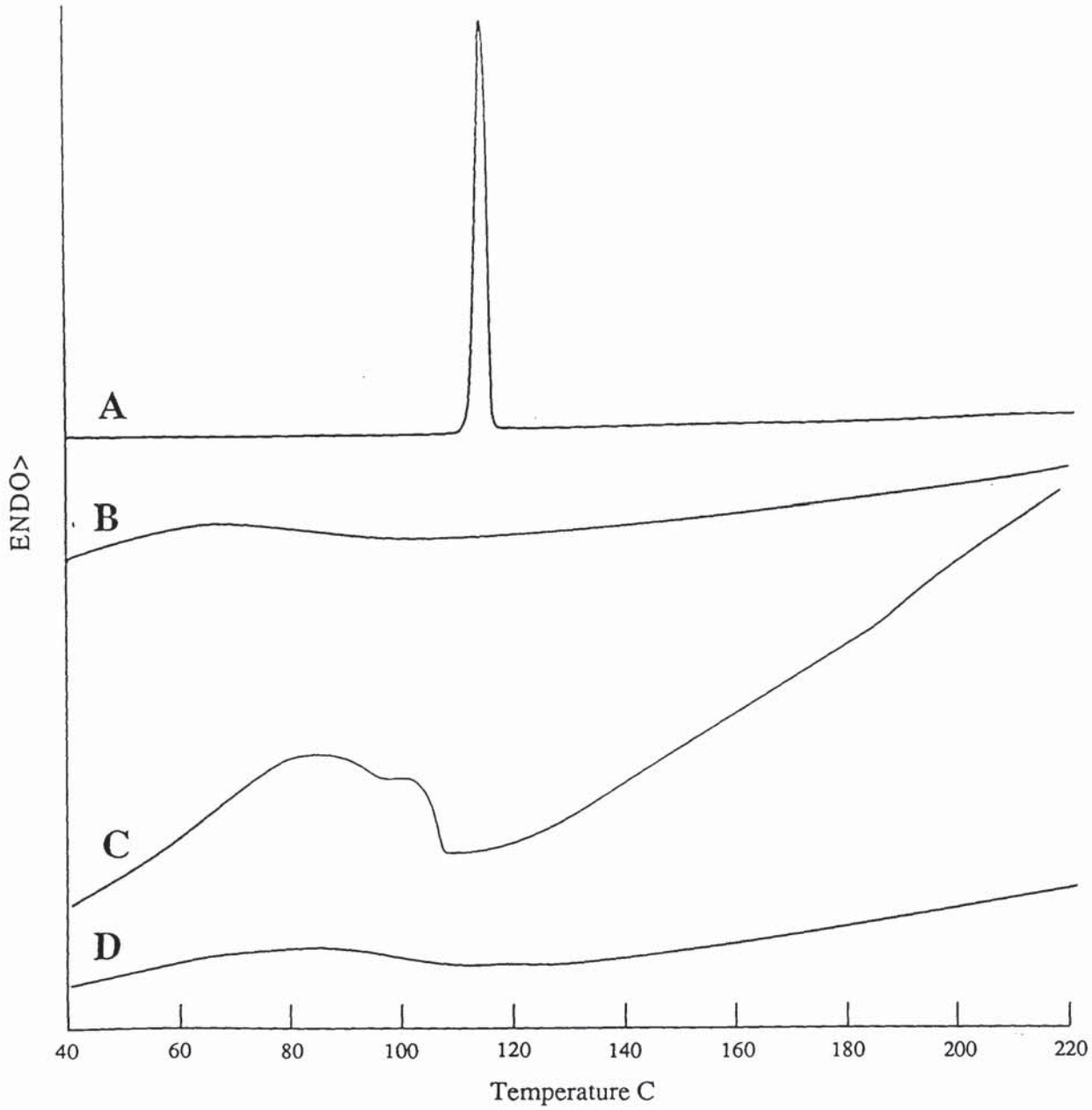

Figure 3.5 DSC thermograms of: A) ethyl paraben (EtP) B) HP-β-CyD, C) the physical mixture of EtP and HP-β-CyD (molar ratio 1:1), and D) the EtP-HP-β-CyD complex

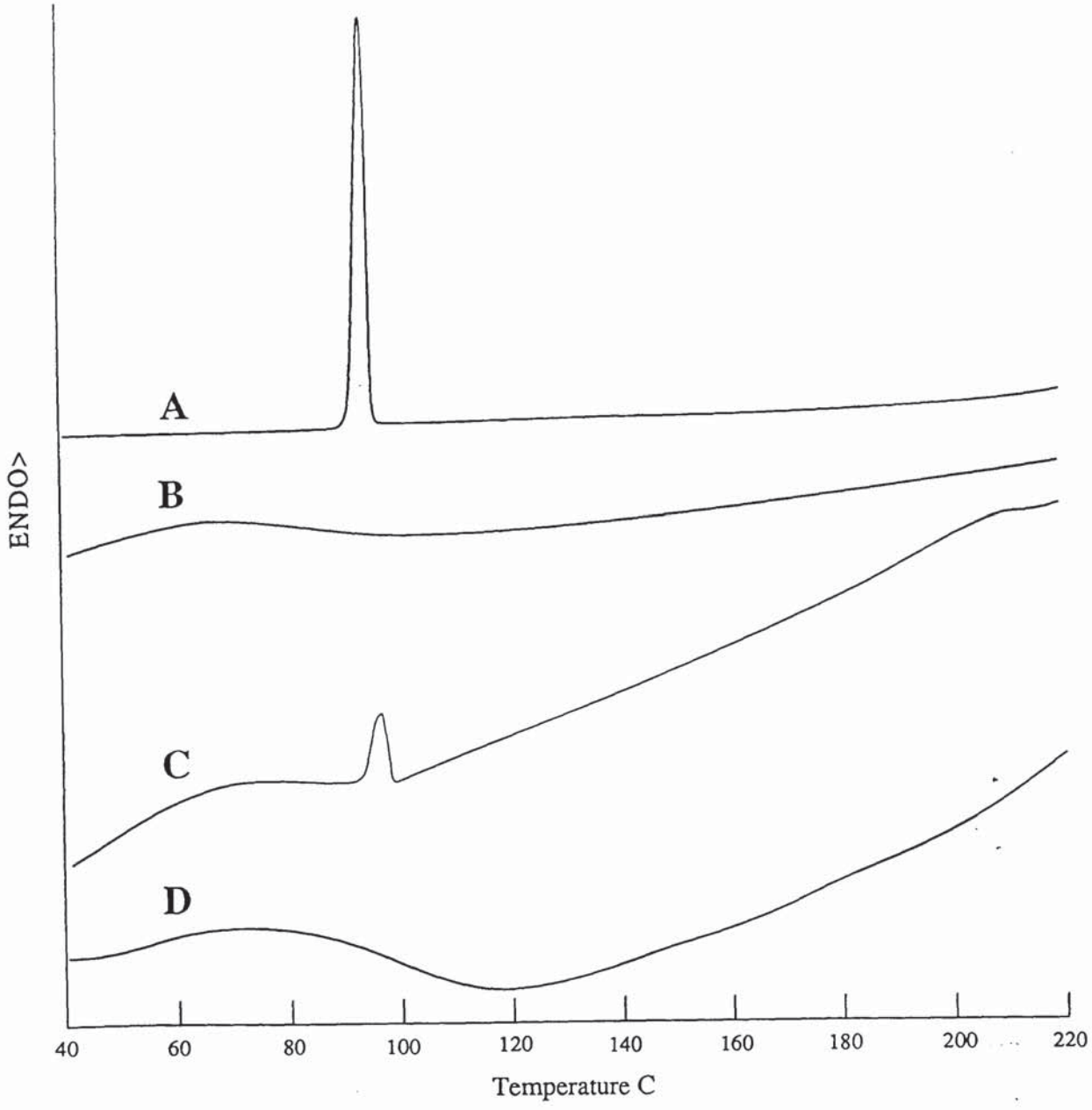

Figure 3.6 DSC thermograms of: A) propyl paraben (PrP) B) HP-β-CyD, C) the physical mixture of PrP and HP-β-CyD (molar ratio 1:1), and D) the PrP-HP-β-CyD complex

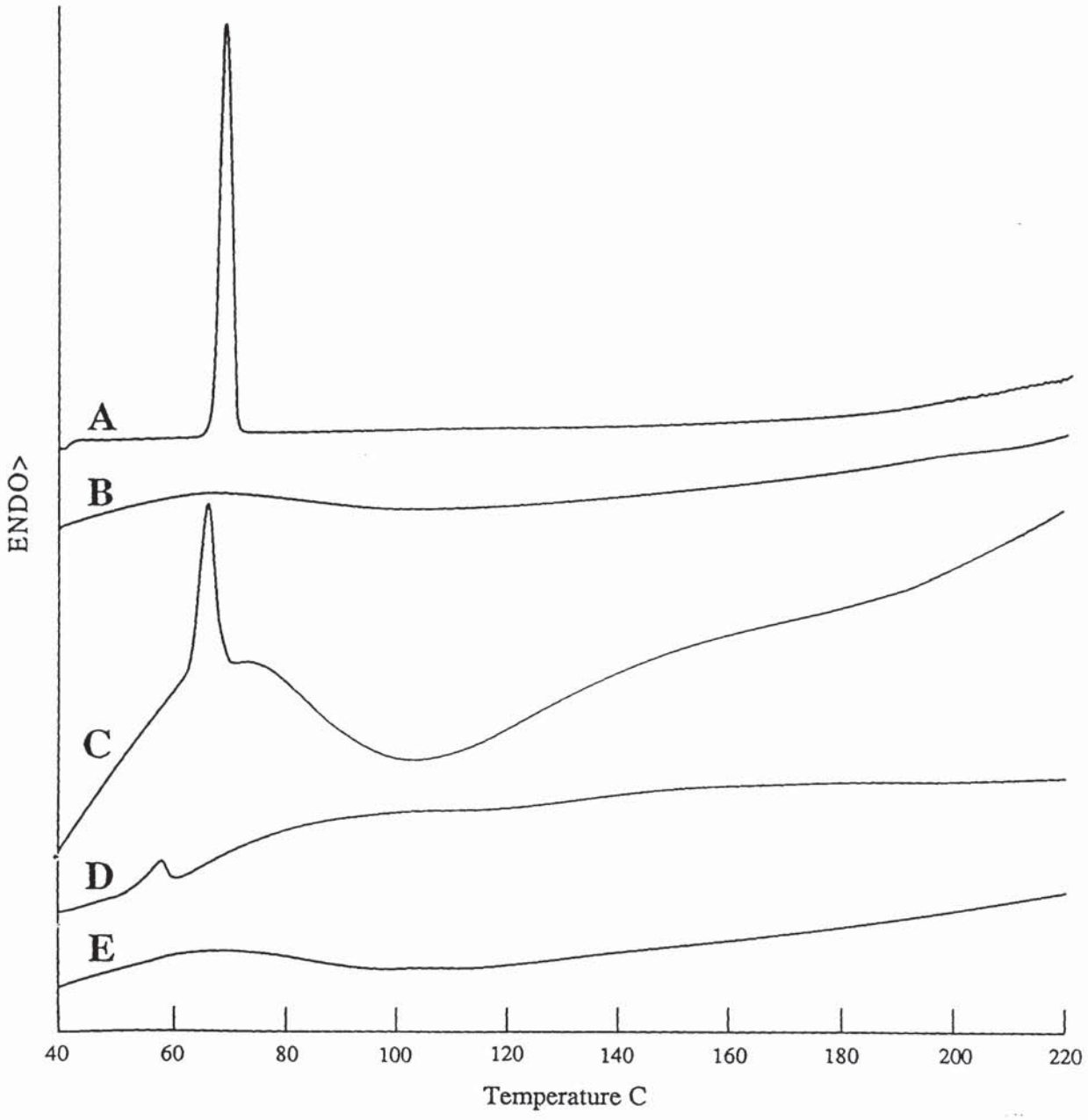

Figure 3.7 DSC thermograms of: A) butyl paraben (BuP) B) HP-β-CyD, C) the physical mixture of BuP and HP-β-CyD (molar ratio 1:1), D) the BuP-HP-β-CyD complex before washing and E) the complex after washing

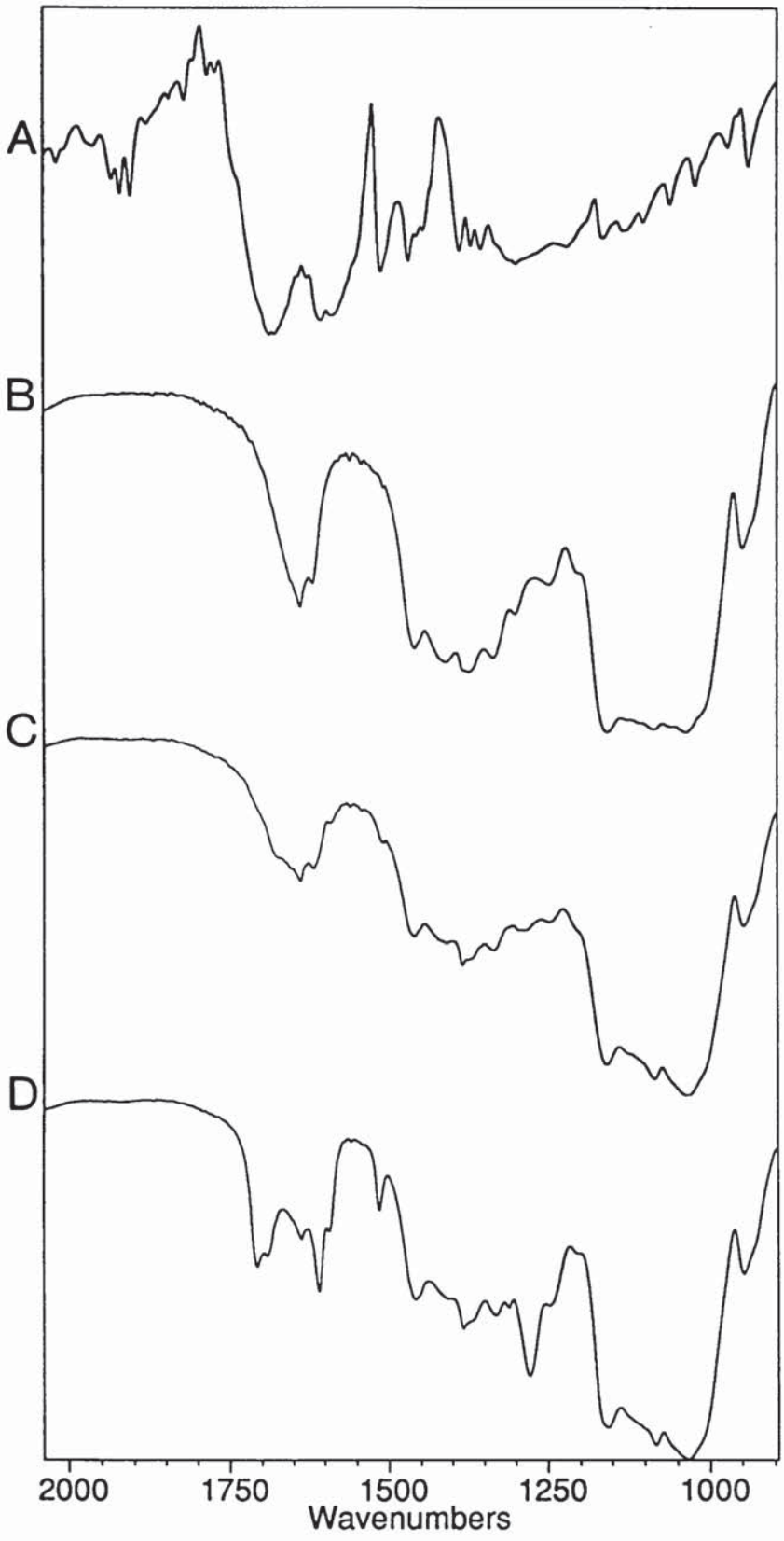

Figure 3.8 Examples of IR spectra: A) butyl paraben (BuP) B) HP-β-CyD C) physical mixture of BuP and HP-β-CyD (molar ratio 1:1) D) the BuP-HP-β-CyD complex

X-ray powder diffraction studies were performed on the BuP-HP-β-CyD system only. The BuP diffractogram (figure 3.9A) showed continual sharp peaks revealing its highly crystalline nature. In contrast, HP-β-CyD (figure 3.9B) revealed a diffuse pattern with few broad peaks illustrating its amorphous nature as discussed previously in 2.6.2. As expected, the diffractogram of the equimolar physical mix, illustrated in figure 3.9C, was simply the superposition of each component. However, the frequency and intensity of the peaks of BuP were reduced due to the relative low weight present. The diffractogram of the freeze-dried physical mixture (figure 3.9D) was similar to the behaviour of the untreated mix suggesting that the freeze-drying process had no major effect on the crystallinity of BuP. However, it is also probable that if changes in crystallinity had occurred they were be difficult to see due to small amount of BuP present relative to the weight of amorphous CyD. The HP-β-CyD complex (figure 3.9E) gave an overall diffuse pattern suggesting that all of the BuP was encapsulated within the CyD; thus, no crystalline parts were observed in its diffractogram. The significant differences between diffraction patterns of the freeze-dried physical mixture and the BuP-HP-β-CyD complex adds to the existing evidence that a true inclusion complex was formed.

The water content of the solid paraben-HP-β-CyD complexes was determined by TGA on a percentage weight per weight basis. Only single batches of complex were prepared for MeP, EtP and PrP, whereas 3 batches of the BuP complex were prepared on separate occasions. The water content of all of the complexes, as illustrated in table 3.5, was less than 5 % of their total weight. The differences between their degrees of hydration is probably due to the variations in freeze-dryer efficiency encountered on a day-to-day basis.

Table 3.5 Percentage weight per weight water-content of the paraben-HP-β-CyD complexes as determined by TGA. Values represent the mean ± s.d., $n = 3$.

	% w/w water content ± s.d.
methyl paraben-HP-β-CyD complex	4.54 ± 0.44
ethyl paraben-HP-β-CyD complex	4.36 ± 0.11
propyl paraben-HP-β-CyD complex	4.60 ± 0.59
butyl paraben-HP-β-CyD complex:	
Batch I	4.35 ± 0.11
Batch II	2.60 ± 0.42
Batch III	1.96 ± 0.09

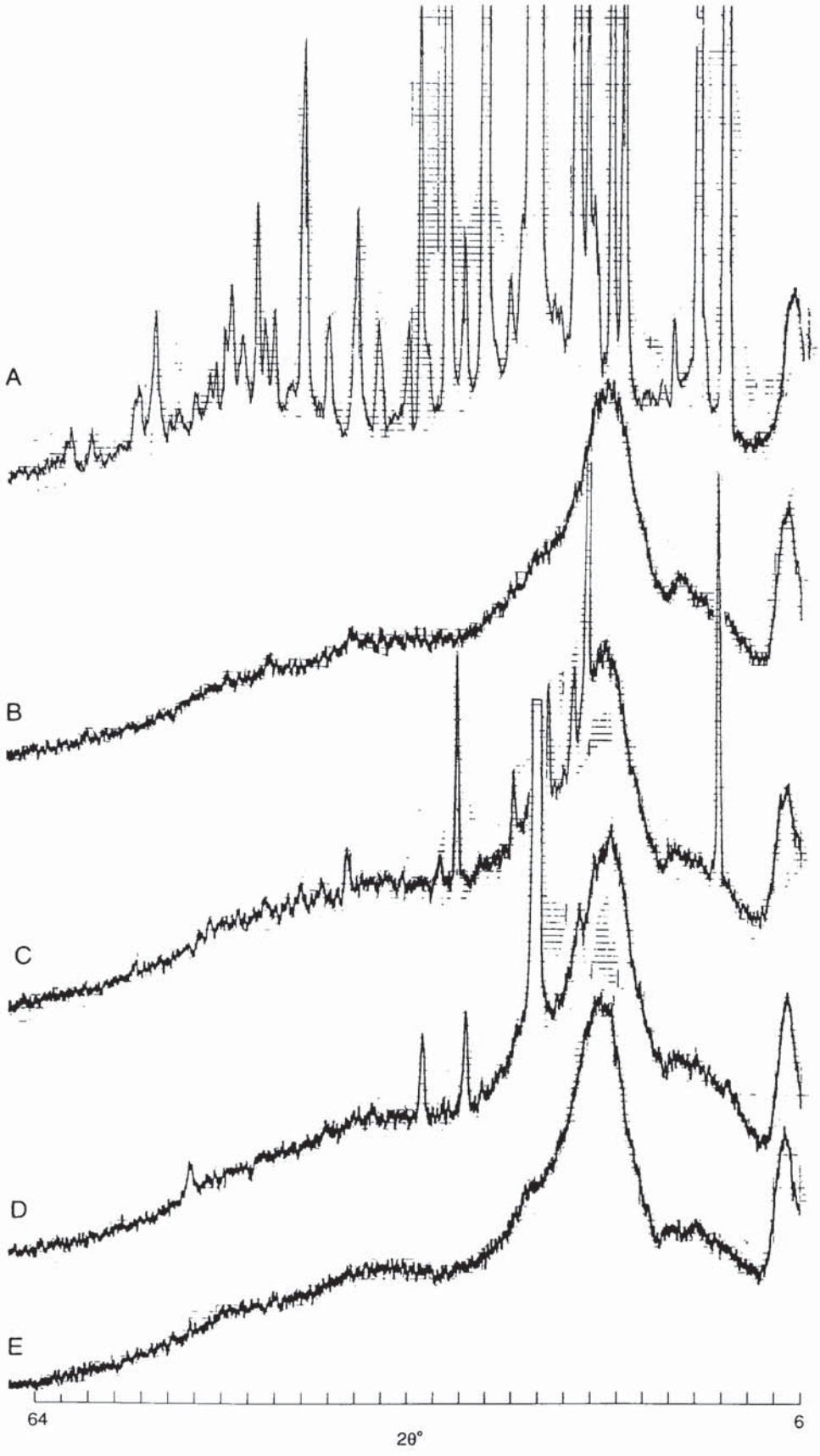

Figure 3.9 Examples of X-ray powder diffractograms: A) BuP, B) HP-β-CyD, C) equimolar physical mix of BuP and HP-β-CyD, D) freeze dried equimolar physical mix of BuP and HP-β-CyD and E) BuP-HP-β-CyD complex

Interestingly, even though the melting point of all parabens were within the temperature range used for TGA (25-150°C), none of the paraben-HP-β-CyD complexes showed major weight loss suggesting that the volatility of the parabens had been reduced. Uekama and co-workers (1980) observed similar behaviour with the paraben-β-CyD complexes, from which it was concluded that thermally stable complexes were formed by CyD inclusion processes.

The water content of the complexes as found by TGA was used during chemical analysis of the paraben complexes, for the determination of the stoichiometric ratios of guest to host in the paraben-HP-β-CyD complexes as discussed later.

From a consideration of the various physical tests performed on the solid phase paraben-HP-β-CyD complexes, the results of DSC and IR analysis confirm the formation of a real inclusion complex of all paraben-HP-β-CyD systems prepared. For the BuP-HP-β-CyD complex, further evidence of complexation was obtained from X-ray powder diffraction studies.

The investigations so far have involved the CyD complex formed in the solid state. The interactions between HP-β-CyD and the parabens in solution were further studied by phase solubility studies (section 3.6.5) and UV spectroscopy (section 3.6.6) which also revealed the existence of the paraben-HP-β-CyD complexes in solution. The solid phase paraben-HP-β-CyD complexes were also used in diffusion experiments (section 3.6.6), performed to determine the diffusion of free drug from which the extent of complex dissociation could be assessed.

3.6.3 Chemical analysis of the solid phase paraben-HP-β-CyD complexes

The theoretical and experimental drug content of the paraben complexes were found using the method of calculation illustrated for the chemical content determination of the CHX-CyD complexes in section 2.6.3. An example calculation for the MeP-HP-β-CyD complex is shown as follows.

The theoretical weight of the 1:1 MeP-HP-β-CyD complex can be considered to be the sum of the M.W. of both HP-β-CyD and MeP, *i.e.*

$$1377.97 \text{ (HP-β-CyD M.W.)} + 152.2 \text{ (MeP M.W.)} = 1530.17$$

Taking into account the water content of the MeP-HP-β-CyD complex (4.54 % w/w) as determined by TGA (section 3.6.2):

1530.17 x 1.0454 = 1599.64 = theoretical molecular weight of complex

The theoretical percentage weight of MeP per weight of its HP-β-CyD complex is therefore:

152.2/1599.64 x 100 = **9.51** % w/w MeP

An example calculation of the experimental drug content determination is as follows:
5.04 mg of the MeP-HP-β-CyD complex dissolved in 1 ml of distilled water gave a final MeP concentration of 3.325 mM which is equivalent to 5.061 mg MeP per ml, hence,

5.061/5.04 x 100 = 10.04 % w/w MeP

The theoretical and experimental chemical contents of the EtP, PrP and BuP-HP-β-CyD complexes were determined in a similar way. A stoichiometry of 1:1 (paraben-HP-β-CyD) was expected for all paraben complexes since equimolar quantities of both complex components were used. As illustrated in table 3.6 the HP-β-CyD complexes of MeP, EtP and PrP all have values close to this ideal stoichiometric ratio.

With the BuP complex however, the experimental drug content values were approximately 2 % less than expected, which consequently resulted in the stoichiometric ratio being less than one. During the preparation of the BuP complex, the complex solution was rapidly cooled from 50°C to approximately -20°C which caused precipitation of BuP. Even though a large proportion of the solubilised BuP would be complexed, some would still remain free which may have precipitated due to the large fall in temperature. This was further confirmed during DSC analysis which showed an endothermic peak equivalent to BuP in the complex thermogram indicating the presence of some uncomplexed BuP. However, after washing with diethyl ether, in which BuP is freely soluble, the peak disappeared. On this basis, it therefore seems that a stoichiometric ratio of 1:1 cannot be expected for the BuP-HP-β-CyD complex since by washing away the precipitated BuP the total amount of BuP initially used during the preparation of the complex was reduced. Hence, the ratio of BuP to HP-β-CyD will be less than unity as observed with the experimental data in table 3.6. The ratio of BuP for all three batches of complex was within the range 0.80 to 0.89 showing good reproducibility of the preparation method.

Table 3.6 Theoretical and experimental determinations of the paraben content of the respective HP-β-CyD complexes. Values represent the mean ± s.d., $n = 3$.

	% w/w paraben		stoichiometry paraben:CyD
	Theoretical value	Experimental value	
methyl paraben-HP-β-CyD complex	9.51±0.04	10.04±0.13	1.06±0.02:1
ethyl paraben-HP-β-CyD complex	10.31±0.01	10.54±0.16	1.02±0.02:1
propyl paraben-HP-β-CyD complex	11.05±0.06	10.69±0.04	0.97±0.01:1
butyl paraben-HP-β-CyD complex:			
Batch I	11.83±0.01	10.24±0.00	0.87±0.00:1
Batch II	12.04±0.08	9.75±0.01	0.81±0.01:1
Batch III	12.11±0.01	10.48±0.27	0.87±0.02:1

3.6.4 Determination of the solubility limit of the butyl paraben-HP-β-CyD complex

Attempts were made to determine the solubility limit of the BuP-HP-β-CyD complex by adding increasing amounts of complex to 1 ml of distilled water at 37°C. However, even after 325 mg of BuP-HP-β-CyD complex (*Batch III*) had been added, which was equivalent to approximately 34 mg BuP per ml, saturation had not been reached. The BuP concentration of the solution of the complex was found to be 0.171 ± 0.002 M, which is approximately 100 times greater than the saturation solubility of BuP itself at 37°C (1.6898 ± 0.041 mM; from phase solubility studies, section 3.6.5). Since, the concentration of HP-β-CyD in solution was also high (~ 29 % w/v; 0.205 M) a viscous solution was formed, thus no further additions of complex were made as sampling was very difficult. *Batches I* and *II* of the HP-β-CyD complex behaved in a similar manner. On leaving the solutions of the BuP-HP-β-CyD complex standing for 7 days at room temperature (~ 20°C), no precipitation of any solid material was observed. The solutions of the BuP complex was therefore supersaturated with respect to BuP. The high stability of the BuP-HP-β-CyD solution has also been reported by Matsuda and co-workers (1993) who found that on storage of a BuP solution containing HP-β-CyD for 30 days, no precipitation of BuP was observed.

The increased solubility of the complex is possibly due to a combination of factors. Firstly, HP-β-CyD which is acting as a carrier of BuP in solution, is itself highly water-soluble (> 45% w/v). The amorphous nature of the CyD derivative contributes to its

solubility characteristics. X-ray diffraction studies have further illustrated the low crystallinity of the BuP-HP-β-CyD complex which is due to the lyophilization process used during preparation of the complex as well as inclusion of BuP within the CyD cavity. Thus, it therefore seems that, as a consequence of the solubilising effect of the HP-β-CyD together with the amorphous nature of the complex, the saturation solubility of the BuP-HP-β-CyD complex could not determined.

Similar attempts were made to determine the solubility limit of MeP, EtP and PrP complexes, however a saturation point was not reached in any case.

Further experiments which involved the solid-phase complexes were the diffusion studies in section 3.6.7. Ideally, a saturated complex solution should have been used for these experiments. However, since this was not known, the amount of complex used for each paraben, except for MeP, was such that the total paraben concentration in solution was approximately 40 times greater than the equilibrium saturation solubility of the respective paraben alone at 37°C, the same temperature at which the diffusion experiments were performed. The solubilities of the parabens at 37°C were found during phase solubility analysis as discussed in section 3.6.5. With MeP, the amount of MeP complex used was such that the total MeP concentration in solution was approximately 10 times greater than the equilibrium saturation solubility of the MeP alone at 37°C. Less complex was used in the latter case due to the large host to guest ratio (by weight) which would consequently increase the viscosity of the solution. Details of the procedure followed for the diffusion experiments are given in section 3.5.8 with their results discussed in section 3.6.7.

3.6.5 Phase solubility studies of the parabens in the presence of HP-β-CyD

The interactions between the parabens and HP-β-CyD in solution were studied by phase solubility analysis. The solubility isotherms obtained for all parabens showed a linear increase in paraben concentration up to the maximum concentration of HP-β-CyD used as illustrated in figures 3.10 and 3.11. The solubility diagrams can be classified as the A_L type as discussed earlier in section 1.5.6.4, which indicate the formation of a soluble complex between HP-β-CyD and the parabens with a probable stoichiometry of 1:1.

Linear regression was used to find the slope and intercept of each diagram, from which the K_S values were found using equation A3.13 in Appendix 3. Table 3.7 contains the slope of each line, S_0, the K_S values found for each paraben, and the solubility enhancement of each paraben achieved with 0.069 M HP-β-CyD. Also included in table

3.7, are the experimental values of the solubilities of the parabens in the absence of CyD, *i.e.* $S_{0\text{-Exp}}$.

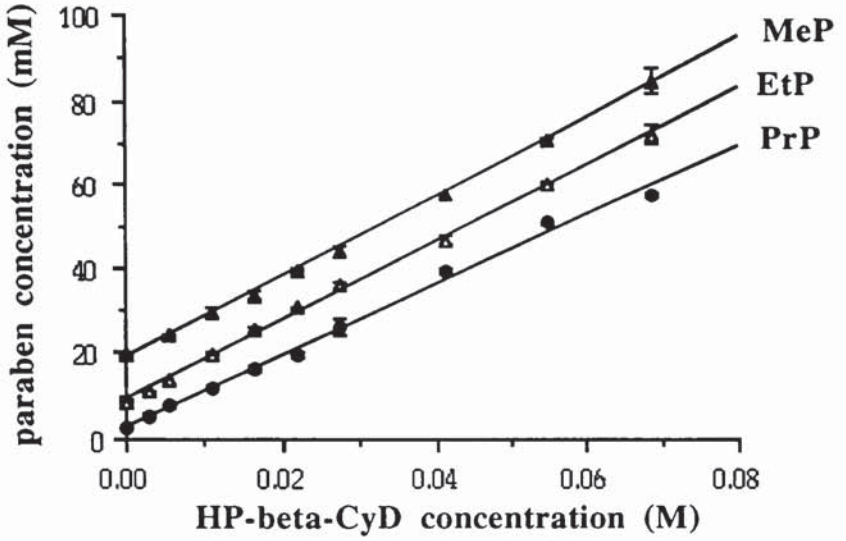

Figure 3.10 Phase solubility diagrams of methyl (MeP), ethyl (EtP) and propyl (PrP) paraben-HP-β-CyD systems in distilled water at 37°C. Points represent the mean ± s.d., $n = 3$.

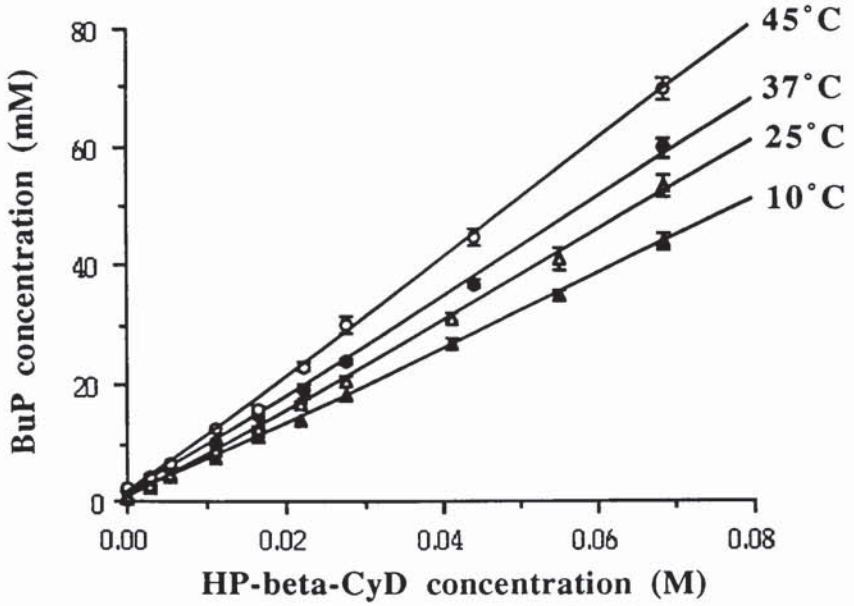

Figure 3.11 Phase solubility diagram of the BuP-HP-β-CyD system in distilled water at various temperatures. Points represent the mean ± s.d., $n = 3$.

Table 3.7 Summary of paraben solubility data. ($S_{0\text{-}Exp}$ are the experimental values for the equilibrium solubility of paraben in the absence of CyD and are the mean ± s.d., n = 3).

Paraben	slope	S_0 ($Mx10^3$)	$S_{0\text{-}Exp}$ ($M \times 10^3$)	K_S (M^{-1})	r^2	Solubility increase with 0.069 M HP-β-CyD
methyl	0.9481	18.647	18.385±0.352	980	0.999	4-fold
ethyl	0.9242	9.3240	8.7977±0.053	1308	0.999	8-fold
propyl	0.8330	2.9075	2.7587±0.170	1715	0.995	21-fold
butyl: 10°C	0.6519	0.5905	0.6123±0.075	3172	0.999	71-fold
25°C	0.7174	1.0287	1.0150±0.021	2467	1.000	52-fold
37°C	0.7913	1.7408	1.6898±0.041	2179	0.999	35-fold
45°C	0.8176	2.2480	2.3924±0.023	1994	0.999	29-fold

The experimental S_0 values were in close agreement with the values obtained from linear regression. The solubility of the alkyl *p*-hydroxybenzoates decreased with increasing chain length. However, the effect of HP-β-CyD on paraben solubilisation was inversed. For example, with 0.069 M HP-β-CyD at 37°C, a 4-fold solubility enhancement was observed with the methyl ester whereas a 33-fold increase occurred with BuP. A similar pattern was seen with the K_S values which showed the complex stability to rise with increasing chain length. By plotting the K_S values obtained at 37°C as a function of the respective paraben solubility ($S_{0\text{-}Exp}$), a linear relationship ($r^2 = 0.968$) was observed as illustrated in figure 3.12. Further linear correlation ($r^2 = 0.999$) was seen between the complex stability constants and the respective log P values for the parabens (shown in table 3.1, section 3.1) as shown in figure 3.13. These results indicate that the greater the hydrophobicity of the paraben guest as indicated by its relative partition coefficient, the greater its affinity for the CyD cavity. As discussed previously, several researchers have observed similar trends between the hydrophobicity of the guest and the complex stability constant. In particular, Lehner and co-workers (1993) observed similar correlations for the interaction of HP-β-CyD with the series of alkyl hydroxybenzoates.

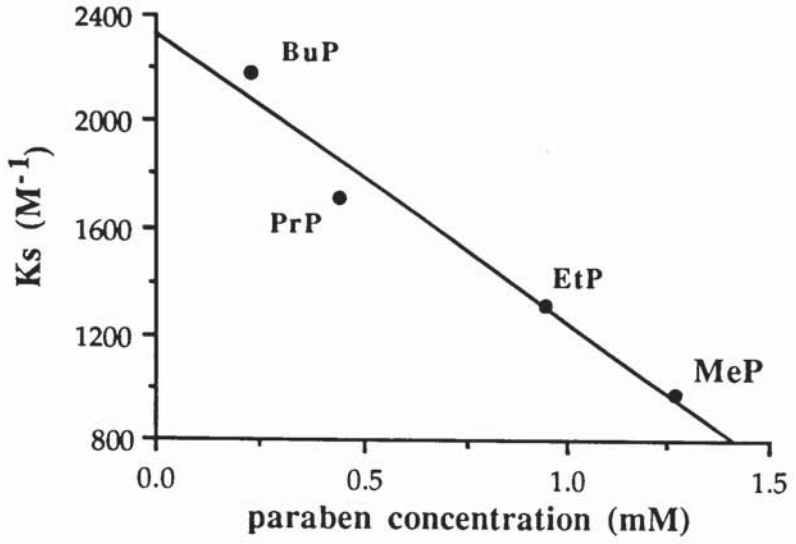

Figure 3.12 Correlation between paraben-HP-β-CyD complex stability constants (K_S) and paraben solubilities ($S_{0\text{-}Exp}$) ($r^2 = 0.968$)

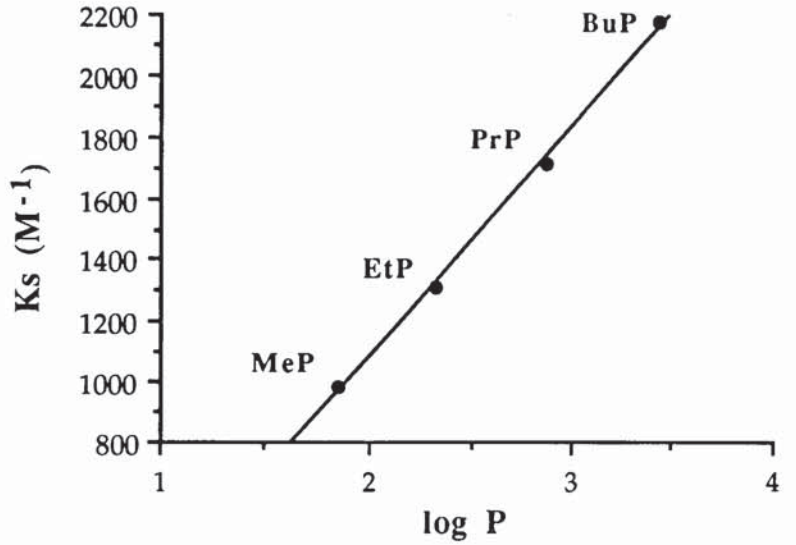

Figure 3.13 Correlation between paraben-HP-β-CyD complex stability constants (K_S) and paraben lipophilicity (log P) ($r^2 = 0.999$)

The solubility behaviour of the parabens in the presence of HP-β-CyD can be compared to solubility studies performed between β-CyD and BuP (Uekama *et. al.*, 1980) where a K_S value of 2561 M^{-1} (25°C) was determined for the respective 1:1 complex formed in solution. Comparing this value with that obtained for the BuP-HP-β-CyD complex (2467 M^{-1}), it can be seen that the magnitude of K_S is virtually identical. Theoretically, the complexing ability of β-CyD and HP-β-CyD should be similar as the molecular

dimensions of the cavity are essentially the same. However, differences are expected between the CyDs in their relative soluble enhancement of a particular guest since the solubilities of the CyDs themselves are different. Again comparing the BuP-HP-β-CyD system to the corresponding β-CyD system, it was found that whereas a soluble complex was formed in solution with HP-β-CyD, in contrast, the BuP-β-CyD complex formed was insoluble (Uekama *et. al.*, 1980), which is possibly a consequence of the limited aqueous solubility of β-CyD.

The K_S values obtained for the respective paraben-HP-β-CyD complexes during this study were comparable with other recently published findings. Matsuda and co-workers (1993) and also Lehner, Müller and Seydel (1993) have reported K_S values of similar magnitude.

The solubility behaviour of BuP in the presence of HP-β-CyD was studied at various temperatures in order to assess the effect of temperature on complex stability and to evaluate the thermodynamic parameters of the inclusion process. With a rise in temperature from 10 to 45°C, an approximate 3.8-fold increase in BuP solubility occurred, however, the relative solubility enhancement with the CyD decreased with increasing temperature. In contrast to the CHX-β-CyD system (section 2.6.4.1), an increase in the slope of the solubility isotherms occurred with a rise in temperature suggesting a greater affinity of the guest for the CyD. However, the K_S values for the BuP-HP-β-CyD complex decreased with increasing temperature, ranging from 3172 M^{-1} at 10°C to 1994 M^{-1} at 45°C which was similar to the behaviour of the CHX-β-CyD complex. The decrease in complex stability with an increase in temperature reflects dissociation of the complex. Using equation A4.20 in Appendix 4, the concentration and percentage of free BuP in the presence of 0.069 M HP-β-CyD were found at each temperature. With a rise in temperature, the percentage of free BuP was expected to increase due to complex dissociation. However, as shown in table 3.8, over the temperature range studied there was very little variation in the percentage of free BuP in the presence of 0.069 M HP-β-CyD. These data indicate that with a rise in temperature, the concentration of the BuP-HP-β-CyD complex increased despite the fact that a parallel reduction in complex stability occurred. The increasing slopes of the solubility isotherms of the BuP-HP-β-CyD system with temperature can therefore also be attributed to the increasing concentration of the BuP-HP-β-CyD complex. Similar temperature effects were observed by Hoshino and co-workers (1993) for the solubility of carbamazepine, dexamethasone and griseofulvin in the presence of HP-β-CyD. These researchers concluded that the increase in water solubility of the guest from solution heating

counterbalances the simultaneously occurring dissociation of complex, which consequently leads to an increase in the concentration of complexed drug.

Table 3.8 Concentration and of percentage of free BuP in the presence of 0.069 M HP-β-CyD at various temperatures calculated using equation A4.20 and the K_S values shown in table 3.7.

Temperature (°C)	Total BuP concentration (M x 10^3)	Concentration of free BuP (M x 10^3)	Percentage of total BuP as free
10	43.521 ± 1.183	3.55 ± 0.05	8.16 ± 0.11
25	52.896 ± 1.978	4.43 ± 0.09	8.38 ± 0.15
37	59.297 ± 1.520	4.99 ± 0.07	8.42 ± 0.10
45	69.264 ± 1.804	5.64 ± 0.08	8.15 ± 0.09

The effect of temperature on the equilibrium constant was illustrated by the van't Hoff plot which was obtained by plotting ln K_S against absolute temperature as described in section 2.6.4. As shown in figure 3.14, the van't Hoff plot was close to linear over the temperature range employed ($r^2 = 0.998$). From the slope and intercept on the y-axis, the enthalpy and entropy changes found respectively are contained in table 3.9 together with the free energy change at 37°C found using equation 2.4 (in section 2.6.4).

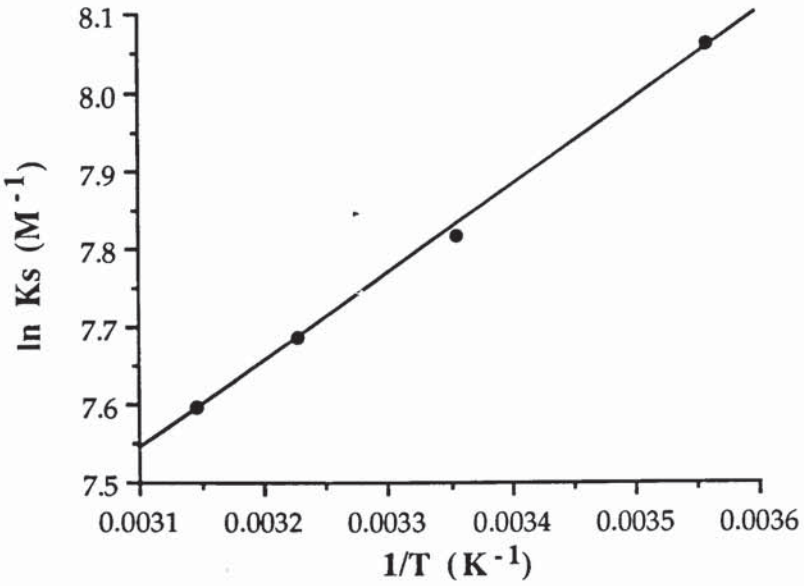

Figure 3.14 Temperature dependence of the equilibrium constant of BuP-HP-β-CyD complex illustrated by the van't Hoff plot
($y = 4.0843 + 1115.8x$, $r^2 = 0.998$)

Table 3.9 Thermodynamic parameters of the BuP-HP-β-CyD complexation process

ΔH	-9.28 kJ mol^{-1}
ΔS	33.96 J K^{-1} mol^{-1}
ΔG	-19.81 kJ mol^{-1}(37°C)

The negative free energy change (-19.81 kJ mol^{-1} at 37°C) for the complexation process enables the reaction to be energetically feasible. The determinants of free energy are the enthalpic and entropic changes of the complexation reaction, thus, both ΔH and ΔS or only one of these parameters may be energetically favourable. For the BuP-HP-β-CyD system, the negative enthalpy change of the complexation process (-9.28 kJ mol^{-1}) reflected the exothermic nature of the reaction. This favourable enthalpy change could be due to increased guest-host interactions and also an increase in solvent-solvent interaction such as intermolecular hydrogen bonding between the water molecules. A positive entropy change was found (33.96 J K^{-1} mol^{-1}) indicating that inclusion of BuP within the CyD cavity was followed by a favourable decrease in solvent order. The hydroxypropyl groups of the CyD derivative extend from the rim of the CyD into the aqueous solvent. It has been suggested (Uekama *et. al.*, 1985) that the hydroxypropyl moieties of the HP-β-CyD may be hydrated and therefore, as a result of the formation of the inclusion complex, the removal of these water molecules from the ordered structure may result in a favourable ΔS. To summarise, therefore, the thermodynamic parameters indicate that the complexation process was driven by favourable enthalpic and entropic processes.

As discussed previously (section 1.5.5), various bonding mechanisms participate in complex formation in aqueous solution. These include hydrogen bonding, van der Waals-London dispersion forces, hydrophobic bonding interactions and energy release by substitution of the water molecules contained within the CyD cavity. The magnitude of the thermodynamic parameters found in the presence study suggest that van der Waal-London dispersion forces and hydrophobic interactions were involved in complex formation between the BuP and HP-β-CyD.

Phase solubility studies have indicated the solubility enhancement of the parabens with HP-β-CyD. The antimicrobial activity of the parabens is limited by their aqueous solubility, there is therefore a possibility that this problem may be overcome with the use of the CyD. However, Lehner and co-workers (1993), suggested that only uncomplexed drug has antimicrobial activity. These researchers performed microbiological studies

using parabens solutions with and without the addition of HP-β-CyD in equimolar proportion to the preservative. The total concentration of paraben in these solutions did not exceed their respective saturation solubilities. In the presence of CyD, a proportion of the total paraben in solution would exist as the complexed form, therefore, the concentration of free paraben was less than in the solution of preservative alone. Hence, the activity of paraben alone was greater than in the presence of HP-β-CyD. Further discussion on other microbiological studies performed on CyD complexes is contained in chapter 5.

A potential paraben-HP-β-CyD solution may still be advantageous in providing a reservoir from which both free and complexed drug will diffuse to the site of bacteria. As already mentioned, free drug is important for activity. The percentage of free drug will depend on the concentration of CyD and the extent of the paraben-CyD interaction as indicated by the respective K_S value. In contrast to the work performed by Lehner and co-workers (1993), if the paraben concentration of paraben-HP-β-CyD solution was greater than the saturation solubility of ester alone, the situation may arise whereby the concentration of free drug in solution exceeds its saturation solubility, *i.e.* is supersaturated. As a result of free paraben supersaturation, a steep concentration gradient would exist between the site of delivery and the site of bacteria, which facilitates further diffusion of free active antimicrobial agent. The diffusion behaviour of parabens from both free drug suspensions and solutions of their respective HP-β-CyD complexes were assessed as discussed in section 3.6.7.

3.6.6 Analysis of the interaction between butyl paraben and HP-β-CyD in solution using UV spectroscopy

The interaction between BuP and HP-β-CyD in solution was further studied by UV spectroscopy. The concentration of BuP was maintained constant and the effect of increasing concentrations of HP-β-CyD (0.00001-0.100 M) on its absorption spectrum was observed. The λ_{max} peak of BuP which occurred at 256 nm, shifted slightly to 258 nm with increasing HP-β-CyD concentrations. A significant reduction in the intensity of the absorption maxima also occurred. However, it was found that with HP-β-CyD concentrations above 0.01 M, no further reductions were observed in the intensity of absorbance at λ_{max}. Figure 3.15 illustrates the absorption spectrum of BuP alone and some examples of the spectra obtained in presence of various concentrations of HP-β-CyD. These results indicated that interactions occurred between BuP and HP-β-CyD in solution which were observed as spectral changes.

Changes similar to those observed in the UV spectrum of BuP in the presence of HP-β-CyD have also been reported for other drug-CyD systems. The UV spectra of ibuprofen also exhibited a shift in its λ_{max} and a reduction in its absorption intensity in the presence of β-CyD (Chow and Karara, 1986). Similar changes were reported by Ikeda and co-workers (1975) for the mefenamic-β-CyD system. The spectral changes observed are thought to be similar to the effects caused by changes in the polarity of the solvent, suggesting that the chromophore of the guest is transferred from an aqueous medium to the non-polar CyD cavity (Hirayama and Uekama, 1987). These changes may be due to a perturbation of the electronic energy levels of the guest caused either by direct interaction with the CyD, by exclusion of solvating water molecules or by a combination of these two effects (Clarke, Coates and Lincoln, 1988).

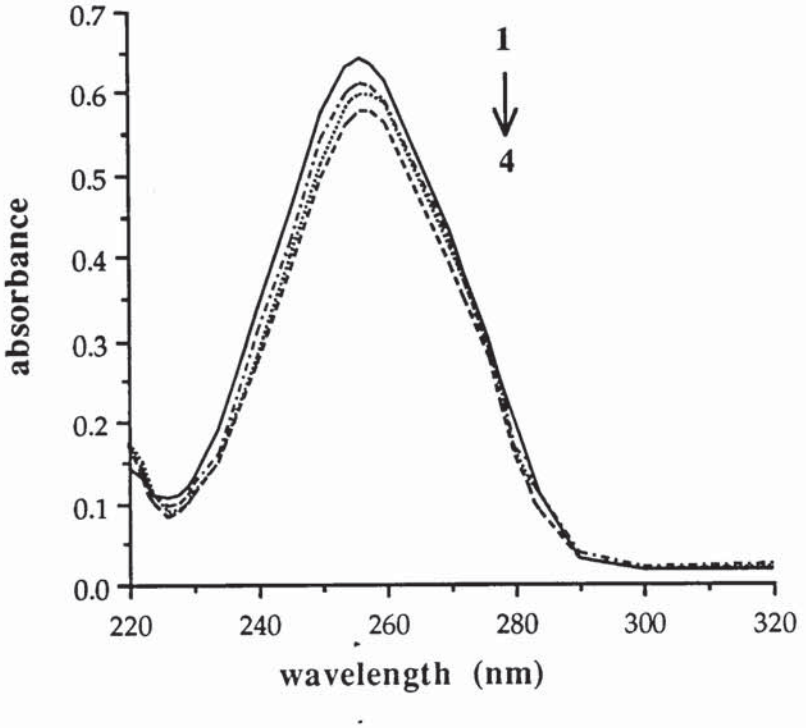

Figure 3.15 Effect of HP-β-CyD on the UV absorption spectrum of 4.13 x 10^{-5} M butyl paraben (BuP): curve (1) BuP alone; (2) 0.0005 M HP-β-CyD; (3) 0.001 M HP-β-CyD; (4) 0.01 M HP-β-CyD.

Phase solubility studies (section 3.6.5) have already shown the formation of a complex between BuP and HP-β-CyD in solution, therefore, it is most likely that the changes observed during UV spectroscopy is further evidence that a complex was formed between BuP and HP-β-CyD which consequently lead to changes in the absorption spectra of the paraben.

Above 0.01 M HP-β-CyD no further reductions in the absorption intensity of BuP occurred, suggesting that the proportion of BuP in solution existing as the complex had reached a saturation level. The molar extinction coefficient (E, L mol^{-1} cm^{-1}) of BuP was found at each concentration of HP-β-CyD using the absorbance value of the respective solution at 256 nm. By plotting E as a function of HP-β-CyD concentration, it was found that E decreased with increasing concentrations of HP-β-CyD and eventually reached a plateau at HP-β-CyD concentrations above 0.01 M as illustrated in figure 3.16.

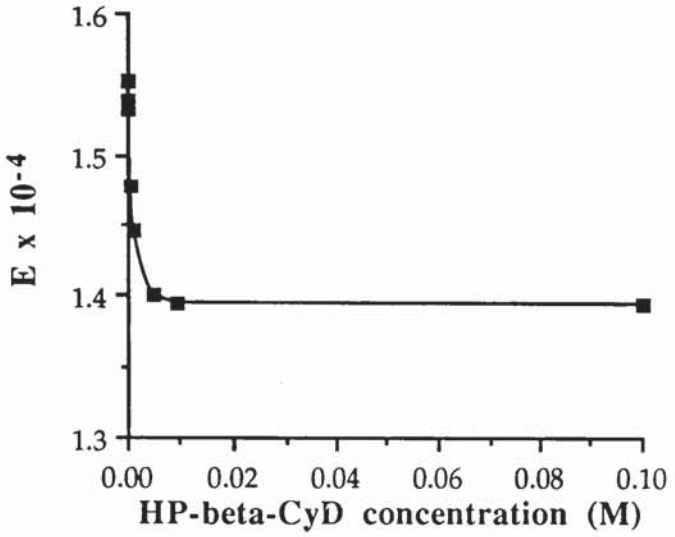

Figure 3.16 Changes in the molar extinction coefficient (E) of butyl paraben in the presence of increasing HP-β-CyD concentration.

By using the changes in guest UV absorption in the presence of CyD, the following model can be used to calculate the concentration of free and complexed guest (Wells, 1988):

$$A\lambda_1 = {}^{G}[C_1E\lambda_1] + {}^{G\text{-}CyD}[C_1E\lambda_1] \qquad (3.1)$$

$$A\lambda_2 = {}^{G}[C_2E\lambda_2] + {}^{G\text{-}CyD}[C_2E\lambda_2]$$

A is the absorbance at λ_1 and λ_2, where λ_1 is the wavelength of maximum absorption (λ_{max}) of guest (G) in the absence of CyD, and λ_2 is the λ_{max} in the presence of CyD. ${}^{G}C$ is the concentration of free guest. ${}^{G}E_{\lambda_1}$ and ${}^{G}E_{\lambda_2}$ are the molar extinction coefficients of free guest at the respective wavelengths. ${}^{G\text{-}CyD}C$ is the concentration of complexed guest, and, ${}^{G\text{-}CyD}E_{\lambda_1}$ and ${}^{G\text{-}CyD}E_{\lambda_2}$ are the molar extinction coefficients of complexed guest at λ_1 and λ_2.

Applying this model to the BuP-HP-β-CyD system, λ_{max} for the guest alone was 256 nm at which the absorbance was 0.641. In the presence of 0.1 M HP-β-CyD, the λ_{max} was shifted slightly to 258 nm at which the absorbance was 0.578. However, due to the fact that only small changes in the absorption maxima occurred in the presence of CyD, the simultaneous equations above could not be used to find the concentration of free drug.

Further attempts were made to calculate the free and complexed BuP by using a BASIC computer programme written by W. J. Irwin as shown in Appendix 4. Very simply, the concentration of free guest concentration was estimated assuming a competitive guest was present. The initial concentration of BuP in solution was 4.13×10^{-5} M, which was used as the variable $[A_0]$, and the K_S of the BuP-HP-β-CyD (25°C, 2467 M^{-1}) was used as K_A. The effect of the competitor was minimised by using very small values for the competitor concentration (4.036×10^{-5} M, $[B_0]$) and the K_S of competitor-HP-β-CyD complex (1.04×10^{-5} M^{-1}, K_B). The initial concentration of HP-β-CyD (variable $[CyD_0]$) was varied from 0.00001 - 0.1 M. Using these parameters, the relative proportions of BuP existing as free drug and as the HP-β-CyD complex at equilibrium, at each HP-β-CyD concentration was estimated as shown in table 3.10. Following this, the expected absorbances at the concentrations of free BuP at 256 nm were calculated as shown below and are also contained in table 3.10.

$$A = Ecl \qquad (3.2)$$

where A = absorbance at λ_{max}
E = molar extinction coefficient (L mol^{-1} cm^{-1})
c = concentration of BuP (mol l^{-1})
l = path length (1 cm)

Rearrangement of equation 3.2:

$$E = \frac{A}{cl} \qquad (3.3)$$

With BuP alone (4.13×10^{-5} M), absorbance at 256 nm was 0.641, therefore

$$^{BuP}E_{256} = \frac{0.641}{4.13 \times 10^{-5} \times 1} = 15520.6 \text{ L mol}^{-1} \text{ cm}^{-1}$$

In the presence of 0.01 M HP-β-CyD and above, the absorbance of BuP at 256 nm remained constant at 0.576, therefore, the molar extinction coefficient of the BuP-HP-β-CyD complex can be calculated as follows:

$$^{BuP\text{-}CyD}E_{256} = \frac{0.576}{4.13 \times 10^{-5} \times 1} = 13946.7 \text{ L mol}^{-1} \text{ cm}^{-1}$$

Table 3.10 Computer simulated estimations for the concentration and percentage of free BuP in the presence of HP-β-CyD of increasing concentration obtained from using the computer programme in Appendix 4 and the variables given in the text.

HP-β-CyD conc (M)	Conc of free BuP (^{BuP}C, M x 10^5)	Conc of complex ($^{BuP\text{-}CyD}C$, M x 10^5)	measured absorbance	calculated absorbance
0	4.13	0	0.641	--
0.00001	4.13	0	0.635	0.641
0.00005	3.711	0.419	0.634	0.634
0.0001	3.364	0.766	0.633	0.629
0.0005	1.896	2.234	0.610	0.606
0.001	1.217	1.217	0.597	0.595
0.005	0.3119	3.818	0.587	0.581
0.01	0.1615	3.969	0.576	0.579
0.1	0.0167	4.113	0.576	0.576

From table 3.10, it can be seen that in the presence of 0.01 M HP-β-CyD, the concentration of free BuP was found to be 1.615 x 10^{-6} M ($^{BuP}C_{calc}$) and the concentration of complexed BuP was 3.969 x 10^{-5} M ($^{BuP\text{-}CyD}C_{calc}$). Hence, using these values, the expected absorbance of BuP in the presence of 0.01 M HP-β-CyD at 256 nm is:

$$\begin{aligned} A_{calc\text{-}256} &= {}^{BuP}[C_{calc} \cdot E_{256}] + {}^{BuP\text{-}CyD}[C_{calc} \cdot E_{256}] \\ &= [1.615 \times 10^{-6} \times 15520.6] + [3.969 \times 10^{-5} \times 13946.7] \\ &= 0.579 \end{aligned} \qquad (3.4)$$

The expected absorbances of the various solutions of BuP-HP-β-CyD were calculated in a similar manner. The measured absorbances were plotted *versus* the calculated values to

determine the extent of deviation. As illustrated in figure 3.17, the plot shows a reasonable fit of the data (r^2=0.988) with the intercept being close to zero (7.1575×10^{-3}) and the slope being approximately one (0.98553). On the basis of these data, it can therefore be concluded that the computer simulated estimations of the concentration of free BuP correlated well with the changes observed in UV absorbance of BuP in the presence of various concentrations of HP-β-CyD.

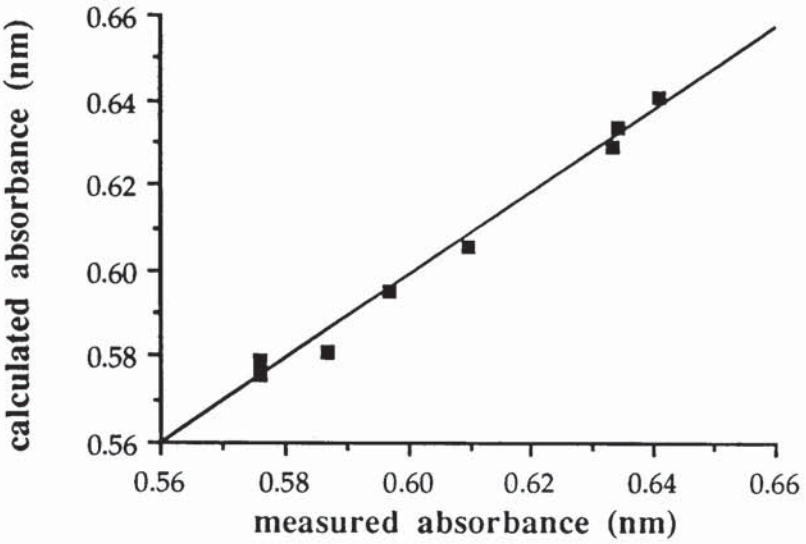

Figure 3.17 Plot of measured absorbance *versus* expected values from calculation [$y = (7.1575 \times 10^{-3}) + 0.98553x$, $r^2 = 0.988$]

3.6.7 Diffusion of parabens through silicone membrane from free and complexed donor phases

Previous diffusion experiments performed on the CHX-β-CyD system were unsuccessful due to the properties of CHX. The lipophilic nature of the alkyl *p*-hydroxybenzoates enabled the use of silicone membrane as the barrier between donor and receiver cells.

Experiments were performed using both solutions and suspensions of parabens alone and of their respective HP-β-CyD complexes as the donor phases. For each paraben system, triplicate diffusion experiments were performed from which the mean flux ± standard deviation were found from the steady-state portion of the diffusion profiles. The theoretical aspects of drug diffusion have previously been discussed in section 2.6.9. Statistical analysis was performed on the flux measurements using the unpaired-sample t-test, described by equation 3.5 (Bolton, 1984).

$$t = \frac{X_1 - X_2}{(\sigma_1^2/ N_1 + \sigma_2^2/N_2)^{1/2}} \qquad (3.5)$$

where, X_1 and X_2 are the means of samples 1 and 2 respectively; σ_1 and σ_2 are the standard deviations of the means of samples 1 and 2 and N_1 and N_2 are the respective sample sizes.

Samples were tested at the 5 % significance level using 2-tailed analysis.

3.6.7.1 Diffusion of parabens from donor phases of drug suspensions alone

The permeation profiles for all parabens, as illustrated in figure 3.18, were linear over the 7-hour period of study, indicating steady-state diffusion. The steady-state fluxes, permeability coefficients (K_p), lag times (t_L) and diffusion coefficients (D) were determined from the linear portions of the rate curves by linear regression as previously described by equations 2.14 to 2.22 in chapter 2. The results are summarised in table 3.11 together with the concentration of each paraben in the donor compartment.

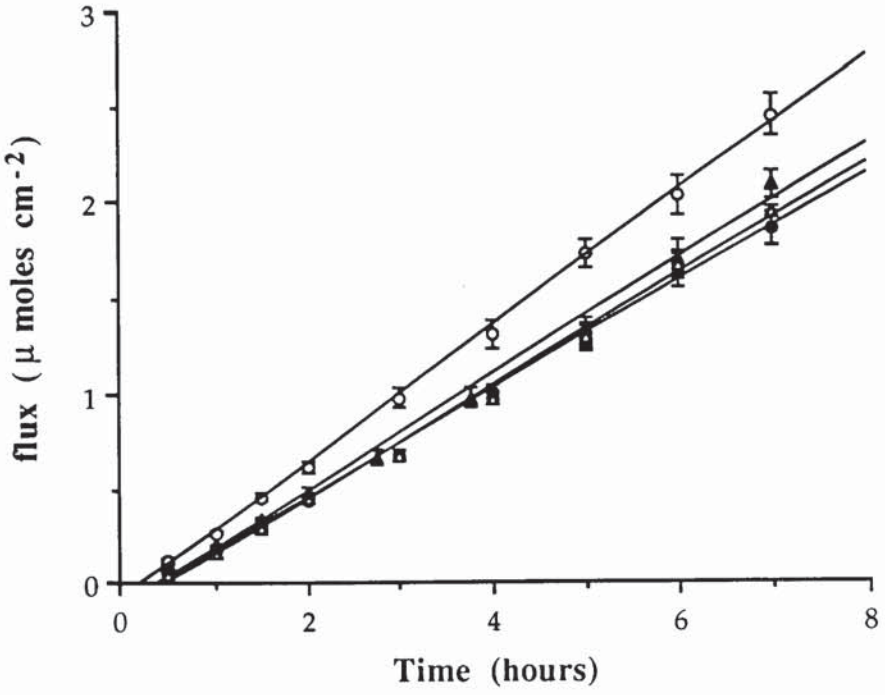

Figure 3.18 Diffusion profiles of the parabens through silicone membrane at 37°C from aqueous donor suspension of drug alone (• MeP; o EtP; ▲ PrP; ∆ BuP). Points represent the mean ± s.d., $n = 3$.

Table 3.11 Diffusion data for parabens transport through silicone membrane from aqueous donor suspensions of drug alone. Values represent mean ± s.d., n = 3.

paraben	**methyl**	**ethyl**	**propyl**	**butyl**
donor concentration (C_d, M x10^3)	17.633 ± 0.118	8.597 ± 0.021	2.348 ± 0.044	1.653 ± 0.056
flux (μmoles cm^{-2} h^{-1})	0.2993 ± 0.018	0.3592 ± 0.017	0.3053 ± 0.015	0.2951 ± 0.008
r^2	0.997	0.995	0.992	0.992
K_p (x 10^2) cm h^{-1}	0.1697 ± 0.025	0.4178 ± 0.240	1.3304 ± 0.091	1.7852 ±0.011
lag time (t_L, hours)	0.3882 ± 0.069	0.2508 ± 0.035	0.3108 ± 0.234	0.4704 ± 0.104
diffusion coefficient (D x 10^3, cm^2 h^{-1})	1.108 ± 0.167	1.715 ± 0.210	1.384 ± 0.595	0.914 ± 0.165

The donor concentrations (C_d) of the parabens shown in table 3.11 are their respective aqueous saturation solubilities. These values were greater than the literature values shown in table 3.1 (section 3.1) due to the fact that in this instance a higher temperature was used. Since the receiver cells were maintained at 37°C, there was transfer of heat to the donor compartment which was found to have a temperature of 34°C. The saturation solubility of the parabens decreased with increasing ester chain length as would be expected. As shown in figure 3.19, the logarithm of the solubilities of the alkyl *p*-hydroxybenzoates are linearly related to the chain length. Similar correlation was observed with the solubilities of the homologous series of alkyl *p*-aminobenzoates (Flynn and Yalkowsky, 1972). Despite the fact the donor concentrations of the parabens varied significantly, these differences was not reflected in their respective flux measurements. The fluxes of the parabens ranged from (0.2951 ± 0.008) to (0.3592 ± 0.017) μmoles cm^{-2} h^{-1}. Statistical analysis of the data found only the flux of EtP (0.3592 ± 0.017 μmoles cm^{-2} h^{-1}) to be significantly greater ($p < 0.05$) than other paraben systems.

The concentration differential is usually considered to be the driving force for diffusion, therefore, for maximum flux, the donor drug solution should be saturated. On the basis of the concentration of the paraben donor suspensions, MeP, which is the most soluble ester may have been expected to shown the greatest flux. When the log of the flux is plotted *versus* the alkyl chain length (n = number of carbons in alkyl chain) an indication of a possible parabolic curve was obtained with the maxima at n = 2, *i.e.* EtP (figure

3.20). This may suggest that the donor concentration is not the sole determinant of flux and that other factors may also be involved in the diffusion of the solute.

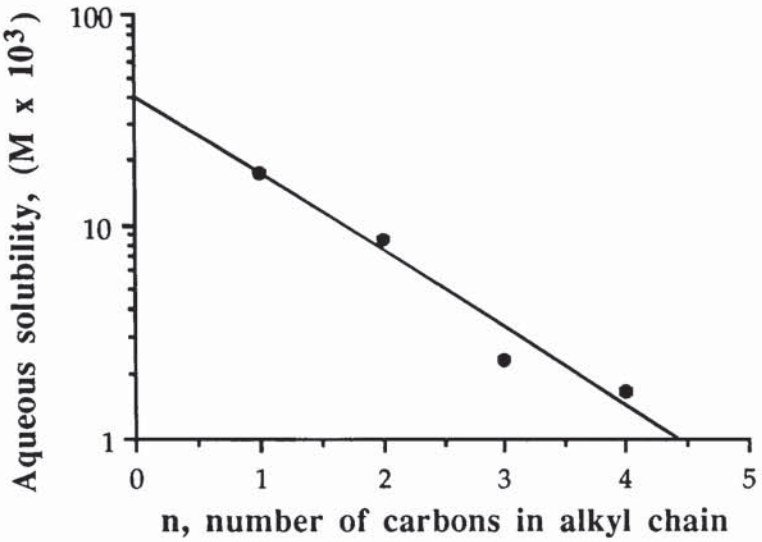

Figure 3.19 Solubility of the alkyl *p*-hydroxybenzoates in water at 34°C *versus* alkyl chain length

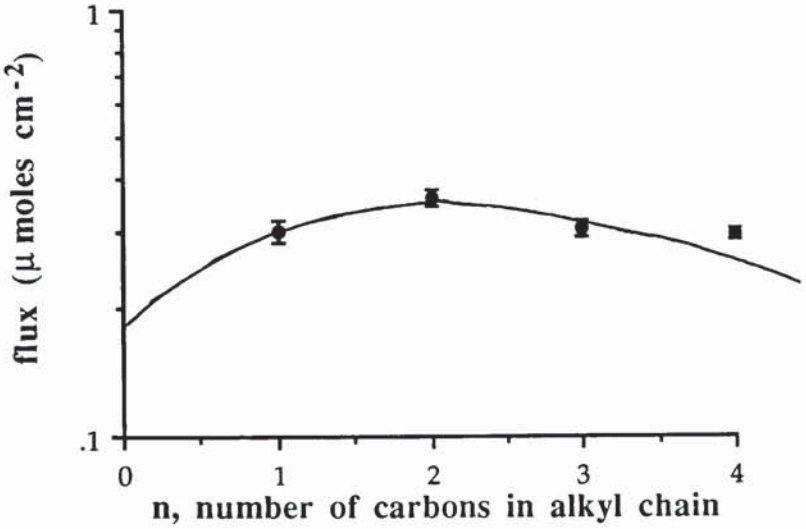

Figure 3.20 Plot of paraben flux *versus* alkyl chain length of paraben esters showing possible parabolic relationship

One parameter of particular importance is the partition coefficient of the drug between the membrane and the bathing solution; this is incorporated into the permeability coefficient, Kp (defined by equation 2.19). The paraben partition coefficients (from table 3.1) are linearly dependent on the chain length as illustrated by plotting paraben partition coefficient as a function of alkyl chain length (figure 3.21). Yalkowsky, Flynn and Slunick (1972) reported a similar linear relationship between the partition coefficients and the chain lengths for the homologous series of alkyl *p*-aminobenzoates. It therefore follows that a plot of log flux *versus* log P will also reveal a parabolic profile with its maxima at EtP, as shown in figure 3.22.

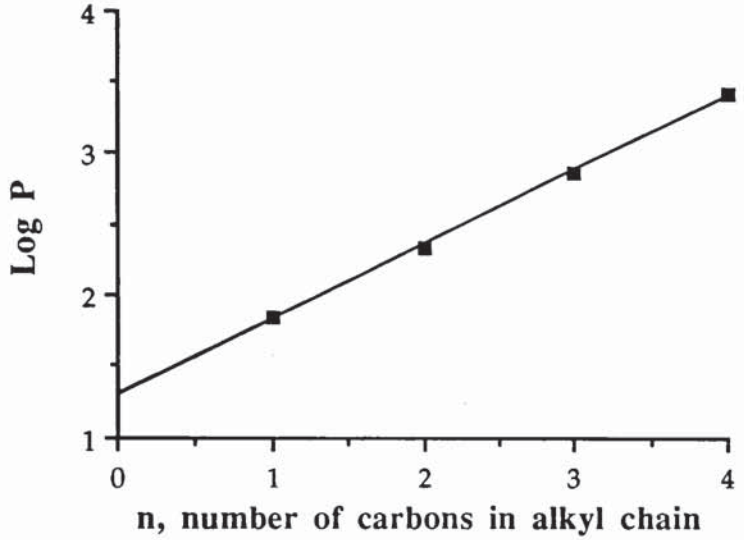

Figure 3.21 Paraben partition coefficient as a function of ester chain length

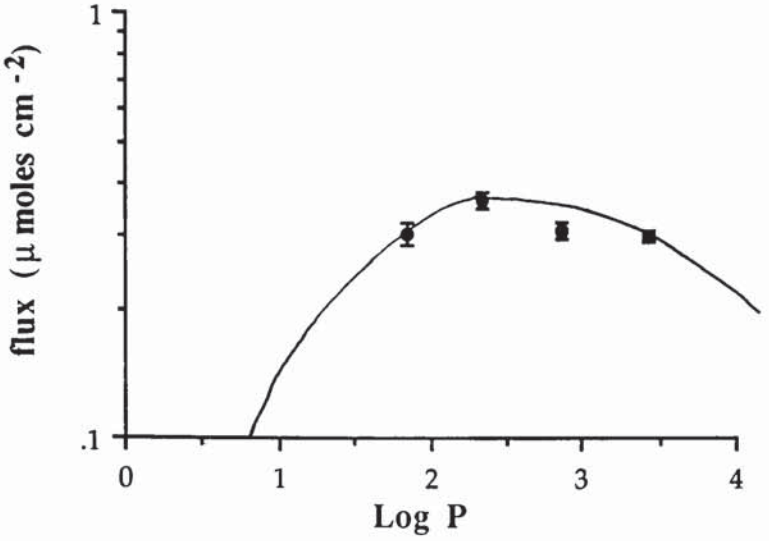

Figure 3.22 Plot of paraben flux *versus* Log P showing possible parabolic relationship

Kp values for the parabens ranged from (0.1697 ± 0.025) x 10^{-2} cm h^{-1} for MeP to (1.7852 ± 0.011) x 10^{-2} cm h^{-1} for BuP. The approximate 10-fold increase in the magnitude of Kp with the increase in ester chain length from MeP to BuP reflected the greater affinity of the more poorly soluble paraben for the lipophilic silicone membrane. By plotting Kp values as a function of paraben Log P (from table 3.1) a linear relationship was observed as shown in figure 3.23. This correlation further confirms the greater hydrophobic nature of the esters with increasing chain length.

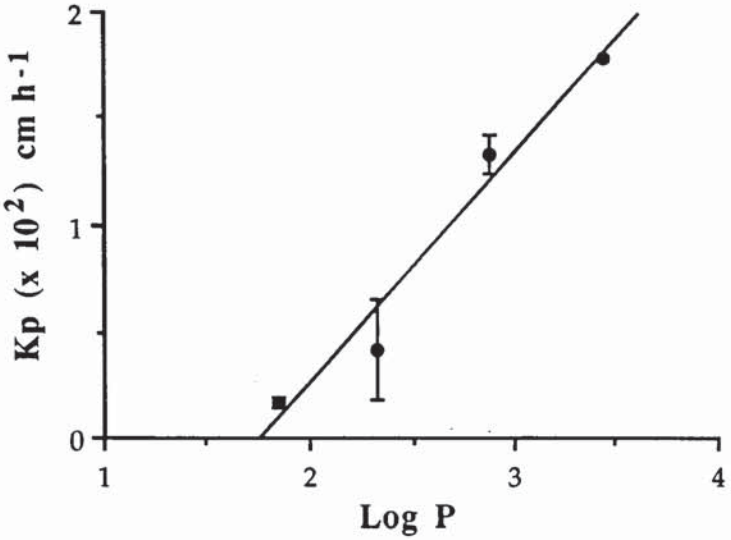

Figure 3.23 Permeability coefficient (K_p) as a function of paraben Log P (r^2=0.964)

The possible parabolic profiles obtained may be explained as follows. Based on the donor concentrations of the solutes, the MeP system had the potential to have the greatest flux. However, its partition into the membrane was limited due its relatively low lipophilic nature (Log P=1.85; Lehner, Müller and Seydel, 1993). The greatest paraben flux obtained with EtP was attributable to both its relatively high donor concentration (8.597 ± 0.021 mM) and its favourable partitioning characteristics as indicating by Kp, (0.4178 ± 0.020) x 10^{-2} cm h^{-1}. However, an increase in the magnitude of Kp does not guarantee an increase in solute flux. If Kp is too large, the solute cannot leave the membrane readily and thus there may be a change from membrane to diffusion layer control of the flux. Basically, for short esters the concentration gradient is essentially within the membrane. However, as the alkyl chain length increases, and therefore, also a parallel increase in partition coefficient, the location of the concentration gradient shifts from the membrane to the aqueous diffusion layer with the membrane acting as a reservoir of the diffusant (Flynn and Yalkowsky, 1972); when this occurs a parabolic relationship is expected. The reduced flux of PrP (0.3053 ± 0.015 μmoles cm^{-2} h^{-1}) and

BuP (0.2951 ± 0.008 μmoles cm^{-2} h^{-1}) is therefore possibly a consequence of their lower donor concentrations (2.348 ± 0.044 mM and 1.653 ± 0.056 mM respectively) and their increased affinity for the silicone membrane as demonstrated by their K_p values of (1.3304 ± 0.091) x 10^{-2} cm h^{-1} and (1.7852 ± 0.011) x 10^{-2} cm h^{-1} for PrP and BuP respectively, and also their increasing Log P values controlling their partition between the membrane and aqueous receptor phase. Flynn and Yalkowsky (1972) reported similar behaviour for a series of alkyl *p*-aminobenzoates. They found that factors such as aqueous solubility of the esters together with the partition coefficients affected their diffusion behaviour. Similar parabolic relationships were observed between the flux of the homologous series and the alkyl chain length with a maximum between the ethyl and butyl esters.

The diffusion lag times (t_L) were obtained from extrapolation of the diffusion plot to the x-axis. As shown in table 3.11, t_L was similar for all parabens. For the homologous series of alkyl p-aminobenzoates (Flynn and Yalkowsky, 1972), the diffusion lag times for esters methyl to butyl were also similar. These researchers suggested that this was due to the adsorption mechanisms for methyl, ethyl, propyl and butyl esters being similar qualitatively but not quantitatively. Since, there was no marked difference in paraben diffusion lag times, it follows that their diffusion coefficients (D) were also similar as shown in table 3.11.

As well as the partition coefficient of the drug, other physicochemical properties of both the solute and the barrier may affect the diffusion process. The frictional resistance to diffusion is also important, and for solids is dependent mainly on the particle size and shape in addition to the type of solvent. Distilled water was used as the solvent throughout all experiments. Interactions between the diffusing drug molecules such as self-aggregation and micellisation, which may alter the particle size, shape and thermodynamic activity coefficient, will similarly exert an effect on the diffusion rate. In this study, the molecular interaction between the paraben and CyD is another factor affecting the diffusion process.

The experiments discussed so far involved the use of aqueous paraben suspensions as the donor phase. Therefore, due to the presence of excess solid, a constant driving force for diffusion was maintained throughout each experiment. The diffusion of BuP was further assessed using a saturated donor solution of the solute (no excess solid). A linear increase in diffusion rate was only observed up to 3.5 hours after which a decline was seen as illustrated in figure 3.24. Using the first seven points of the solution diffusion profile, the steady-state flux of BuP found by linear regression was 0.2794 ± 0.021 μmoles cm^{-2}

h^{-1} ($r^2 = 0.990$). There was no significant difference ($p < 0.05$) between this value and the flux of BuP from its suspension (0.2951 ± 0.0081 μmoles cm^{-2} h^{-1}). The BuP concentration of the donor solution decreased from 1.7393 ± 0.015 mM to 0.2927 ± 0.016 mM over the 7 hour of study. The decrease in diffusion rate observed after the initial linear phase was therefore due to the concentration in the donor phase being continuously depleted. Consequently, the concentration differential, and hence the driving force of diffusion between the donor and receiver phases, was reduced.

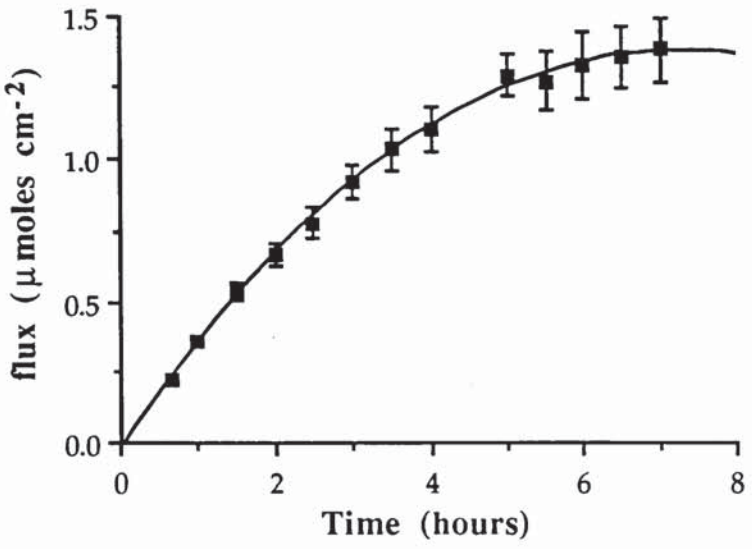

Figure 3.24 Diffusion of BuP through silicone membrane from a saturated aqueous solution. Points represent the mean ± s.d., $n = 3$.

3.6.7.2 Diffusion of parabens from donor solutions of the paraben-HP-β-CyD complexes

The diffusion of parabens from their respective HP-β-CyD complex solutions was assessed in a similar manner. A control experiment was performed initially to determine whether HP-β-CyD itself diffused through the silicone membrane. Visual examination of the freeze-dried receiver solutions after the 7-hour experiment showed the absence of any material indicating that due to the hydrophilic nature of the CyD, it did not cross the lipophilic membrane. It was, therefore, also assumed that the paraben-HP-β-CyD complexes were also unable to diffuse across the membrane. During the diffusion experiments with the solutions of the paraben-HP-β-CyD complexes in the donor compartment, the paraben flux was therefore a measure of free drug transport only.

The flux of BuP from its free drug suspension was compared to the flux from a donor solution of the BuP-HP-β-CyD complex of equivalent concentration to the saturation solubility of paraben alone. Since equimolar drug concentrations were used, it could perhaps be assumed that the driving force in each system was equivalent and therefore a similar flux should be obtained. However, as illustrated in figure 3.25, a constant diffusion rate was observed over the initial 2 hours after which it declined. Using the first four points of the rate curve, the flux of BuP from a solution of its HP-β-CyD complex found by linear regression was (0.1011 ± 0.002) μmoles cm^{-2} h^{-1}. The flux of BuP from its HP-β-CyD complex was significantly less than the flux from a free drug suspension (0.2951 ± 0.008 μmoles cm^{-2} h^{-1}). The diffusion data of BuP from its free drug suspension and a solution of its HP-β-CyD complex is summarised in table 3.12. The concentration of the solution of the HP-β-CyD complex is the concentration determined at time zero. The lag time for BuP diffusion from the solution of the complex (0.0439 ± 0.017 hours) was approximately 10 times less than that for the free drug suspension (0.4704 ± 0.104 hours). Theoretical, there should be no significant difference since a pre-saturated suspension was used and in both systems the diffusing solute is the same. The t_L is obtained by extrapolation of the linear portion of the diffusion plot to the x-axis which may therefore account for the unexpected results. Due to the errors in t_L, the diffusion coefficients were not calculated.

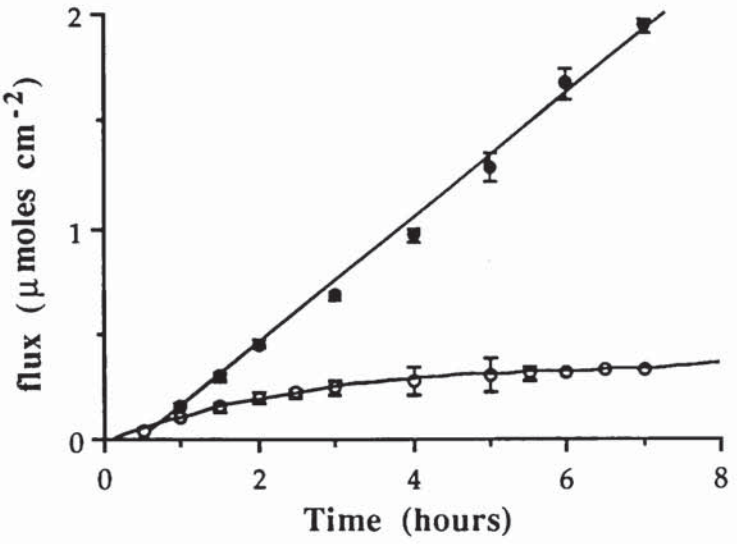

Figure 3.25 Diffusion of BuP from its free drug suspension (•) and from a solution of its HP-β-CyD complex (o) of equivalent BuP concentration. Points represent the mean ± s.d., $n = 3$.

Table 3.12 Diffusion data for butyl paraben (BuP) transport through silicone membrane from an aqueous donor suspension of drug alone and a solution of its HP-β-CyD complex of equivalent BuP concentration. Values represent the mean ± s.d., $n = 3$.

donor sample	**free drug suspension**	**solution of complex**
donor concentration (M x10^3)	1.653 ± 0.056	1.720 ± 0.071
flux (μmoles cm^{-2} h^{-1})	0.2951± 0.008	0.1011 ± 0.002
r^2	0.992	0.993
K_p (x 10^2) cm h^{-1}	1.7852 ± 0.011	0.5878 ± 0.014 (apparent) 1.4690 ± 0.062 (true)
lag time (hours)	0.4704± 0.104	0.0439 ± 0.017

Following dissolution of the complex, dissociation of the complex into its respective free components occurs; however, the dissociation equilibrium is influenced by various factors. The concentration of drug in the non-complexed form and, therefore, the drug available for diffusion, is governed by the temperature, the magnitude of the respective K_S value and the relative concentrations of the free components in solution (Habon and Szejtli, 1981). The receptor solutions during all diffusion experiments were heated to 37°C from which there was a transfer of heat to the donors solution; measured temperature of donor solution was 34°C. The effect of temperature on the complex dissociation equilibria was therefore considered to be constant in all paraben systems studied.

The magnitude of K_S for the BuP-HP-β-CyD complex is relatively high (2179 M^{-1}; 37°C), therefore the dissociation equilibrium will be shifted in favour of complexation as illustrated in scheme 4 below. However, the K_S value may not be the sole determinant of complex dissociation since other factors such as the affinity of the drug for the silicone membrane will be involved.

$$\text{BuP-HP-}\beta\text{-CyD}_{\text{solution}} \rightleftharpoons \text{BuP}_{\text{solution}} + \text{HP-}\beta\text{-CyD}_{\text{solution}}$$

Scheme 4: Dissociation equilibrium of the BuP-HP-β-CyD complex

The permeability coefficient of BuP diffusing from the solution of its HP-β-CyD complex solution was found to be (0.5878 ± 0.014) x 10^{-2} cm h^{-1} which was lower than the respective value for the diffusion of BuP from its free drug suspension (1.7852 ± 0.011) x 10^{-2} cm h^{-1}. However, the K_p value for the solution of the complex is only an apparent value. Even though the total BuP concentration of the free and complexed systems were equivalent, the concentration of free BuP available for diffusion at equilibrium in the HP-β-CyD complex solution, was less than in the saturated solution of BuP alone. Consequently, the flux of BuP from the solution of the complex was reduced. Using equation A4.20 in Appendix 4, the concentration and percentage of BuP existing as the non-complexed form in the donor solution of HP-β-CyD complex was found as summarised in table 3.13. Using the concentration of free BuP at time zero (0.6882 ± 0.176 mM), the true K_p for the solution of the complex was found to be (1.469 ± 0.061) x 10^{-2} cm h^{-1}. This value is still significantly less than the respective K_p of BuP suspension [(1.7852 ± 0.011) x 10^{-2} cm h^{-1}] suggesting that in the presence of CyD, the affinity of BuP for the silicone membrane is relatively lower than when present alone. This may be a consequence of the equilibrium existing between free and complexed forms.

Table 3.13 Concentration and percentage of free BuP in the BuP-HP-β-CyD complex donor solution at time zero and at the end of the 7 hours experiment calculated using equation A4.20 and K_S = 2179 M^{-1}. Values represent the mean ± s.d., n = 3.

Time (hours)	Total BuP concentration of donor solution (M x 10^3)	Concentration of free BuP (M x 10^3)	Percentage of total BuP concentration as free
0	1.7203 ± 0.071	0.6882 ± 0.018	40.0 ± 2.8
7	0.3994 ± 0.006	0.2563 ± 0.003	64.2 ± 1.6

The BuP concentration of the donor solution of the BuP-HP-β-CyD complex decreased from 1.7203 ± 0.071 mM to 0.3994 ± 0.006 mM over the 7 hour period of study. The ratio of the donor concentration of the suspension of BuP alone (1.653 ± 0.056 mM), to the initial concentration of free BuP in the solution of the complex (0.6882 ± 0.018 mM), was 2.4. This correlates well with the ratio of the flux from a donor suspension of BuP alone (0.2951 μmoles cm^{-2} h^{-1}), to the solution of the complex (0.1011 μmoles cm^{-2} h^{-1}) which was 2.9. The percentage of the total BuP in the system which was in a non-complexed form was greater with the lower concentration of the complex (64.2 ± 1.6 %) at the end of the experiment. This was to be expected since in more dilute systems, the

equilibrium governing complex dissociation is shifted to the free components of the complex (Szejtli, 1988).

The decrease in diffusion rate of BuP from its HP-β-CyD complex solution after the initial linear phase was similar to that observed with a saturated solution of BuP alone (figure 3.24). Due to the decrease in the total donor BuP concentration of the BuP-HP-β-CyD solution, the concentration differential, and hence the driving force of diffusion between the donor and receiver phases was also reduced; this consequently reduced the diffusion rate of the solute.

To summarise, it has been shown that when comparing the diffusion of free drug from equimolar solutions of either saturated drug alone or its HP-β-CyD complex, the flux from the latter system is reduced due to the fact that only a proportion of the total paraben concentration will be free drug, and therefore, available for diffusion. For a paraben-CyD product to be advantageous, the flux of paraben from a solution of its HP-β-CyD complex must be greater that the flux from a free drug suspension. This can only be achieved by increasing the total donor concentration of the paraben HP-β-CyD complex in an attempt to increase the proportion of drug in the non-complexed form in solution.

Ideally, saturated solutions of the paraben complexes should have been used so that the maximum flux achievable could be assessed. However, as discussed in section 3.6.4, the solubility limit of the BuP complex was not reached. It was therefore decided to use sufficient amounts of each paraben-HP-β-CyD complex (with the exception of MeP) such that the total concentration of dissolved paraben was approximately 40 times its equilibrium solubility at 37°C (S_0) as determined during phase solubility studies (section 3.6.5). The concentration of the parabens-HP-β-CyD complexes could have been further increased to provide a greater concentration differential between the donor and receiver phases. However, since the relative guest to host ratio is small, by increasing the amount of complex dissolved in solution the increase in total paraben concentration is relatively small compared to the effect in the HP-β-CyD concentration which consequently increases the viscosity of the donor solution. Therefore, since the diffusion of solutes is retarded by an increase in viscosity, no further increases were made in the amount of the parabens-HP-β-CyD complex used. With MeP, since the drug alone is relatively water-soluble (18.385 ± 0.352 mM), the amount of complex required to give a MeP concentration which was 40 times its saturation solubility would have been approximately 1.0 g dissolved in 1 ml of distilled water. The theoretical concentration of HP-β-CyD in this solution would be have been 100 % w/v which clearly would have been a highly viscous solution. Therefore, the diffusion of MeP from solution of its HP-β-CyD

complex was assessed using sufficient MeP complex such that the total MeP concentration in solution was approximately 10 times greater than the saturation solubility of the MeP alone at 37°C. In this way, the concentration of HP-β-CyD solution was reduced to approximately 25 % w/v and thus the viscosity was also reduced.

The diffusion profiles for all parabens from donor solutions of their respective HP-β-CyD complexes were linear over the 7-hour period of study indicating steady-state diffusion. Figures 3.26 to 3.29 compare the permeation behaviour of the parabens from donor suspensions of drug alone to diffusion from solutions of their HP-β-CyD complexes. The steady-state fluxes, permeability coefficients and lag times were determined from the linear portions of the rate curves by linear regression and are summarised in tables 3.14 to 3.17 for each paraben respectively. The concentration of the donor solutions of the respective HP-β-CyD complexes were determined at time zero and at 7 hours from the initiation of the experiment, however, no significant differences were found between them. The donor concentrations determined at time zero, together with the data obtained for the diffusion of the parabens from their free drug suspensions, are also included in the appropriate table.

For each paraben system, MeP being the exception, the flux of drug from the donor solution of the respective HP-β-CyD complexes were significantly ($p < 0.05$) greater than the flux from free drug suspensions. With the BuP-HP-β-CyD complex, the diffusion experiments were performed with all three batches of complex that were prepared to assess the reproducibility of the procedure. Figure 3.29 illustrates the diffusion profile of BuP from *Batch III* complex, however, as shown in table 3.17, the flux of BuP from all three batches of complex were all similar. There was no significant difference between the flux of MeP from its saturated drug suspension and the flux from a donor solution of its HP-β-CyD complex.

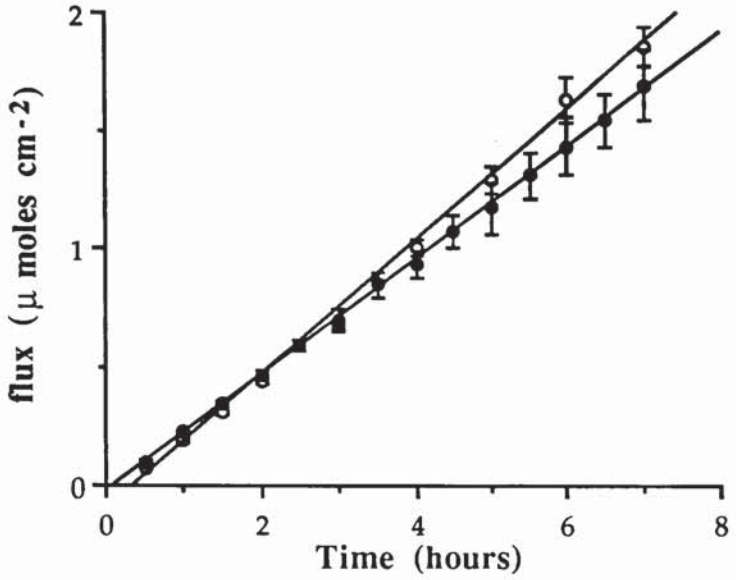

Figure 3.26 Diffusion of methyl paraben through silicone membrane from an aqueous donor suspension of drug alone (o) and a solution of its HP-β-CyD complex (•). Points represent the mean ± s.d., $n = 3$.

Table 3.14 Diffusion data for methyl paraben (MeP) transport through silicone membrane from an aqueous donor suspension of drug alone and a solution of its HP-β-CyD complex. Values represent the mean ± s.d., $n = 3$.

donor sample	**free drug suspension**	**solution of complex**
donor concentration (M x10^3)	17.633 ± 0.118	172.930 ± 3.356
flux (μmoles cm^{-2} h^{-1})	0.2993 ± 0.018	0.2436 ± 0.024
r^2	0.997	0.999
K_p (x 10^2) cm h^{-1}	0.1697 ± 0.025	0.0141 ± 0.002 (apparent) 0.1905 ± 0.021 (true)
lag time (t_L; hours)	0.3882 ± 0.069	0.0414 ± 0.123

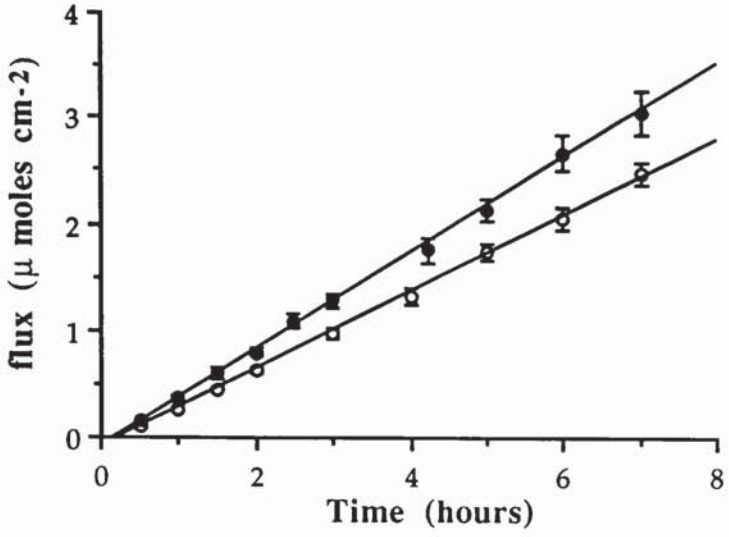

Figure 3.27 Diffusion of ethyl paraben through silicone membrane from an aqueous donor suspension of drug alone (o) and a solution of its HP-β-CyD complex (•). Points represent the mean ± s.d., $n = 3$.

Table 3.15 Diffusion data for ethyl paraben (EtP) transport through silicone membrane from an aqueous donor suspension of drug alone and a solution of its HP-β-CyD complex. Values represent the mean ± s.d., $n = 3$.

donor sample	free drug suspension	solution of complex
donor concentration (M x10^3)	8.597 ± 0.021	353.46 ± 13.62
flux (μmoles cm^{-2} h^{-1})	0.3592 ± 0.017	0.4450 ± 0.045
r^2	0.995	0.998
K_p (x 10^2) cm h^{-1}	0.4178 ± 0.021	0.0126 ± 0.002 (apparent) 0.2770 ± 0.330 (true)
lag time (t_L; hours)	0.2508 ± 0.035	0.1588 ± 0.150

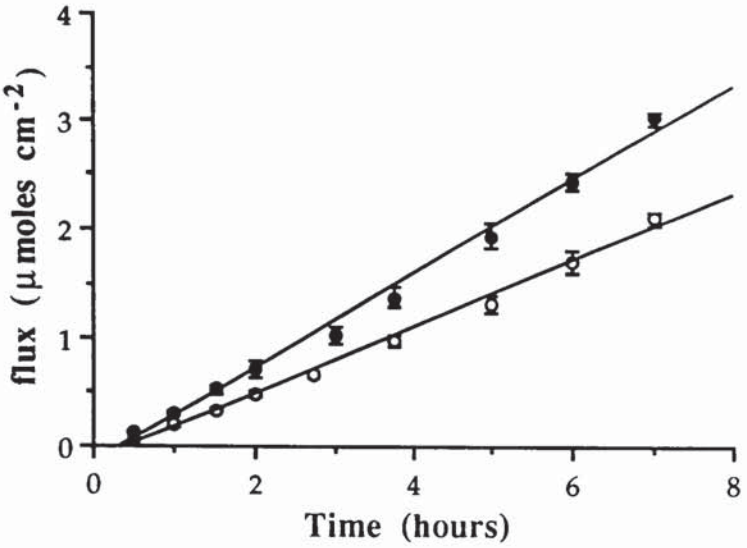

Figure 3.28 Diffusion of propyl paraben through silicone membrane from an aqueous donor suspension of drug alone (o) and a solution of its HP-β-CyD complex (•). Points represent the mean ± s.d., $n = 3$.

Table 3.16 Diffusion data for propyl paraben (PrP) transport through silicone membrane from an aqueous donor suspension of drug alone and a solution of its HP-β-CyD complex. Values represent the mean ± s.d., $n = 3$.

donor sample	free drug suspension	solution of complex
donor concentration (M x10^3)	2.348 ± 0.044	93.935 ± 2.949
flux (μmoles cm^{-2} h^{-1})	0.3053 ± 0.015	0.4332 ± 0.014
r^2	0.992	0.993
K_p (x 10^2) cm h^{-1}	1.3004 ± 0.091	0.0461 ± 0.003 (apparent) 0.6094 ± 0.029 (true)
lag time (t_L; hours)	0.3108 ± 0.234	0.3647 ± 0.078

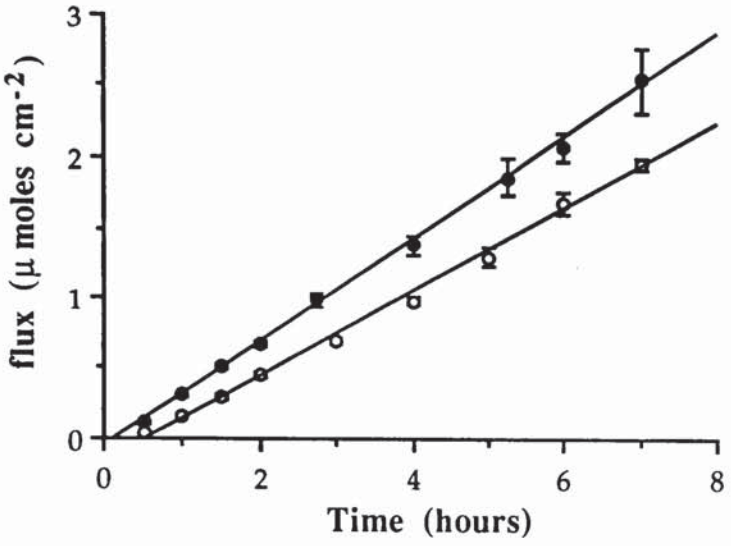

Figure 3.29 Diffusion of butyl paraben through silicone membrane from an aqueous donor suspension of drug alone (o) and a solution of its HP-β-CyD complex, *Batch III* (•). Points represent the mean ± s.d., $n = 3$.

Table 3.17 Diffusion data for butyl paraben (BuP) transport through silicone membrane from an aqueous donor suspension of drug alone and a solution of its HP-β-CyD complex. Values represent the mean ± s.d., $n = 3$.

donor sample	free drug suspension	complex		
		Batch I	*Batch II*	*Batch III*
donor concentration ($M \times 10^3$)	1.653 ± 0.056	58.417 ± 2.394	57.345 ± 1.885	61.394 ± 2.193
flux (μmoles cm^{-2} hr^{-1})	0.2951 ± 0.008	0.3600 ± 0.018	0.3617 ± 0.029	0.3968 ± 0.019
r^2	0.992	0.995	0.998	0.992
K_p ($\times 10^2$) cm h^{-1} (apparent values)	---	0.0616 ± 0.006	0.0631 ± 0.007	0.0646 ± 0.006
K_p ($\times 10^2$) cm h^{-1} (true)	1.7852 ± 0.011	0.7268 ± 0.051	0.7372 ± 0.070	0.7805 ± 0.052
lag time (t_L; hours)	0.4704 ± 0.104	0.2551 ± 0.168	0.0794 ± 0.061	-0.1989 ± 0.049

Even though the total paraben concentration of paraben-HP-β-CyD systems were approximately 40 times the concentration of the respective free drug suspensions, an equivalent enhancement in flux was not observed. As explained previously, this is due to the fact that the concentration of the donor solution of the paraben complex is a measure of both free and complexed drug. Due to the membrane properties, only free drug diffused into the receiver compartment. Therefore, using the total paraben concentrations of the donor solutions of the paraben-HP-β-CyD complexes and their respective complex stability constants as determined in section 3.6.5, the percentage of free paraben in the donor solutions was calculated using equation A4.20 in Appendix 4. Table 3.18 summarises the K_S values of the parabens-HP-β-CyD complexes, the total paraben concentration of the donor solutions of the complex, and the concentration and percentage of the total paraben in the system which was in a non-complexed form. Also shown are the saturation solubilities of the parabens alone. The data shown for the BuP-HP-β-CyD system is based on the flux of BuP from a solution of *Batch III* complex.

Table 3.18 Summary of paraben data. Values represent mean ± s.d., $n = 3$.

paraben-HP-β-CyD system	**methyl**	**ethyl**	**propyl**	**butyl**
K_S (M^{-1})	980	1308	1718	2179
Total concentration of complex solution (M x 10^3)	172.939 ± 3.356	353.461 ± 13.622	93.935 ± 2.949	61.394 ± 2.193
Concentration of free paraben (M x 10^3)	12.784 ± 0.129	16.061 ± 0.314	7.109 ± 0.115	5.084 ± 0.093
Percentage of total paraben concentration as free	7.39 ± 0.22	4.54 ± 0.28	7.57 ± 0.37	8.28 ± 0.46
paraben concentration of free drug suspension (Mx 10^3)	17.633 ± 0.118	8.597 ± 0.021	2.348 ± 0.044	1.653 ± 0.056
degree of supersaturation	0.73	1.87	3.03	3.08

The concentration of the total paraben in the EtP, PrP and BuP-HP-β-CyD systems which was in a non-complexed form was significantly greater ($p<0.05$) than their respective free drug saturation solubilities, *i.e.* these systems were supersaturated with respect to free paraben. As a consequence, the flux of parabens from these systems was greater that their respective diffusion from suspensions of drug alone. With MeP however, the concentration of free drug was significantly less ($p<0.05$) than its saturation concentration. Although the flux of MeP from the MeP-HP-β-CyD system (0.2436 ± 0.024 μmoles cm^{-2} h^{-1}) appeared to be less than that obtained with the

saturated drug suspension (0.2993 ± 0.018 μmoles cm^{-2} h^{-1}), this difference was not significant.

The concentration of EtP in the non-complexed form in the EtP-HP-β-CyD system (16.061 ± 0.314 mM) was approximately 87 % greater than the saturation solubility of EtP itself (8.597 ± 0.021 mM), however, the flux of EtP from a solution of its EtP-HP-β-CyD complex (0.4450 ± 0.045 μmoles cm^{-2} h^{-1}) was only 24 % greater than the flux from a free drug suspension (0.3592 ± 0.017 μmoles cm^{-2} h^{-1}). Similarly, the flux of PrP from a solution of its HP-β-CyD complex (0.4332 ± 0.014 μmoles cm^{-2} h^{-1}), was 42 % greater than the flux from its free drug suspension (0.3053 ± 0.015 μmoles cm^{-2} h^{-1}); however, the concentration of PrP in the non-complexed form (7.109 ± 0.115 mM) was approximately 3 times the saturation solubility of PrP alone (2.384 ± 0.044 mM). With the BuP-HP-β-CyD, the flux of BuP observed with *Batch III* complex (0.3968 ± 0.019 μmoles cm^{-2} h^{-1}) was approximately 34 % greater than the flux from a drug suspension of BuP alone (0.2951 ± 0.008 μmoles cm^{-2} h^{-1}). In this system, the concentration of BuP existing as the non-complexed form (5.048 ± 0.093 mM) was again approximately 3 times the saturation solubility of BuP alone (1.653 ± 0.056 mM). Since the concentration differential is the driving force for diffusion, a correlation was expected between the increase in the concentration of free drug in the solutions of the paraben-HP-β-CyD complexes and the flux enhancement of the paraben. However, as shown by the results, the flux enhancement is lower that the relative enhancement of free drug concentration. Since the solutions are supersaturated with respect to the paraben alone, it could be that at high concentrations there may be some association such as hydrogen bonding between the free parabens and exterior of CyD torus which would consequently reduce diffusion.

For all parabens, the apparent K_p values of the respective solutions of the parabens complexes were less than the respective values for the drug suspensions alone. This was a direct consequence of the fact that the total donor paraben concentration was used in the calculation. However, since only free drug can diffuse through the silicone membrane, K_p was recalculated using the concentration of free paraben in the each donor system (taken from table 3.18). For the MeP system, there was no significant ($p<0.05$) difference between the K_p of the drug suspension alone [(0.1697 ± 0.025) x 10^{-2} cm h^{-1}] and the true K_p of the solution of the complex [(0.1905 ± 0.021) x 10^{-2} cm h^{-1}]. Even though the true K_p values of the solutions of the EtP, PrP and BuP complexes were higher than their respective apparent K_p values, they were still significantly less than the K_p values of the suspensions of drug alone. The reduction in permeability coefficient of the parabens in the presence of HP-β-CyD may be attributed to some form of association

as previously discussed and also due to the equilibrium existing free and complexed paraben. The concentration of the solution of MeP-HP-β-CyD solution was approximately 10 times the solubility of drug alone. However, with the other parabens, the total concentration of the solutions of the complexes were approximately 40 times the solubility of drug alone. Therefore, since the concentration of the MeP-HP-β-CyD system was relatively dilute in comparison, it follows that the extent of association was less pronounced and thus there was no significant difference between the K_p values of the complex and drug alone.

For all paraben-HP-β-CyD systems, the lag times showed great variation which was possibly due to the errors incurred from extrapolation as discussed previously. Hence, the diffusion coefficients were not calculated.

As previously discussed, following dissolution of the complex, the dissociation of the complex into its respective free components is influenced by various factors including the magnitude of K_S of the respective guest-CyD complex and the concentration of CyD in solution.

The effect of K_S on the concentration of free drug in the donor solutions of the complexes can be illustrated by the comparing the EtP, PrP and BuP-HP-β-CyD systems. The percentage of total paraben concentration as the non-complexed form increased in the order BuP > PrP > EtP for their respective paraben-HP-β-CyD systems. However, the K_S values of the respective paraben complexes decreased in the same order. If the magnitude of K_S is considered alone, in the case of BuP, which has the largest K_S value of 2179 M^{-1}, the shift of the dissociation equilibrium to favour complexation of BuP would be expected to be relatively greater than in the EtP system (K_S = 1308 M^{-1}) due to the greater stability of the BuP-HP-β-CyD complex. As a consequence therefore, the concentration of paraben in the non-complexed form was greater for the EtP-HP-β-CyD system (16.061 ± 0.314 mM), however, the percentage of the total EtP concentration in the non-complexed form was the smallest (4.54 ± 0.28 %). This effect can be explained by consideration of the CyD concentration in solution.

Dissociation of the CyD complex will also be influenced by the relative CyD concentration in solution. The amount of paraben-HP-β-CyD complex used during the diffusion experiments was such that the total concentration of paraben in solution (with the exception of MeP) was 40 times its respective saturation solubility. Since the stoichiometry of the paraben-HP-β-CyD complexes was approximately 1:1, with the EtP complex which was used in the greatest concentration (353.461 ± 13.622 mM), the CyD

concentration was also approximately 0.35 M, which was the highest of all the paraben-HP-β-CyD systems. Consequently, a larger percentage of the total paraben in solution existed as the complexed form. In the remaining parabens-CyD systems, which were relatively dilute compared to the EtP system, the percentage of total drug existing in the non-complexed form was greater due to the lower concentration of HP-β-CyD present.

With consideration of the influence of K_S and CyD concentration, the concentration and percentage of MeP found in the non-complexed form can be explained as follows. The MeP complex is the least stable of the paraben-HP-β-CyD complexes studied, having a K_S of 980 M^{-1}. Therefore, on dissolution and dissociation of the complex, the greatest concentration of free drug will exist due to is low stability relative to the other paraben complexes. However, the concentration of free paraben was greater with the EtP-HP-β-CyD system since the total concentration of EtP, both free and complexed (353.461 ± 13.622 mM), was greater than the total concentration of MeP in the MeP-HP-β-CyD system (172.939 ± 3.356 mM). However, if the percentages of free drug in the systems are considered, the free drug in the MeP-HP-β-CyD system (7.39 ± 0.22 % of total MeP concentration) is greatest due to the dilute system as well as the weaker complex.

To assess the effect of K_S alone on the permeation behaviour of guest from its CyD complex, the quantities of paraben-HP-β-CyD complexes used should be such that the concentration of HP-β-CyD in each paraben system was constant. If this procedure had been followed, the difference in flux between the respective paraben-CyD systems might be expected to be greater. Nevertheless, it has been shown that, provided the total concentration of drug in the solution of the paraben-HP-β-CyD complex is sufficiently high, the concentration of drug existing as the non-complexed form will exceed its saturation solubility. Consequently, the solution is supersaturated with respect to paraben alone and will therefore have a greater thermodynamic activity. The greater concentration of free drug in the donor compartment increases the differential across the membrane which ultimately leads to an enhanced flux. In applying this system to the treatment of localised bacterial infections where drug access is a problem such as in the oral cavity or the GI tract (*H. pylori*), the paraben-HP-β-CyD complex will provide a supersaturated solution of antimicrobial agent which will readily diffuse to the site of action. The potential microbiological activity of the paraben will therefore be greater than the administration of drug alone. The microbiological testing of this diffusion system is discussed in chapter 5.

To further increase the flux of the parabens from solutions of their HP-β-CyD complexes, a competitor may be added to displace the drug from the complex, making it

more available for diffusion. The effect of competitors will be discussed in the following section.

3.6.8 Diffusion of butyl paraben in the presence of competitors

As demonstrated in section 3.6.7, the concentration of BuP in the non-complexed form in a solution of its HP-β-CyD complex (total BuP concentration, 61.394 ± 2.193 mM; *Batch III* complex) was greater that the saturation solubility of drug alone which consequently lead to an increased flux. By the addition of a competitive guest to the solution of BuP-HP-β-CyD complex, displacement of BuP would follow enabling the flux of BuP to be enhanced further. Certain properties are required for a compound to be a suitable competitor candidate. Firstly, the competitive agent (CA) must have a high affinity for the CyD cavity so that the paraben is displaced. The BuP-HP-β-CyD complex is relatively stable as indicated by its K_S value of 2179 M^{-1} (37°C); therefore, the K_S of the CA-CyD complex should ideally be of greater magnitude. However, Tokumara and co-workers (1986) found DL-phenylalanine (Phe) to be a suitable competitor for the cinnarizine-β-CyD system, despite the fact that the K_S of the Phe-β-CyD complex was smaller than the respective cinnarizine complex ($K_S = 6.2 \times 10^3$ M^{-1}, Tokumura *et. al*, 1984). Since Phe is highly water-soluble, a high concentration of the competitor was used which may have counteracted the effect of the relatively small K_S. It therefore seems that if a suitable CA is poorly water soluble it competes for the CyD on the basis of its K_S value. Alternatively, the CA may be highly water-soluble, and due to its concentration being greater than complexed drug, the guest is displaced from the cavity. The geometric properties of the CA must also be favourable for a CA-CyD complex to form and the CA must also be pharmaceutically acceptable. Furthermore, for this study, the ideal CA should not interact with the membrane in any way. Figure 2.23 illustrates the role of the competing agent in the dissolution process of the complex.

The competitors used in this study were ascorbyl palmitate (AsP) and the surfactants sodium dodecyl sulphate (SDS) and dodecyl tetraammonium bromide (DTAB). Ascorbyl palmitate (L-Ascorbic 6-palmitate) is used as an antioxidant in foods and has also been considered as an antiatherosclerotic agent (SmithKline Beecham, personal communication, T. Grattan), it may, therefore, be considered as being pharmaceutically acceptable. The only reported interaction of AsP with CyD was by Kanebo (1978) who prepared the solid AsP-β-CyD complex for incorporation into cosmetic products, however, no information was given on the extent of the interaction. Since AsP has limited water-solubility, it was expected to have a strong affinity for the CyD cavity, hence AsP was chosen as a potential competitive agent for the displacement of BuP from its HP-β-CyD complex.

The surfactants SDS and DTAB were chosen as competitive agents due to their strong interaction with β-CyD as reported by Wan Yunnus and co-workers (1992); the magnitude of the K_S for SDS-β-CyD and DTAB-β-CyD complexes were found to be 21,000 M^{-1} and 18,100 M^{-1} respectively at 25°C. It was assumed that the surfactants would interact with HP-β-CyD to a similar extent. The K_S value of the BuP-HP-β-CyD complex was found to be 2467 M^{-1} at 25°C, therefore the surfactants should theoretically displace BuP due to their greater affinity for the cavity, as exhibited by their higher K_S values. The use of surfactants as competitive agents may not be pharmaceutically acceptable; however they were chosen to simply model the effects of displacement of complexed drug.

3.6.8.1 Diffusion of butyl paraben from donor phases of drug alone and the BuP-HP-β-CyD complex in the presence of ascorbyl palmitate

The diffusion of BuP from a solution of its HP-β-CyD complexed was assessed in the presence of AsP as a potential competitor. A control experiment was performed initially to determine whether AsP itself diffused through the silicone membrane from a donor suspension of drug alone. The UV absorbance of the receiver solution increased by 0.04 absorbance units over the 6 hour study. Even though the diffusion of AsP was very slight as indicated by the small change in absorbance, UV spectroscopy could not be used for the quantification of BuP in the experiments involving AsP since both AsP and BuP would contribute to the absorbance of the donor and receiver solutions. HPLC was therefore used for the quantification of BuP in the donor and receiver solutions of the experiments involving AsP as the competing agent. AsP did not interfere with the HPLC assay of BuP.

The diffusion profile of BuP from its HP-β-CyD complex (*Batch III*) in a suspension of AsP was initially linear but exhibited curvature in the latter stages of its profile. Figure 3.30 compares the diffusion behaviour of BuP from its HP-β-CyD complex with and without the presence of AsP. Using the first 10 data points of the rate curve for BuP diffusion in the presence of AsP, the steady-state flux of BuP was determined by linear regression to be 0.6468 ± 0.0353 μmoles cm^{-1} h^{-1}, which is approximately 1.6-fold greater than the flux of BuP from a solution of its complex alone (0.3968 ± 0.0188 μmoles cm^{-1} h^{-1}, section 3.6.7). In the presence of AsP therefore, the flux of BuP from its solution of complex was significantly enhanced ($p < 0.05$). There was no significant change in total BuP concentration of the donor solution of the complex in the presence of AsP measured at time zero and at the end of the experiments which was found to be (58.052 ± 0.691) x 10^{-3} M. This BuP concentration was a similar to that of the donor solution of complex alone (61.394 ± 2.193) x 10^{-3} M. Table 3.19 summarises the

diffusion data obtained from donor systems of the BuP-HP-β-CyD complex alone and in the presence of excess AsP.

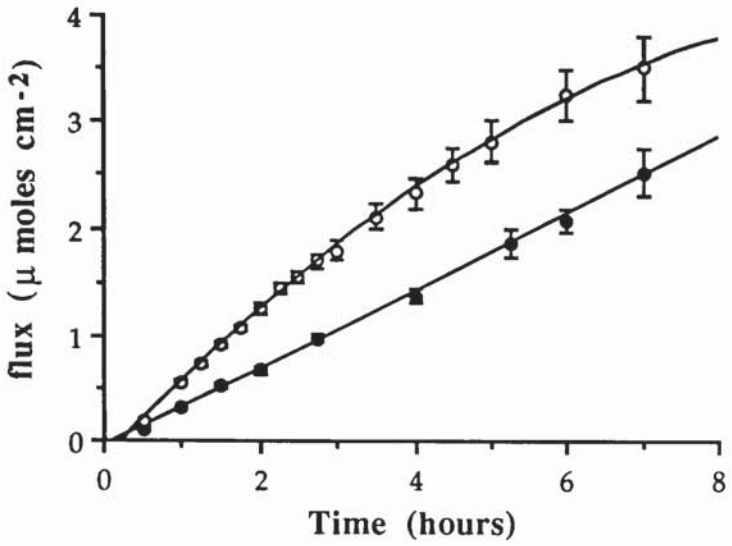

Figure 3.30 Diffusion of butyl paraben through silicone membrane from a solution of its HP-β-CyD complex alone (•) and in the presence of ascorbyl palmitate (o). Points represent the mean ± s.d., $n = 3$.

Table 3.19 Diffusion data for butyl paraben (BuP) transport through silicone membrane from solution of its HP-β-CyD complex alone and in the presence of ascorbyl palmitate. Values represent the mean ± s.d., $n = 3$.

donor sample	complex solution alone	complex with AsP
donor concentration (M x10^3)	61.394 ± 2.193	58.052 ± 0.691
flux (μmoles cm^{-2} h^{-1})	0.3968 ± 0.019	0.6468 ± 0.035
r^2	0.992	0.993
K_p (x 10^2) cm h^{-1} (apparent)	0.0646 ± 0.006	0.1114 ± 0.008
K_p (x 10^2) cm h^{-1} (true)	0.7805 ± 0.052	1.2755
lag time (hours)	0.1989 ± 0.049	0.1288±0.047

The enhanced flux of BuP in the presence of AsP as compared to the flux from complex alone, suggests that AsP displaced BuP from its HP-β-CyD complex and therefore increased the concentration of free drug in solution. The curvature of the diffusion profile

of BuP from a solution of its complex in the presence of AsP could be due to depletion of free BuP in the donor cell, thus steady state diffusion could not be maintained. To calculate the concentration of free BuP in the presence of AsP, the K_S of the complex formed between HP-β-CyD and AsP and the concentration of AsP in the system needs to be known. The interaction of AsP and HP-β-CyD in solution was assessed by phase solubility analysis (section 3.6.9) from which the K_S of their respective complex was found to be 539 M^{-1} and the saturation solubility of AsP alone (S_0) at 37°C determined as (1.2721 ± 0.113) x 10^{-5} M. In comparing this phase solubility data to the respective BuP-HP-β-CyD system, the interaction of BuP with HP-β-CyD is of greater magnitude as indicated by its K_S of 2179 M^{-1}, thus its is perhaps surprising that a competitive effect was observed.

To further clarify the competitive effect, the BASIC computer programme illustrated in figure A4.1 in Appendix 4, was used for the calculation of free drug concentration in the presence of AsP as a competitor. The variables required were the initial concentration of BuP which was equivalent to the total BuP concentration of the donor system ([A_0], (58.052 ± 0.691) x 10^{-3} M) the initial concentration of AsP which in this case was its saturation solubility ([B_0], (1.2721 ± 0.113) x 10^{-5} M), the K_S of the BuP-HP-β-CyD complex (K_A, 2179 M^{-1}) and the K_S of the AsP-HP-β-CyD complex (K_B, 539 M^{-1}). Since the stoichiometric ratio of the BuP-HP-β-CyD complex was approximately one, the concentration used for [CyD_0], *i.e.*, the initial CyD concentration, was assumed to be the same as the concentration of BuP in the donor phase, (58.052 ± 0.691) x 10^{-3} M. A summary of these data is given in table 3.20.

Table 3.20 Summary of free drug concentrations in the BuP-HP-β-CyD complex system with and without AsP calculated using computer programme in Appendix 4 and the variables given in the text.

	complex solution alone	complex with AsP
Total BuP concentration of complex solution (M x 10^3)	61.394 ± 2.193	58.052 ± 0.691
flux (μmoles cm^{-2} h^{-1})	0.3968 ± 0.019	0.6468 ± 0.035
Concentration of free paraben (M x 10^3)	5.084 ± 0.093	5.071
Percentage of total paraben concentration as free	8.28 ± 0.46	8.31

In the presence of AsP, the concentration of BuP which is in the non-complexed form (5.071×10^{-3} M) was not significantly different from the concentration in the BuP-HP-β-CyD solution alone. The increase in flux of BuP observed with the AsP system is therefore due to some reason other than the displacement of BuP from the CyD cavity. In the presence of AsP, the true permeability coefficient of BuP was significantly greater than for the system of complex alone indicating that the partition of BuP between the membrane and aqueous donor phases was greater in the presence of AsP. Previous experiments have shown that AsP itself diffused through the membrane, however, its effect on the membrane also needed to assessed.

The diffusion experiments were repeated using a donor suspension of BuP in the presence of AsP from which the diffusion of BuP was linear over the 7 hour study period. Using linear regression, the steady state flux of BuP was found to be 0.5730 ± 0.046 μmoles cm^{-1} h^{-1} which is twice the flux of BuP from its drug suspension alone (0.2951 ± 0.008 μmoles cm^{-1} h^{-1}). The diffusion profiles of BuP from a donor suspension of BuP with and without the presence of AsP are illustrated in figure 3.31 with a summary of the respective diffusion data given in table 3.21. Since there was no significant difference between the donor concentration of BuP in both systems, theoretically, the driving force for diffusion should be equivalent, following which similar fluxes would be expected. However, in the presence of AsP the flux of BuP and also its permeability coefficient ($[3.3222 \pm 0.008] \times 10^{-2}$ cm h^{-1}) were significantly enhanced ($p < 0.05$). Furthermore, in comparing the flux of BuP from a free drug suspension in the presence of AsP (0.5730 ± 0.046 μmoles cm^{-1} h^{-1}) to the flux of BuP from a solution of its HP-β-CyD complex in the presence of AsP (0.6468 ± 0.035 μmoles cm^{-1} h^{-1}), there was no significant difference ($p < 0.05$). With both BuP alone and a solution of its complex, in the presence of AsP, the permeability coefficient of BuP is significantly increased ($p < 0.05$). Due to the linear nature of the diffusion profiles in the presence of AsP, it is unlikely that AsP causes any mechanical destruction of the membrane. It therefore seems probable that the enhanced flux of BuP from its HP-β-CyD complex in the presence of AsP was not due to displacement of BuP by AsP, but due to the increased membrane permeability of BuP in the presence of AsP.

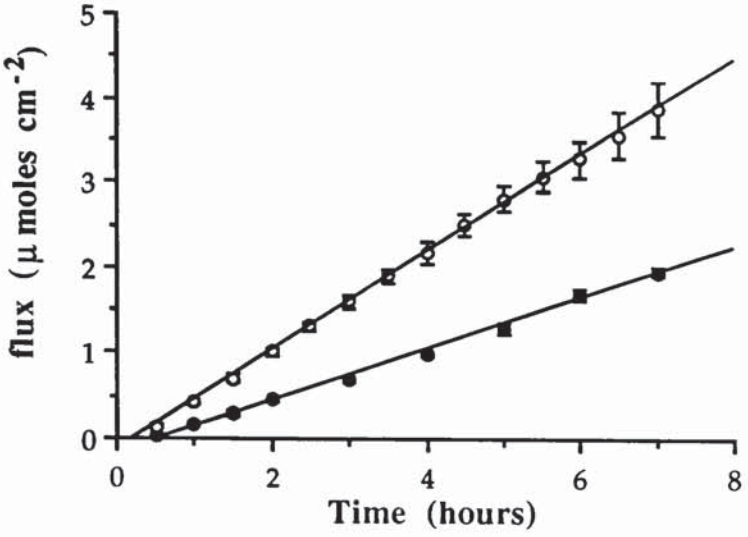

Figure 3.31 Diffusion of butyl paraben through silicone membrane from a suspension of drug alone (•) and in the presence of ascorbyl palmitate (o). Points represent the mean ± s.d., $n = 3$.

Table 3.21 Diffusion data for butyl paraben (BuP) transport through silicone membrane from a suspension of drug alone and in the presence of ascorbyl palmitate. Values represent the mean ± s.d., $n = 3$.

donor sample	**BuP suspension alone**	**BuP with AsP**
donor concentration (M x10^3)	1.653 ± 0.056	1.7247 ± 0.006
flux (μmoles cm^{-2} h^{-1})	0.2951 ± 0.008	0.5730 ± 0.046
r^2	0.992	0.999
K_p (x 10^2) cm h^{-1}	1.7852 ± 0.011	3.3222 ± 0.008
lag time (t_L, hours)	0.4704 ± 0.104	0.2358 ± 0.100

3.6.8.2 *Diffusion of butyl paraben from donor phases of drug alone and the BuP-HP-β-CyD complex in the presence of SDS and DTAB*

Since it was found that AsP increased the permeability of silicone membrane, prior to assessing the competitive nature of the surfactants, their effect on silicone membrane was also determined.

The concentrations of surfactants used were 7.5 mM and 13.5 mM for SDS and DTAB respectively which were below their literature critical micelle concentrations (CMC values: 8.1 mM and 14.4 mM for SDS and DTAB respectively; Elworthy and Florence, 1968). When excess BuP was added to a solution of the surfactants, the solubility of BuP increased from 1.7874 ± 0.018 mM (aqueous solubility at 37°C) to 6.1775 ± 0.013 mM and 3.3598 ± 0.163 mM with SDS and DTAB respectively. The solubility enhancement of BuP suggests that even though the concentration of the surfactants were below their CMC values, interactions occurred to solubilise the excess BuP present. The control experiment performed during the experiments involving AsP as a potential competitor involved measuring the flux of BuP from a donor suspension of excess BuP and AsP. No significant difference was found between the saturation solubility of BuP with and without AsP. However, in the case of the surfactants as competitor agents, the solubility of BuP is significantly greater in the presence of the SDS and DTAB. Therefore, on this occasion the control experiment was performed by initially pretreating the silicone membrane with the surfactants and then measuring the flux of BuP from a donor suspension of drug alone through the treated membrane. During membrane pretreatment with the surfactants, no significant change in the UV absorbance of the receiver solution was measured, indicating that any residual SDS or DTAB remaining in the membrane after washing would not effect the absorbance measurements during quantification of BuP.

Linear diffusion of BuP from a donor suspension of drug alone through silicone membrane pretreated with SDS and DTAB was observed. Figure 3.32 compares the diffusion behaviour of BuP before and after membrane treatment. The steady-state fluxes, permeability coefficients and lag-times were determined from the linear portions of the rate curves by linear regression. The results are summarised in table 3.22 which also shows the data for the diffusion of BuP through untreated membrane (from section 3.6.7). The flux of BuP through membrane pretreated with both surfactants (0.5984 ± 0.017 μmoles cm^{-2} h^{-1} and 0.5111 ± 0.016 μmoles cm^{-2} h^{-1} for SDS and DTAB respectively) were significantly greater ($p<0.05$) than the flux through untreated membrane (0.2951 ± 0.008 μmoles cm^{-2} h^{-1}). The concentration of BuP in the donor suspensions in all cases was comparable suggesting that the concentration differential

between the donor and receiver phases should also have been identical and therefore there should have been no significant difference in the flux of BuP.

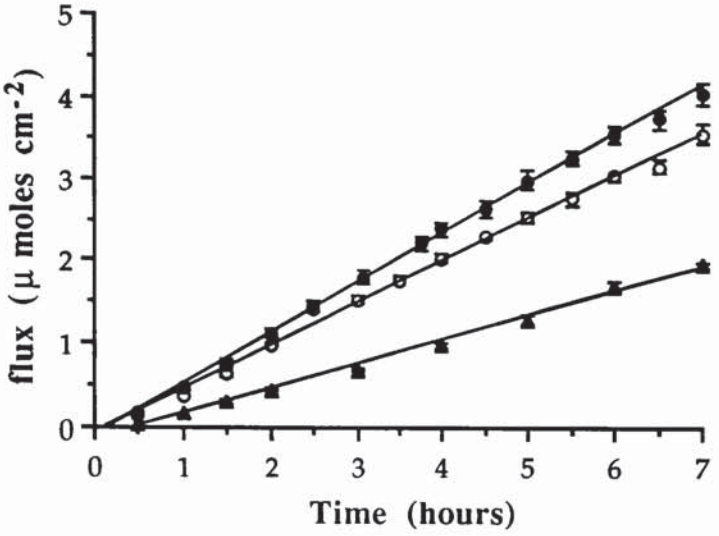

Figure 3.32 Diffusion of butyl paraben from a suspension of drug alone through silicone membrane before (▲) and after pretreatment with SDS (●) and DTAB (o). Points represent the mean ± s.d., $n = 3$.

Table 3.22 Diffusion data for butyl paraben (BuP) transport from a suspension of drug alone through silicone membrane before and after pretreatment with SDS and DTAB. Values represent the mean ± s.d., $n = 3$.

membrane:	untreated	SDS treated	DTAB treated
BuP concentration of donor (M x10^3)	1.653 ± 0.056	1.689 ± 0.011	1.623 ± 0.092
flux (μmoles cm^{-2} h^{-1})	0.2951 ± 0.008	0.5984 ±0.017	0.5111 ± 0.016
r^2	0.992	0.998	0.995
K_p (x 10^2) cm h^{-1}	1.7852 ± 0.011	3.5411 ± 0.127	3.1149 ± 0.330
lag time (hours)	0.4704 ± 0.104	0.1475 ± 0.039	0.1120 ± 0.032

The permeability coefficients of BuP for the SDS and DTAB pretreated membranes were $(3.5411 \pm 0.127) \times 10^{-2}$ and $(3.1149 \pm 0.330) \times 10^{-2}$ $cm^2\ h^{-1}$ respectively, which were significantly greater ($p < 0.05$) than the respective value for untreated silicone membrane, $(1.7852 \pm 0.011) \times 10^{-2}$ $cm^2\ h^{-1}$. The lag time of BuP through untreated membrane was significantly longer ($p < 0.05$) than with surfactant-treated membrane. The differences observed between the flux of BuP, the lag-time for diffusion and the permeability coefficients of BuP for treated and untreated membrane suggests that the surfactants increased membrane permeability. Consequently, the diffusion of BuP occurred faster than through untreated membrane. The surfactants therefore were not appropriate competitor agents due to their effect on the membrane and thus the diffusion of BuP from its HP-β-CyD complex in the presence of SDS and DTAB was not studied.

Both the surfactants and AsP have proved to be inappropriate competitive agents for the paraben-HP-β-CyD systems. Potential competitive guests should initially be screened on the basis of the magnitude of the K_S for their respective complexes with HP-β-CyD. If the K_S value is greater than that for the paraben-HP-CyD complex, the effect of the potential agent on the silicone membrane should be assessed. If no changes in membrane permeability occur, the diffusion experiments with the paraben-HP-β-CyD complexes should be performed.

3.6.9 Phase solubility of ascorbyl palmitate in the presence of HP-β-CyD at 37°C

The interactions between AsP and HP-β-CyD in solution were assessed by phase solubility analysis. A linear increase in AsP solubility was observed with increasing concentrations of HP-β-CyD. With the highest concentration of HP-β-CyD used, 0.069 M, the aqueous solubility of AsP was enhanced approximately 43-fold. The solubility diagram illustrated in figure 3.33 is of the A_L type indicating the formation of a soluble complex between AsP and HP-β-CyD with a probable stoichiometry of 1:1 (Higuchi and Connors, 1965). Using linear regression, the slope and intercept of the solubility isotherm were found, from which the respective K_S of the AsP-HP-β-CyD complex formed was calculated using equation A3.13 in Appendix 3.

The AsP-HP-β-CyD complex formed in solution was found to have a K_S of 539 M^{-1}, which is smaller than the respective BuP-HP-β-CyD complex K_S of 2179 M^{-1}. In comparing the saturation solubilities of both guests as determined from phase solubility studies at 37°C, BuP ($[1.6898 \pm 0.41] \times 10^{-3}$ M) has a greater aqueous solubility that AsP ($[1.2721 \pm 0.113] \times 10^{-5}$ M). Therefore, on the basis of solubility, a larger K_S may have been expected for the AsP-HP-β-CyD complex, however, sterically, the inclusion

of AsP into the CyD cavity may not have been as favourable as the inclusion of BuP. From the structure of AsP, as illustrated in figure 3.34, it is possible that the palmitate ester moiety was incorporated into the cavity rather than the hydrophilic ascorbic acid residue.

It can therefore be concluded that due to the relatively weak interaction between AsP and HP-β-CyD, AsP was not a suitable competitor for the displacement of BuP from its HP-β-CyD complex.

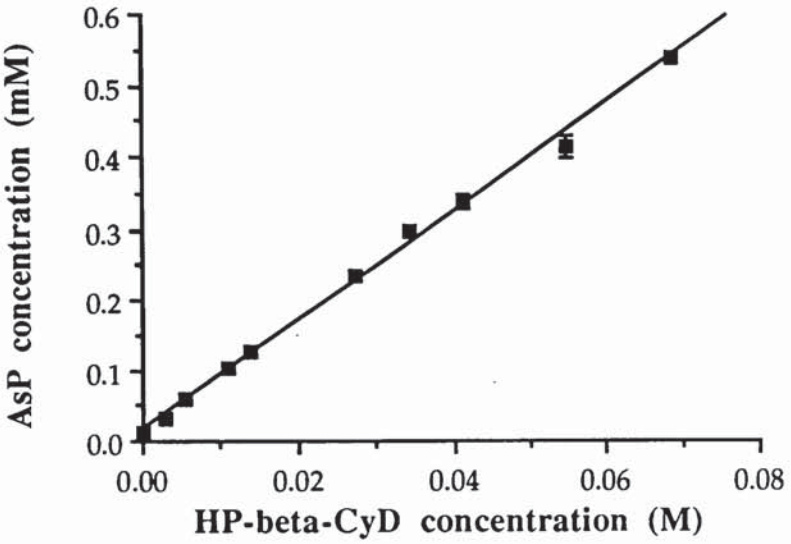

Figure 3.33 Phase solubility diagram of the AsP-HP-β-CyD system in distilled water at 37°C. Points represent the mean ± s.d., $n = 3$.
[$y = (7.6946 \times 10^{-3})x + 1.4399 \times 10^{-5}$, $r^2 = 0.998$)

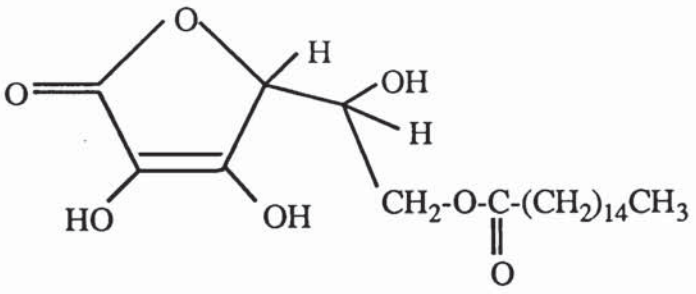

Figure 3.34 Structure of ascorbyl palmitate

3.7 CONCLUSIONS

The interactions between the parabens and HP-β-CyD were studied in both solution and solid phases. The solid complexes were prepared by the freeze-drying method. Investigation of the solid paraben-HP-β-CyD complexes was performed by DSC, IR analysis and X-ray powder diffraction which revealed the existence of real inclusion complexes. Experiments performed to determine the solubility limit of the paraben-HP-β-CyD complexes did not find a saturation limit.

Investigation of the interactions between parabens and HP-β-CyD in solution were studied by phase solubility analysis and UV spectroscopy. Phase solubility studies showed the enhanced solubility of the parabens in the presence of HP-β-CyD by the formation of a soluble complex with a probable stoichiometry of 1:1. The solubility enhancement was greater as the alkyl chain of the ester increased. The magnitude of K_S also increased from the methyl to butyl ester which further confirmed that the greater the hydrophobic nature of the guest, the greater its affinity for the CyD cavity. Using the BuP-HP-β-CyD system, the temperature dependence of the complex stability constant was illustrated. With a rise in temperature, K_S values decreased due to dissociation of the complex. The thermodynamic parameters for the complexation reaction showed favourable enthalpic and entropic changes indicating that the inclusion of BuP within the CyD cavity was a feasible process.

Phase solubility studies have illustrated the enhanced solubility of parabens due to complex formation in aqueous solution and the solid phase paraben-HP-β-CyD complexes also showed their superior solubilities. Therefore, due to the higher concentration of parabens available in aqueous solution due to solubilisation by HP-β-CyD, the wider use of the parabens as antimicrobial agents may by possible. Furthermore, by administration of a high concentration of antimicrobial agent, the driving force for diffusion would be greater; this would consequently enhance its microbiological action. However, for antimicrobial activity, the concentration of free drug is important and therefore the dissociation of the HP-β-CyD complex is an important consideration.

Diffusion experiments performed using silicone membrane to assess the dissociation of paraben-HP-β-CyD complex have illustrated the enhanced flux of paraben provided that the donor solution of the paraben complex is of a sufficiently high concentration. In these systems, the concentration of drug in the non-complexed form was greater than the saturation solubility itself. Therefore, with a solution of the complex, the solution is supersaturated with respect to the paraben and thus will have a greater thermodynamic

activity than a saturated solution of drug alone. Consequently, the flux of paraben was greater from a solution of its HP-β-CyD complex than from a suspension of paraben alone. In applying this system for the potential treatment of localised bacterial infections, the paraben-HP-β-CyD complex would provide a reservoir of antimicrobial agent from which free drug would readily diffuse to the site of bacterial infection due to the concentration differential. The rate of diffusion would be greater than from a saturated suspension of drug alone and hence the microbiological activity would also be enhanced. The microbiological activity of drug released from the paraben complex system was assessed as discussed in chapter 5. The rate of diffusion of free drug may be further increased in the presence of a competitor, although, no suitable competitor was found during this study.

In conclusion therefore, it has been shown that paraben-HP-β-CyD complex systems may have potential use for the local treatment of bacterial infections. Some of the practical considerations for this putative antimicrobial-CyD system include the form in which the product would be administered and also the retention of the product in the oral cavity or the G.I. tract so that sufficient drug can diffuse to the site of action. For treatment of bacteria in the oral cavity a gum form of the product may be suitable.

Further work on the paraben-HP-β-CyD system would include the search for a suitable competitor to demonstrate the displacement of complexed drug and therefore enhancement in diffusion rate. Also, investigations into suitable mechanisms for the retention of a potential antimicrobial-CyD product in an *in vivo* system should be performed.

CHAPTER FOUR
INVESTIGATION OF THE INTERACTION BETWEEN TRICLOSAN AND HYDROXYPROPYL-β-CYCLODEXTRIN

4.1 INTRODUCTION

Triclosan (5-chloro-2-(2,4-dichlorophenoxy) phenol) is a bis-phenol antimicrobial agent. The poor water-solubility of triclosan (0.6 mg/100 ml, 25°C) limits its usable concentration, hence, triclosan has bacteriostatic properties only against Gram-positive and most Gram-negative bacteria. Practical application of triclosan is limited to medicated soaps and washing creams. Triclosan is also used in toothpastes and mouthrinses as an antiplaque agent. The structure of triclosan is shown in figure 4.1.

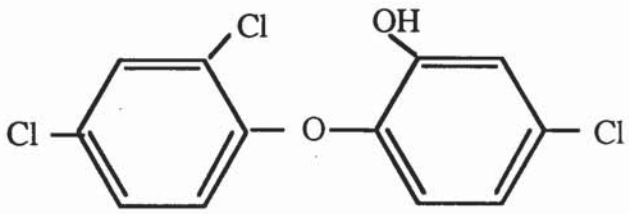

Figure 4.1 Structure of triclosan

The mode of action of triclosan can be considered to be similar to other phenolic antimicrobial agents. Generally, phenols target the bacterial cell wall resulting in lysis, inhibit active transport mechanisms in the cytoplasmic membrane and increase membrane permeability leading to leakage of the cytoplasmic constituents (Hugo, 1992). At high concentrations, phenols cause coagulation of the cytoplasm (Hugo, 1992). The actions described will depend on various factors including the concentration of the antimicrobial agent present as well as contact time with the bacteria. Due to the poor water-solubility of triclosan, its bacteriostatic actions are possibly restricted to cell wall lysis only, which occurs with low concentrations of disinfectants (Hugo, 1992).

Various methods can be used to increase the solubility of triclosan; these include the use of solvents, surfactants and also by pH adjustment, thus an enhancement in clinical effect may be expected. Triclosan has a pK_a of 7.9, thus, at high pH, an increase in solubility is observed. A recent study by Kjarheim and co-workers (1994) found triclosan dissolved in alkali to have an insignificant antiplaque effect whereas there was a marked effect with triclosan dissolved in propylene glycol. At high pH, the increase in triclosan

solubility is due the hydrophilicity of the phenol anion, the charge of which has an unfavourable effect on its antibacterial activity. These researchers suggested that repulsion occurred between the negatively charged triclosan molecule and the negatively charged tooth surface. Furthermore, the solutions containing triclosan in the presence of surfactants also showed a reduced activity compared to the triclosan dissolved in propylene glycol. The triclosan molecules are trapped in the surfactant micelles and thus less is available for an antibacterial effect. It therefore seems that the nature of the solvent is an important consideration for the formulation of a suitable antimicrobial product such that its clinical effect is retained. Although triclosan is soluble in organic solvents, these may cause irritation and can also have toxic effects. Ideally, an aqueous system is required in which triclosan is both highly soluble and also microbiologically active. Thus, the use of CyDs may enable an efficacious aqueous triclosan antiplaque product to be formulated.

As previously discussed, the aims of this study are concerned with the delivery of antimicrobial agents to difficult to access bacteria in both the oral cavity and in the stomach *i.e. H. pylori.* The use of a triclosan-CyD product against dental plaque has already been discussed above. *In-house* microbiological studies performed by SmithKline Beecham found triclosan to be an effective agent against *H. pylori.* The use of triclosan against *H. pylori* has already been reported in a patent application by Dettmar and Lloyd-Jones (1991). These researchers present triclosan-containing formulations in various dosage forms which include solutions, suspensions, tablets and capsules. Due to the limited aqueous solubility of triclosan, the solution formulations were prepared in propylene glycol and polyethylene glycol. An alternative solubilising agent is HP-β-CyD.

This study investigates the solubility enhancement of triclosan in the presence of HP-β-CyD. The interactions between triclosan and HP-β-CyD in both solution and solid phases were assessed. Assuming that the clinical effect of triclosan is retained, the solubility increase may consequently enable its wider usage as an effective bacteriostatic, and possibly bactericidal antimicrobial agent. To date, no publications regarding the interaction of triclosan with CyDs have appeared in the literature.

4.2. MATERIALS

Triclosan was supplied by SmithKline Beecham and was used as received. Details of all other chemicals and solvents used are listed in Appendix 2. An enzymatic diagnostic test was purchased from Sigma Chemicals for the quantitative determination of ammonia.

4.3 EQUIPMENT

Details of all equipment used is contained in section 2.3.

4.4 ASSAY PROCEDURES FOR TRICLOSAN

Quantitative assay of triclosan was achieved by HPLC. UV spectroscopy was used for the determination of a suitable wavelength for UV detection during HPLC analysis. Details of these assay procedures will be discussed in this section.

4.4.1 UV spectroscopy

The UV spectrum of triclosan was determined in the range 200-350 nm using a 0.0265 mM solution of triclosan prepared in 50:50 methanol:water (v/v). The λ_{max} of triclosan occurred at 283 nm, however, the intensity of absorbance at this wavelength was relatively small; the molar extinction coefficient (E) at this wavelength was 4906 L mol^{-1}. Absorbance was greater in the shoulder region of the spectrum, therefore for greater sensitivity, UV detection of triclosan during HPLC assay was performed at 245 nm; E = 9434 L mol^{-1}.

4.4.2 HPLC method development

Reversed-phase HPLC was used for the quantitative analysis of triclosan. By systematic and quantitative changes in solvent composition it was found that a mobile phase in the ratio of 80:20 methanol:water (v/v) gave optimum peak resolution whilst maintaining a relatively short analysis time. Detection of the elutes was monitored at 245 nm for reasons discussed above. Butyl paraben was selected as the internal standard and quantification of sample peak responses was achieved using peak area ratios (triclosan:I.S). Table 4.1 summarises the HPLC conditions employed for the triclosan assay. A sensitivity of 0.005 AUFS, the maximum possible with the instrumentation was used. Due to the limited solubility of triclosan in water alone, samples for HPLC assay were prepared using 50:50 methanol:water (v/v) solvent mix. The injection volume varied depending on the experiments performed. When a greater sensitivity was required, for example, during diffusion experiments (section 4.5.8), a 200 µl injection volume was used. For all other experiments, a 100 µl injection volume was adequate. Figures 4.2 and 4.3 illustrate examples of a typical chromatogram and a calibration plot respectively. The calibration graph shows the concentration range of triclosan used when injecting 100 µl samples. When using 200 µl injection volumes, the concentration of

triclosan ranged from 0.26 x 10^{-4} to 1.6 x 10^{-4} M and the final concentration of butyl paraben internal standard in the samples was also reduced to 3 x 10^{-5} M.

Table 4.1 HPLC conditions for the quantitative assay of triclosan

mobile phase	80:20 methanol-water
flow rate	1.0 ml min^{-1}
column	10 cm, ODS2 5 µm Spherisorb particles
wavelength	245 nm
sensitivity	0.005 AUFS
injection solvent	50:50 methanol:water mix
injection volume	100-200 µl
internal standard	Butyl paraben (3 - 6 x 10^{-5} M)

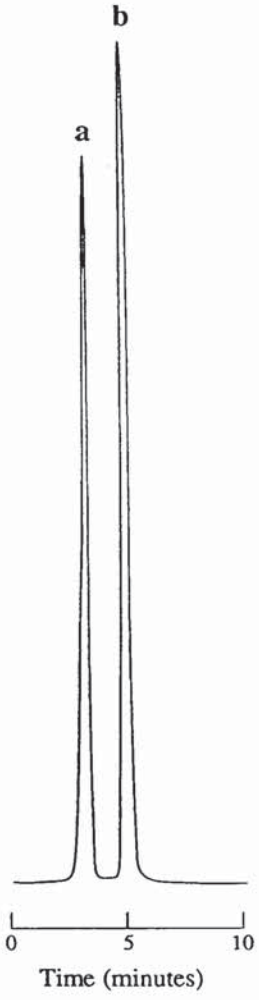

Figure 4.2 Example of a typical chromatogram of triclosan (peak b, 1.9 x 10^{-4} M; t_R = 5.0 minutes) with butyl paraben (peak a, 6 x 10^{-5} M; t_R = 2.7 minutes) as internal standard

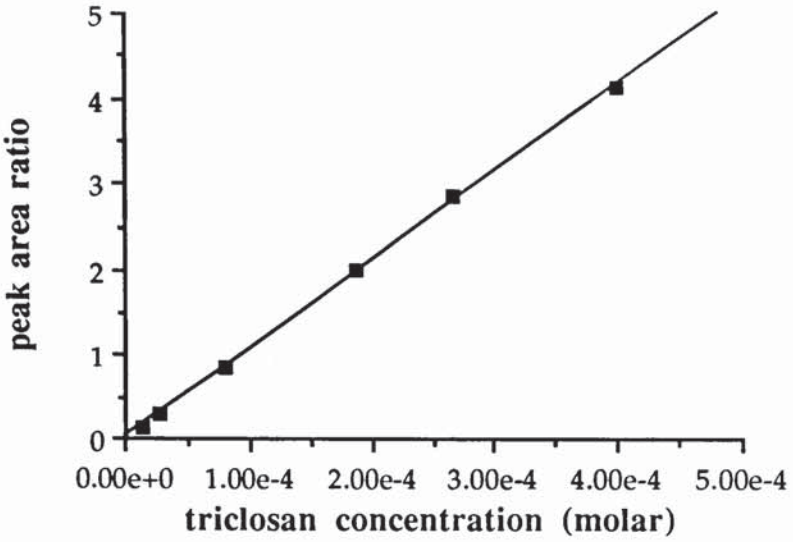

Figure 4.3 Example of a typical calibration curve for triclosan with 6 x 10^{-5} M butyl paraben as I.S. (y = [1.0356 x 10^{-4}]x + 2.3613 x 10^{-2}, r^2 = 1.000)

4.5 EXPERIMENTAL

4.5.1 Preparation of the solid phase triclosan-HP-β-CyD complex

4.5.1.1 Method 1: Use of an aqueous system for preparation of the complex

Equimolar quantities of the guest and host components were used. To 100 ml distilled water, 0.2 mmoles of HP-β-CyD was added (0.2856 g) and the solution heated to 45°C in a flask. When the CyD had dissolved, 0.2 mmoles (0.0579 g) of triclosan was added. The mixture was left stirring until a clear solution was visible. If a solution had been formed it would have been quickly cooled to room temperature by immersion in an ice water-bath, transferred to a freeze-drying flask (500 ml) and quickly frozen by immersion in a acetone/dry ice bath and then lyophilised to a white solid.

4.5.1.2 Method 2: Use of organic solvents for preparation of the complex

Equimolar quantities (0.2 mmoles) of triclosan (0.057 g) and HP-β-CyD (0.2856 g) were added to 20 ml volumes of 50:50 solvent:water (v/v) mix. The solvents used were ethanol, methanol, acetone and isopropanol. These samples were left shaking overnight at 45°C after which the solvent was removed from each solution by rotary evaporation performed at 45°C.

4.5.1.3 Method 3: Use of ammonia for preparation of the complex

Equimolar quantities of the host and guest were used. The molecular weight of HP-β-CyD was corrected for its water content as determined in section 2.6. To 50 ml of distilled water in a flask, 0.4343 g (1.5 mmol) of triclosan and 2.1419 g (1.5 mmol) of HP-β-CyD were added, together with 1.5 ml of aqueous ammonia solution (28 % w/v). The final concentration of ammonia in the solution was therefore approximately 0.82 % w/v. Dissolution of solid material was complete after 5 minutes with the aid of sonication. The resulting solution was frozen using an acetone/dry ice bath and was then freeze-dried.

4.5.2 Preparation of the equimolar physical mix of triclosan and HP-β-CyD

The physical mix was prepared by careful mixing of 0.4343g (1.5 mmol) of triclosan and 2.1419g (1.5 mmol) of HP-β-CyD in a similar manner to that described in section 2.5.2.

4.5.3 Investigation of the solid phase triclosan-HP-β-CyD complex

The solid phase triclosan-HP-β-CyD complex and the corresponding equimolar physical mixture were subjected to DSC, TGA, and IR spectroscopy. The experimental procedures followed were similar to those described for the investigation of the CHX-CyD complexes in section 2.5.3.

4.5.4 Chemical analysis of the triclosan-HP-β-CyD complex

Approximately 4 mg of each batch of complex was accurately weighed and dissolved in 10 ml distilled water in a volumetric flask. The triclosan content of the resulting solution was determined by adding 1 ml to 1 ml butyl paraben I.S. stock solution (1.2×10^{-4} M). Quantification of triclosan in the diluted sample was achieved by injection of 100 µl under the HPLC conditions described in section 4.4.2. This procedure was repeated in triplicate for each batch of complex.

4.5.5 Determination of ammonia content

Analysis was performed according to the procedure outlined in the manufacturers handbook (Sigma Chemicals). A series of plastic cuvettes were set up for the blank, control and test samples to which 1 ml of Ammonia Assay Solution (included in diagnostic kit) was initially added. Further additions included, 100 µl of distilled water to the blank cuvette, 100 µl of Ammonia Control Solution to the control cuvette and 100 µl of the test solution was added to the test cuvettes. Test solutions were prepared in triplicate by dissolving 10 mg (accurately weighed) of the triclosan-HP-β-CyD complex

in 1 ml distilled water. A saturated solution of triclosan alone and a solution of 0.069 M HP-β-CyD were also used as test solutions.

All cuvettes were covered with Parafilm and mixed by gentle inversion. The cuvettes were equilibrated at 37°C for 3 minutes after which the initial absorbance of the sample in each cuvette was recorded at 340 nm using distilled water as the reference solution. To each cuvette, 10 µl of L-Glutamate Dehydrogenase solution was added and the samples mixed by gentle inversion. After allowing approximately 5 minutes for the reaction to occur, the final absorbance of each solution was recorded again at the same wavelength.

Using the absorbance readings, the concentration of ammonia was calculated using the method outlined in the manufacturers handbook.

4.5.6 Phase solubility studies of triclosan in the presence of HP-β-CyD

The experimental procedure was similar to that described in section 2.5.5 for the CHX-HP-β-CyD system. Excess amounts of triclosan were added to 2 ml of HP-β-CyD solutions (0.003-0.069 M) in screw-capped bottles. Each concentration of CyD was prepared in triplicate by appropriate dilution of a stock solution of 0.069 M HP-β-CyD. Triplicate controls were also set up containing excess triclosan in 2 ml distilled water. All suspensions were shaken in a water bath at constant temperatures (8, 25, 37 and 45°C). After equilibrium was reached (5 days), a 1.5 ml aliquot from each suspension was centrifuged at 13000 *rpm* for 5 minutes. The supernatants were diluted prior to quantification of triclosan by the HPLC assay method described in section 4.4.2. For the control samples, 1 ml of the supernatant was diluted 2-fold with I.S. stock solution (butyl paraben, 1.2×10^{-4} M prepared in methanol). The CyD-containing supernatants were diluted 10 to 60-fold. For example, a 10-fold dilution was performed with the most dilute triclosan-CyD system (0.003 M HP-β-CyD) by adding 200 µl of its supernatant to 0.8 ml distilled water and 1 ml of I.S. stock solution in a HPLC vial. For a 60-fold dilution, performed with the strongest triclosan-CyD system (0.069 M HP-β-CyD) equilibrated at 45°C, 200 µl of the supernatant was initially added to 400 µl of distilled water contained in an Epindorf tube which was then vortexed in a whirl mix. This solution was further diluted by adding 100 µl to 0.9 ml distilled water together with 1 ml I.S. stock solution. In this way, the internal standard solution was always diluted 2-fold prior to HPLC assay thus minimising any variation in its peak response. An injection volume of 100 µl was used with all samples.

At each temperature, a constant amount of triclosan was added to each 2 ml CyD solution ranging from 8 mg at 8°C to 20 mg at 45°C. The presence of HP-β-CyD did not interfere with the HPLC assay of triclosan. Solubility diagrams were constructed for each temperature by plotting the concentration of triclosan solubilised as a function of HP-β-CyD concentration. Stability constants were calculated from the linear portion of the solubility diagrams assuming a 1:1 stoichiometry and using equation A3.13 in Appendix 3 as previously discussed.

4.5.7 Dissolution studies on the triclosan-HP-β-CyD complex

Distilled water (5 ml) was placed in triplicate dissolution vessels each maintained at 37°C by a Churchill thermostatic water pump which circulated water through a jacket surrounding the vessel body. Uniform mixing of the solvent was achieved by a small teflon coated magnetic stirring bar driven by an external motor. When the dissolution medium had reached the desired temperature, the equivalent amount of 32 mg of triclosan, as the HP-β-CyD complex (225 mg; *Batch II*) was accurately weighed and placed in each dissolution vessel. At appropriate time intervals, 200 µl samples were removed from each vessel with a Gilson automatic pipette and placed into Epindorf tubes. The samples were centrifuged for 5 minutes at 13000 *rpm* using a microcentrifuge. The supernatants were diluted 40-fold by adding 100 µl of the supernatant to 1.9 ml of distilled water and 2 ml of butyl paraben I.S. stock solution (1.2×10^{-4} M; prepared in methanol) in a HPLC vial. Quantification of triclosan was achieved by injection of a 100 µl volume under the HPLC conditions described in section 4.4.2. After sample removal, no additional solvent was added to the dissolution medium.

The above dissolution procedure was repeated with excess triclosan (32 mg added to 20 ml distilled water) and the equimolar physical mix of triclosan and HP-β-CyD (225 mg of mix was added to 5 ml). For each test powder, triplicate experiments were performed. Sampling during the dissolution experiment of triclosan alone was performed by removal of 1.5 ml samples, their centrifugation, followed by dilution of 1 ml of the supernatant with 1 ml I.S. stock solution. A 40-fold dilution was performed with the samples from the dissolution of the equimolar mix as described above.

4.5.8 Diffusion studies on the triclosan-HP-β-CyD complex

4.5.8.1 General procedure

Franz diffusion cells were employed for diffusion studies. The cells were assembled as previously described and illustrated in section 2.5.10, however, minor modifications were made to the experimental procedure. Firstly, on this occasion, experiments were performed using only Spectra/Por dialysis membrane (500 molecular weight cut-off level)

as the barrier between donor and receiver compartments. Secondly, a 40% v/v methanolic solution was used as the receiver solvent used. A stock solution of methanol and water in the ratio 40:60 (v/v) was prepared and left to equilibrate overnight at 37°C, following which it was sonicated to eliminate any air bubbles. All experiments were performed in triplicate.

Quantification of drug diffusion into the receiver phase was achieved by HPLC. At set time points (usually every 30 minutes up to 7 hours) 1 ml samples were removed from the receiver compartment and this was replaced by an equal volume of 40 % methanolic solution (v/v). Since this procedure produced a dilution of the receiver phase, the sample concentrations were adjusted by applying a similar correction factor to that described in section 2.5.10 (equation 2.1). This correction factor was applied to experimental data using a BASIC computer program written by W. J. Irwin, which also converted the molar concentrations to μmoles cm^{-2} membrane.

4.5.8.2 Diffusion of triclosan through Spectra/Por membrane (500 Da. molecular cut-off limit) from a donor suspension of drug alone

The general experimental procedure followed was as described in section 4.5.8.1. A pre-saturated suspension of triclosan was prepared by adding excess drug to 20 ml distilled water and shaking overnight at 37°C. To each donor chamber, 5 ml of the pre-saturated suspension was added. Receiver samples were diluted 2-fold by adding 1 ml to 1 ml BuP I.S. stock solution (6×10^{-5} M, prepared in 40:60 methanol-water v/v), following which 200 μl of the resulting solution was quantified by the HPLC method described in section 4.4.2. At time zero and the end of the experimental procedure (7 hours), the concentration of triclosan in the donor chamber was also determined by centrifuging 1.5 ml of the donor suspension at 13 000 *rpm* for 5 minutes. The recovered supernatant was diluted 2-fold with I.S. following which 200 μl of the diluted sample was injected under the HPLC conditions described in section 4.4.2.

4.5.8.3 Diffusion of HP-β-CyD through Spectra/Por membrane (500 Da. molecular cut-off limit)

To assess the diffusion behaviour of HP-β-CyD through Spectra/Por membrane, the general experimental procedure described in section 4.5.8.1 was followed using a 0.069 M HP-β-CyD solution as the donor phase. However, on this occasion no sampling of the receiver phase was done until after 7 hours when the receiver solution from each diffusion cell was carefully poured into a round bottom flask. The receiver solutions were then frozen by immersion into a dry ice-acetone bath and then lyophilised.

4.5.8.4 *Diffusion of triclosan through Spectra/Por membrane (500 Da. molecular cut-off limit) from a donor solution of its HP-β-CyD complex*

The experimental procedure described in section 4.5.8.1 was followed. On this occasion donor samples consisted of a solution of the triclosan-HP-β-CyD complex (*Batch II*). The equivalent amount of 1.8 mg of triclosan, as the HP-β-CyD complex (12 mg) was dissolved in 10 ml distilled water. To each donor chamber, 3 ml of this complex solution was added. The concentration of the receiver phase was monitored as previously described by adding 1 ml of BuP I.S. stock solution (6×10^{-5} M) to 1 ml of the receiver sample. Quantification of triclosan in the diluted samples was achieved by HPLC assay using an injection volume of 200 µl as discussed in section 4.4.2.

The triclosan concentration of the solution in each donor cell was determined after the initial 5 minutes and then at the end of the experimental procedure (7 hours). A 10-fold dilution was performed by adding 200 µl of the donor solution to 0.8 ml distilled water and 1 ml I.S. stock solution. Using an injection volume of 200 µl, the concentration of triclosan was determined by HPLC as described in section 4.4.2.

4.5.8.5 *Diffusion of triclosan through Spectra/Por membrane (500 Da. molecular cut-off limit) from a donor suspension of the triclosan-HP-β-CyD complex*

The general procedure previously described in section 4.5.8.1 was followed. On this occasion, the diffusion of triclosan from a donor suspension of its HP-β-CyD complex (*Batch II*) was assessed. To 1 ml distilled water contained in each donor compartment, an equivalent amount of 6.5 mg of triclosan, as the HP-β-CyD complex (45 mg), was added. The concentration of the receiver phase was monitored as previously described by adding 1 ml of BuP I.S. stock solution (6×10^{-5} M) to 1 ml of the receiver sample. After the initial 5 minutes and at the end of the experimental procedure (7 hours), the concentration of triclosan in the donor chamber was also determined by centrifuging 200 µl of the donor suspension at 13000 *rpm* for 5 minutes. The recovered supernatant was diluted 20-fold by adding 100 µl of the supernatant to 0.9 ml distilled water and 1 ml I.S stock solution. HPLC assay was performed using an injection volume of 200 µl as described in section 4.4.2

4.5.8.6 *Effect of SDS on Spectra/Por membrane permeability*

The general procedure described in section 4.5.8.1 was followed, however, on this occasion distilled water was used as the receiver solvent and a solution of 7.5 mM SDS was used as the donor phase. After 7 hours exposure of the membrane to SDS, the diffusion apparatus was carefully dismantled leaving the membrane mounted on the donor compartments. The donor chambers and the surface of the membrane exposed to SDS

were rinsed with distilled water to remove any remaining SDS. The receiver cell was also rinsed with distilled water and refilled with the 40 % methanolic solvent. The diffusion apparatus was reassembled and 5 ml of a pre-saturated aqueous triclosan suspension was placed in each donor chamber. The experimental procedure as described in section 4.5.8.2 was then followed.

4.6 RESULTS AND DISCUSSION

4.6.1 Preparation of the solid phase triclosan-HP-β-CyD complex

Various procedures were followed for the preparation of the triclosan-HP-β-CyD complex. Initially, equimolar quantities of triclosan and HP-β-CyD were mixed in distilled water in a manner similar to the preparation of the CHX-CyD complexes (section 2.5.1). However, due to the low melting point of triclosan (55-57°C), this method was limited to a relatively low temperature (45°C) to aid solubilisation. Consequently, the combination of a purely aqueous solvent together with a low temperature failed to solubilise triclosan sufficiently to favour complex formation, and therefore this method of complex preparation was not pursued any further.

The second method involved the use of organic solvents to aid triclosan dissolution. Triclosan was initially soluble in the solvent-water mixtures, however, during the evaporation procedure, volatile solvent was lost. Thus the solution became more aqueous and as a consequence triclosan was precipitated. This method therefore also proved to be inappropriate.

From the above two methods, it was evident that an additional agent was required to aid dissolution of triclosan in an aqueous medium, however, this additive has to be easily removable without precipitation of triclosan. Since triclosan is a weak acid having a pK_a of 7.9, it was expected to be readily soluble in an alkaline environment. The pH of the aqueous medium was increased by the addition of ammonia solution following which triclosan was solubilised. After lyophilization of the triclosan-HP-β-CyD solution, the complex was recovered as an amorphous white powder. Aqueous ammonia has been used to aid the solubilisation of various other acidic drugs during CyD complex preparation such as non-steroidal antiinflammatory drugs (Kurozumi, Nambu, and Nagai, 1975), pancratistatin (Torres-Labandeira, Davignon and Pitha, 1991) and amphotericin B (Pitha *et. al.*, 1992). The resulting drug-CyD solutions were freeze-dried during which the ammonia was removed due to its volatility.

The use of aqueous ammonia to aid solubilisation of triclosan for preparation of the solid phase HP-β-CyD complex appeared to be successful. However, the existence of a true inclusion complex needs to confirmed by various investigative procedures, the results of which are discussed in the proceeding section. An additional procedure evaluated the residual ammonia content of the complex as discussed later.

4.6.2 Investigation of the solid phase triclosan-HP-β-CyD complex

Various methods were used for the characterisation of the solid phase triclosan-HP-β-CyD complex which included DSC, IR spectroscopy and TGA. In each of these procedures, the behaviour of the equimolar physical mixture of triclosan and HP-β-CyD was compared to the behaviour of the CyD complex.

DSC analysis of triclosan alone showed a melting endotherm at 58°C (figure 4.4A) which was also present in the thermogram of the equimolar triclosan-HP-β-CyD physical mix (figure 4.4C). However, the triclosan peak had completely disappeared in the thermogram for the HP-β-CyD complex (figure 4.4D). Example thermograms of the triclosan-HP-β-CyD system are illustrated in figure 4.4. These results are consistent with the formation of a real inclusion complex between triclosan and HP-β-CyD. As previously discussed, the changes in thermal behaviour between the physical mix and the complex may be due to the lack of intermolecular association of triclosan which is a consequence of monomolecular dispersion of the guest within the CyD cavity, thus no melting endotherm was seen.

IR spectroscopy was further used for the investigation of the triclosan-HP-β-CyD system. The spectrum of triclosan (figure 4.5A) shows strong absorption bands in range 1000-1400 cm^{-1} due to the presence of the ether linkage and phenolic group. The spectrum of the equimolar physical mix (figure 4.5C) showed a combination of absorption bands due to the presence of both the triclosan and HP-β-CyD. However, due to the relatively low weight of triclosan present, the majority of the bands seen in the spectrum were those of the CyD alone. The IR spectrum of the triclosan-HP-β-CyD complex (figure 4.5D) was virtually identical to the spectrum of the respective physical mixture. Figure 4.5 illustrates examples of spectra obtained for the triclosan-HP-β-CyD system. As discussed previously, since the CyD constitutes a high proportion of the total complex, inclusion of the guest will not induce any major changes. From these results it was concluded that, in this instance, IR spectroscopy could not be used to confirm the existence of a true inclusion complex.

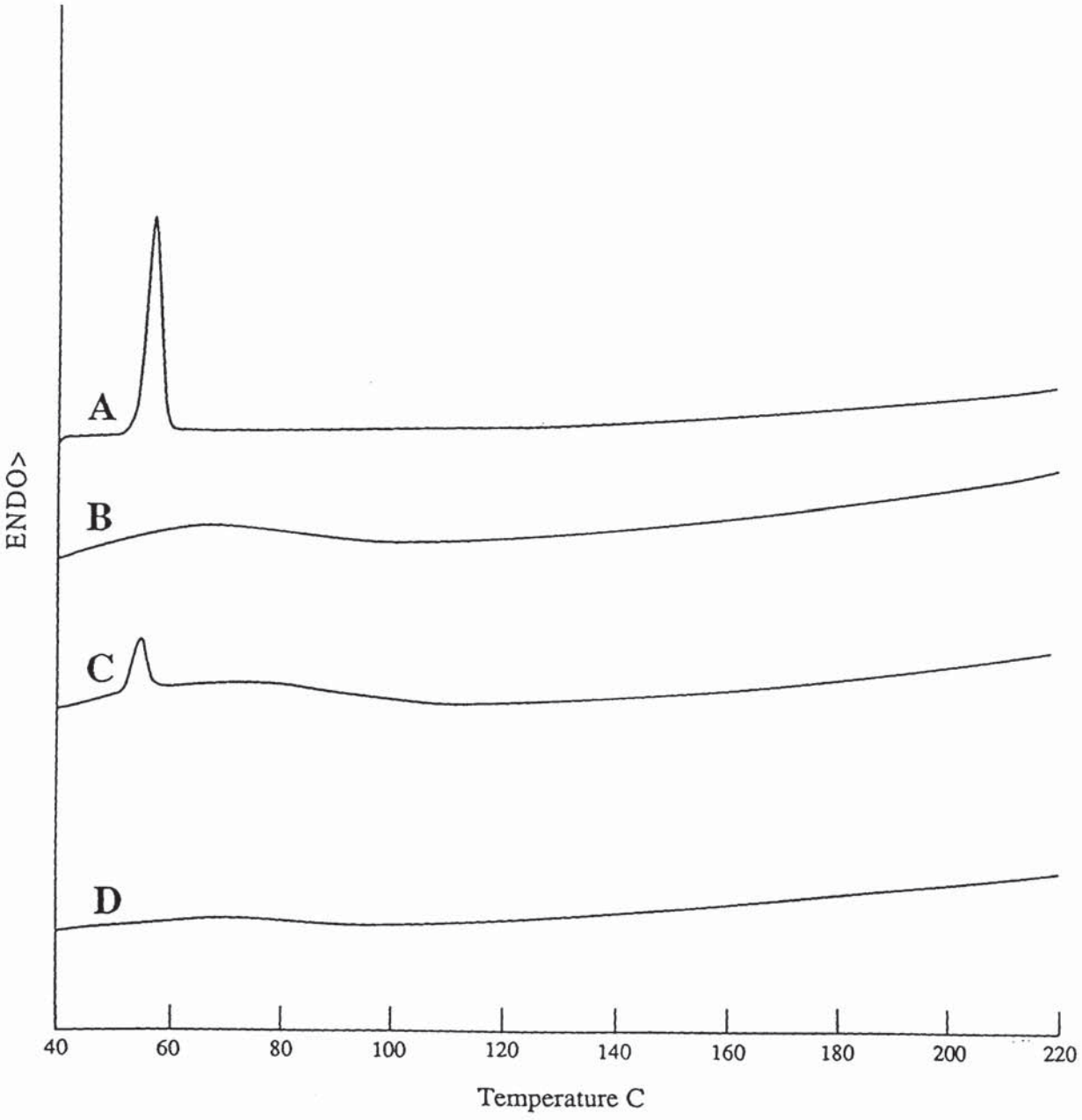

Figure 4.4 DSC thermograms of: A) triclosan, b) HP-β-CyD, C) the physical mixture of triclosan and HP-β-CyD (molar ratio 1:1), and D) the triclosan-HP-β-CyD complex

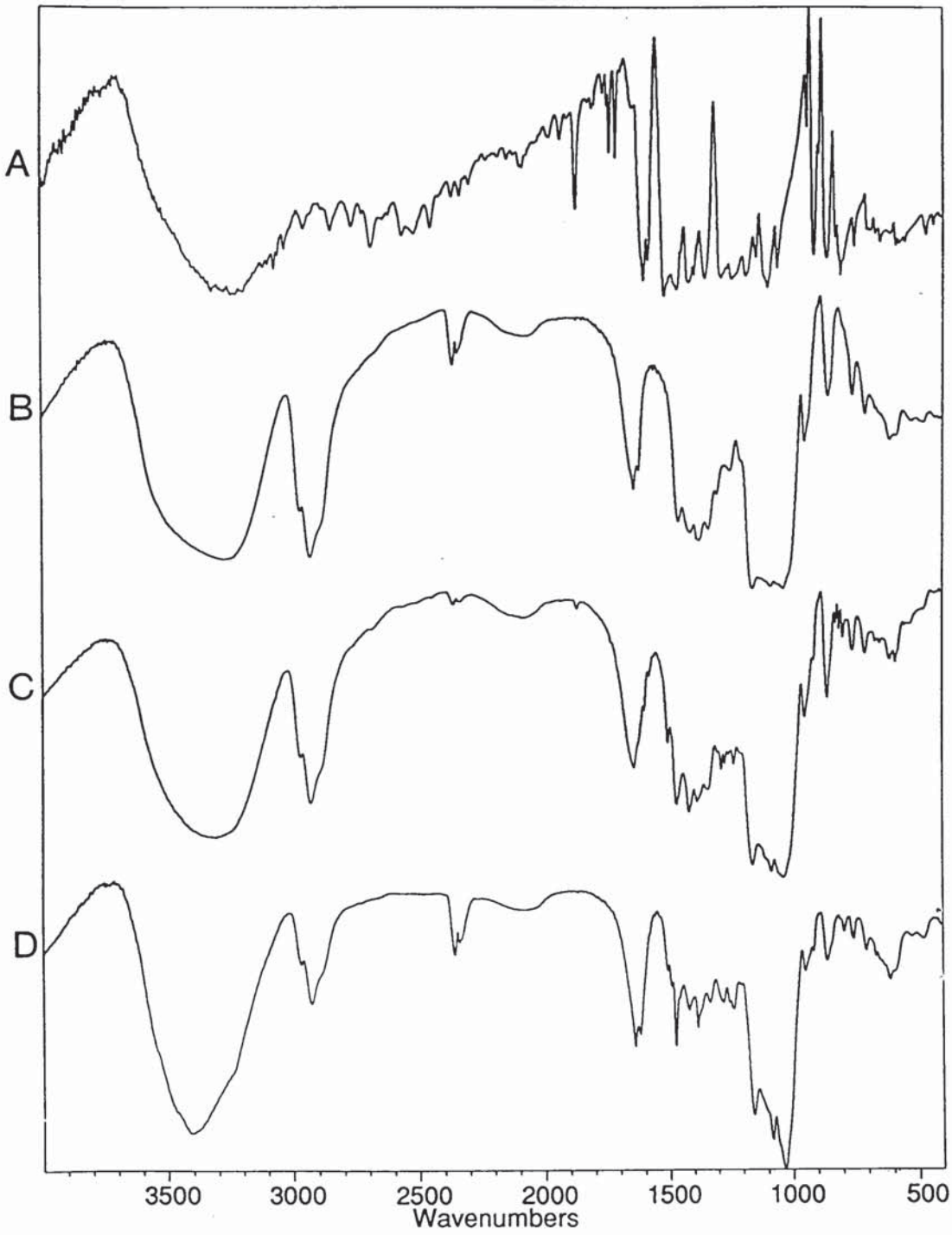

Figure 4.5 Examples of IR spectra of: A) triclosan, B) HP-β-CyD, C) physical mix of triclosan and HP-β-CyD (molar ratio 1:1) and D) the triclosan-HP-β-CyD complex

The water content of the solid phase triclosan-HP-β-CyD complex was determined by TGA on percentage weight per weight basis. Two batches of the triclosan-HP-β-CyD complex were prepared on separate occasions. The differences between the water of both batches of complex, as illustrated in table 4.2, are probably due to differences in freeze-dryer efficiency.

Table 4.2 Percentage water content of the triclosan-HP-β-CyD complex as determined by TGA. Values represent the mean ± s.d., $n = 3$.

Sample	% w/w water content ± s.d.
Batch I	1.558 ± 0.298
Batch II	3.210 ± 0.159

The water content of the triclosan-HP-β-CyD complex as found by TGA was used during chemical analysis of the complex for the determination of the stoichiometric ratio of guest to host as discussed in the following section.

To summarise, of the investigative procedures performed on the triclosan-HP-β-CyD system, only DSC confirmed the formation of a real inclusion complex.

4.6.3 Chemical analysis of the solid phase triclosan-HP-β-CyD complex

The theoretical and experimental drug contents of the triclosan complex were found using the method of calculation illustrated for the chemical content determination of the CHX-CyD complexes in section 2.6.4. The theoretical weight of the 1:1 triclosan-HP-β-CyD complex can be considered to be:

1378.6 (HP-β-CyD M.W.) + 289.5 (triclosan M.W.) = 1668.1

Taking into account the water content of both batches of complex as determined by TGA (section 4.6.2), the corrected molecular weights of the 2 batches of complex were calculated from which the theoretical triclosan content of the complex was found in a manner similar to that shown in section 2.6.4. The experimental values for the triclosan content of the triclosan-HP-β-CyD complex were also calculated in a similar manner to that shown for the CHX-CyD complexes.

Both batches of triclosan-HP-β-CyD complex had similar experimental drug content values; (14.13±1.00) and (14.49± 0.51) % weight of triclosan per complex weight for *Batches I* and *II* respectively. However, these values were approximately 2 to 3 % lower than expected. The theoretical and also the experimentally determined values for triclosan content of the HP-β-CyD complex are contained in table 4.3. Ideally, a 1:1 stoichiometric ratio should have been obtained since equimolar quantities of both complex components were used. The percentage deviation of the drug content values are similar to the water content of the complexes as determined by TGA. From DSC, the melting point of triclosan was found to be approximately 58°C. Furthermore, during TGA, weight loss started to occur at temperature of ~ 50°C and continued until ~ 110°C. It therefore seems probable that some triclosan sublimed out of the triclosan-HP-β-CyD system during the heating process of TGA. On the basis of these assumptions, the actual water content of the complex must be minimal. As previously discussed, Karl Fischer titrimetry is another method which may be used for the determination of water content. However, a larger sample size (0.5 g) was needed to perform the assay thus this method was not pursued.

Table 4.3 Theoretical and experimental determinations of the triclosan content of its HP-β-CyD complexes. Values represent the mean ± s.d., $n = 3$.

	% w/w triclosan		stoichiometry (CyD:triclosan)
	Theoretical value	Experimental value	
Batch I	17.09 ± 0.04	14.13 ± 1.00	1:0.83 ± 0.05
Batch II	16.82 ± 0.02	14.49 ± 0.51	1:0.86 ± 0.03

4.6.4 Determination of ammonia content

Ammonia was used to aid the solubilisation of triclosan by increasing the pH of the solvent during preparation of the complex. Hirsch and co-workers (1987) have shown that ammonia itself forms an inclusion complex with β-CyD which has a K_S value of 1.5×10^4 M^{-1} (23°C), thus it was important to determine the amount of ammonia retained in the complex.

The quantitative determination of the residual ammonia in the triclosan-HP-β-CyD complex was performed using an enzymatic diagnostic test purchased from Sigma Chemicals.

For all samples, the difference between the initial and final absorbance reading was found (ΔA). The concentration of ammonia in the test and control samples were calculated using the following formulae:

$$\text{CONTROL Ammonia } (\mu g/ml) = (\Delta A_{CONTROL} - \Delta A_{BLANK}) \times 30.3 \quad (4.1)$$

$$\text{TEST Ammonia } (\mu g/ml) = (\Delta A_{TEST} - \Delta A_{BLANK}) \times 30.3 \quad (4.2)$$

where: $$\text{Factor } 30.3 = \frac{1.11 \times 17}{6.22 \times 0.1}$$

1.11	=	volume of liquid in cuvet
17	=	Weight (μg) of 1 μmol of ammonia
6.22	=	Millimolar absorbtivity of NADPH at 340 nm
0.1	=	Volume (ml) of specimen

A quality control test was performed on the detection procedure using the Ammonia Control Solution. Using equation 4.1 above, the concentration of ammonia in the control sample was found to be 4.67 μg/ml. This value was within ±10% of the concentration stated on the vial (5 μg/ml), *i.e.* acceptable range was 4.5-5.5 μg/ml, thus the test procedure was considered to be satisfactory.

No difference was seen between ΔA of the blank and ΔA of both triclosan and HP-β-CyD test samples indicating that they did not interfere with the ammonia assay.

Using equation 4.2, the ammonia content of the test solutions of the complex was calculated. These values were then divided by the weight of complex used, to obtain the percentage ammonia content per unit weight of complex. The ammonia content of the complex was found to be 0.0067 % (± 0.0007); the mean of 3 determinations ± s.d. Despite the fact that CyD complexes of ammonia have high stability, the small amount of residual ammonia detected in the complex suggests that, due to its volatility, most of ammonia was removed during the freeze-drying process.

4.6.5 Phase solubility studies of triclosan in the presence of HP-β-CyD

At all temperatures, a linear increase in triclosan solubility was observed up to the maximum concentration of HP-β-CyD used. The solubility isotherms can be classified as the A_L type indicating the formation of a soluble complex in solution with a probable stoichiometry of 1:1 (triclosan:HP-β-CyD). Figure 4.6 illustrates the solubility diagram obtained for the triclosan-HP-β-CyD system.

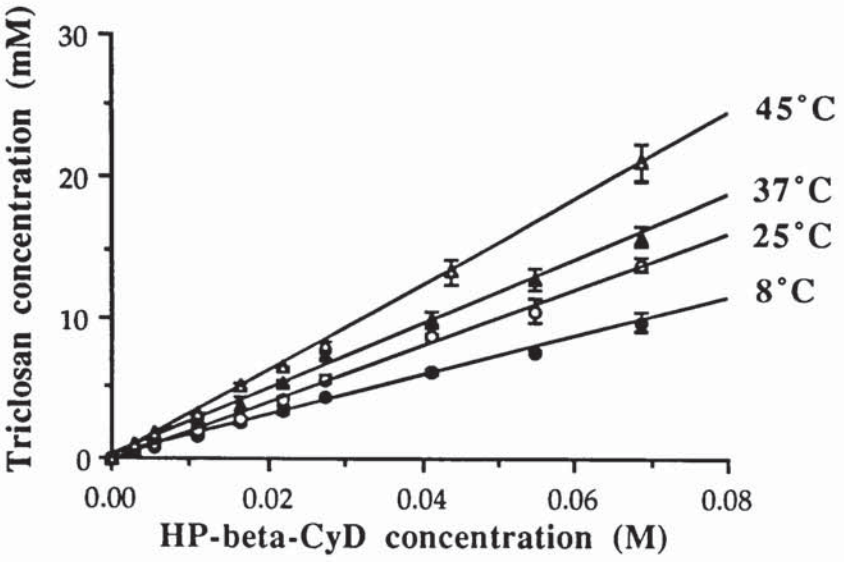

Figure 4.6 Phase solubility diagram of the triclosan-HP-β-CyD system in distilled water at various temperatures. Points represent the mean ± s.d., $n = 3$.

Linear regression was used to find the slope and intercept of each diagram, from which the K_S values were found using equation A3.13 in Appendix 3. Table 4.4 contains the slope of each line, S_0, the K_S values found at each temperature, and the solubility enhancement of each triclosan achieved with 0.069 M HP-β-CyD. Also shown are the experimental values of the solubility of triclosan in the absence of CyD ($S_{0\text{-}Exp}$).

Table 4.4 Summary of solubility data for the triclosan-HP-β-CyD phase solubility system. ($S_{0\text{-}Exp}$ are the experimental values for the equilibrium solubility of triclosan in the absence of CyD and are the mean ± s.d., $n = 3$).

Temp. (°C)	Slope	S_0 (M x 10^5)	$S_{0\text{-}Exp}$ (M x 10^5)	K_S (M^{-1})	r^2	solubility increase with 0.069 M HP-β-CyD
8	0.14230	0.9102	0.85 ± 0.04	18232	0.997	1134-fold
25	0.19344	2.0437	2.74 ± 0.13	11735	0.996	500-fold
37	0.24382	3.8860	4.10 ± 0.50	8297	0.996	385-fold
45	0.28941	5.9167	5.63 ± 0.51	6368	0.999	372-fold

The solubility of triclosan alone increased approximately 7-fold from $(0.85 \pm 0.04) \times 10^{-5}$ M at 8°C to $(5.63 \pm 0.51) \times 10^{-5}$ M at 45°C. The experimental S_0 values correlated well with the values obtained from linear regression. With an increase in temperature, the extent of triclosan solubilisation by CyD decreased; at 8°C, an approximate 1135-fold increase in triclosan solubility was observed with the maximum concentration of HP-β-CyD (0.069 M) used and at 45°C, the solubility of triclosan was increased approximately 350-fold. As expected, a similar trend was observed with the K_S values which decreased from 18232 M^{-1} at 8°C to 6368 M^{-1} at 45°C due to dissociation of the complex. In contrast, with a rise in temperature, the slopes increased in a manner similar to that observed for BuP-HP-β-CyD system (section 3.6.5). Using equation 4.20 in Appendix 4, the concentration and percentage of free triclosan in the presence of 0.069 M HP-β-CyD was found at each temperature. With a rise in temperature, the percentage of triclosan existing in the non-complexed form was expected to increase due to complex dissociation. However, as shown in table 4.5, over the temperature range studied, there was very little variation in the percentage of free triclosan in the presence of 0.069 M HP-β-CyD. Similar temperature effects were observed for the BuP-HP-β-CyD system, and as previously discussed, this type of behaviour was thought to be due to the increased aqueous solubility of guest with temperature which counterbalances dissociation of the complex. Hence, there is an increase in the concentration of complexed drug.

Table 4.5 Concentration and percentage of free triclosan in the presence of 0.069 M HP-β-CyD at various temperatures calculated using equation A4.20 and the K_S values shown in table 4.4.

Temperature (°C)	Total triclosan concentration (M x 10^3)	Concentration of free triclosan (M x 10^3)	Percentage of total triclosan as free
8	9.642 ± 0.713	0.700 ± 0.026	7.26 ± 0.88
25	13.794 ± 0.466	1.042 ± 0.018	7.56 ± 0.40
37	15.766 ± 0.750	1.320 ± 0.032	8.37 ± 0.63
45	20.947 ± 1.804	1.737 ± 0.055	8.29 ± 0.83

With consideration of the phase solubility data of all the guest species (CHX, parabens and triclosan) used for this study, it can be seen that triclosan has the greatest affinity for the CyD cavity as indicated by the K_S value. Table 4.6 summarises the K_S values for the guest-CyD complexes determined at 37°C. As previously discussed, the extent of interaction between guest and CyD will depend on the geometric characteristics of the

guest and also its polarity. From the magnitude of the K_S values, these properties of triclosan appear to be more favourable than those of CHX and the parabens derivatives.

Table 4.6 Summary of K_S values for the guest-HP-β-CyD complexes from this study determined at 37°C

Guest	K_S (M^{-1})
CHX	41
Methyl paraben	980
Ethyl paraben	1308
Propyl paraben	1715
Butyl paraben	2179
Triclosan	8297

From consideration of the structure of triclosan, as illustrated in figure 4.1, it can be seen that two aromatic moieties are present. Thus, it is possible that complex formation occurs by inclusion of one or both of these groups in the CyD cavity. However, since the aromatic moieties are linked together by an ether linkage only, the distance between them is probably relatively short indicating that is unlikely that both aromatic moieties are encapsulated at the same time. On the basis of these considerations and the fact that slope of the solubility diagrams were less that unity, it is probable that the triclosan-HP-β-CyD complex formed in solution has a stoichiometry of 1:1.

The effect of temperature on the equilibrium constant was illustrated by the van't Hoff plot which was obtained by plotting ln K_S against absolute temperature as described in section 2.6.4. As illustrated in figure 4.7, the plot was almost linear over the temperature range employed ($r^2 = 0.994$). From the slope and intercept on the y-axis, the enthalpy and entropy changes found respectively are contained in table 4.7, together with the free energy change at 37°C found using equation 2.4 (in section 2.6.4).

All thermodynamic parameters showed favourable changes indicating the feasibility of the complexation reaction. The negative enthalpy change (-21.3 kJ mol^{-1}) further confirmed the exothermic nature of the complexation process as also seen with the CHX-β-CyD and BuP-HP-β-CyD systems. As previously discussed, this favourable enthalpy change indicates increased guest-host interactions and solvent-solvent interactions possibly by the formation of hydrogen bonds. The positive entropy change (6.04 J K mol^{-1}) indicates a favourable decrease in the structural order of the system following complexation. The BuP-HP-β-CyD system behaved in a similar manner. As previously discussed, the

hydroxypropyl moieties of the CyD may be hydrated. The inclusion process of a guest within the CyD cavity may lead to the removal of these water molecules from the ordered structure which consequently results in a favourable entropy change.

The thermodynamic parameters for the triclosan-HP-β-CyD system indicate that the complexation reaction was driven by favourable enthalpic and entropic processes. Various bonding mechanisms are thought to participate in complex formation as discussed previously. The magnitude of thermodynamic parameters found in the present study suggest that van der Waals-London dispersion forces and hydrophobic bonding mechanisms were primarily involved in formation of the triclosan-HP-β-CyD complex.

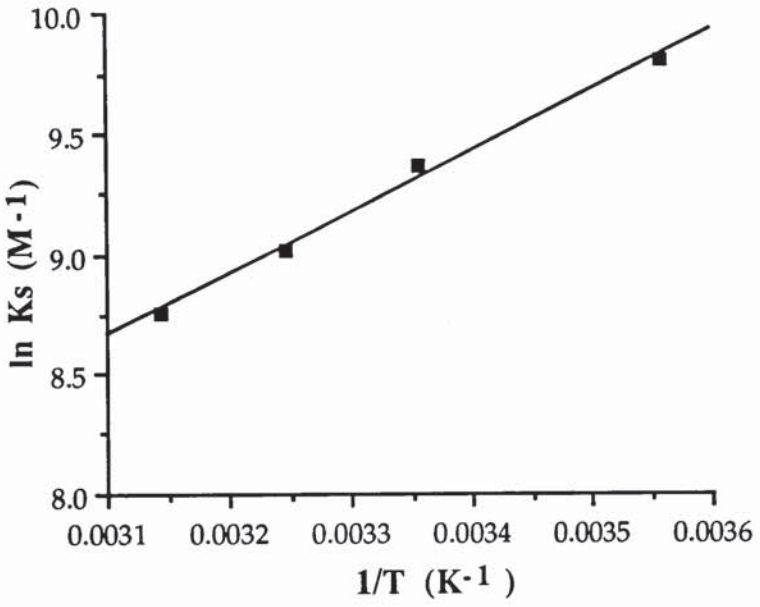

Figure 4.7 Temperature dependence of the equilibrium constant of triclosan-HP-β-CyD complex illustrated by the van't Hoff plot
($y = 0.72682 + 2559.3x$, $r^2 = 0.994$)

Table 4.7 Thermodynamic parameters of the triclosan-HP-β-CyD complexation process

ΔH	-21.3 kJ mol^{-1}
ΔS	6.04 J K^{-1} mol^{-1}
ΔG	-23.26 kJ mol^{-1}(37°C)

To summarise, phase solubility studies have demonstrated the interaction of triclosan with HP-β-CyD in solution with the formation of the soluble complex. Complex stability constants ranged from 18232 M^{-1} to 6368 M^{-1} indicating the relative high affinity of triclosan for the CyD cavity. Further studies were performed to assess the solubility and diffusion behaviour of the solid phase triclosan-HP-β-CyD complex.

4.6.6 Dissolution studies on the triclosan-HP-β-CyD system

Dissolution studies were performed using the dispersed powder technique to assess the saturation solubility of the triclosan-HP-β-CyD complex.

The equilibrium solubility of triclosan at 37°C was found to be 0.0391 ± 0.002 mM which correlated well with the solubility concentration found during phase solubility studies performed at this temperature. The equilibrium solubility of the equimolar physical mixture of triclosan and HP-β-CyD was 6.164 ± 0.171 mM; this is approximately 158 times greater the solubility of triclosan alone. The triclosan-HP-β-CyD complex dissolved much more rapidly than triclosan alone and the equimolar mix of the complex components. The solubility of the complex reached a peak after 5 minutes dissolution at a concentration of 9.536 ± 0.482 mM; this was approximately 240 times greater than the solubility of drug alone. Following the attainment of this supersaturated level, the solubility of the complex gradually declined reaching an equilibrium concentration of 6.121 ± 0.063 mM after 5 hours. This concentration was similar to the value approached by the physical mixture after this time period. Figure 4.8 illustrates the dissolution behaviour of triclosan, the equimolar physical mix and the triclosan-HP-β-CyD complex.

The equilibrium solubility of the complex (6.121 ± 0.063 mM) was approximately 158-times the solubility of triclosan alone. The dissolution experiment was performed by adding 225 mg of the triclosan-HP-β-CyD complex to 5 ml of distilled water. Due to the enhanced water-solubility of HP-β-CyD, it was assumed that any free CyD would be in solution, thus the theoretical concentration of HP-β-CyD was 0.027 M; this was calculated in a manner similar to that previously described in section 2.6.5 for the dissolution of the CHX-HP-β-CyD complex (section 2.6.5.). During phase solubility studies at 37°C (section 4.6.4), an approximate 165-fold enhancement in triclosan solubility was observed with 0.028 M HP-β-CyD which therefore correlates well with the results of the dissolution study.

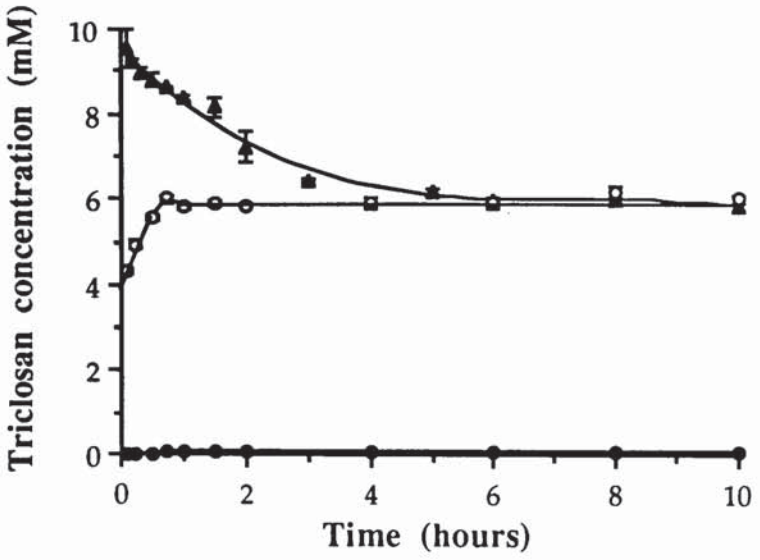

Figure 4.8 Dissolution profiles of triclosan (●), its equimolar mix with HP-β-CyD (o) and its HP-β-CyD complex (▲) in water at 37°C, measured by the dispersed powder technique. Points represent the mean ± s.d., $n = 3$.

In a similar manner to that observed for the CHX-CyD complexes (section 2.6.5), a supersaturation effect was observed for the triclosan-HP-β-CyD complex. For the triclosan system, the difference between the initial saturated solubility of the complex (9.536 ± 0.482 mM) and the equilibrium solubility of the complex (6.121 ± 0.063) was approximately 1.6-fold. In contrast, this difference was greater for the CHX-CyD systems; 2.2 fold and 4.3-fold for β-CyD and HP-β-CyD complexes respectively. Following dissolution of the guest-CyD complex, the complex dissociates into the respective components but the relative proportions of free and complexed species are dictated by the K_S. The concentration of triclosan existing as the free and complexed species at the supersaturated level and at equilibrium was estimated by using equation A4.20 (Appendix 4). Table 4.8 contains these estimations and compares these data with respective data for the CHX-CyD systems.

With both CHX and triclosan systems, following dissolution of their respective CyD complexes, both systems were supersaturated with respect to the solubility of drug alone. With the triclosan-HP-β-CyD complex, 5 minutes after dissolution, the concentration of free triclosan (1.014 mM) was approximately 26 times greater than the solubility of triclosan alone (0.0391 ± 0.002 mM). Although the solubility of the complex declined after reaching an optimum, even at equilibrium, this system was supersaturated with respect to free triclosan. Therefore, at the saturation solubility of the complex (9.536 mM), ~ 10 % of the total triclosan dissolved in the system exists as the non-

complexed form. In contrast, with the CHX-CyD systems, a much greater proportion of the total solubilised CHX (~ 65-74 %) was free. The differences between the CHX and triclosan guest systems can be explained by consideration of the K_S values for the respective complexes. The relatively low K_S values for the CHX-CyD complexes (54 M^{-1} and 40 M^{-1} for β-CyD and HP-β-CyD; section 2.6.4) reflected the poor affinity of CHX for the CyD which consequently reduces the amount of complexed CHX in solution. Furthermore, due to the weak interaction, the overall solubility enhancement of CHX in the presence of the CyDs was not great (2-fold) and therefore the equilibrium solubility of the CHX-CyD complexes was also reduced.

In contrast, triclosan has a much greater affinity for the CyD cavity as evident from its K_S value of 8297 M^{-1} (37°C). Therefore, as shown in table 4.8, following dissolution of the complex, a larger proportion of the solubilised triclosan existed as the complexed form rather than free. Consequently, the equilibrium solubility of the triclosan complex is greater than the CHX-CyD complexes. On the basis of these observations, it is evident that with high K_S values more drug is complexed and therefore a greater enhancement in drug solubility is expected. As previously discussed, the single most important factor controlling precipitation is supersaturation. It is can therefore be hypothesised that, low K_S values allow extensive release of drug which may be faster than the crystallisation process. Hence, the difference between the saturation solubility of the complex and its equilibrium solubility is greater for relatively weak CyD complexes.

Table 4.8 Estimations of the concentration of free guest following dissolution of excess CyD complexes using equation A4.20 in Appendix 4.

	CHX-β-CyD *(Batch I)*	CHX-HP-β-CyD *(Batch II)*	Triclosan-HP-β-CyD *(Batch II)*
K_S, M^{-1} (37°C)	54	40	8297
At supersaturation:			
total guest conc. (mM)	9.293	21.029	9.536
free guest conc. (mM)	6.798	13.614	1.014
percentage of free guest	73.2 %	64.7 %	10.6 %
At equilibrium:			
total guest conc. (mM)	4.246	4.853	6.121
free guest conc. (mM)	3.561	4.161	0.801
percentage of free guest	83.9 %	85.7 %	13.1 %

Dissolution studies have revealed the enhanced solubility of the triclosan complex compared to drug alone. Furthermore, the triclosan-HP-β-CyD system was supersaturated with respect to drug alone. The greater concentration of free and therefore active drug in such a system may enable the wider usage of triclosan as an effective antimicrobial agent. For a potential triclosan-CyD product to be targeted against bacteria residing in areas which are difficult to access, such as *H. pylori,* the active drug would need to diffuse across the mucus barrier to the site of bacterial infection. For the triclosan-CyD product to be advantageous, the diffusion of free drug released from the CyD complex would need to be greater than the diffusion from drug alone. The diffusional behaviour of triclosan-HP-β-CyD is discussed in the following section.

4.6.7 Diffusion studies on the triclosan-HP-β-CyD system

Diffusion experiments were performed to assess the diffusion of triclosan from donor phases containing either free or complexed triclosan. The experiments undertaken were similar to those performed with the CHX-β-CyD (section 2) and paraben derivatives-CyD systems (section 3), but, as a consequence of the greater lipophilic nature of triclosan, minor modifications in experimental procedure were necessary.

Two types of membrane were tested for use in this study, namely silicone membrane and Spectra/Por Molecularporous dialysis membrane. As previously discussed, drugs are transported through silicone membrane by initially partitioning into the membrane from the solution in the donor chamber and then diffusing out into the receiver chamber. The diffusion process will depend on the partitioning of the drug between the membrane and the receiver solvent. For hydrophobic compounds however, the membrane may become saturated with respect to the solute and thus aqueous diffusion layer transport will be dominant. Due to the hydrophobic nature of triclosan, its affinity for a purely aqueous receiver phase was expected to be very low and consequently retention of triclosan in the membrane may occur. Furthermore, if distilled water was used, saturation of the receiver phase, with respect to triclosan, may occur rapidly due to its limited water-solubility which would restrict further diffusion. To aid transport of triclosan into the receiver phase, the polarity of the receiver solvent was adjusted by the addition of methanol. Preliminary experiments with various concentrations of methanol found 40 % to be an optimum concentration. At lower methanol concentrations, diffusion was too slow to be quantified appropriately. At higher methanol concentrations, evaporation of methanol during the experiment caused problems in reproducibility. Initial experiments were performed using triplicate Franz diffusion cells containing suspensions of triclosan alone in the donor chamber with silicone membrane of 0.02 inch thickness. The results of these experiments showed wide variations between the three diffusion cells with very

small fluxes of triclosan (~ 0.07 μmoles cm^{-2} h^{-1}), both of which were thought to be due to retention of triclosan in the silicone membrane despite the methanolic receiver solvent. It was evident from these preliminary investigations that the use of silicone membrane was unsuitable for the study of triclosan diffusion.

An alternative choice of membrane was the Spectra/Por dialysis membrane with 500 Da. molecular weight cut-off. As previously discussed, theoretically only compounds of a molecular weight less that 500 Da. will diffuse through this membrane. These membrane properties make it ideal for use in this study as triclosan, with a molecular weight of 289.5 Da., would be transported through the membrane whereas the respective triclosan complex and HP-β-CyD were expected be retained in the donor chamber due to their larger size. To confirm this, a control experiment was performed initially to determine whether HP-β-CyD itself diffused through this membrane. Visual examination of the freeze-dried solutions after the 7-hour experiment showed the absence of any material confirming that HP-β-CyD was too large to pass through the pores of this membrane. It was, therefore, assumed that the triclosan-HP-β-CyD complex was also unable to diffuse through this membrane. During the diffusion experiments performed with donor systems of complexed triclosan, the triclosan flux was therefore a measure of free drug transport only.

Experiments were performed using both solutions and suspensions of free and complexed triclosan as the donor phases. For each test system, triplicate diffusion experiments were performed from which the mean flux ± standard deviation was found from the steady-state portion of the diffusion profiles. The theoretical background to drug diffusion has previously been discussed in section 2. Statistical analysis was performed on the flux measurements using the unpaired-sample t-test as described previously by equation 3.5 (section 3.6.7).

4.6.7.1 Diffusion of triclosan from donor phases of free and complexed drug

Diffusion of triclosan from donor phases of both free and complexed drug showed an initial lag phase. With a donor suspension of triclosan alone, after this lag phase, a constant diffusion rate was observed over the 7 hour study period, indicating steady-state diffusion. In contrast, with both the donor solution and suspension of the triclosan complex, a constant diffusion rate was observed over the initial 3 hours after which it declined. The steady-state fluxes, permeability coefficients (K_p) and lag times (t_L) were determined from the linear portion of the rate curve by linear regression as previously described by equations 2.14 to 2.22 in chapter 2. The permeation profiles of triclosan from donor systems of free and complexed drug are illustrated in figure 4.9 with the

corresponding data summarised in table 4.9. Also shown are the initial and final donor concentrations of triclosan in the donor phase of each test system.

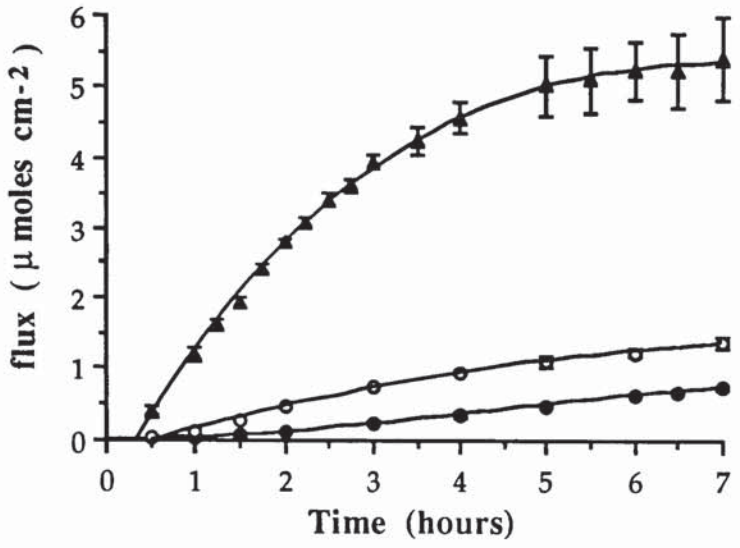

Figure 4.9 Diffusion of triclosan through Spectra/Por membrane from donor phases containing: ●, suspension of triclosan alone; o, solution of the triclosan-HP-β-CyD complex; ▲, suspension of triclosan-HP-β-CyD complex. Points represent the means ± s.d., $n = 3$.

Table 4.9 Diffusion data for triclosan transport through Spectra/Por membrane from donor phases containing free and complexed drug. Values represent the means ± s.d., $n = 3$.

donor sample	free drug suspension	solution of complex	suspension of complex
initial donor conc. ($M \times 10^3$)	0.0418 ± 0.002	0.5930 ± 0.051	8.217 ± 0.201
final donor conc. ($M \times 10^3$)	0.0412 ± 0.004	0.2453 ± 0.019	5.499 ± 0.115
flux (μmoles cm^{-2} h^{-1})	0.1223 ± 0.003	0.3018 ± 0.002	1.4087 ± 0.074
r^2	0.999	0.996	0.993
K_p (x 10) cm h^{-1}	2.9258 ± 0.212	0.5089 ± 0.052	0.1714 ± 0.014
lag time (t_L; hours)	0.990 ± 0.093	0.509 ± 0.010	0.170 ± 0.027

In comparing the initial donor concentrations of triclosan in all systems, the concentration of the solution (0.593 ± 0.051 mM) and suspension (8.271 ± 0.210 mM) of the complex was approximately 15 and 200-fold respectively, greater than the saturation solubility of triclosan alone (0.0418 ± 0.002). The enhanced donor concentration of triclosan in the CyD systems consequently resulted in a significant ($p<0.05$) increase in flux. The flux of triclosan from the solution (0.3018 ± 0.002 μmoles cm^{-2} h^{-1}) and the suspension of the complex (1.4087 ± 0.074 μmoles cm^{-2} h^{-1}) was approximately 2.5 and 11.5 times respectively greater than the flux from a suspension of triclosan alone (0.1223 ± 0.003 μmoles cm^{-2} h^{-1}; hereafter known as control flux).

The total triclosan concentration of the donor solution of the triclosan complex decreased from 0.593 ± 0.051 mM to 0.2453 ± 0.019 mM over the 7 hour study. The decrease in diffusion rate observed after the initial linear phase was therefore due to the concentration in the donor phase being continuously depleted. Consequently, the concentration differential, and hence the driving force of diffusion between the donor and receiver phases was reduced.

The donor suspension of the complex behaved in a similar manner with the triclosan concentration falling from 8.217 ± 0.210 mM to 5.499 ± 0.115 mM over the same time period. During dissolution studies (section 4.6.5) performed on the triclosan-HP-β-CyD complex, the solubility of the complex reached a peak after 5 minutes dissolution at a concentration of 9.536 ± 0.482 mM, after which the solubility declined to an equilibrium concentration of 6.121 ± 0.063 mM. These values are slightly higher than the concentrations obtained for the donor suspension of the complex which can be explained by the fact that the temperature of the donor cell was 34°C whereas dissolution studies were performed at 37°C. Due to the decrease in the total triclosan concentration of the donor suspension of the complex over the study period, the concentration differential and therefore the driving force of diffusion between the donor and receiver phase was also reduced; hence after an initial linear flux a decrease in diffusion rate was observed.

The total concentration of triclosan in the donor phase containing the triclosan-HP-β-CyD complex represents both free and complexed drug, the relative proportions of which are governed by the K_S value (8297 M^{-1}, 37°C). As previously discussed, HP-β-CyD and the complex are unable to pass through the membrane due to their molecular weight being greater than 500 Da. The flux from the donor systems of the complex is therefore a measure of free drug transport only. Hence, the increase in triclosan solubility by CyD complexation and the enhancement in flux of triclosan is not expected to be equivalent. The flux however, can be related to the concentration of free triclosan in the CyD

systems. Using equation A4.20 in Appendix 4, the concentration and percentage of triclosan existing as the non-complexed form in both the donor solution and suspension of the HP-β-CyD complex was calculated as summarised in table 4.10.

Table 4.10 Concentration and percentage of free triclosan in the donor systems of the triclosan-HP-β-CyD complex estimated using equation A4.20 and $K_S = 8297\ M^{-1}$.

	free drug	solution of complex		suspension of complex	
	suspension	initial	final	initial	final
Total conc. of triclosan (M x 10^3)	0.0418 ± 0.002	0.5930 ± 0.051	0.2453 ± 0.019	8.217 ± 0.201	5.499 ± 0.115
Conc. of free triclosan (M x 10^3)	0.0418 ± 0.002	0.2138 ± 0.011	0.1219 ± 0.006	0.9367 ± 0.012	0.7561 ± 0.005
Percentage of total triclosan as free	100	36.1	49.7	11.4	13.7

The concentration of free triclosan in the complex systems was found on the basis of the initial and final donor concentrations. The free triclosan concentrations of the donor systems of the CyD complex were significantly ($p<0.05$) greater than a saturated solution of triclosan alone (0.0418 ± 0.002 mM), *i.e.* these systems were supersaturated with respect to free triclosan. As a consequence, the flux of triclosan from these systems was greater than the diffusion of triclosan from a suspension of drug alone. The percentage of total triclosan in the system which is in the non-complexed form, is greater with the lower concentration of complex (0.539 mM); this was to be expected since in more dilute systems, the dissociation equilibrium of the complex is shifted to favour the free components of the complex (Szejtli, 1988). The increased flux from the donor systems of the complex was now expected to correlate with the enhancement in free drug concentration.

The initial concentration of free drug (0.2138 mM ± 0.011 mM) in the donor solution of the triclosan-HP-β-CyD complex was approximately 5-fold the saturation solubility of triclosan alone (0.0418 ± 0.002 mM). However, the flux of triclosan from the donor solution of the complex (0.3018 ± 0.002 μmoles $cm^{-2}\ h^{-1}$) was approximately 2.5 times greater than the control flux (0.1223 ± 0.003 μmoles $cm^{-2}\ h^{-1}$). The initial free drug concentration in the donor suspension of the complex (0.9367 ± 0.012 mM) was

approximately 22-fold greater than the saturated solubility of triclosan alone, however, the flux from the suspension (1.4087 ± 0.074 μmoles cm^{-2} h^{-1}) was approximately 11.5-fold greater than the control flux. It can therefore be seen that the enhancement in triclosan flux was approximately half the increase in free drug concentration. This was similar to the diffusional behaviour of free drug from donor solutions of the paraben-CyD complexes; the relative flux enhancement was less than the increase in free drug concentration. As previously discussed, since the donor systems are supersaturated with respect to the free drug, it is possible that at high concentrations there may be some association such as hydrogen bonding between the guest molecules or even with the exterior of the CyD torus. These interactions would therefore reduce diffusion.

The difference between the flux of triclosan from the donor solution and suspension of the triclosan-HP-β-CyD complex was approximately 4.7-fold, and the difference between their estimated free drug concentrations was approximately 4.4-fold, indicating that in this instance, experimental data correlated well with the estimations. This correlation was further observed by plotting the flux of triclosan as a function of free drug concentration, as illustrated in figure 4.10. Although a limited number of data points were used, a linear plot (r^2 = 0.997) was obtained with the intercept being close to zero (2.8668 $x10^{-2}$). These results therefore indicated that even though the flux enhancement was not equivalent to the increase in free drug concentration, a linear relationship existed between these two variables.

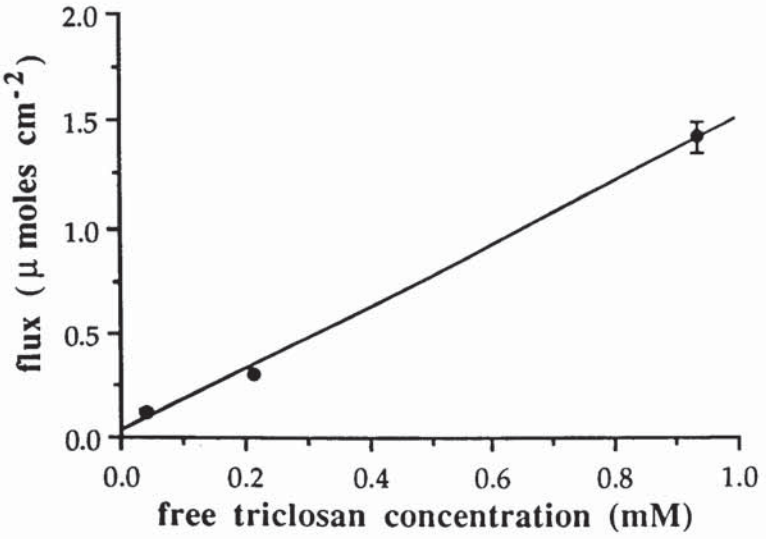

Figure 4.10 Flux of triclosan as a function of free drug concentration ($y = (2.8668 x10^{-2}) + 1.4651x$, $r^2 = 0.997$)

The lag times for triclosan diffusion from all three systems were significantly ($p<0.05$) different. The lag time was greatest for the donor suspension of drug alone ($t_L = 0.990 \pm 0.093$ hours) due to the relatively low concentration of triclosan present. The donor systems of the complex were supersaturated with respect to free triclosan, therefore the driving force for diffusion was greater, and as a consequence, the lag times for diffusion were reduced. As expected, since the concentration of free drug was greatest in the donor suspension of the complex, this system showed the shortest lag time ($t_L = 0.170 \pm 0.027$ hours).

The permeability coefficients (K_p) shown in table 4.9 for the donor systems of the triclosan-HP-β-CyD are only apparent values since these were calculated using the total concentration of triclosan in the donor phase. Since only free triclosan diffused through the membrane, the K_p values were recalculated using the concentrations of drug in the non-complexed form in these systems; these values are summarised in table 4.11 The true K_p values for donor systems of the complex were significantly less than the respective K_p of the triclosan suspension; $(2.9258 \pm 0.212) \times 10$ cm h^{-1}. The K_p values of the solutions of the parabens-CyD complexes were also significantly less than the respective K_p values of the free drug suspensions. These results therefore suggest that due to the equilibrium existing between free and complexed species, the affinity of free drug for the membrane is reduced in the presence of CyDs.

Table 4.11 True permeability coefficients of triclosan as diffused from donor systems of the triclosan-HP-β-CyD complex

	solution of complex		suspension of complex	
	initial	final	initial	final
Total conc. of triclosan ($M \times 10^3$)	0.5930 ± 0.051	0.2453 ± 0.019	8.217 ± 0.201	5.499 ± 0.115
Conc. of free triclosan ($M \times 10^3$)	0.2138 ± 0.011	0.1219 ± 0.006	0.9367 ± 0.012	0.7561 ± 0.005
True K_p (x 10) cm h^{-1}	1.4115 ± 0.087	2.4758 ± 0.132	1.5039 ± 0.079	1.8631 ± 0.111

Diffusion experiments have illustrated that the concentration of free triclosan in solution can exceed its saturation solubility (*i.e.* supersaturated) by CyD complexation which consequently leads to an enhanced diffusion rate. This drug-CyD system may be advantageous for the treatment of bacteria where drug access is a problem, such as in the oral cavity and in the stomach against *H. pylori*. The high concentration of triclosan administered as the complex would provide a reservoir of drug, from which diffusion would rapidly occur to the site of action due to the steep concentration gradient. Furthermore, due to greater concentration of free triclosan available, its microbiological activity may also be enhanced. This activity may be further enhanced by displacement of more triclosan by an effective competitor. However, the search for a suitable competitor remains.

This study has demonstrated the potential application of an antimicrobial-CyD complex. Future considerations for the use of such a product include the form in which the triclosan complex would be administered and also retention of the product in the oral cavity and GI tract. Several triclosan-containing dental products are formulated with a co-polymer (polyvinylmethyl ether maleic acid; PVA/MA) to increase the retention of the triclosan by oral tissues (Urquhart and Addy, 1991). Dettmar and Lloyd-Jones (1991) formulated triclosan as muco-adherent granules to provide a sustained release medicament for the treatment of *H. pylori*. Similar approaches could be used for the retention of a triclosan-CyD product in the oral cavity and GI tract.

4.6.7.2 Effect of SDS on membrane permeability

Prior to the use of SDS as a competing agent, the effect of SDS on the membrane was assessed by comparing the control triclosan flux to the flux obtained with SDS treated membrane. Instead of pretreating the membrane, the flux of triclosan from a donor suspension of triclosan in SDS could have been measured. However, in this instance, although the concentration of SDS used (7.5 mM) was below its CMC (8.1 mM), interactions between SDS and triclosan may have occurred leading to an increase in triclosan solubility. For fair comparison to the control triclosan experiment, the donor concentration of triclosan should be the same on both occasions. The concentration of the donor triclosan suspension used with the pretreated membrane was found to be 0.0423 ± 0.003 mM, which was similar to the concentration of control donor suspension (0.0418 ± 0.002 mM).

When performing the diffusion experiment with the pretreated membrane, the membrane of one of the diffusion cells ruptured during the procedure. Figure 4.11 illustrates the mean diffusion profile of triclosan obtained with the remaining two diffusion cells,

together with the profile obtained from the triclosan control experiment performed without any membrane treatment. Using linear regression, the steady-state flux of triclosan through pretreated membrane was found to be (1.6464 ± 0.278) μmoles cm^{-2} h^{-1}; this was approximately 13 times greater than the control flux of triclosan (0.1223 ± 0.003 μmoles cm^{-2} h^{-1}). The lag time for triclosan diffusion through the treated membrane (0.906 ± 0.013 hours) was similar to the respective value for the untreated membrane (0.990 ± 0.093 hours). In contrast, the permeability coefficient of triclosan with the treated membrane (3.8922 ± 1.004 cm h^{-1}) was approximately 10-fold greater than the respective value for untreated membrane (0.2926 ± 0.021 cm h^{-1}). The steady-state fluxes, lag times and K_p values for diffusion of triclosan through treated and untreated membrane are summarised in table 4.12.

To summarise, it was evident that the surfactant SDS increased the permeability of the membrane, possibly by enlargement of the pores. Furthermore, the error bars of the SDS-treated permeation profile indicated wide variations between the flux of the 2 diffusion cells indicating that the process was not very reproducible. On the basis of these observations, the use of SDS as competitive agent was not pursued.

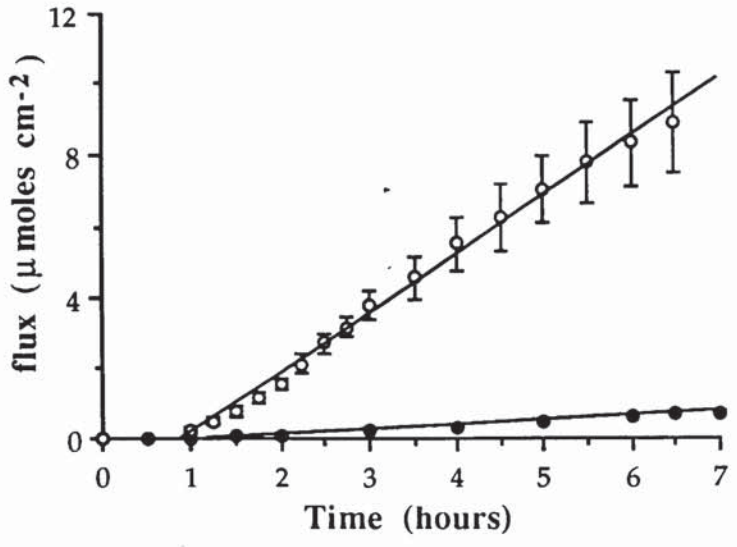

Figure 4.11 Diffusion of triclosan from a suspension of drug alone through Spectra/Por membrane before (•) and after pretreatment with SDS solution (o). Points represent the mean ± s.d., n = 3 for untreated membrane and n = 2 for treated membrane.

Table 4.12 Diffusion data for triclosan transport from a suspension of drug alone through Spectra/Por membrane before and after pretreatment with 7.5 mM SDS solution. Values represent the mean ± s.d., n = 3 for untreated membrane and n = 2 treated membrane.

	untreated membrane	SDS treated membrane
triclosan concentration of donor (M x10^3)	0.0418 ± 0.002	0.0423 ± 0.003
flux (μmoles cm^{-2} h^{-1})	0.1223 ± 0.003	1.6464 ± 0.278
r^2	0.997	0.994
K_p (x 10^2) cm h^{-1}	0.2953 ± 0.021	3.8922 ± 1.004
lag time (t_L; hours)	0.990 ± 0.093	0.906 ± 0.013

4.7 CONCLUSIONS

The present study investigated the solubility enhancement of triclosan by complexation with HP-β-CyD in an attempt to increase its antimicrobial effectiveness. The interactions between the complex components in solution and solid phases were assessed.

A solid phase complex of triclosan and HP-β-CyD was prepared (section 4.5.1) with the aid of aqueous ammonia as a co-solubiliser. DSC analysis of the complex showed the absence of the triclosan peak indicating the formation of a true inclusion complex.

Phase solubility studies (section 4.6.5) showed a linear enhancement in the triclosan solubility due to the formation of a soluble complex in solution. The slope of the solubility isotherm was less than unity, thus a 1:1 stoichiometry was assumed for the complex. At 37°C, in the presence of 0.069 M HP-β-CyD, the solubility of triclosan was enhanced 385-fold and the value of the respective complex stability constant was 8297 M^{-1}. The magnitude of the K_S values indicated the strong affinity of triclosan for the CyD cavity. The highly lipophilic nature of triclosan together with its geometric characteristics make it an ideal candidate for CyD inclusion complexation. The thermodynamic parameters of the inclusion process were found to be energetically favourable and indicated the involvement of van der Waals interactions and hydrophobic bonding mechanisms in complex formation.

Dissolution studies performed on the solid phase triclosan-HP-β-CyD complex revealed an initial peak solubility of the complex which was approximately 240 times greater than the solubility of triclosan alone. The concentration of free triclosan in this system was greater than the saturation concentration of drug alone, *i.e.* the system was supersaturated with respect to free triclosan. The flux of triclosan from the same concentration of complex used during the diffusion experiments was approximately 11.5 times greater than the flux from a suspension of triclosan alone. These results suggested that due to the supersaturated concentration of free drug in the complex system, an enhancement in the clinical effect of triclosan may be observed. Furthermore, the bulk concentration of triclosan administered as the CyD complex would enable a steep concentration gradient to exist, thus facilitating the rapid diffusion of triclosan to the site of bacterial infection.

The experiments performed so far indicate both solubility and flux enhancements of triclosan as a consequence of complexation with HP-β-CyD. However, the clinical effect of a potential triclosan-CyD product has to be greater than triclosan alone if it is to be of any advantage. Therefore, a suitable microbiological test needs to be performed to assess the clinical efficacy of the triclosan-CyD system. Details of *in-vitro* microbiological testing of CyD complexes are given in chapter 5, however, due to limited time the experiments on the triclosan-HP-β-CyD complex could not be pursued.

CHAPTER FIVE
MICROBIOLOGICAL TESTING OF CYCLODEXTRIN COMPLEXES OF ANTIMICROBIAL AGENTS

5.1 INTRODUCTION

The interaction of various antimicrobial agents with cyclodextrins has been studied by many researchers. Rajapopalan and co-workers (1986) investigated the formation of the inclusion complex of amphotericin-B with γ-CyD; the interactions between the antimycotic imidazole derivatives and CyDs were studied by Van Doorne, Bosch and Lerk (1988) and Pedersen *et. al.* (1993); Van Doorne and Bosch (1991) also studied the interactions between nystatin and γ-CyD. In all these cases, an increase in the aqueous solubility of the poorly soluble antimicrobial agents was required in an attempt to enhance their respective microbiological activity. The antimicrobial activity of these guest-CyDs systems will be discussed later.

Another area of interest has been the interaction of preservative agents with CyDs (Loftsson *et. al.*, 1992; Lehner, Müller and Seydel, 1994). Liquid formulations of drug-CyD products would require the incorporation of a suitable preservative agent to prevent contamination by microorganisms. However, the preservative agents themselves may interact with the CyD and thus their antimicrobial effect may be affected. In the presence of HP-β-CyD, the antimicrobial efficacy of benzalkonium chloride was reduced (Dechandt, Mehner and Frömming, 1994). Loftsson and co-workers (1992) found that depending on the nature of the preservative agent, the drug molecule was displaced from the CyD cavity and consequently the antimicrobial activity of the preservative was decreased due to the formation of the preservative-CyD complex. However, the loss of antimicrobial activity will depend on the fraction of the preservative molecule which is included in the CyD cavity. Uekama *et. al.* (1980) observed an increase in the minimum inhibitory concentration (MIC) of the *p*-hydroxybenzoic acid esters (parabens) when they were complexed with α- and β-CyD. Similar results were reported by Lehner and co-workers (1993) for the HP-β-CyD complexes of the parabens who also observed a correlation between the magnitude of the respective paraben-HP-β-CyD complex stability constant and the antimicrobial activity of the agent.

Various methods have been used to assess the microbiological activity of antimicrobial agents in the presence of CyDs. One method used by several researchers (Uekama *et. al.*, 1980; Lehner, Müller and Seydel, 1993) involved the measurement of the MIC of the

antimicrobial agent with and without the presence of the CyD. In all cases, in the presence of the CyD, the MIC of the antimicrobial agent increased indicating a reduction in microbiological activity. However, Matsuda *et. al.* (1993) found that in the presence of HP-β-CyD, butyl paraben maintained its antimicrobial activity. In this latter system however, equimolar ratios of guest and host were not present. As previously discussed, the activity of the paraben derivatives increases with alkyl chain length indicating that their mechanism of action is associated with their solubility in the cell membrane. The phenolic moiety of the esters may also be involved in their antimicrobial activity. Using NMR and circular dichroism spectroscopic studies these researchers proposed that the active phenolic moiety of BuP extruded outside the CyD cavity to explain the maintenance of the antimicrobial activity of the BuP when complexed with HP-β-CyD.

The solutions of antimicrobial agent used for MIC testing were either of saturated concentrations or below since, in this instance, the preservative ability of the antimicrobial agents was assessed. The potential application of the antimicrobial-CyD product from this study was for the treatment of localised bacterial infections. The MIC method was, therefore, unsuitable for microbiological testing during this study since saturated drug-CyD solutions were required to achieve supersaturation of the antimicrobial agent which may potentially enhance its microbiological activity.

Inhibition zone measurements is another method used to assess the activity of antimicrobial-CyD complexes. Pedersen *et. al.* (1993) added saturated solutions of the imidazoles (econazole and miconazole) containing various CyD concentrations (β- and HP-β-CyD) to wells in agar plates and then measured the zone of inhibition produced. A similar method was used by Van Doorne and co-workers (1988) on the imidazole derivatives-β-CyD systems and by Uekama *et. al.* (1980) on the parabens with α- and β-CyD. At higher concentrations of CyD, the zones of inhibition may be expected to be reduced since the equilibrium should favour complexation due to the large excess of CyD. However, all groups of researchers reported an increase in the inhibition zones with increasing CyD concentration. These findings were explained by Van Doorne and co-workers (1988) as follows. In the absence of CyD, the concentration of drug alone is low due to its poor aqueous solubility. In the presence of CyD, the solubility of drug is enhanced by formation of the complex *in situ* which, therefore, increases the concentration differential across the agar and enhances diffusion from the drug-CyD reservoir. Diffusion of both free and complexed drug will occur. However, due to the larger molecular weight of the CyD complex, its diffusion is relatively slower than that of free drug alone. Since the activity of the drug-CyD complex itself is negligible, the enhanced microbiological activity observed in the presence of the CyD is due to

dissociation of the complex in the agar resulting in a higher concentration of active free drug. Furthermore, interactions may occur between the CyD and components of the agar which may lead to displacement of the complexed drug.

A further microbiological method used by Pedersen *et. al.* (1993) assessed the effect of the solid econazole-β-CyD complex on the viability of a bacterial culture over a timed period. The antimicrobial activity of the econazole complex was greater than an equivalent amount of the physical mixture of the components of the complex. It was suggested that the enhanced activity of the solution of the complex was possible, due to an increase in the solubility of econazole by complexation or the formation of a supersaturated econazole solution.

The aim of the present study was to compare the antimicrobial activity of drug alone to the complexed drug. As discussed, several different methods have been used for the testing of antimicrobial-CyD complexes. In contrast to both the MIC method and the inhibition zone measurements, the viability assay performed by Pedersen *et. al.* (1993) involved the use of the solid-phase econazole-β-CyD complex (stoichiometric ratio 1:1). This latter method therefore seemed appropriate for use in this study since dissolution studies have demonstrated the superior solubilities of the solid phase CHX-CyD (section 2.6.5) and paraben-HP-β-CyD complexes (section 3.6.4). Furthermore, the concentration of drug in the non-complexed form in these antimicrobial-CyD systems was found to be greater than the saturation solubility of drug alone. Theoretically, the microbiological activity of these supersaturated solutions (with respect to the drug alone) should be greater that the drug alone. Also, with supersaturated solutions, maximal flux of the drug to the site of bacteria will occur which is important for the treatment of bacteria which are difficult to access such as in oral cavity and beneath the gastric mucus (*H. pylori*).

Two methods were used therefore, for microbiological testing during this study. The first method was similar to the bacterial viability assay used by Pedersen *et. al.* (1993) and involved direct contact of the bacteria with the complexed drug. The second method was based on the diffusion studies performed on the paraben-HP-β-CyD systems (section 3.6) which have already demonstrated the enhanced flux of paraben from a solution of the paraben-HP-β-CyD complex. By incorporating organisms into the receiver compartment of the diffusion cells, the microbiological activity of the enhanced paraben flux was observed. This method therefore examined the activity of free paraben as released from the paraben-HP-β-CyD complex and did not involve direct contact of the solution of the complex with the bacteria.

The test organisms used throughout all reported methods depended on the specificity of the antimicrobial-CyD product. For example, the activity of the imidazole-CyD complexes were tested against *Candida albicans* (Van Doorne, Bosch and Lerk, 1988; Pedersen *et. al.*, 1993). The CyD complexes of the preservative agents, which included the paraben esters, were tested against various microorganisms which included *Pseudomonas aeruginosa* and *Escherichia coli* (Loftsson *et. al.*, 1992; Lehner, Müller and Seydel, 1994). One of the potential applications of the antimicrobial-CyD product from this study is for the treatment of *H. pylori* making this an ideal candidate for use as the test organism. This organism is grown on blood agar base supplemented with 5 % horse blood with a microaerophilic gas mixture of 80 % nitrogen, 10 % carbon dioxide and 10 % oxygen at 37°C for 4 days (SKB, personal communication). However, due to these stringent conditions required for the cultivation of this bacteria, great problems were encountered with its use. Thus, the test organisms used to demonstrate the microbiological activities of the antimicrobial-CyD systems were *E. coli*, *Ps. aeruginosa* and *Bacillus subtilis* .

5.2 MATERIALS

Chlorhexidine dihydrochloride and butyl paraben were purchased from Sigma chemicals. Nutrient Agar and Nutrient Broth were purchased from Oxoid (Basingstoke, U.K.). Letheen Broth was purchased from Difco Laboratories (Michigan, USA). Test solutions were sterilised by filtration using 0.2 μm γ-irradiated cellulose filters purchased from Sigma Chemicals.

5.3 EXPERIMENTAL

5.3.1 Testing of the chlorhexidine dihydrochloride-β-CyD complex

5.3.1.1 Preparation of CHX test solutions

A saturated solution of CHX was prepared by equilibrating excess drug in distilled water at 37°C overnight in a shaking water bath. The suspension was filtered using a 0.45 μm Whatman cellulose nitrate filter. The solution of the CHX-β-CyD complex was prepared by dissolving the equivalent amount of 110 mg of CHX, as the β-CyD complex (340 mg) in 20 ml of distilled water pre-heated to 37°C. After shaking for 5 minutes, any solid was removed from the solution by filtration through a 0.45 μm Whatman cellulose nitrate filter. The concentration of CHX in both solutions of drug alone and complex was determined by HPLC by diluting 0.5 ml of the solution 50-fold in a 25 ml volumetric

flask. Prior to making up to volume, 1 ml of propyl paraben I.S. stock solution (1.25×10^{-3} M) was added. Quantification of CHX in the final solutions was achieved by injection of 100 µl under the HPLC conditions as described in section 2.4.2. Duplicate assays were performed for each test solution. A saturated solution of β-CyD was also prepared by dissolving 0.9 g in 50 ml distilled water. Prior to assessment of their antimicrobial activities, all test solutions were sterilised by filtration through a 0.2 µm cellulose acetate filter (Sigma).

5.3.1.2 Effect of free and complexed CHX on the viability of Escherichia coli and Pseudomonas aeruginosa

E. coli (NCTC 10418) and *Ps. aeruginosa* (ATCC 9027) were used as the test organisms. To obtain a stationary-phase bacterial culture, 50 ml sterile nutrient broth was inoculated with a single bacterial colony taken from a nutrient agar plate containing the organism, and continuously stirred overnight at 37°C. The stationary-phase bacterial suspension was diluted with nutrient both to give 10^{10} organisms per ml. To 10 ml each of sterile nutrient broth, used as the control, and to the same volume of the test solutions prepared in section 5.3.1.1, 100 µl of the *E. coli* bacterial suspension was added. At set time-points, usually every 5 minutes up to 30 minutes, 10 µl aliquots were removed from the test systems containing CHX alone and the CHX-β-CyD complex and were serially diluted (10^{-3} to 10^{-5}) with Letheen broth which was used as the inactivation liquid. From each dilution, 100 µl was spread onto nutrient agar plates and incubated overnight at 37°C. Two nutrient agar plates were used for each dilution. With the nutrient broth and β-CyD controls, 10 µl aliquots of the test solution were removed at zero time and 30 minutes and serially diluted with Letheen broth in a similar manner as previously described. After incubation of all plates overnight at 37°C, the colony-forming units on each plate were counted.

The above procedure was repeated with *Ps. aeruginosa* as the test organisms.

5.3.1.3 Effect of free and complexed CHX on the viability of Bacillus subtilis

Spores of *Bacillus subtilis* (ATCC 6633) were used as the test organism. *B. subtilis* was cultured at 37°C in Ciba Medium B (5 g polypeptone, 3 g beef extract, 8 g sodium chloride, 15 g agar, 2 mg manganese chloride, 2 mg sodium nitrate made with water to 1000 ml, adjusted to pH 7.3) for one week at 65°C. The organisms were collected by washing the surface of the agar with 50 ml of sterile water following which the suspension was heated to 70°C for 15 minutes to kill any vegetative organisms present. The spore suspension was then diluted with sterile saline (0.9 % NaCl) to result in 10^8 organisms per ml. To 1 ml each of nutrient broth, the solutions of β-CyD, CHX

alone and the solution of the CHX-β-CyD complex as prepared in section 5.3.1.1, 100 µl of the spore suspension was added. At set time-points usually every hour from zero time up to 3 hours, 100 µl aliquots were removed from the test systems containing CHX alone and the CHX-β-CyD complex and were serially diluted (10^3 to 10^4-fold) with Letheen broth. From each dilution, 100 µl was spread onto nutrient agar plates and incubated overnight at 37°C. Two nutrient agar plates were used for each dilution. With the nutrient broth and β-CyD controls, 100 µl aliquots of the test solutions were removed at zero time and 30 minutes and serially diluted with Letheen broth in a similar manner as previously described. After incubation of all plates overnight at 37°C, the colony-forming units on each plate were counted.

5.3.2 Testing of the butyl paraben-HP-β-CyD complex

5.3.2.1 Preparation of the butyl paraben (BuP) test solutions

A saturated solution of BuP was prepared by equilibrating excess drug in distilled water at 37°C overnight in a shaking water bath. The suspension was filtered using a 0.45 µm Whatman cellulose nitrate filter. A solution of the complex was prepared by dissolving the equivalent amount of 55 mg of BuP, as the HP-β-CyD complex (595 mg) in 5 ml of distilled water pre-heated to 37°C. The concentration of BuP in both solutions of drug alone and the complex were determined by HPLC. The concentration of the saturated BuP solution was determined by diluting 1 ml to 25 ml. For the quantification of BuP in the solution of the complex, 50 µl of the solution was diluted 500-fold in a 25 ml volumetric flask. In both cases, prior to making up to volume, 1 ml of propyl paraben I.S. stock solution (1.66×10^{-3} M) was added. Quantification of BuP in the final solutions was achieved by injection of 100 µl under the HPLC conditions as described in section 3.4.2. Duplicate assays were performed for each test solution. A solution of HP-β-CyD, of 0.069 M (~10% w/v) was also prepared in distilled water. Prior to assessment of their antimicrobial activities, all test solutions were sterilised by filtration through a 0.2 µm cellulose acetate filter (Sigma).

5.3.2.2 Effect of free and complexed BuP on the viability of Pseudomonas aeruginosa

Ps. aeruginosa (ATCC 9027) was used as the test organism. After cultivation in nutrient broth at 37°C overnight, the stationary phase bacterial suspension was diluted with nutrient broth to give 10^8 organisms per ml. To 1 ml of sterile nutrient broth, used as the control, and to the same volume of the test solutions prepared in section 5.3.2.1, 100 µl of the *Ps. aeruginosa* bacterial suspension was added. At set time-points, usually every 5 minutes up to 30 minutes, 100 µl aliquots were removed from separate test solutions containing saturated BuP alone or the BuP-HP-β-CyD complex and were serially diluted (10^2 to 10^5-fold) with Letheen broth which was used as the inactivation liquid. From

each dilution, 100 µl was spread onto nutrient agar plates and incubated overnight at 37°C. Two nutrient agar plates were used for each dilution. This procedure was repeated with the nutrient broth and HP-β-CyD controls at time zero and 30 minutes. After incubation of all plates overnight at 37°C, the colony-forming units on each plate were counted. The experiment was performed on 3 separate occasions for each test solution.

5.3.2.3 Effect of BuP on the viability of E. coli using Franz diffusion cells

Franz diffusion cells, as previously described in section 3.5.7.1, were adapted for use during the microbiological testing of the BuP-HP-β-CyD complex. On each occasion duplicate cells (control and test) were used and the procedure was performed in a warm room maintained at 37°C. Both donor and receiver compartments, which also contained a small magnetic flea were sterilised prior to use. The test organism used was *E. coli* (NCTC 10418). A log-phase bacterial suspension was required which was prepared in a manner similar to the preparation of the stationary-phase culture described previously in section 5.3.1.2. However, on this occasion, the inoculated suspension was cultivated at 37°C for 3 hours only. The 3-hour log-phase bacterial culture was diluted with nutrient broth to result in 10^8 organisms per ml. The medium for the receiver compartment was prepared by adding 2 ml of diluted bacterial suspension to 50 ml sterile phosphate buffered saline (PBS) followed by gentle stirring for even distribution of the bacterial suspension within the solution. The receiver compartments were filled with the bacterial PBS solution and then clamped above a Camlab Variomag multipoint stirrer enabling uniform mixing of the medium at a rate of 100 *rpm*. A piece of silicone membrane (~ 3 cm^2) of 0.02 thickness was carefully washed with sterile distilled water and then mounted onto the donor cell with Parafilm. The donor cell was then secured to the receiver chamber with Parafilm and held together by a spring clamp. Samples for testing included a pre-saturated suspension of BuP alone and solution of the BuP-HP-β-CyD complex (prepared in section 5.3.2.1), of which 1 ml was placed into the test donor cell. With the suspension of BuP alone, 1 ml of distilled water was placed in the control donor cell. With the solution of the complex, 1 ml of HP-β-CyD was placed in the control donor compartment. At set time points from zero to 6 hours, 100 µl aliquots were removed from the receiver compartments and serially diluted (10^2 to 10^5-fold) with Letheen broth. From each dilution, 100 µl was spread onto nutrient agar plates and incubated overnight at 37°C. Two nutrient agar plates were used for each dilution. After incubation of all plates overnight at 37°C, the colony-forming units on each plate were counted. The experiment was repeated on 3 separate occasions for both free and complexed BuP. The growth of bacteria in the appropriate control receptor compartment was compared to the viability of the bacteria in the test receptor compartment. A

diagrammatic representation of the Franz diffusion cell as used during the microbiological investigations is illustrated in figure 5.1.

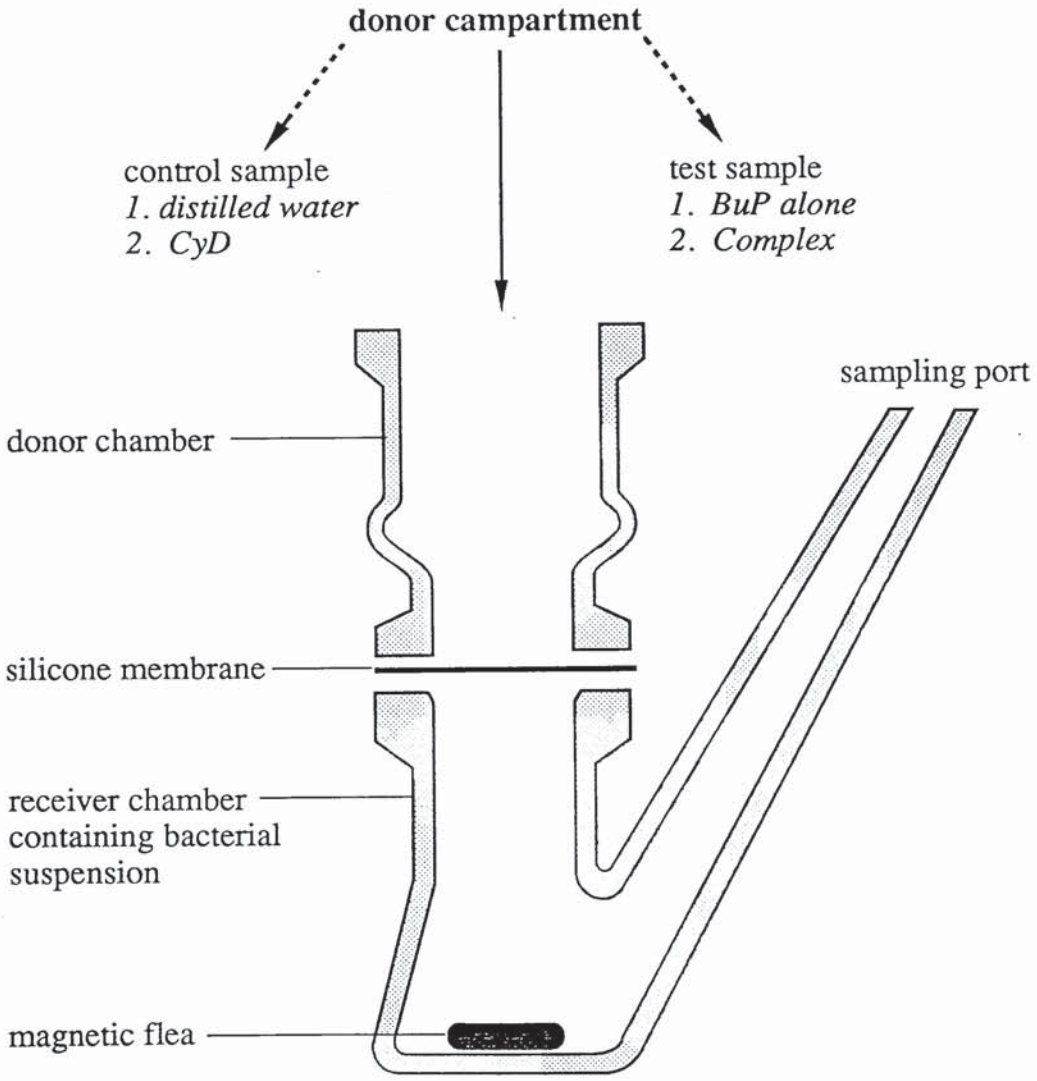

Figure 5.1 Diagram of Franz diffusion cell used for microbiological assay

5.4 RESULTS AND DISCUSSION

5.4.1 Microbiological activity of the chlorhexidine dihydrochloride-β-CyD complex

The viable bacterial count in the nutrient broth control for *E. coli* in the stationary phase, increased from (2.09 ± 0.22) x 10^8 organisms per ml to (2.13 ± 0.41) x 10^8 organisms per ml over the 30 minutes study period indicating no significant changes in bacterial viability. The viable bacterial count in the presence of β-CyD was similar changing from (2.11 ± 0.32) x 10^8 organisms per ml to (2.05 ± 0.61) x 10^8 organisms per ml over the 30 minutes study period. The static behaviour of the bacteria in the β-CyD control suggests that the CyD itself was devoid of any antibacterial activity. However, in contrast, no growth was observed on any of the nutrient agar plates for the test solutions of CHX alone and the CHX complex. The CHX concentration of the solution of the β-CyD complex (11.240 ± 0.139 mM) was approximately 6-fold greater than the solubility of CHX itself (1.896 ± 0.005 mM). The results indicated that *E. coli* was too sensitive to the relatively high concentrations of CHX available here. Even when the more resistant *Ps. aeruginosa* was used as the test organism, the CHX solutions were too potent. Thus, it was decided to increase the resistance of the test organism further by examining the potential of bacterial spores in this experiment

The results for the effects of free and complexed CHX on spore viability were expressed as percentages of the initial spore count in each test sample determined at zero time. The viable spore count for the nutrient broth control changed from (7.25 ± 0.355) x 10^6 spores per ml to (7.85 ± 0.636) x 10^6 spores per ml over the 3 hour contact period indicating no significant changes in viability. Similar results were observed with the β-CyD control in which the viable spore count changed from 7.71 x 10^6 to 7.34 x 10^6 spores per ml, indicating that the CyD itself had no activity against the bacterial spores. By plotting the log of the percentage of viable spores in each test solution as a function of time, a linear correlation was observed as illustrated in figure 5.2. Using linear regression, the slopes for the viability changes in the presence of free and complexed CHX were found to be 0.2132 (r^2 = 0.845) and 0.2389 (r^2 = 0.923) respectively. Although the error bars of these two systems overlapped, the microbiological effect of the solution of the complex CHX appeared to be superior to that of free CHX. Over the 3 hours study, an approximate 45 % reduction in the viable spore population was observed.

In the presence of CyDs, the activity of the antimicrobial may be affected depending on the extent of the interaction between the drug and the CyD, as indicated by the magnitude of the K_S , and also the part of the molecule entrapped within the CyD cavity. Using

equation A4.20 in Appendix 4, together with the K_S value for the CHX-β-CyD complex (54 M^{-1}; section 2.6.4) and the total CHX concentration of the solution of the complex (11.240 ± 0.139 mM), the concentration of CHX existing as the non-complexed form was estimated to be 7.884 ± 0.075 mM; this is approximately four times the saturation solubility of CHX alone (1.896 ± 0.005 mM). The solution of the CHX-β-CyD complex was therefore supersaturated with respect to CHX, and, therefore its microbiological activity may be expected to be greater than a saturated solution of CHX alone. However, the results failed to show a marked difference between the antimicrobial activity of CHX in solutions with and without CyD. It is possible that, due to the high resistance of the spores, a greater difference is required between the free drug concentrations in solutions of CHX alone and its β-CyD complex to exhibit changes in their antimicrobial activities.

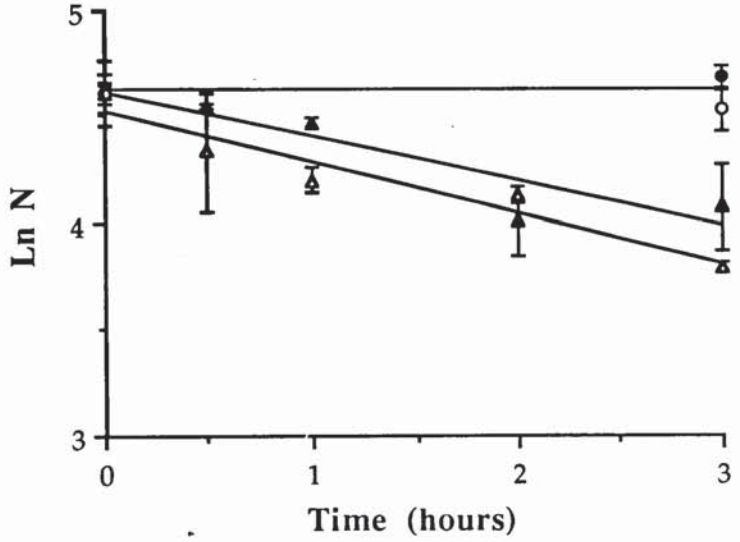

Figure 5.2 Time-dependent viability changes of *B. subtilis* spores when added to the following solutions at zero time: (•) nutrient broth; (o) β-CyD control; (▲) CHX alone; (Δ) CHX-β-CyD complex. N is the number of spores as a percentage of the viable population in each test solution at zero time. Points represent the mean ± s.d. of duplicate nutrient plates.

5.4.2 Microbiological activity of the butyl paraben-HP–β-CyD complex

5.4.2.1 Effect of free and complexed BuP on the viability of Pseudomonas aeruginosa

The stoichiometric ratio of the BuP-HP-β-CyD complex (*Batch III*) was found to be 0.87:1 (BuP:CyD respectively; section 3.5.4). The concentration of HP-β-CyD in the solution of the dissolved BuP complex prepared in section 5.3.2.1 was approximately 0.069 M . Hence, an equivalent concentration of HP-β-CyD was used as a control with which no significant effect on the growth of the test organism, *Ps. aeruginosa*, was observed. Similar results were reported by Loftsson *et. al.* (1992) who found no bacterial damage below concentrations of 20 % w/v. However, in contrast, Lehner and co-workers (1994) observed inhibition of bacterial growth with HP-β-CyD concentrations of 10 %. The variation in results are possibly due to the differences in the contact times between the bacteria and CyD. The experiments performed by Loftsson *et. al.* (1992) used a incubation time of 24 hours whereas a longer incubation time of 72 hours was used by Lehner and co-workers (1994).

The effect of both free and complexed BuP solutions on the viability of *Ps. aeruginosa* was assessed over a 30 minute period. Since stationary-phase bacteria were used, the action of BuP on the micro-organism was due to a bactericidal effect. Parabens are considered to be bacteriostatic in nature, however, during these experiments relatively high concentrations of antimicrobial agent were used at which a bactericidal effect was observed. The experiment was performed on 3 separate occasions using solutions of both free and complexed BuP each time. The bacterial count measured in the nutrient broth control at zero time was considered to be the initial viable bacterial count for all test solutions. The initial bacterial counts were not taken at zero time from the test solutions themselves due to the presence of the antimicrobial agent which may have had an immediate action. The bacterial cell counts determined for the test solutions at each time point indicated the number of viable cells remaining. These results were expressed as a percentage of the total initial bacterial count. For each test solution, the mean ± s.d. of the percentage of viable cells remaining at each time point during the 3 experiments was found and plotted as illustrated in figure 5.3.

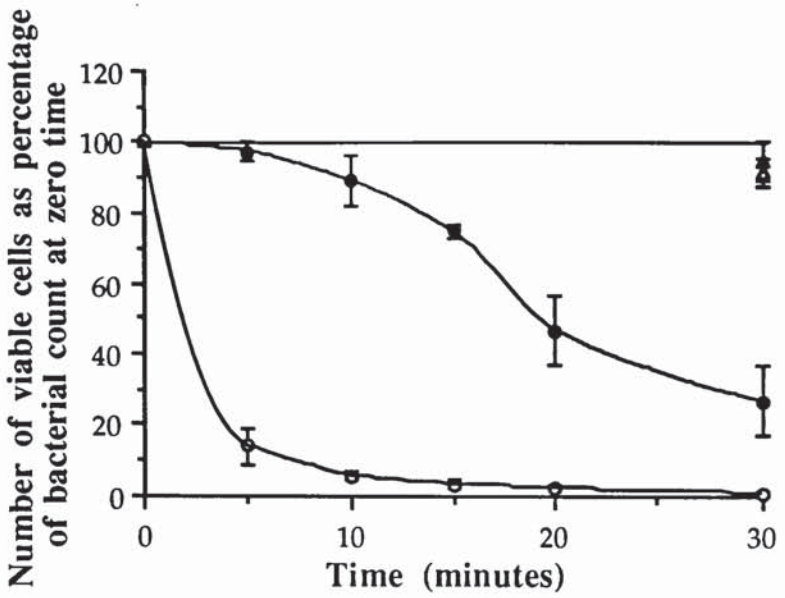

Figure 5.3 Time-dependent changes in the viability of *Ps. aeruginosa* when added to the following solutions at zero time: (▲) nutrient broth; (Δ) HP-β-CyD, 0.069 M; (•) BuP, 1.6756 ± 0.043 mM; (o) BuP-HP-β-CyD complex, 0.05936 ± 0.003 M. Points represent the mean ± s.d. of 3 experiments.

Approximately 30 % of the initial bacterial population remained after 30 minutes exposure to a saturated solution of BuP alone. Initially, the bactericidal effect of BuP was minimal, however, after 10 minutes contact with the bacteria, the rate of bacterial kill was increased. In contrast, an immediate bactericidal effect was observed with the solution of the BuP-HP-β-CyD complex which reduced the viable bacterial population to virtually zero over the 30 minute exposure period. With the solution of BuP alone, the viable bacterial population was reduced to half its initial count over 19 minutes, whereas with the solution of the BuP complex only 2.5 minutes exposure was required.

The viability assay has demonstrated the enhanced microbiological activity of the BuP-HP-β-CyD complex as compared to drug alone. This is in contrast to the general opinion of antimicrobial drug-CyD complexes being inactive. If equimolar concentrations of free and complexed drug solutions had been used against the bacteria, a reduction in the microbiological activity of the complexed drug may have been observed since the proportion of free, and therefore active drug in the complex system would be less than in the solution of drug alone. During this study however, sufficient BuP-HP-β-CyD complex was used such that the total BuP concentration was greater than the saturated

solubility of drug alone. The BuP concentration of the complex solution was found to be 0.05936 ± 0.003 M which was approximately 35 times greater than a saturated solution of BuP alone [(1.6756 ± 0.043) x 10^{-3} M]. The concentration of BuP in the BuP-HP-β-CyD system existing as the non-complexed form, was calculated to be (4.995 ± 0.130) x 10^{-3} M, which was approximately three times the saturation solubility of BuP alone. The greater antimicrobial activity of the complex solution may therefore be attributed to the presence of a supersaturated solution with respect to the BuP. Pedersen *et. al.* (1993) observed similar behaviour with the econazole-β-CyD complex. Furthermore, the BuP-HP-β-CyD complex itself may have contributed to the enhanced activity since it has been reported that the phenolic moiety of BuP extruded outside the CyD cavity enabling the complex to maintain its antimicrobial activity (Matsuda *et. al.*, 1993).

5.4.2.2 Effect of BuP on the viability of E. coli using Franz diffusion cells

The results of the viability assay of *Ps. aeruginosa* (section 5.4.2.1) have demonstrated the enhanced activity of the BuP complex which may be attributed to the supersaturation of BuP and also to the activity of the complex itself. In an *in vivo* situation, the antimicrobial agent may have to overcome a biological barrier prior to reaching the site of bacterial infection, such as the gastric mucus for *H. pylori*. Diffusion studies (section 3.6) using silicone membrane as a barrier have illustrated the enhanced flux of the free BuP from a solution of its HP-β-CyD complex due to supersaturation of BuP itself. The diffusion cells were therefore adapted in order to assess whether the enhanced flux of paraben also demonstrated a greater microbiological activity.

Previous microbiological experiments were performed with saturated solutions of antimicrobial agent which were therefore able to exert a bactericidal effect on the stationary-phase test organisms. During the diffusion experiments (section 3.6.6), even though solutions of high BuP concentration were added to the donor compartments of the Franz cells, the actual concentration of BuP in the receiver compartments would be considerably less; the concentration range of BuP in the receiver compartment from a donor phase of saturated BuP suspension was 4 μM to 240 μM over the 7-hour period. Therefore, due to the lower concentrations of antimicrobial agent a more susceptible test organism was used, *i.e. E. coli*.

Preliminary experiments were performed to assess the effect of low concentrations of BuP on stationary-phase bacteria. The procedure involved adding 100 μl of stationary phase bacterial suspensions of *E. coli* (10^7 organisms per ml) to 5 ml of nutrient broth containing BuP in the concentration range 1 μM to 500 μM. After incubation overnight at

37°C, growth was observed at all concentrations of BuP, indicating that the concentration of BuP was too low to have a bactericidal effect. Therefore, to increase the susceptibility of the bacteria to BuP, log-phase *E. coli* were used to enable the antimicrobial agent to exert a bacteriostatic effect which does not require concentrations as high as those required to kill stationary-phase bacteria.

Incorporation of nutrient broth into the receiver compartment was essential for the experiment to be successful. The primary mechanism of action of the paraben is the inhibition of uptake processes in the bacteria (Eklund. 1980), therefore actively growing bacteria are required for the antimicrobial agents to exert a bacteriostatic effect. By adding 2 ml of nutrient broth to 50 ml PBS the bacteria had sufficient nutrient to maintain growth. Further increases in the proportion of nutrient broth were not made since extensive bacterial growth would have occurred over the 6 hour study period which would have been an unfair challenge to the antimicrobial agent.

The diffusion experiments were performed with either a pre-saturated suspension of BuP or a solution of the BuP-HP-β-CyD complex as the test donor phase on 3 separate occasions with the appropriate control. At each time point over the 6 hour study, the bacterial growth in the receiver compartment for the test system was compared to the bacterial growth in the control receiver medium. With the BuP suspension as the donor phase, distilled water was used as the control donor, and with the donor solution of the BuP complex, 10% HP-β-CyD solution was used as the control. Over the 6 hour study, the bacterial population increased by a factor of 3.057 (± 0.418) in the distilled water control and by a factor of 3.203 (± 0.366) in the HP-β-CyD control. The similarity between these results further confirms that HP-β-CyD was impermeable to the silicone membrane due to its hydrophilic nature, as previously demonstrated in section 3.6.6.

Despite the fact that log-phase bacteria were used, the diffusion of BuP from the donor suspension of paraben alone had little effect on the inhibition of bacterial growth as illustrated in figure 5.4. The relatively poor microbiological activity of BuP in this system was due to the low concentration of antimicrobial present; the concentration of BuP accumulated in the receiver phase over the 6 hour study period can be estimated from previous diffusion studies to be ~ 190 μM (0.037 mg/ml). In contrast, the diffusion of BuP from a solution of the BuP-HP-β-CyD complex showed a much greater antimicrobial activity. As illustrated in figure 5.5, the growth of bacteria in the control increased steadily over the 6 hours. The bacterial count in the receiver of the BuP-HP-β-CyD system also increased up to the initial 4 hours, however the rate of bacterial growth was considerably less than that observed for the control system. After 4 hours, the viable

bacterial population in the receiver medium of the BuP-HP-β-CyD system was maintained at a constant level suggesting that no further bacterial growth occurred. The changes observed in the growth of the bacteria with the complex test solution were due to the diffusion of BuP across the silicone membrane into the receiver medium which consequently exerted a bacteriostatic effect on the microorganisms. The concentration of BuP in the receiver compartment increased over the 6 hour period and thus a greater antimicrobial effect was observed with time; the concentration of BuP accumulated in the receiver phase over the 6 hour study period can be estimated from previous diffusion studies to be ~ 275 μM (0.053 mg/ml).

To standardise the findings from the experiments performed using both free and complexed BuP, the bacterial counts in each test system were expressed as a percentage of the bacterial count in the appropriate control system at each time point which indicated the number of viable cells remaining. For each test system, the mean ± s.d. of the percentage of viable cells remaining at each time point during the 3 experiments was found and plotted as illustrated in figure 5.6.

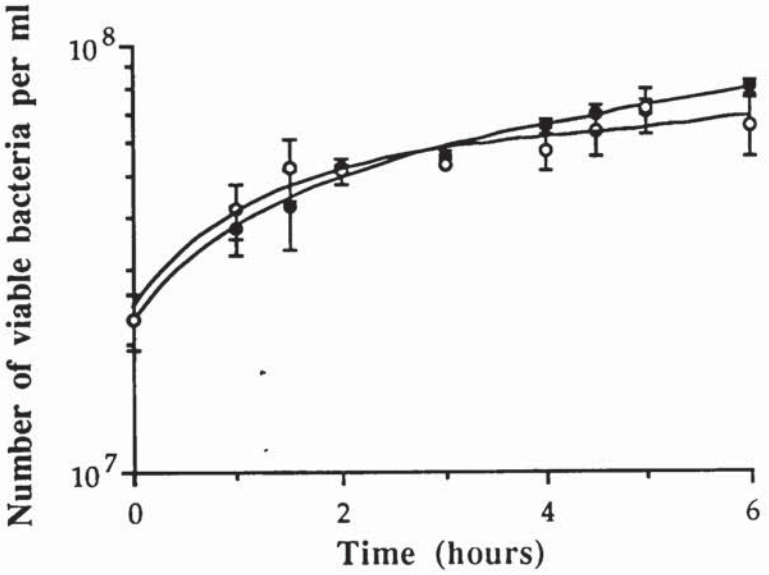

Figure 5.4 Time-dependent changes in the viability of *E. coli* in the receiver medium with the respective donor compartment containing distilled water as a control (•) or a suspension of BuP (o). Points represent the mean ± s.d. of duplicate nutrient agar plates

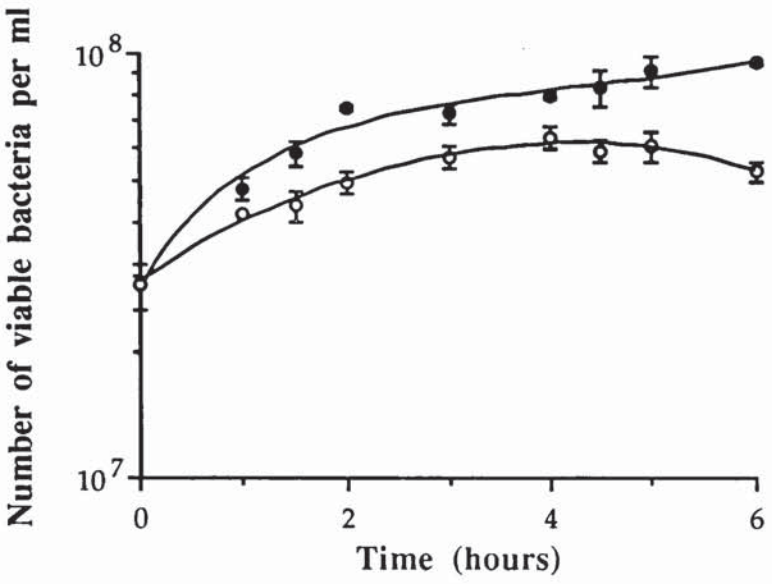

Figure 5.5 Time-dependent changes in the viability of *E. coli* in the receiver medium with the respective donor compartment containing HP-β-CyD as a control (•) or a solution of the BuP-HP-β-CyD complex (o). Points represent the mean ± s.d. of duplicate nutrient agar plates.

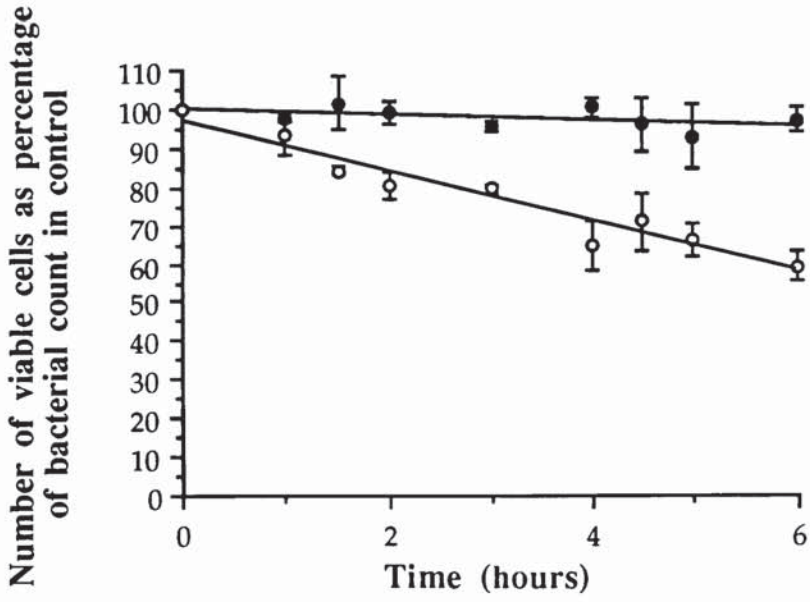

Figure 5.6 Time-dependent changes in the viability of *E. coli* in the receiver medium with the respective donor compartment containing a suspension of BuP (•) and a solution of the BuP-HP-β-CyD complex (o), expressed as a percentage of the viable bacterial population in the appropriate control system. Points represent the mean ± s.d. of triplicate experiments

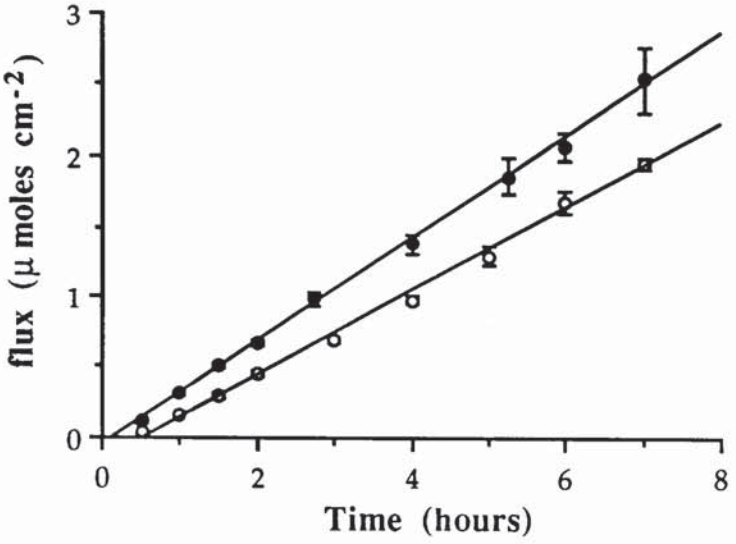

Figure 5.7 Diffusion of butyl paraben through silicone membrane from an aqueous donor suspension of drug alone (o) and a solution of its HP-β-CyD complex, *Batch III* (•). Points represent the mean ± s.d., $n = 3$.

With a donor suspension of BuP, the viable bacterial population was almost static, indicating that the diffusion of BuP from a donor suspension of drug alone had little bacteriostatic effect. In contrast, the plot for the donor solution of the BuP-HP-β-CyD complex, showed a linear decrease in bacterial viability with time. Over the 6 hour period, the concentration of BuP (~ 275 μM) in the receiver phase which had accumulated by diffusion from the BuP-HP-β-CyD solution, was sufficient to reduce the viable bacterial population by approximately 60 %. Using linear regression, the slope of the profile for the complex was found to be 6.5592 ($r^2 = 0.936$), which could be considered to be the rate of bacterial kill. From previous diffusion studies (section 3.6.6), the flux of BuP from a saturated donor suspension of drug alone was found to be 0.2951 ± 0.0081 μmoles cm^2 h^{-1}, whereas the flux from a solution of the BuP-HP-β-CyD (total BuP concentration, 61.394 ± 2.193 mM) was found to be 0.3968 ± 0.0188 μmoles cm^2 h^{-1}; the permeation profile of BuP from these systems are illustrated in figure 5.7. The enhanced flux of BuP was due to the concentration of BuP in the non-complexed form being approximately 3 times greater than the saturation solubility of BuP itself. It is evident from the microbiological studies that the supersaturated solution of BuP, present as the solution of the BuP-HP-β-CyD complex in the donor compartment, exhibited enhanced flux across the membrane into the receiver compartment which consequently exerted an antimicrobial effect. With a donor suspension of BuP alone having a lower concentration, the concentration differential cross the membrane was

reduced. Therefore, since the flux of BuP was much less, the concentration of BuP in the receiver phase was too low to observe any antimicrobial effect.

The flux of BuP, and therefore its antimicrobial activity could be further increased in the presence of the competitor. Once a suitable competitor has been found as discussed in section 3.6.7, the microbiological experiments performed with the Franz diffusion cells should be repeated with a donor solution of the BuP-HP-β-CyD complex in the presence of the competitor. Displacement of complexed BuP by the competitor should further increase the concentration of free BuP in solution and also enhance its flux across the silicone membrane. Therefore, due to the higher concentration of BuP in the receiver phase, a greater microbiological activity of BuP may be observed.

By using Franz diffusion cells, the possible benefits of an antimicrobial-CyD product for the treatment of localised bacterial infections which are difficult to access has been demonstrated. Future work would include the use of other microbiological methods which would utilise a more realistic barrier to diffusion than silicone membrane. An outline of these methods is given below.

1. Agar plate method using gastric mucus as a barrier to diffusion

This method involves the use of gastric mucus as a barrier to diffusion in an attempt to simulate the problems encountered for treatment of *H. pylori*. Very simply, agar plates of a suitable medium to support growth of the bacterium are prepared. The bacterial culture of the test organism is spread evenly over the plates. A strip of agar is cut out and the space filled with gastric mucus. Wells are cut into the agar adjacent to the mucus into which the test solutions are added. After incubation of the plates at the required temperature and conditions suitable for bacterial growth, the zone of inhibition produced adjacent to the mucus strip is measured. Figure 5.8 illustrates an example of an agar plate with the mucus strip. The test solutions will consist of either saturated drug alone, and the drug-CyD complex with and without the presence of a suitable competitor. Control experiments would also be performed using the appropriate solutions (distilled water, CyD alone, competitor alone). The zones of inhibition produced by the respective test solutions will give an indication of their microbiological effect *i.e.* the larger the zone of inhibition the greater the activity. Diffusion of the complex will be relatively slow compared to the free drug due to its larger molecular size. However, if the solution of the complex is supersaturated with respect to the drug alone, the potential exists for maximal flux of the drug across the mucus and a greater antimicrobial activity as compared to drug alone.

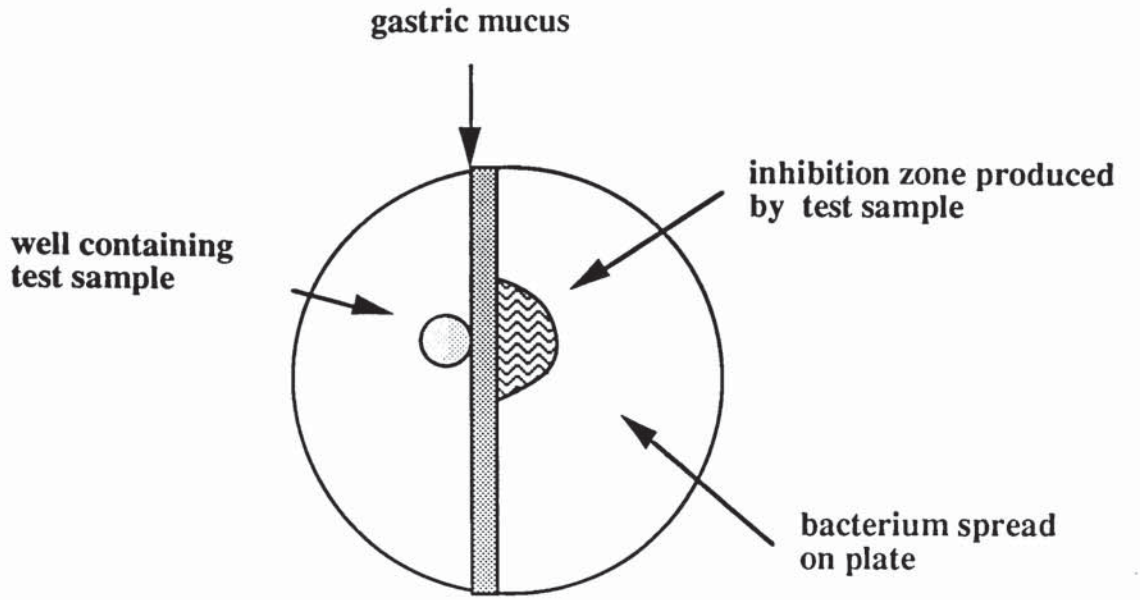

Figure 5.8 Diagram of an agar plate with gastric mucus for the microbiological testing of the drug-CyD complex

2. Biofilm method

By using oral cavity bacteria as the test organisms, the biofilm method may be used to simulate an *in vitro* dental plaque model to test the activity and penetration of the drug-CyD complexes. The biofilms would be grown on microtitre plates using a suitable bacteria. The biofilm would be exposed to the test solutions for 5 minutes and then washed off with phosphate buffer. A constant volume of growth medium would be added to each biofilm well and incubated overnight under conditions suitable for bacterial growth. After the incubation period, the extent of re-growth of the biofilm would be assessed using optical density (OD) measurements. The contact time of the test samples with the biofilm should be varied to observe the effect of increasing drug penetration time on biofilm growth. Samples for testing would include a saturated solution of drug alone, solution of drug-CyD complex alone and in the presence of the competitor. Control experiments would be performed with the appropriate solutions (distilled water, CyD alone, competitor alone).

5.5 CONCLUSIONS

The microbiological activities of the CHX-β-CyD and the BuP-HP-β-CyD systems were assessed by two methods. The first method observed the viability of a bacterial population in the presence of both free and complexed drug. With the CHX-β-CyD

system, the use of a bacterial test organism was unsuccessful due to the relatively high concentrations of antimicrobial agent used. However, by using resistant spores of *B. subtilis* as the test organism, the microbiological activity of the CHX-β-CyD was studied. No significant differences were observed between the activities of free and complexed CHX on the spore viability. Since the aim of the microbiological experiments was to use saturated drug solutions in an attempt to achieve supersaturation, saturated solutions of CHX itself were too potent to test against bacteria therefore no further microbiological experiments were pursued with the CHX-β-CyD system.

The solution of the BuP-HP-β-CyD complex showed a superior antimicrobial effect on the viability of *Ps. aeruginosa* as compared to the effect of a saturated solution of BuP alone. The enhanced activity of the complex solution was possibly due to the supersaturation of BuP and the enhanced activity of the complex itself.

The second method assessed the microbiological effect of BuP as it diffused through silicone membrane from a donor suspension of either drug alone or a solution of the BuP-HP-CyD complex. The flux of BuP from the complex was greater due to supersaturation of BuP in the complex solution which consequently had a greater microbiological effect.

To conclude, therefore, it has been demonstrated that, by formation of the BuP-HP-β-CyD complex, the solubility of the drug was increased and, at sufficiently high concentrations of the complex, the concentration of BuP in the non-complexed form was greater than the saturation solubility of drug alone. Consequently, the microbiological activity of the complex solution was greater, as demonstrated by the viability assay on *Ps. aeruginosa*. Furthermore, the diffusion of free drug from its complex was also enhanced and therefore it is assumed that in an *in vivo* situation, the flux of drug to the site of bacterial infection will also be increased as will the microbiological potential of the antimicrobial agent.

Future work will include microbiological testing of the HP-β-CyD complexes of MeP, EtP, PrP and triclosan using the time-dependent viability assay, the Franz diffusion cell method as well as the agar plate and biofilm methods described. Furthermore, once a suitable competitor agent has been found, its effect on the antimicrobial behaviour of the drug-CyD systems will be also assessed using these methods.

CHAPTER 6
GENERAL SUMMARY

Over the last decade, the increasing application of CyDs in the pharmaceutical field has become evident by the growing number of publications concerning their use. By forming inclusion complexes with various types of guest, the pharmaceutical properties of the complexed guest are modified with improvements in aqueous solubility, dissolution rate, bioavailability and stability. Although no marketed products are available in the United Kingdom, elsewhere these advantages have led to the introduction of cyclodextrin-containing pharmaceuticals as previously shown in table 1.4.

This study investigated the solubility enhancements of poorly water-soluble antimicrobial agents with CyDs, in an attempt to increase their antimicrobial efficacy. The drugs chosen for study were chlorhexidine dihydrochloride (CHX, chapter 2), *p*-hydroxy-benzoic acid esters (parabens, chapter 3) and triclosan (chapter 4). As previously discussed, several papers have recently been published regarding the interaction of some of these agents with CyDs. The published studies involving chlorhexidine were concerned with a reduction in its side effects such as bitter taste, irritation and tooth staining by complexation with β-CyD. The objective of the literature work performed with the parabens was to assess the changes in the preservative action of the esters in the presence of HP-β-CyD. As yet, no work has been reported on the interactions between triclosan and CyDs.

In contrast to the published literature, the aim of the present study was to use the antimicrobial-CyD product as a potential treatment for localised bacteria infections which are difficult to access such as *H. pylori* in the GI tract and pathogens of the oral cavity. The guest compounds used during the present study were found to be active against *H. pylori*. However, since these antimicrobial agents are poorly water-solubility, their microbiological effect and also their diffusion to the site of action may be limited. It was anticipated that, by interaction with CyDs, the solubility of the antimicrobial agents would be increased, following which, diffusion would also enhanced due to the greater concentration differential existing between the site of delivery and the site of bacterial infection.

The two CyDs used during this study were β-CyD and its highly water-soluble hydroxypropyl derivative (HP-β-CyD). The interactions between CHX and both CyDs were studied, but with the other guests species only HP-β-CyD was used. The

interactions between the CyDs and antimicrobials were studied in solution and solid phases.

Phase solubility studies, NMR and UV spectroscopy investigated the interactions in solution. The former method gave an indication of the complex stability constant (K_S) and also illustrated the effect of temperature on complex stability. Over the temperature range studied (8-45°C), the magnitude of K_S ranged from 30 M^{-1} (CHX-HP-β-CyD complex; 10°C) to 18232 M^{-1} (triclosan-HP-β-CyD complex; 8°C). With increasing concentrations of CyD, the aqueous solubility of all guests was increased. Phase solubility diagrams obtained for all guest-CyD systems (except CHX-HP-β-CyD) were of the A_L type indicating the formation of a soluble complex in solution with a probable stoichiometry of 1:1 (guest:CyD). With the CHX-HP-β-CyD system, negative deviation of the solubility diagrams was observed which was possibly due to a change in the nature of the solvent.

The following comparisons of the phase solubility studies are made with the exception of the CHX-HP-β-CyD system. The stability constant (K_S) of the complexes obtained for the guest-CyD complexes at 37°C was smallest for the CHX-β-CyD complex (54 M^{-1}), and largest for the triclosan-HP-β-CyD complex (8297 M^{-1}). Similarly, the greatest solubility enhancement was observed with the triclosan-HP-β-CyD system; with 0.069 M HP-β-CyD, the aqueous solubility of triclosan was increased 385-fold at 37°C. The affinity of triclosan for the HP-β-CyD cavity is due to both its favourable geometry and its highly hydrophobic nature. With the homologous series of the parabens, the magnitude of K_S increased with an increase in the alkyl chain length of the ester. Furthermore, a linear correlation was observed between the K_S values of the parabens-HP-β-CyD complexes and the respective paraben log P values (figure 3.13; section 3), indicating that complexation of lipophilic guests are favoured. Future work would include the determination of the water/*n*-octanol partition coefficients for both triclosan and CHX to relate their lipophilic nature to the extent of their interaction with CyDs.

The guest-CyD systems (CHX-β-CyD, BuP-HP-β-CyD, triclosan-HP-β-CyD) studied at various temperatures illustrated a decrease in complex stability with an rise in temperature indicating dissociation of the complex. Furthermore, the thermodynamic parameters of the complexation process determined from the van't Hoff plot suggested that, in all cases, inclusion of the guest with the CyD cavity was energetically feasible. The magnitude of the enthalpic and entropic changes for the complexation reaction suggested that hydrogen bonding, van der Waals-London dispersion forces and hydrophobic interactions participated in complex formation.

The ^{1}H-NMR studies performed on the CHX-β-CyD system further confirmed the existence of an inclusion complex in solution which has a probable stoichiometric ratio of 1:1. Furthermore, the results indicated that complex formation occurred by inclusion of the chlorophenyl moiety of the CHX in the CyD cavity. Future work would include similar NMR studies performed on the paraben-HP-β-CyD and triclosan-HP-β-CyD systems to ascertain the stoichiometry and mode of inclusion of these respective complexes. Further conclusive information regarding the geometry of the guest-CyD inclusion complex could be obtained from NMR experiments involving the nuclear overhauser effect (NOE).

UV spectroscopy further confirmed the interaction of BuP with HP-β-CyD in solution suggesting the possibility that complexation of BuP occurred *via* inclusion of its aromatic moiety in the CyD cavity.

Solid-phase CyD complexes of the various guests were prepared by the freeze-drying method. Various investigative procedures were performed on the solid-phase complexes to confirm the existence of true inclusion complexes. DSC analysis showed clear differences between the thermograms of the complex systems and the respective equimolar physical mixtures. The melting endotherm of the guest was lost on complexation due to the dispersion of the guest within the CyD cavity. Further evidence of complexation for the paraben-HP-β-CyD systems was obtained from IR analysis. The carbonyl moiety of the paraben derivatives when complexed, was shifted to a higher frequency due to the reduced intermolecular association between the guest molecules. Powder X-ray diffraction studies performed on the CHX-CyD and BuP-HP-β-CyD systems revealed significant differences between the diffractograms of the respective equimolar physical mixtures and the complexes. The reduced crystallinity of the complexes suggested that the guests were encapsulated within the CyD cavity.

Dissolution studies of guest-CyD complexes illustrated their superior solubilities. In the case of the CHX-CyD and triclosan-HP-β-CyD systems, metastable supersaturated solutions were initially formed after which the solubility of the complexes declined to an equilibrium level. With the paraben-HP-β-CyD systems however, saturation limits of the respective complexes were not reached. The concentration of free drug existing in these systems was estimated using the proposed model (Appendix 4). With the CHX and triclosan-CyD systems, at the saturation level of the complex, the concentration of drug in the non-complexed form was greater than the saturation solubility of drug alone. With the parabens systems, when sufficient complex was dissolved, the concentration of free drug was also greater than the saturation solubility of the respective paraben. Therefore,

in all these systems the solutions were supersaturated with respect to the free drug. Using equation A4.20, the effect of K_S on free drug concentration in the various guest-CyD systems studied was compared; the K_S values of the various guest-CyD complexes were used and a fixed concentration of guest and CyD *i.e.* the variables $[A]_0$ and $[C]_0$ were equal to 0.05 M. The percentages of free and complexed drug in the various systems are shown in table 6.1. As would be expected, the greater the stability constant of the complex, the greater the percentage of complexed guest.

Table 6.1 Percentage of free and complexed guest in the various guest-CyD systems from this study estimated using equation A4.20 and a total guest and CyD concentration of 0.05 M

guest-CyD system	K_S (M^{-1})	Percentage of free guest (%)	Percentage of complexed guest (%)
CHX-β-CyD	54	45.1	54.9
CHX-HP-β-CyD	41	49.6	50.4
MeP-HP-β-CyD	980	13.3	86.7
EtP-HP-β-CyD	1308	11.6	88.4
PrP-HP-β-CyD	1715	10.2	89.8
BuP-HP-β-CyD	2179	9.1	90.9
Triclosan-HP-β-CyD	8297	4.8	95.2

An important consideration for treatment of bacteria in difficult to access areas is the diffusion of antimicrobial agent to the site of action. The concentration differential, which is the driving force for diffusion, would be greater between the supersaturated antimicrobial-CyD solution and the drug concentration at the site of bacterial infection, than that between a solution of drug alone and the site of action. Diffusion experiments were performed on the parabens-HP-β-CyD and triclosan-HP-β-CyD systems. As a consequence of the physicochemical properties of these guests, the membranes used enabled preferentially transport of non-complexed drug only. These experiments were thus performed to assess the flux of free drug from donor phases containing either drug alone or a solution of the respective CyD complex. The flux of drug from donor solutions of the CyD complexes, which were supersaturated with respect to the free drug, was greater than the flux from a suspension of drug alone. Unfortunately, a suitable membrane to assess the flux of free CHX was not found. Future work would include the use of radiolabelled CHX and β-CyD to demonstrate the diffusional behaviour of CHX.

The general consensus seems to be that depending on whether the active part of the antimicrobial agent is included within the CyD cavity, the drug-CyD complex itself is inactive. However, the potential antimicrobial activity of supersaturated solutions (with respect to free drug) should be greater than solutions of drug alone. Microbiological testing (chapter 6) of the CHX-β-CyD system found no significant difference between the activities of saturated solutions of drug alone and the CHX-β-CyD complex against *B. subtilis* spores, despite the fact that in the latter solution, the concentration of free CHX was approximately 4 times greater than the saturation concentration of CHX itself. In contrast, the microbiological activity of the BuP-HP-β-CyD was significantly greater than a saturated solution of drug alone. This was due to the solution of the complex being supersaturated (3 times saturation solubility of BuP alone) with respect to free and therefore active BuP, and also possibly due to the activity of the BuP-HP-β-CyD itself as previously discussed. Further microbiological testing involved the use of Franz diffusion cells to simulate an *in vivo* barrier to diffusion of the antimicrobial agent to the site of bacterial growth. Since the flux of BuP from a donor solution of its HP-β-CyD complex (supersaturated with respect to free BuP) was enhanced, the microbiological activity of this system was also greater than that of a donor suspension of BuP alone. Future work would include assessment of the microbiological activities of the other paraben-HP-β-CyD and also the triclosan-HP-β-CyD systems. As outlined in chapter 5, the agar plate method and biofilm method could be further used to demonstrate both the diffusion and activity of free and complexed drug.

A further consideration for future work would be the search for a suitable competitor candidate which would displace complexed drug enabling more free for diffusion to the site of bacterial infection and for microbiological activity.

In conclusion, the results of this study have demonstrated the use of CyDs in enhancing the solubility of poorly soluble antimicrobial agents by formation of inclusion complexes. The advantages of using the more soluble HP-β-CyD were also observed. At sufficiently high concentrations of the CyD complexes, the concentration of dissolved drug existing as the non-complexed form exceeded its saturation solubility concentration enabling a larger concentration differential to exist across the membrane. It was shown that the flux of free drug from these supersaturated solutions was enhanced. If an *in vivo* system is considered, the driving force for diffusion of a drug to a difficult to access area should also be increased. Consequently, the concentration of antimicrobial agent at the site of action will be greater enabling efficient eradication of the bacterium. Further issues which need to be addressed include the retention of a putative antimicrobial-CyD product in the oral cavity or the GI tract such that efficacious concentrations of antimicrobial agent may

be delivered. Although oral administration of CyDs is considered to be safe, the concentrations of these antimicrobial agents delivered as the CyDs complexes would be greater than the concentrations used in currently available products. Thus, further toxicological testing would be required to assess their safety profiles at higher concentrations.

This study has presented a potential solution to the problem of efficient delivery of antimicrobial agents for the treatment of localised bacterial infections. However, the theory behind the use of CyDs to obtain supersaturated solutions of free drug could be applied to other drug formulations where drug delivery is a problem due to both a limited solubility of the active agent and the biological barriers which need to be overcome to reach the site of action.

REFERENCES

Aalto TR, Firman MC, Rigler NE, *p*-Hydroxybenzoic acid esters as preservatives 1. Uses, antibacterial and antifungal studies, properties and determination. *J Am pharm Ass, scient Edn*, 41 (1953) 449-456

Albert A, Serjeant EP, *The Determination of Ionization Constants. A Laboratory Manual,* Third Edition, Chapman and Hall, London (1984)

Amdidouche D, Darrouzet H, Duchene D, Poelman M, Inclusion of retinoic acid in β-Cyclodextrin. *Int J Pharm,* 54 (1989) 175-179

Andersen GH, Robbins FM, Domingues FJ, Moores RG, Long CL, The utilisation of Schardinger dextrins by the rat. *Tox Applied Pharm*, 5 (1963) 257-266

Backensfeld T, Müller BW, Kolter K, Interaction of NSA with cyclodextrins and hydroxypropyl cyclodextrin derivatives. *Int J Pharm*, 74 (1991) 85-93

Bekers O, Kettenes-Van Den Bosch JJ, Van Helden SP, Seijkens D, Beijen JH, Bult A, Underberg WJM, Inclusion complex formation of anthracycline antibiotics with cyclodextrins; A proton nuclear magnetic resonance and molecular modelling study. *J Inclus Phenom*, 11 (1991a) 185-193

Bekers O, Uijtendaal EV, Beijnen JH, Bult A, Underberg WJM, Cyclodextrins in the pharmaceutical field. *Drug Dev Ind Pharm*, 17 (1991b) 1503-1549

Bellamy LJ, *The Infra-Red Spectra of Complex Molecules,* Second Edition, John Wiley & Sons Inc, New York (1958) pp 166

Bergeron R, Rowan R, The molecular disposition of sodium *p*-nitrophenolate in the cavitites of cycloheptaamylose and cyclohexaamylose in solution. *Biorg Chem*, 5 (1976) 425-436

Brewster ME, Estes KS, Bodor N, An intravenous toxicity study of 2-hydroxypropyl-β-cyclodextrin, a useful drug solubiliser, in rats and monkeys. *Int J Pharm*, 59 (1990) 231-243

Brewster ME, Hora MS, Simpkins JW, Bodor N, Use of 2-hydroxypropyl-β-cyclodextrin as a solubilising and stabilising excipient for protein drugs. *Pharm Res*, 8 (1991) 792-795

Brewster ME, Loftsson T, Baldvinsdóttir J, Bodor N, Stabilisation of aspartame by cyclodextrins. *Int J Pharm*, 75 (1991) RS-R8

Broughan L, HPLC determination of chlorhexidine in urine and serum. *J Chrom*, 383 (1986) 365-373

Bolton S, *Drugs and the Pharmaceutical Sciences, Volume 25. Pharmaceutical Statistics.* Marcel Dekker Inc, New York (1984) pp 105-161

Buvári A, Barcza I, Complex formation of inorganic salts with β-cyclodextrin. *J Inclusion Phenom Mol Recognit Chem*, 7 (1989) 379-389

Cabral Marques HM, Hadgraft J, Kellaway IW, Studies of cyclodextrin inclusion complexes. I. The Salbutamol-cyclodextrin complex as studied by phase solubility and DSC. *Int J Pharm,* 63 (1990), 259-266

Cabral Marques HM, Hadgraft J, Kellaway IW, Pugh PJ, Studies of cyclodextrin inclusion complexes. II. Molecular modelling and ^{1}H-NMR evidence for the Salbutamol-β-cyclodextrin complex. *Int J Pharm*, 63 (1990), 267-274

Caldwell SH, Marshall BJ, Campylobacter pylori and peptic disease: Therapeutic implications. *Drug Therapy*, (1989) 92-106

Catena GC, Bright FV, Thermodynamic study of the effects of β-cyclodextrin inclusion with anilinonaphthalenesulfonates. *Anal Chem*, 61 (1989) 905-909

Chatjigakis AK, Donzé C, Coleman AW, Solubility behaviour of β-cylcodextrin in water/co-solvent mixtures. *Anal Chem*, 64 (1992) 1632-1634

Chow D, Karara A, Characterisation, dissolution and bioavailability in rats of Ibuprofen-β-cyclodextrin complex system. *Int J Pharm*, 28 (1986) 95-101

Christensen F, Jensen JE, The effect of chlorhexidine on some biochemical parameters of rat liver microsomes. *Acta pharmacol et toxicol*, 35 (1974) 33-41

Ciancio SG, Agents for the management of plaque and gingivitis. *J Dent Res*, 71 (1992) 1450-1454

Clarke RJ, Coates JH, Lincoln SF, Kinetic and equilibrium studies of cyclomalto-octaose (γ-cyclodextrin)-methyl orange inclusion complexes. *Carb Res*, 127 (1983) 181-191

Clarke RJ, Coates JH, Lincoln SF, Inclusion complexes of the cyclomalto-oligosaccharides (cyclodextrin). *Adv Carbohyd Chem Biochem*, 46 (1988) 205-249

Cohen J, Lach JL, Interactions of pharmaceuticals with Schardinger dextrins I. Interaction with hydroxybenzoic acids and *p*-hydroxybenzoates. *J Pharm Sci*, 52 (1963) 132-136

Corrigan OI, Stanley CT, Mechanism of drug dissolution rate enhancement from β-cyclodextrin-drug systems. *J Pharm Pharmacol*, 34 (1982) 621-626

Coussement W, Van Cauteren H, Vandenberge J, Vanparys P, Teuns G, Lampo A, Marsboom R, Toxicological profile of hydroxypropyl-β-cyclodextrin (HP-β-CD) in laboratory animals. In: Duchêne D (ed), *Minutes of the Fifth International Symposium on Cyclodextrins*, Editons de Santé, Paris (1990) pp 522-524

Cramer F, Saenger W, Spatz C H, Inclusion compounds XIX. The formation of inclusion compounds of α-cyclodextrin in aqueous solutions. Thermodynamics and kinetics. *J Am Chem Soc*, 89 (1967) 14-20

Croft AP, Bartsch RA, Synthesis of chemically modified cyclodextrins. *Tetrahedron*, 39 (1983) 1417-1474

Cutler RA, Diana GD, Cschalt S, Bisbiguanides: A new series of antimicrobial agent. *Soap and Chemical Specialist*, 42 (1966) 45-49; 101-103

Darrington RT, Xiang T, Anderson BD, Inclusion complexes of purine nucleosides with cyclodextrin. I. Complexation and stabilisation of a dideoxypurine nucleoside with 2-hydroxypropyl-β-cyclodextrin. *Int J Pharm*, 59 (1990) 35-44

Darrouzet H, Practical considerations concerning the use of cyclodextrins as complex agents. In: Hegdes AR (ed), *Minutes of the Sixth International Symposium on Cyclodextrins*, Editions de Santé, France (1992) pp 301-307

Davies A, The mode of action of chlorhexidine. *J peridont Res*, 8; Suppl.12 (1973) 68-75

Davies A, Disinfection. *Reports on The Progress of Applied Chemistry*, 54 (1969) 366-374

Davis AF, Hadgraft J, Effect of supersaturation on membrane transport: 1. Hydrocortisone acetate. *Int J Pharm*, 76 (1991) 1-8

Dechandt J, Mehnert W, Frömming KH, Influence of hydroxypropyl-β-cyclodextrin on the antimicrobial efficacy of benzalkonium chloride. *Eur J Pharm Sci*, 2 (1994) 179

Dermaco PV, Thakkar AL, Cyclohepta-amylose inclusion complexes. A proton magnetic resonance study. *Chem Comm*, (1970) 2-4

Dettmar PW, Lloyd-Jones JG, Medicament containing triclosan for treating gastrointestinal disorders. *UK Pat. Appl. GB 2243549 (1.5.1991)*

Djedäini F, Lin SZ, Perly B, Wouessidjewe D, High-field nuclear magnetic resonace techniques for the investigation of a β-cyclodextrin: Indomethacin inclusion complex. *J Pharm Sci*, 79 (1990) 643-646

Documenta Geigy, Scientific Tables, Sixth Edition, Geigy Pharmaceutical Company Ltd, Manchester (1965) pp 520-521

Eklund T, Inhibition of growth and uptake processes in bacteria by some chemical food preservatives. *J appl Bact*, 48 (1980) 423-432

El-Gendy GA, Terada K, Yamamoto K, Nakai Y, Molecular behaviour, dissolution characteristics and chemical stability of aspirin in the ground mixture and in the inclusion complex with di-O-methyl-β-cyclodextrin. *Int J Pharm*, 31 (1986) 25-31

Elworthy PH, Florence AT, Macfarlane CB, *Solubilization by surface-active agents*. Chapman and Hall Ltd, London (1968) pp 41

Erden N, Çelebi N, A study of the inclusion complex of naproxen with β-cyclodextrin. *Int J Pharm*, 48 (1988) 83-89

Fenyvesi E, Shirakura O, Szejtli J, Nagai T, Properties of cyclodextrin polymer as a tabletting aid. *Chem Pharm Bull*, 32 (1984) 665-669

Flourie B, Molis C, Franchisseur, Dupas H, Hatat C, Rambaud JC, Digestibility of β-cyclodextrin in the human intestine. In: Hegdes AR (ed), *Minutes of the Sixth International Symposium on Cyclodextrins*, Editions de Santé, France (1992) pp 284-287

Flynn GL, Yalkowsky SH, Correlation and prediction of mass tranpsort across membranes I: Influence of alkyl chain length on flux-determining properties of barrier and diffusant. *J Pharm Sci*, 61 (1972) 838-852

Frank HS, Evans MW, Free volume and entropy in condensed systems III. Entropy in binary liquid mixtures; partial molal entropy in dilute solutions; structure and thermodynamics in aqueous electrolytes. *J Chem Phys*, 13 (1945) 507-532

Frank DW, Gray JE, Weaver RN, Cyclodextrin nephrosis in the rat. *Am J Path*, 83 (1976) 367-373

Frijlink HW, Eissens AC, Hefting NR, Poelstra K, Lerk CF, Meyer DKF, The effect of parenterally administered cyclodextrins on cholesterol levels in the rat. *Pharm Res*, 8 (1991) 9-16

Frömming KH, Cyclodextrins in the pharmaceutical industry. In: Szejtli J (ed), *Proceedings of the First International Symposium on Cyclodextrins*, Reidel Publishing Company, Dordrecht (1981) pp 367-376

Fronza G, Mele A, Redenti E, Ventura P, Proton nuclear magnetic resonance spectroscopy studies of the inclusion complex of piroxicam with β-cyclodextrin. *J Pharm Sci*, 81 (1992) 1162-1165

Gaffney MH, Cooke M, Improved method for the determination of chlorhexidine in urine. *J Chrom*, 306 (1984) 303-313

Gallopo AR, Lynch DM, Cyclodextrin complexes of bis-biguanide hexane compounds. *Eur. Pat. Appl. EP 306455 (3.8.1989):* CA, 111:180501f (1991)

Gelb RI, Schwartz LM, Cardelino B, Fuhrman HS, Johnson RF, Laufer, Binding mechanisms in cyclohexaamylose complexes. *J Am Chem Soc*, 103 (1981) 1750-1757

Gerlóczy A, Antal S, Szatmari I, Muller-Horvath R, Szejtli J, Absorption, distribution and excretion of ^{14}C-labelled hydroxypropyl-β-cyclodextrin in rats following oral administration. In: Duchêne D (ed), *Minutes of the Fifth International Symposium on Cyclodextrins*, Editons de Santé, Paris (1990) pp 507-513

Gerlóczy A, Fonagy A, Keresztes P, Perlaky L, Szejtli J, Absorption, distribution, excretion and metabolism of orally administered ^{14}C-β-cyclodextrin in the rat. *Arzneim Forsch*, 7 (1985) 1042-1047

Gerlóczy A, Fonagy A, Szejtli J, Absorption and metabolism of β-cyclodextrin by rats. In: Szejtli J (ed), *Proceedings of the First International Symposium on Cyclodextrins*, Reidel Publishing Company, Dordrecht (1981) pp 101-108

Griffiths DW, Bender M, Cycloamyloses as catalysts. *Advances in Catylsis*, 83 (1973) 209-261

Habon I, Szejtli J, Complex equilibrium and bioavailability. In: Szejtli J (ed), *Proceedings of the First International Symposium on Cyclodextrins*, Reidel Publishing Company, Dordrecht (1981) pp 413-422

Hall ES and Ache HJ, Study of the forces responsible for polar substrates in the cyclohexaamylose cavity by positron annihalation techniques. *J Phys Chem*, 83 (1979) 1805-1807

Han SM, Atkinson WM, Purdie N, Solute induced circular dichroism: Drug discrimination by cyclodextrin. *Anal Chem*, 56 (1984) 2827-2830

Häusler O, Müller-Goyman, Properties and structure of aqueous solutions of hydroxypropyl-beta-cyclodextrin. *Starch*, 45 (1993) 183-187

Hersey A, Robinson BH, Thermodynamic and kinetic study of the binding of azo-dyes to α-cyclodextrin. *J Chem Soc, Faraday Trans. 1*, 80 (1984) 2039-2052

Higuchi T, Connors KA, Phase solubility techniques. *Adv Anal Chem Instr*, 4 (1965) 117-212

Hirayama F, Hirashima N, Abe K, Uekama K, Litsu T, Ueno M, Utilization of diethyl-β-cyclodextrin as a sustained release carrier for isosorbide dinitrate. *J Pharm Sci*, 77 (1988) 233-236

Hirayama F, Uekama K, Methods of investigating and preparing inclusion compounds. In: Duchêne D (ed), *Cyclodextrin and their Industrial Uses*, Editions de Santé, Paris (1987) pp 133-172

Hirsch W, Dimartini C, Fried V, Ling W, Complexation of aqueous ammonia by cyclodextrins. *Can J Chem*, 65 (1987) 2661-2664

Horiuchi Y, Hirayama F, Uekama K, Slow-release characteristics of diltiazem from ethylated-β-cyclodextrin complexes. *J Pharm Sci*, 79 (1990) 128-132

Hoshino T, Uekama K, Pitha J, Increase in temperature enhances solubility of drugs in aqueous solutions of hydroxypropyl cyclodextrins. *Int J Pharm*, 98 (1993) 239-242

Hostetler JS, Hanson LH, Stevens DA, Effect of cyclodextrin on the pharmacology of antifungal oral azoles. *Antimicrob Agents Chemother*, 36 (1992) 477-480

Hugo WB, Mode of action of non-antibiotic antibacterial agents. In: Hugo WB, Russell AD (eds), *Pharmaceutical Microbiology*, Fifth Edition, Blackwell Scientific Publications, London (1992) pp 288-294

Hugo WB, Longworth AR, Some aspects of the mode of action of chlorhexidine. *J Pharm Pharmacol*, 16 (1964) 655-662

Huston CE, Wainwright P, Cooke M, High performance liquid chromatographic method for the determination of chlorhexidine. *J Chrom*, 237 (1982) 457-464

Hybl A, Rundle RE, Williams DE, The crystal and molecular structure of the cyclohexaamylose-potassium acetate complex. *J Am Chem Soc*, 87 (1965) 2779-2788

Ikeda K, Uekama K, Otagiri M, Inclusion complexes of β-cyclodextrin with antiinflammatory drugs fenamates in aqueous solution. *Chem Pharm Bull*, 23 (1975) 201-208

Imai T, Otagiri M, Saito H, Uekama U, Inclusion mode of flurbiprofen with β-cyclodextrin and heptakis (2,3,6-tri-O-methyl)-β-cyclodextrin, and improvements of some pharmaceutical properties of flurbiprofen by complexation. *Chem Pharm Bull*, 36 (1988) 354-359

Inoue Y, Miyata Y, Formation and molecular dynamics of cycloamylose inclusion complexes with phenylalanine. *Bull Chem Soc Jpn*, 54 (1981) 809-816

Irwin WJ, Dwivedi AK, Holbrook PA, Dey M, The effect of cyclodextrins on the stability of peptides in nasal enzymic systems. *Pharm Res*, 11 (1994) 1698-1703

Irwin WJ, Scott DK, Hplc in pharmacy. *Chemistry in Britain*, (1982) 708-718

Jencks WP, *Catalysis in Chemistry and Enzymology*, McGraw-Hill Book Company, New York (1969) pp 393-436

Job P, Research on the formation of mineral complexes in solution and on their stability. *Ann Chim*, 9 (1928) 113-134

Jodal I, Kandra L, Harangi J, Nanasi P, Szejtli J, Hydroylsis of cyclodextrin by *Aspergillus oryzae* α-amylase. *Starch*, 36 (1988) 140-143

Johnson JR, Electrochemical methods. In: Beckett AH, Stenlake JB (eds), *Practical Pharmaceutical Chemistry, Part 2*, Fourth Edition, The Athlone London Press, London, (1988) pp 175-254

Jones SP, Grant DJW, Hadgraft J, Parr G, Cyclodextrins in the pharmaceutical sciences, Part 1: Preparation, structure and properties of cyclodextrin inclusion compounds. *Acta Pharm Technol*, 30 (1984) 213-223

Jones SP, Parr GD, The acetoluides as models for studying cyclodextrin inclusion complexes. *Int J Pharm*, 36 (1987) 223-231

Kanebo Ltd, Toyko, Japan. *Appl 78/137.652 (7.11.1978)*: CA, 93:191911a (1980)

Kirschbaum JJ, Inter-laboratory transfer of HPLC methods: Problems and solutions. *J Pharm Biomed Anal*, 7 (1989) 813-833

Kjaerheim V, Waaler SM, Rolla G, Significance of choice of solvents for the clinical effect of triclosan-containing mouthwashes. *Scand J Dent Res*, 102 (1994) 202-205

Kobayshi N, Osa T, Complexation of aromatic carboxylic acids with heptakis (2,6-di-O-methyl) cyclomaltoseheptaose in chloroform and water. *Carb Res*, 182 (1989) 149-157

Kondo S, Sugimoto I, Enhancement of transdermal delievery by superfluous thermodynamic potential. I. Thermodynamic analysis of nifedipine transport across the lipoidal barrier. *J Pharmacobio-Dyn*, 10 (1987) 587-594

Kumar PJ, Clark ML, Gastroenterolgy. In: Kumar PJ, Clark ML (eds), *Clinical Medicine*, Second Edition, Baillere Tindall, London (1990) pp 173-237

Kurozumi M, Nambu N, Nagai T, Inclusion compounds of non-steroidal antiinflammatory and other slightly water soluble drugs with α- and β-cyclodextrin in powdered form. *Chem Pharm Bull*, 23 (1975) 3062-3068

Lehner SI, Müller BW, Seydel JK, Interactions between *p*-hydroxybenzoic acid esters and hydroxypropyl-β-cyclodextrin and their antimicrobial effect against *Candida albicans*. *Int J Pharm*, 93 (1993) 201-208

Lehner SI, Müller BW, Seydel JK, Effect of hydroxypropyl-β-cyclodextrin on the antimicrobial action of preservatives. *J Pharm Pharmacol*, 46 (1994) 186-191

Lewis EA, Hansen LD, Thermodynamics of binding of guest molecule to α- and β-cyclodextrin. *J Chem Soc Perkins Trans 2* (1973) 2081-2085

Lin SZ, Wouessidjewe D, Poelman M, Duchene D, In vivo evaluation of indomethacin/cyclodextrin complexes. Gastrointestinal tolerance and dermal anti-inflammatory activity. *Int J Pharm*, 106 (1994) 63-67

Li Wan Po A, Irwin WJ, High-performance liquid chromatography. Techniques and applications. *J Clin Hosp Pharm*, 5 (1980) 107-144

Loftsson T, Stefánsdóttir Ó, Frioriksdóttir H, Guòmundsson Ö, Interactions between preservatives and 2-hydroxypropyl-β-cyclodextrin. *Drug Dev Ind Pharm*, 18 (1992) 1477-1484

Lumry R, Rajender S, Enthalpy-entropy compensation phenomena in water solutions of proteins and small molecules: A ubiquitous property of water. *Biopolymers*, 9 (1970) 1125-1227

Makita T, Ojima N, Hashimoto Y, Ide H, Tsuji M, Fujisaki Y, Chronic oral toxicity study of β-cyclodextrin (β-CD) in rats. *Oyo Yakuri*, 10 (1975) 449-458 (English abstract)

Manson JD, *An outline of peridontics*. John Wright & Sons Ltd, Bristol (1983)

Marsh P, Microbiological aspects of chemical control of plaque and gingivitis. *J Dent Res*, 71 (1992) 1431-1438

Martindale, Thirtieth edition, The Pharmaceutical Press, London, 1993

Matsuda H, Ito K, Sato Y, Yoshizava D, Tanaka M, Taki A, Sumiyoshi, Utsuki, Hirayama, Uekama K, Inclusion complexation of *p*-hydroxybenzoic acid esters with 2-hydroxypropyl-β-cylcodextrins. On changes in solubility and antimicrobial activity. *Chem Pharm Bull*, 41 (1993) 1448-1452

Matsuda K, Mera Y, Segawa Y, Uchida I, Yokomine A, Takagi K, Acute toxicity study of γ-cyclodextrin (γ-CD) in mice and rats. *Oya Yakuri*, 26 (1983) 287-291 (English abstract)

Melville TH, Russell C, *Microbiology for dental students*. William Heinemann Medical Books Ltd, London (1981)

Menard FA, Dedhiya MG, Rhodes CT, Studies of the effect of pH, temperature and ring size on the complexation of phenytoin with cyclodextrins. *Pharm Acta Helv*, 63 (1988) 303-308

Merck Index, Tenth Edition, Merck & Co. Inc. USA, 1983

Mularz EA, Cline-Love LJ, Petersheim M, Structural basis for enantiomeric resolution of pseudoephedrine and the failure to resolve ephedrine by using β-cyclodextrin mobile phases. *Anal Chem*, 60 (1988) 2751-2755

Müller BW, Brauns U, Solublization of drugs by modified β-cylcodextrins. *Int J Pharm*, 26 (1985) 77-88

Müller BW, Brauns U, Hydroxypropyl-β-cyclodextrin derivatives: Influence of average degree of substitution on complexing ability and surface activity. *J Pharm Sci*, 75 (1986) 571-572

Munson JW, HPLC:Theory, instrumentation and pharmaceutical application. In Munson JW (ed), *Drugs in the Pharmaceutical Sciences, Volume II, Pharmaceutical Analysis, Modern Methods, Part B*, Marcel Dekker Inc, New York (1984) pp 15-154

Nakai Y, Nakajima S, Yamamoto K, Terada K, Konno T, Effects of grinding on physical and chemical properties of crystalline medicinals with microcrystalline cellulose III. Infrared spectra of medicinals in ground mixture. *Chem Pharm Bull*, 36 (1978) 3419-3425

Nakai Y, Nakajima S, Yamamoto K, Terada K, Konno T, Effects of grinding on physical and chemical properties of crystalline medicinals with microcrystalline cellulose V. Comparison with tri-O-methyl-β-cyclodextrin ground mixture. *Chem Pharm Bull*, 28 (1980) 1552-1558

Nakai Y, Yamamoto, Terada K, Watanbe D, New methods for preparing cyclodextrin inclusion compounds. I. Heating in a sealed container. *Chem Pharm Bull*, 35 (1987) 4609-4615

Nishijo J, Nagai M, Inclusion complex of 8-Anilinonaphthalene-1-sulphonate with β-cyclodextrin. *J Pharm Sci*, 80 (1991) 58-62

Oguchi ZT, Terada K, Yamamoto K, Nakai Y, Freeze-drying of drug-additive binary systems. *Chem Pharm Bull*, 37 (1989) 1881-1885

Okada Y, Kubota Y, Koizumi K, Hizukuri S, Ohfuji T, Ogata K, Some properties and the inclusion behaviour of branched cyclodextrins. *Chem Pharm Bull*, 36 (1988) 2176-2185

Orienti I, Fini A, Zecchi V, Zuman P, Diffusion of naproxen in the presence of β-cyclodextrin across a silicone rubber membrane. *Pharm Acta Helv*, 66 (1991) 204-208

Otagiri M, Imai T, Hirayama F, Uekama K, Inclusion complex formation of the antiinflammatory drug flurbiprofen with cyclodextrins in aqueous solution and in solid state. *Acta Pharm Suec*, 20 (1983) 11-20

Otagiri M, Imai T, Matsuo N, Uekama K, Improvements to some pharmaceutical properties of flurbiprofen by β- and γ-cyclodextrin complexation. *Acta Pharm Suec*, 20 (1983) 1-10

Otagiri M, Miyaji T, Uekama K, Ikeda K, Inclusion complexation of barbiturates with β-cyclodextrins in aqueous solution. I. Spectroscopic study on the mode of interaction. *Chem Pharm Bull*, 24 (1976) 1146-1154

Otagiri M, Uekama K, Ikeda K, Inclusion complexes of β-cyclodextrin with tranquilizing drug phenothiazines in aqueous solution. *Chem Pharm Bull*, 23 (1975) 199-195

Otero-Espinar FJ, Anguiano-Igea S, Garcia-Gonzalex N, Vila-Jato JL, Blanco-Mendez J, Interaction of naproxen with β-cyclodextrin in solution and in the solid state. *Int J Pharm*, 79 (1992) 149-157

Paginton JS, β-Cyclodextrin: The success of molecular inclusion. *Chemistry in Britain*, 23 (1987) 455-458

Parrish MA, Cyclodextrins - a review. Available from Sterling Organics Limited, Newcastle-upon-Tyne, England.

Pedersen M, Edelsten M, Nielsen VF, Scarpellinie A, Skytte S, Slot C, Formation and antimycotic effect of cyclodextrin inclusion complexes of econazole and miconazole. *Int J Pharm*, 90 (1993) 247-254

Peterson, WL, *Helicobacter pylori* and peptic ulcer disease. *New Eng J Med*, 325 (1991) 1043-1048

Pharr DY, Fu ZS, Smith TK, Hinze WL, Solubilisation of cyclodextrins for analytical applications. *Anal Chem*, 61 (1989) 275-279

Pitha J, Anaissie EJ, Uekama K, γ-Cyclodextrin:Testosterone complex suitable for sublingual administration. *J Pharm Sci*, 76 (1987) 788-790

Pitha J, Harman SM, Michel ME, Hydrophilic cyclodextrin derivatives enable effective oral administration of steroidal hormones. *J Pharm Sci*, 75 (1986) 165-167

Pitha J, Hoshino T, Torres-Labandeira, Irie T, Preparation of drug:hydroxypropyl-cylcodextrin complexes by a method using ethanol or aqueous ammonia hydroxide as co-solubilisers. *Int J Pharm*, 80 (1992) 253-258

Pitha J, Milecki J, Fales H, Pannell L, Uekama K, Hydroxypropyl-β-cyclodextrin: Preparation and characterization: Effects of solubility of drugs. *Int J Pharm*, 29 (1986) 73-82

Pitha J, Pitha J, Amorphous water-soluble derivatives of cyclodextrins: Non-toxic dissolution enhancing excipients. *J Pharm Sci*, 74 (1985) 987-990

Qi T, Nishihata T, Rytting JH, Study of the interaction between β-cyclodextrin and chlorhexidine. *Pharm Res*, 11 (1994) 1207-1210

Rajagopalan N, Chen S, Chow W, A study of the inclusion of amphotericin-B with γ-cyclodextrin. *Int J Pharm*, 29 (1986) 161-168

Rao CT, Fales HM, Pitha J, Pharmaceutical usefulness of hydroxypropylcyclodextrins: "E Pluribus Unum" is an essential feature. *Pharm Res*, 7 (1990) 612-615

Rao VSR, Foster JF, On the conformation of the D-glucopyranose ring in maltose and in higher polymers of D-glucose. *J Phys Chem*, 67 (1963) 951-955

Rees DA, Conformation analysis of polysaccharides. Part V. The characterization of linkage confirmations (chain confirmations) by optical rotation at a single wavelength. evidence for distortion of cyclohexa-amylose in aqueous solution. Optical rotation and the amylose conformation. *J Chem Soc*, B (1970) 877-884

Russell AD, The mechanism of action of some antibacterial agents. *Progress in Med Chem*, 6 (1969) 135-199

Saenger W, Cyclodextrin inclusion compounds in research and industry. *Angew Chem Int Ed Engl*, 19 (1980) 344-362

Saenger W, Structural aspects of cyclodextrins and their inclusion complexes. In: Davies JED, MacNiol DD (eds), *Inclusion compounds*, Volume 2, Academic Press, London (1984) pp 231-259

Sanghavi NM, Mayekar R, Fruitwala M, Inclusion complexes of terfenadine-cyclodextrins. *Drug Dev Ind Pharm*, 21 (1995) 375-381

Schardinger F, Thermophilic bacteria from various foods and milk and some conversion products thereof inn nutrient solutions containing carbohydrate, including crystallised polysaccharides (dextrins) from starch. *Untersuch Nahr u Genussm*, 6 (1903) 865-876

Scrip, *H pylori* peptic ulcers - recipe for success, No 1968 October 21st 1994, pp 23

Sekikawa H, Nakano M, Arita T, Inhibitory effect of polyvinylpyrollidine on the crystallisation of drugs. *Chem Pharm Bull*, 26 (1978) 118-126

Senior N, Some observations on the formulation and properties of chlorhexidine. *J Soc Cosmet Chem*, 24 (1973) 259-278

Seo H, Tsumoka M, Hashimoto T, Fujinaga T, Otagiri M, Uekama K, Enhancement of oral bioavailability of spironolactone by β- and γ-cyclodextrin complexations. *Chem Pharm Bull*, 31 (1983) 286-291

Stern W, Cyclodextrin-based drug delivery. *Drug News and Perspectives*, 2 (1989) 410-415

Sundarajan PR, Rao VSR, Conformational studies on cycloamyloses. *Carb Res*, 13 (1970) 351-358

Suzuki M, Ito K, Fushimi C, Kondo T, A study of cyclodextrin complex formation by a freezing point depression method. *Chem Pharm Bull*, 41 (1993) 942-945

Suzuki M, Sasaki Y, Inclusion compound of cyclodextrin and azo dye I. Methyl Orange. *Chem Pharm Bull*, 27 (1979) 609-619

Szejtli J, Cyclodextrins and their inclusion complexes, Akadémiai Kiadó, Budapest, 1982

Szejtli J, Dimethyl-β-cyclodextrin as parenteral drug carrier. *J Inclus Phenom*, 1 (1983) 135-150

Szejtli J, Industrial applications of cyclodextrins . In: Atwood JL, Davies JE, MacNiol DD (eds), *Inclusion Compounds Volume 3, Physical Properties and Applications*, Academic Press, London (1984) pp 331-390

Szejtli J, Molecular entrapment and release properties of drugs by cyclodextrins. In: Smolen VF, Ball LA (eds), *Controlled Drug Bioavailability Vol 3*, John Wiley & Sons, New York (1985) pp 365-421

Szejtli J, *Cyclodextrin Technolgy*. Kluwer Academic Publishers, Dordrecht (1988)

Szejtli J, Cyclodextrins in drug formulation: Part II. *Pharm Tech Int*, (March 1991) 17-22

Szejtli J, The properties and potential uses of cyclodextrin derivatives. *J Inclus Phenom*, 14 (1992) 25-36

Szejtli J, Gerlóczy A, Fonagy A, Intestinal absorption of ^{14}C-labelled β-cyclodextrin in Rats. *Arzneim-Forsch*, 30 (1980) 808-810

Szejtli J, Sebsetyen G, Resorption, metabolism and toxicity studies of the peroral administration of beta-cyclodextrin. *Starch*, 31 (1979) 385-389

Szeman J, Ueda H, Szejtli, Fenyvesl E, Machida Y, Nagai T, Complexation of several drugs with water-soluble cyclodextrin polymer. *Chem Pharm Bull*, 35 (1987) 282-288

Szente L, Investigation and characterization of cyclodextrin complexes. *Cyclodextrin Workshop Gent*, (1989) 1-20

Szente L, Strattan CE, Hydroxypropyl-β-cyclodextrin, preparation and physiochemical properties. In: Duchene D (ed), *New Trends in Cyclodextrins and their Derivatives*, Editions de Santé, Paris (1991) pp 55-96

Tabushi I, Kiyosuke Y, Sugimoto T, Yamamurak K, Approach to the Aspect of Driving Force of Inclusion by α-Cyclodextrin. *J Am Chem Soc*, 100 (1978) 916-919

Takeo K, Kuge T, Complexes of starch and its related materials with organic compounds. *Starch*, 24 (1972) 281-284

Thakkar AL, Demarco PV, Cycloheptaamylose inclusion complexes of barbiturates: Correlation between proton magnetic resonance and solubility studies. *J Pharm Sci*, 60 (1971) 652-653

Tokumara T, Nanba M, Tsushima Y, Tatsuishi K, Kayano M, Machida Y, Nagai T, Enhancement of bioavailability of cinnarizine from it β-cyclodextrin complex on oral administration with α-phenylalanine as a competing agent. *J Pharm Sci*, 75 (1986) 391-394

Tokumara T, Ueda H, Tsushima Y, Kasai M, Kayano M, Amada I, Nagai T, Inclusion complexes of cinnarizine with β-cyclodextrin in aqueous solution and in the solid state. *Chem Pharm Bull*, 32 (1984) 4179-4184

Tong W, Lach JL, Chin T, Guiloory J, Stuctural effects on the binding of amine drugs with the diphenymethyl functionality to cyclodextrins. I. A microcalorimetric study. *Pharm Res*, 8 (1991) 951-957

Torcelli C, Martini A, Muggetti L, De Ponti R, Stability studies on a steroidal drug/β-cyclodextrin coground mixture. *Int J Pharm*, 71 (1991) 19-24

Torres-Labandeira JJ, Pitha J, Davingnon P, Oversaturated solutions of drugs in hydroxypropyl cyclodextrins, parenteral preparations of pancratistatin. *J Pharm Sci*, 80 (1990) 384-386

Ueda H, Nagai T, Nuclear magnetic resonance (NMR) spectroscopy of inclusion compounds of tolbutamide and chlorpropamide with β-cyclodextrin in aqueous solution. *Chem Pharm Bull*, 28 (1980) 1415-1421

Uekama K, Fujinaga T, Hirayama F, Otagiri M, Yamaski. Inclusion complexation of steroid hormones with cyclodextrins in water and in the solid phase. *Int J Pharm*, 10 (1982) 1-15

Uekama K, Hirayama F, Esaki K, Inoue M, Inclusion complexes of cyclodextrin with cinnamic acid derivatives: Dissolution and thermal behaviour. *Chem Pharm Bull*, 27 (1979) 76-79

Uekama K, Hirayama F, Nasu S, Matsuo N, Irie T, Determination of the stability constants for inclusion complexes of cyclodextrins with various drug molecules by high performance liquid chromatography. *Chem Pharm Bull*, 26 (1978) 3477-3484

Uekama K, Horiuchi Y, Irie T, Hirayama F, O-Carboxymethyl-O-ethylcyclomaltoheptaose as a delayed release-type drug carrier: Improvement of the oral bioavailability of diltiazem in the dog. *Carb Res*, 192 (1989) 323-330

Uekama K, Ikeda Y, Hirayama F, Otagiri M, Shibata M, Inclusion complexation of *p*-hydroxybenzoic acid esters with α- and β-cyclodextrins: Dissolution behaviour and antimicrobial activities. *Yakugaku Zasshi*, 100 (1980) 994-1003

Uekama K, Imai T, Improvement of dissolution and suppository release characteristics of flurbiprofen by inclusion complexation with heptakis-(2,6,di-O-methyl)-β-cyclodextrin. *J Pharm Sci*, 74 (1985) 841-845

Uekama K, Narisawa S, Hiryama F, Otagiri M, Improvement of dissolution and absorption characteristics of benzodiazepines by cyclodextrin complexation. *Int J Pharm*, 16 (1983) 327-338

Uekama K, Narisawa S, Irie T, Otagiri M, Anamolous dissolution behaviour of the diazepam-γ-cyclodextrin complex in polymer solutions. *J Inclus Phenom*, 1 (1984) 309-312

Uekama K, Oh K, Otagiri M, Seo H, Tsuruoka M, Improvement of some pharmaceutical properties of clofibrate by cyclodextrin complexation. *Pharm Acta Helv*, 58 (1983) 338-342

Uekama K, Otagiri M, Cyclodextrins in Drug Carrier Systems. *CRC Critical Reviews in Therapeutic Drug Carier Systems*, 3 (1987) 1-40

Uekama K, Otagiri M, Kame Y, Tanaka S, Ikeda K, Inclusion complexes of cinnamic acids with cyclodextrins: Mode of inlcusion in aqueous solution. *Chem Pharm Bull*, 23 (1975) 1421-1430

Urquhart E, Addy M, Chemical control of plaque. *Dental Health*, 30 (1991) 8-13

Van Doorne H, Bosch EH, Stability and in vitro activity of nystatin and its γ-cyclodextrin complex against *Candida albicans*. *Int J Pharm*, 73 (1991) 43-49

Van Doorne H, Bosch EH, Lerk CF, Formation and antimicrobial activity of complexes of β-cyclodextrin and some antimycotic imidazole deravitives. *Pharm Weekbl Sci Ed*, 10 (1988) 80-85

Van Doorne H, Bosch EH, Lerk CF, Interactions between cyclodextrins and some antimycotic imidazole derivatives: studies on solubility and antimicrobial activity. In: Huber O, Szejtli J (eds), *Proceedings of the Fourth International Symposium on Cyclodextrins*, Kluwer Academic Publishers (1988) pp 285-291

Villiers A, The fermentation of starch by the action of butyric enzyme. *Compt Rend Acad Sci*, 112 (1891) 536-538

Vines G, The enemy within. *New Scientist*, Number 1947 (1994) 12-14

Walton A G, Precipitation. In Parfitt GD (ed), *Dispersion of Powders in Liquids*, Elsevier Publishing Company Ltd, London (1969) pp 122-164

Wan Yunus WMZ, Taylor J, Bloor DM, Hall DG, Wyn-Jones E, Electrochemical measurements on the binding of sodium dodecyl sulphate and dodecyltrimethyl ammonium bromide with α- and β-cyclodextrin. *J Phys Chem*, 96 (1992) 8979-8982

Warren JR, Marshall BJ, Unidentified curved bacilli on gastric epithelium in active chronic gastritis. *Lancet*, 1 (1983) 1273-1274

Wells JI, *Pharmaceutical Preformulation, the physicochemical properties of drug substances*. John Wiley & Sons, New York (1988)

Wells JI, Aulton ME, Preformulation. In: Aulton ME (ed), *Pharmaceutics: The Science of Dosage Form Design*, Churchill Livingstone, London (1988) pp 223-253

Wyle FA, *Helicobacter pylori*: Current Perspectives. *J Clin Gastroent*, 13 (1991) S114-S124

Yalkowsky SH, Flynn GL, Slunick TG, Importance of chain length on physicochemical and crystalline properties of organic homologs. *J Pharm Sci*, 61 (1972) 852-857

Yoshida A, Arima H, Uekama K, Pitha J, Pharmaceutical evaluation of hydroxyalkyl ethers of β-cyclodextrins. *Int J Pharm*, 46 (1988) 217-222

Yoshida A, Yamamoto M, Irie T, Hirayama F, Uekama K, Some pharmaceutical properties of 3-hydroxypropyl- and 2,3-dihydroxypropyl-β-cyclodextrins and their solubilising and stabilising abilities. *Chem Pharm Bull*, 37 (1989)

Yoshida A, Yamamoto M, Itoh T, Irie T, Hirayama F, Uekama K, Utility of 2-hydroxypropyl-β-cyclodextrin in an intramuscular injectable preparation of nimodipine. *Chem Pharm Bull*, 38 (1990) 176-179

Yusuff N, York P, Spironolactone cyclodextrin complexes: Phase solubility and ultrafilitration studies. *Int J Pharm*, 73 (1991) 9-15

Yusuff N, York P, Chrystn H, Bramley PN, Swallow RD, Tuledhar BR, Losowsky MS, Improved bioavailability from a spironolactone beta-cyclodextrin complex. *Eur J Clin Pharmacol*, 40 (1990) 507-511

APPENDICES

APPENDIX 1

ABBREVIATIONS

AsP	ascorbyl palmitate
AUFS	absorbance units full scale
BuP	butyl paraben (*n*-butyl *p*-hydroxybenzoate)
CA	competing agent
CHG	chlorhexidine digluconate
CHX	chlorhexidine dihydrochloride
cm	centimetre
CMC	critical micelle concentration
CyD	cyclodextrin
^{14}C	carbon-14-radiolabelled
D.S.	degree of substitution
DSC	differential scanning calorimetry
DTAB	dodecyl tetraammonium bromide
EtP	ethyl paraben (ethyl *p*-hydroxbenzoate)
f/d	freeze-dried
g	grammes
G	guest
h	hours
HA-CyD	hydroxyalkylated-cyclodextrins
HCl	hydrochloric acid
^{1}H-NMR	proton nuclear magnetic resonance
HP-β-CyD	hydroxypropyl-β-cyclodextrin
HPLC	high-performance liquid chrmoatography
i.d.	internal diameter
IR	infra-red
I.S.	internal standard
KBr	potassium bromide
KF	Karl Fischer
K_p	permeability coefficient
K_s	complex stability constant
MeP	methyl paraben (methyl *p*-hydroxybenzoate)
mg	milligrammes
min	minutes
ml	millitres

mM	millimolar
mmol	millimoles
M	molar
M.S.	molar substitution
MeOH	methanol
n	sample size
NADPH	nicotinamide adenine dinulceotide phosphate (reduced)
NaHSA	sodium salt of heptane sulphonic acid
NMR	nuclear magnetic resonance
ODS	octadecylsilane
P	partition coefficient
Phe	phenylalanine
pK_a	$\log_{10}$ dissociation constant
PrP	propyl paraben (propyl *p*-hydroxybenzoate)
p.o.	peroral
r	correlation coefficient
rpm	revolutions per minute
s.d.	standard deviation
SDS	sodium dodecyl sulphate
SP	spironolactone
TGA	thermogravimetric analysis
UV	ultraviolet
v/v	volume in volume
w/v	weight in volume (g/100 ml)
α-CyD	alpha cyclodextrin
β-CyD	beta cyclodextrin
γ-CyD	gamma cyclodextrin
λ	wavelength (nm)
µg	micrograms
µl	microlitres
%	percentage
°C	degrees Celcius

APPENDIX 2

LIST OF SUPPLIERS

Chemical	*Supplier*
Butyl paraben	Sigma
Chlorhexidine digluconate	Sigma
Chlorhexidine dihydrochloride	Sigma
Deuterated water	Aldrich
Ethyl paraben	Sigma
Glacial acetic acid	Fisons
1-Heptane sulphonic acid (sodium salt)	Sigma
Methanol	Fisons
Methyl paraben	Sigma
Propyl paraben	Sigma